Synthesis and Evaluation of New Antimicrobial Agents and Novel Organic Fluorophores

A thesis submitted by

Xin Qiu B.Sc. (Hons.)

to the

National University of Ireland, Maynooth

For the degree of Masters of Science

Based on the research carried out in the

Department of Chemistry, Faculty of Science and Engineering,

National University of Ireland, Maynooth

under the supervision and direction of

Dr. John C. Stephens & Dr. John McGinley

October 2013

Contents

Chapter 3 Experimental for the synthesis of pyrazole ligands and their metal complexes 54

Instrumentation 54

3.1   Synthesis of pyrazole ligands of compound 1 family 55

Chapter 5 Results and discussion of the synthesis of biphenyl sulfones and their fluorescent properties

Chapter 6 Experimental for the synthesis of biphenyl sulfones

Abstract

As a result of the evolution of antimicrobial resistant bacteria there is a pressing need for novel classes of antibiotics. This project aimed, in part, to design and synthesise a new family of pyrazole ligands, their zinc(II) complexes and to evaluate their antmicrobial activity. The overall goal was to improve the antimicrobial activity of both ligand and metal salt through the formation of the corresponding zinc complex. The first pyrazole ligands synthesized were unable to coordinate with zinc(II) salts. We believe this was due to steric hindrance generated by the relatively large pyrazaole ligands. Several smaller pyrazole ligands were synthesized, some of which successfully complexed with zinc suggesting that steric hindrance had indeed been a factor for the first set of ligands. A family of zinc complexes were generated employing the family of smaller pyrazole liagnds. All the pyrazole-zinc complexes, pyrazole ligands and zinc salts were evaluated for activity against *S.aureus* and *E.coli*. Generally, the susceptibility test results showed that most pyrazole ligands did not exhibit potent activity against either *E. coli* or *S. aureus*. All of the zinc complexes exhibited good antibacterial activity against both *E. coli* and *S. aureus* at 100 μg/mL. As we had expected the zinc complexes greatly improved the antibacterial activity of the pyrazole ligands. However, most zinc complexes were as active as the zinc salts alone indicating that the addition of the pyrazole ligands did not improve the activity of the zinc salts.

Organosulfones are widely used in the field of pharmaceuticals and ploymers. Traditional methodologies for synthesizing biphenyl sulfones include Suzuki-Miyaura coupling, Friedel-Crafts and other multistep reactions. These methodologies require catalysts, solvents and some require long reaction times. We have developed a novel solvent-free methodology for synthesizing fluorescent biphenyl sulfones with a relatively short reaction time and in good yields. This methodology exploits an interesting electrocyclisation of bissulfonyl trienes. A new family of substituted biphenyl sulfones resulted. UV-absorption, emission and excitation spectra were generated for the family of biphenyl sulfones and their photophysical characterisitics studied (e.g. Stokes shift, quantum yield, molar extinction coefficients). The biphenyl sulfones with NO_2 substituents did not exhibit fluorescence due to the strong electron withdrawing nature of the NO_2 group. Other substituted biphenyl sulfones exhibited highly solvatochromic emissions, probably via twisted intramolecular charge transfer (TICT) states. The biphenyl N,N-dimethyl-4'-(phenylsulfonyl)-[1,1'-biphenyl]-4-amine was found to show a very high quantum yield in toluene and dichloromethane (Φ close to 0.9); large Stokes shifts and high molar extinction coefficient in ethylene glycol ($\varepsilon > 80\ 000\ M^{-1}cm^{-1}$). The HOMO-LUMO gaps of a family biphenyl sulfones were plotted against their Stokes shifts (in chloroform) giving an excellent linear correlation ($R^2 = 0.9978$). These results suggested that the underlying photophysical processes are similar for all our biphenyl sulfones, where stronger electron donating groups generate smaller HOMO-LUMO gaps and red-shifted emissions, as compared to weaker electron donating groups.

List of abbreviations

Anal. Calc.	Analytical calculation
Ar	Aryl
Br	Broad
t-Bu	*tert*-Butyl
$CDCl_3$	Deuterated chloroform
cm	Centimetre
cm^{-1}	Wavenumbers
d	Doublet
℃	Degrees Celsius
dd	Doublet of doublets
Δ	Reflux temperature
δ	Chemical shift
DMF	N,N-Dimethylformamide
D_6-DMSO	Deuterated dimethyl sulphoxide
dt	Doublet of triplets
ESI	Electrospray ionization
EtOH	Ethanol
E_T^{30}	Reichardt's solvent plarity parameter
FTIR	Fourier Transform Infrared
FDA	The U.S. Food and Drug Administration
HCl	Hydrochloric acid
HOMO	Highest occupied molecular orbital
HOBT	Hydroxybenzotriazole
Hz	Hertz
J	Coupling constant
KBr	Potassium bromide
KOH	Potassium hydroxide
λ	Wavelength (nm)
LUMO	Lowest unoccupied molecular orbital
M	Molar
m	Multiplet
Me	Methyl
MeOH	Methanol
MeCN	Acetonitrile
MIC	Minimium inhibitory concentration

MIC_{50}	The minimium inhibitory concentration that results in a 50 % kill
MIC_{100}	The minimium inhibitory concentration that results in a 100 % kill
min	Minute
mL	Millilitre
mmol	Millimole
m.p.	Melting point
μL	Microlitre
NMR	Nuclear magnetic resonance
nm	Nanometre
ppm	Parts per million
q	Quartet
s	Singlet
t	Triplet
TBTU	*O*-(Benzotriazol-1-yl)-*N,N,N,N*-tetramethyluronium tetrafluoroborate
TICT	Twisted intramolecular charge transfer
UV/vis	Ultraviolet/visible
Φ	Quantum yield
Cca	coumarin-3-carboxylate

Chapter 1: Introduction to the synthesis of pyrazole ligands, their metal complexes and evaluation of their antibacterial activity

1.1 A brief history of antimicrobial agents

Antimicrobial agent is a general term that refers to a group of drugs including antibiotics, antifungals, antiprotozoals, and antivirals. In recent time, the resistance of bacteria has grown worldwide and is driving the demand for the development of novel antimicrobial agents. The first antimicrobial agent was salvarsan, which was synthesized by a German doctor, Ehrlich, in 1910. Salvarsan was used as a therapy for syphilis and showed low toxicity levels. This discovery opened what is known as the century of antimicrobial chemotherapy. The second class of synthetic antimicrobial agents developed were the sulfonamides. The first sulfonamide drug, Prontosil, was invented by Domagk in 1935, and was found to be active against *Streptococcus pyogenes*.[1,2]

Alexander Fleming discovered penicillin in 1928, when he found that the growth of *Staphylococcus aureus* was inhibited around a contaminated growth of blue mold. This indicated that a substance produced by the microorganism was able to inhibit the growth of *Staphylococcus aureus*. Due to the lack of suitable technology, the active substance, penicillin, was not identified until the 1940s when Chain Ernst Boris and Howard Walter Florey, and their group, extracted and purified penicillin, for the first time. Penicillin was successfully put into clinical use in the 1940s and saved the lives of many wounded soldiers in World War II.[3] The structure of penicillin was subsequently modified generating methicillin and ampicillin in the 1960s, which have broader antibacterial activity spectrums.[4]

In 1943 streptomycin was isolated from the soil bacterium *Streptomyces griseus* by a graduate student, Albert Schatz, in the laboratory of Selman Abraham Waksman at Rutgers University.[1, 5] Streptomycin was used for the treatment of tuberculosis. After that, chloramphenicol was isolated by David Gottlieb from the bacterium *Streptomyces venezuelae* and introduced into clinical practice in 1949. The tetracyclines were discovered as natural products by Benjamin Minge Duggar in 1945 and prescribed in 1948. Macrolides and aminoglycosides were discovered in the 1950s and glycopeptides in 1956. Nalidixic acid was the first synthetic quinolone antibiotic and was discovered by George Lesher as a byproduct of chloroquine manufacture in the 1960s. Nalidixic acid was put into clinical use from 1967 but was only active against Gram-negative bacteria and its use was limited to the treatment of urinary tract infections.[1,6] The cephems, including cephalosporins and cephamycins were developed in 1960s.[1,7]

Modern antimicrobial agent development involves many lines of research: not only is an excellent antibacterial spectrum and excellent efficacy required but also excellent pharmacokinetic and safety profiles. For example: nalidixic acid, the first class of synthetic quinolone antibiotic, as previously described, was limited to the treatment of urinary tract infections. This was a result of its low blood concentration, poor distribution and fast metabolism in the human body. A late generation quinolone, norfloxacin had improved pharmacokinetic properties, good tissue distribution and was more metabolically stable. It also had a broader antibacterial spectrum and was active against both Gram-positive and Gram-negative bacteria.[1] A second example can be found with the cephalosporins. Cephcephaloglycin, a first-generation cephalosporin antibiotic, was metabolized quickly, and required a high blood concentration to function well. A late generation cephalosporin, cefalexin, had much improved pharmacokinetic properties with a superior oral-bioavailability and was more metabolically stable.

1.2 Antimicrobial agents

There are four main classes of antimicrobial agents based on their mechanism of reaction, 1) the agents that inhibit bacterial cell wall biosynthesis, 2) the agents that inhibit protein biosynthesis, 3) the agents that inhibit deoxyribonucleic acid (DNA) or ribonucleic acid (RNA) synthesis, 4) the agents that inhibit folate synthesis.[8]

1.2.1 Agents that inhibit bacterial cell wall biosynthesis

In regard to antimicrobial development the cell wall is one of the most important compositions in bacteria cells as it is not found in mammalian cells. As a result, bacterial cell wall biosynthesis is a promising and exploited target for antimicrobial chemotherapy. The β-lactams and glycopeptides are two families of antimicrobial agents, whose activity is derived from their ability to inhibit bacterial cell wall biosynthesis.[9]

1.2.1.1 β-Lactams

The bacterial cell wall is formed through transpeptidation reactions which are catalyzed by peptidoglycan transpeptidases.[10] β-Lactam antibiotics inhibit the growth of bacteria by the covalent binding to the active site of peptidoglycan transpeptidases (penicillin binding proteins), which catalyze the transpeptidation reactions. As a result, the transpeptidation reactions cannot occur, leading to the inhibition of bacterial cell biosynthesis and cell death.[11]

Penicillin was discovered by Alexander Fleming, also called penicillin G, and was the first antibiotic applied to clinical use.1 It was effective against Gram-positive organisms and since it was first discovered its structure has been modified greatly in order to improve its potency, oral bioavailability, antibacterial spectrum of activity, and to decrease its sensitivity to β-lactamases. These modifications generated methicillin, ampicillin and piperacillin, **Figure 1.1.1**. Methicillin was developed by Beecham in 1959,[4] with decreased sensitivity to β-lactamases. The replacement of two hydrogen atoms by two methoxy groups on the *ortho* position of the phenyl ring introduced additional steric hindrance and protected the β-lactam ring from being cleaved by β-lactamases. Ampicillin has broader antibacterial spectrum of activity when compared to penicillin G. This additional activity stemmed from the inclusion of an amino group on the amide side chain and was essential for activity against Gram-negative bacteria. Piperacillin also showed improved potency and decreased sensitivity to β-lactamases resulting from the modification of the amino group on the amide side chain.

Cephalosporin compounds were first isolated from cultures of *Cephalosporium acremonium* found in a sewer in Sardinia in 1948 by Italian scientist Giuseppe Brotzu.[1] The cephalosporins were applied to clinical use in 1960s and are active predominantly against Gram-positive organisms. Thousands of derivatives have been made since then, and successive generations have increased activity against Gram-negative organisms. The first generation of cephalosporins was active against Gram-positive organisms and *Escherichia Coli*. The second generation of cephalosporins had decreased sensitivity to β-lactamases, and an extended antibacterial spectrum. They were active against both Gram-positive and Gram-negative organisms. The third generation of cephalosporins improved their efficacy against Gram-negative bacteria, but their antimicrobial activity against Gram-positive organisms was generally lower than first generation. They had broader antibacterial spectrum and decreased sensitivity to β-lactamases compared to the second generation. The fourth generations of cephalospoins are zwitter ions that can penetrate the outer membrane of Gram-negative bacteria, and they also showed improved resistance to β-lactamases compared to the third generation.[12] The core structure of cephalosporins is shown in **Figure 1.1.2**. Together with cephamycins, which are very similar to the cephalosporins, they constitute a subgroup of β-lactam antibiotics called cephems.
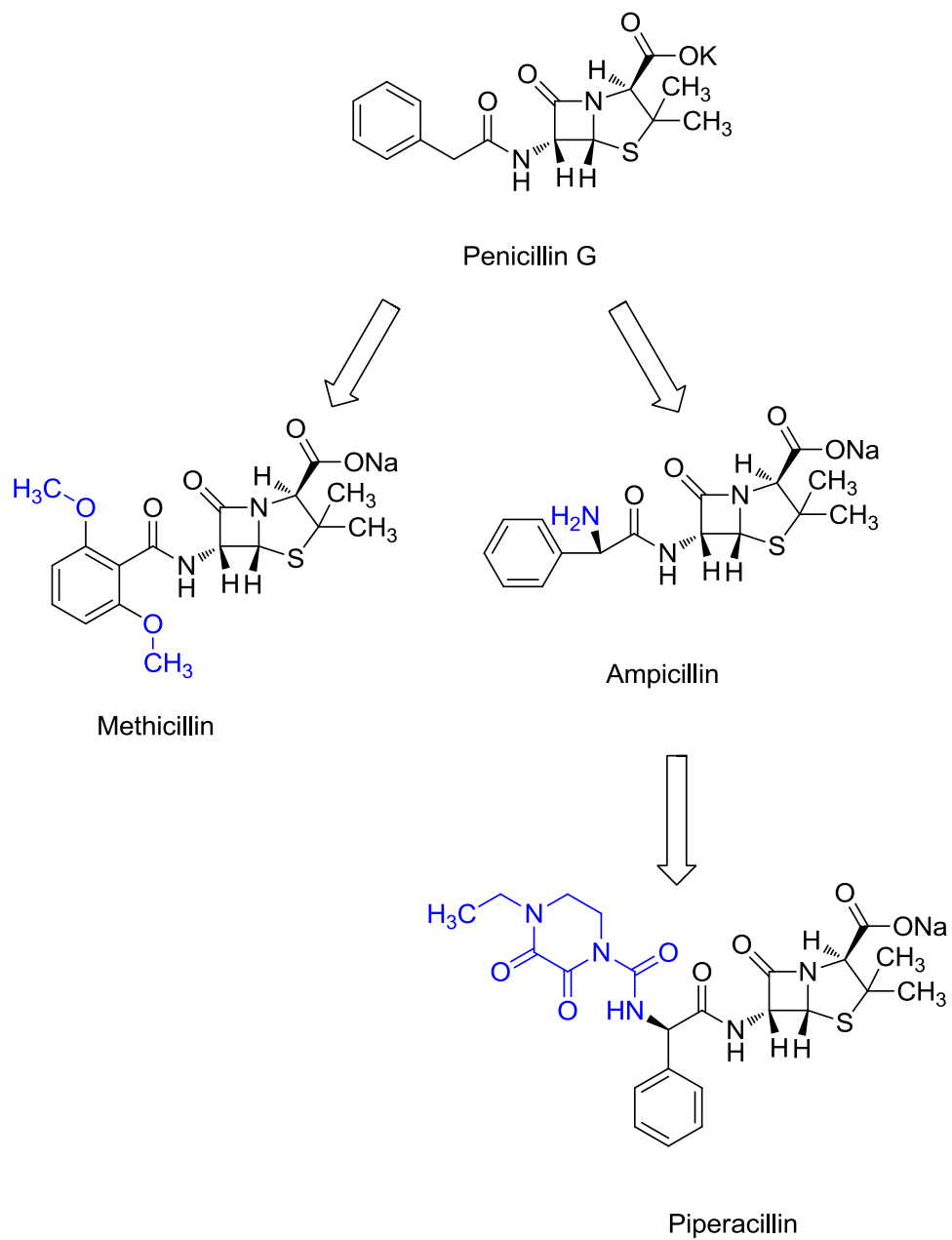
Figure 1.1.1 Penicillin structures
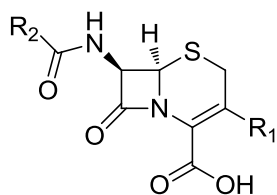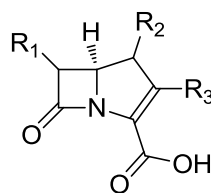
Core structure of cephalosporins   Core structure of carbanpenems backbone

Figure 1.1.2 Core structures of cephalosporins and cabapenems

Carbapenems, which include imipenem (FDA approved in 1985),[13] panipenem (Japanese approval 1993) and meropenem (FDA approval 1996), were the last resort treatment for many bacterial infections.[14] The unsaturated pentacyclic ring structure attached to the core β-lactam structure made them highly resistant to β-lactamases,[15] but they exhibited low bioavailability.[16] Bacterial resistance to the carbapenems has been growing since the appearance of the New Delhi metallo-β-lactamase, "NDM-1" in India.[17] The core structure of a carbapenem is shown in **Figure 1.1.2**.

Monobactams are compounds whose β-lactam ring is not fused to another ring. They are only active against Gram-negative organisms, and the only commercially available monobactam is Aztreonam, **Figure 1.1.3**. Aztreonam was approved by the FDA in 1986. It is resistant to some β-lactamases and only highly active against susceptible Gram-negative bacteria including *Pseudomonas aeruginosa*.[18]
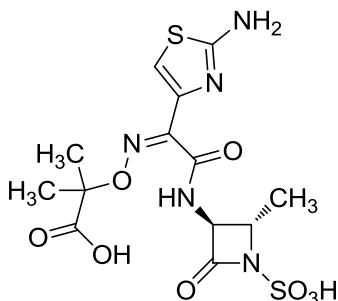
Aztreonam

Figure 1.1.3 Structure of Aztreonam

1.2.1.2 Glycopeptide antibiotics

Glycopeptide antibiotics are a class of antibiotics composed of glycosylated cyclic or polycyclic nonribosomal peptides, which exhibit excellent activity against Gram-positive

bacteria, especially methicillin-resistant *Staphylococcus aureus*.[19] These antibiotics inhibit the growth of bacteria by crossing the bacterial cell wall of Gram-positive bacteria, and binding to the terminal acyl-D-alanyl-D-alanine of the peptidoglycan precursor. As a result, transpeptidation reactions are blocked due to the introduced steric hindrance, and subsequently the biosynthesis of the bacteria cell wall is inhibited.[8] Significant glycopeptide antibiotics include vancomycin, teicoplanin, and bleomyin. Vancomycin, **Figure 1.1.4**, was the first glycopeptide antibiotic and was isolated from a soil sample collected in the interior jungles of Borneo by Edmund Kornfeld (Eli Lilly) in 1953.[20]

Figure 1.1.4 Structure of Vancomycin

1.2.2 Agents that inhibit protein biosynthesis

These agents act by blocking one or more steps of protein biosynthesis, which occurs on 30S or 50S ribosomal subunits. For example, streptomycin binds to the small 16S rRNA of 30S subunits of the bacterial ribosome, interfering with the binding of formyl-methionyl-tRNA to the 30S subunit, which leads to codon misreading, and inhibiting protein synthesis.[21] The major families of these protein biosynthesis inhibitors are aminoglycosides, macrolides, and tetracylines.

Antibiotic aminoglycosides found use primarily against infections involving aerobic, Gram-negative bacteria, such as *Pseudomonas*, *Acinetobacter* and *Enterobacter*. The most frequent use of aminoglycosides was empiric therapy for serious infections such as

septicemia, complicated intra-abdominal infections, complicated urinary tract infections and nosocomial respiratory tract infections. They have also been used in combination with β-lactam antibiotics to treat some Gram-positive bacteria. The most common β-lactam antibiotic used in combination with aminoglycosides is ampicillin.[22] Streptomycin, **Figure 1.1.5**, was the first in the class of aminoglycosides. It was isolated from soil bacterium *Streptomyces griseus* in the laboratory of Selman Abraham Waksman at Rutgers University by Albert Schatz in 1943.[5]
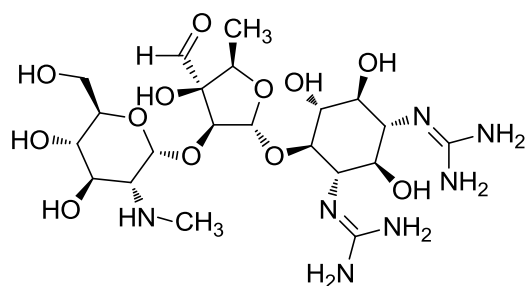
Figure 1.1.5 Structure of Streptomycin

Antibiotic macrolides are active against Gram-positive bacteria, have relatively broad spectrum of antimicrobial activity and newer macrolide agents continue to be developed. Erythromycin, **Figure 1.1.6**, was the first macrolide and was isolated from the metabolic products of a strain of *Streptomyces erythreus* by J. M. McGuire (Eli Lilly). Erythromycin has been used since the early 1950s.[23] Ketolides, a subfamily of macrolides, are used to treat respiratory tract infections caused by macrolide-resistant bacteria. Telithromycin, **Figure 1.1.6**, the first ketolide antibiotic for clinical use, was reached the market (Germany and Spain) as Ketek late in 2001.[24]

Erythromycin
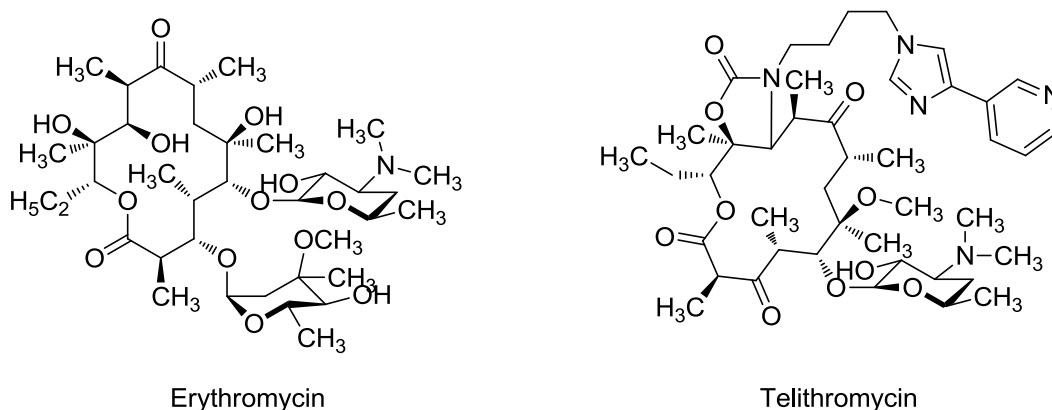
Telithromycin

Figure 1.1.6 Structures of Erythromycin and Telithromycin

15

Antibiotic tetracyclines are considered to be broad-spectrum antibiotics, but due to their side effect, they are rarely choosen as a treatment.[25] The first member of tetracyclines was chlortetracycline, **Figure 1.1.7**, and was discovered by Benjamin Duggar who isolated the substance from *Streptomyces aureofaciens* in 1945.[26]
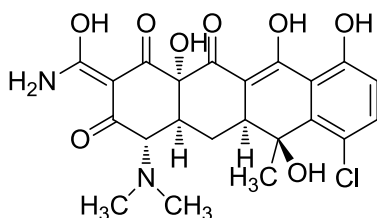
Figure 1.1.7 Structure of Chlortetracycline

1.2.3 Agents that inhibit deoxyribonucleic acid (DNA) or ribonucleic acid (RNA) synthesis

There are two main families of antibiotics that inhibit DNA and RNA synthesis, the quinolone and rifampicin familes. Quinolones were a family of synthetic broad-spectrum antibiotics. They act by binding to the bacterial DNA gyrase or topoisomerase IV, and prevent DNA from unwinding and duplicating, thereby inhibiting biosynthesis of DNA.[22] Nalidixic acid was the first quinolone antimicrobial agent synthesized by George Lesher in 1960s,[1,6] and was only active against Gram-negative bacteria. Since nalidixic acid achieves only low blood concentration, poor distribution and is rapid metabolism, it was limited to the treatment of urinary tract infections. Quinolones were not widely used until the discovery of fluoroquinolones in 1980s.[27] Norfloxacin, which came to market in 1984, had improved pharmacokinetic properties e.g. good tissue distribution and was more metabolically stable. It also had a broader antibacterial spectrum and was active against both Gram-positive and Gram-negative bacteria.[1] Levofloxacin, which is described as a third-generation fluoroquinolone, is the enantiomer of ofloxacin (a second-generation fluoroquinolone) and exhibits higher antimicrobial activity and weaker side effects.[1,28]
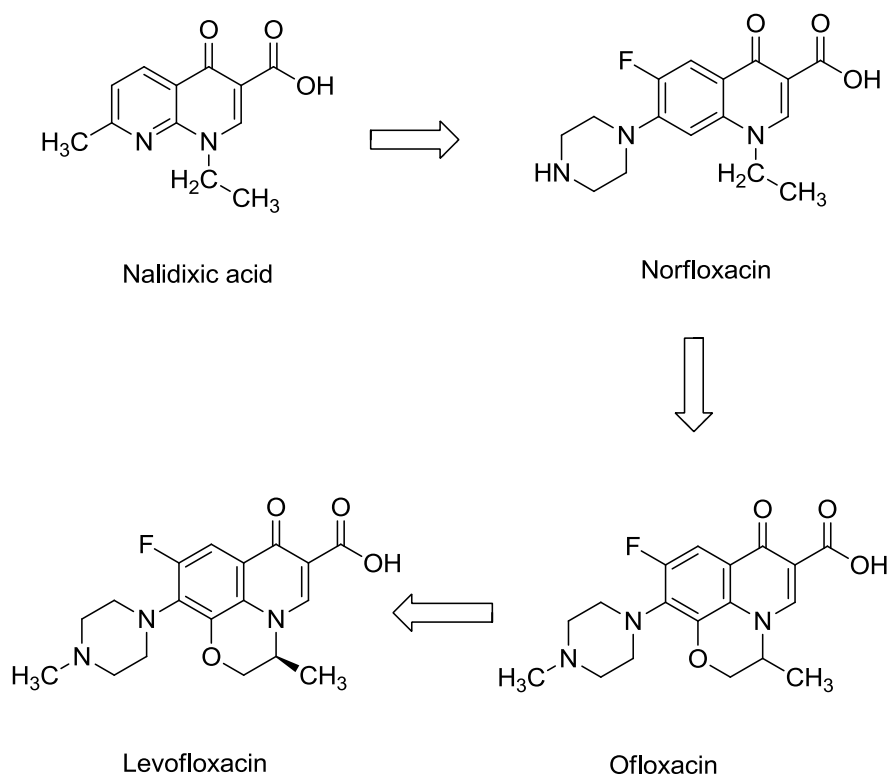
Figure 1.1.8 Evolution of quinolone antimicrobials

Rifamycins were first isolated from a fermentation culture of *Streptomyces mediterranei* by Piero Sensi and Maria Teresa Timbal in 1957.[22] They act by binding to the β-subunit of DNA-directed RNA polymerase thus inhibiting the initiation of chain formation in RNA synthesis.[22] Rifamycins were widely used for the treatment of many diseases, and have been widely used in the treatment of pathogenic bacteria that have become resistant to commonly used antibiotics. Of all the rifamycins discovered, rifamycin B, **Figure 1.1.9**, was the first to come to the market in 1958 and it was widely used for the treatment of drug-resistant tuberculosis.[29]
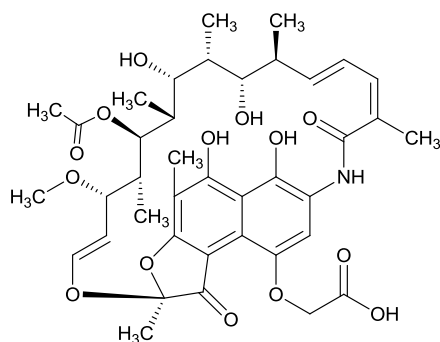
Figure 1.1.9 Structure of Rifamycin B

1.2.4 Agents that inhibit folate synthesis

Folate is very important to the survival of all living organisms, as it serves as the source of methyl, formyl and other single carbon fragments in the biosynthesis of purine nucleotides in DNA synthesis.[30] The way human and bacteria obtain folate is very different. Humans obtain folate through their diet, while bacteria obtain folate through biosynthesis. This makes folate a very attractive target for antimicrobial chemotherapy.[31] There are two enzymes that are targeted: dihydropeteroate (DHPS), an enzyme which sulfonamides act on, and dihydrofolate reductase (DHFR), an enzyme which trimethoprim act on, **Figure 1.2.1**. Sulfonamides inhibit DHPS, which catalyzes the conversion of p-aminobenzoic acid (PABA) to dihydroteroate.[32] Trimethoprim inhibit DHFR which converts dihydrofolate into tetrahydrofolate.[33] Most of the sulfonamide drugs are no longer in use, as bacteria rapidly acquire resistance to them. One of the most commonly used sulfonamides was sulfamethoxazole, **Figure 1.2.1**, which was often used in combination with trimethoprim. This combination was primarily active against *Streptococcus*, *Staphylococcus aureus*, *Escherichia coli* and *Haemophilus influenzae* amongst others.[34]

Folate

Sulfamethoxazole   Trimethoprim
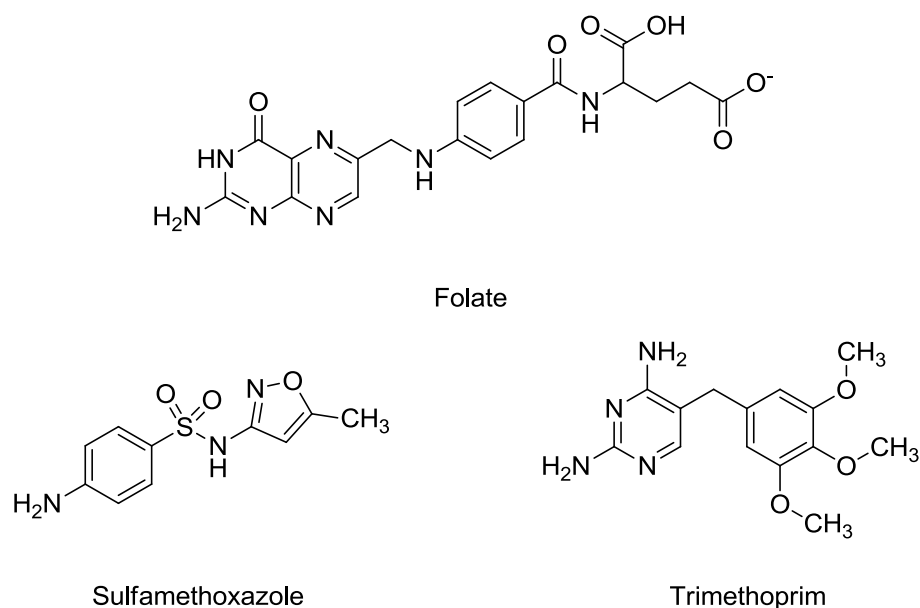
Figure 1.2.1 Structure of folate, sulfamethoxazole and trimethoprim.

1.2.5 Zinc metallotherapeutics

Zinc containing compounds have been reported to have antimicrobial activity, e.g. metal-containing thin films have been incorporated into wound dressings or on surfaces to kill microbes and bacteria in the UK. Andrew Johnson, at the University of Bath, created such a thin film by synthesizing zinc and copper Schiff-base complexes. The zinc complex was found to be particularly successful, and exhibited very high activity against *Staphylococcus aureus* and *Pseudomonas aeruginosa*, **Figure 1.2.2**.[35]
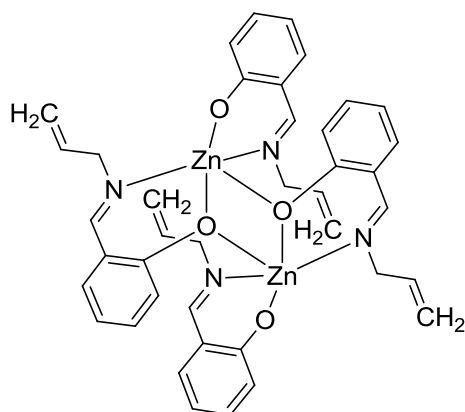
Figure 1.2.2 Structure of Johnson's zinc complexes.[35]

A pyrazole-zinc complex has been reported by Naveen V. Kulkarni in India and is active against *E.coli* and *Pseudomonas aeruginosa*, **Figure 1.2.3**.[46] The mechanism through which zinc produces its antimicrobial effect was unknown until a possible mechanism was proposed by Christopher A. McDevitt in 2011.[36] This report discussed how manganese was found to be essential for the growth and virulence of *Streptococcus pneumoniae*. Zinc was found to be able to prevent manganese uptake and thereby inhibit the bacterial growth.[36]
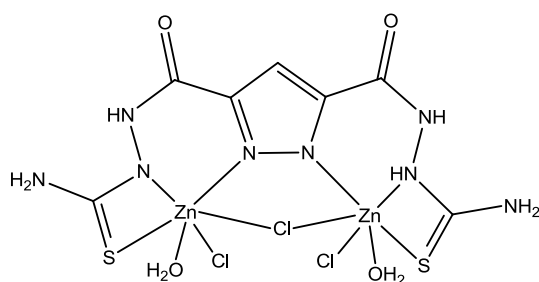
Figure 1.2.3 Structure of pyrazole-zinc complex[46]

An enaminone-zinc complex, **Figure 1.2.4**, has been reported by Tariq Mahmud. The enaminone-zinc complex was tested against bacteria using the disc-diffusion method. They reported the enaminone-zinc complex was very active against *E.coli* and active against *S.aureus*.[37]
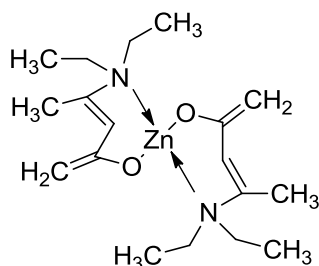
Figure 1.2.4 Structure of Enaminone-zinc complex[37]

A Zn(II) complex with *N*-heteroaromatic Schiff base ligands, **Figure 1.2.5**, exhibiting antibacterial activity has been reported by *Nenad R. Filipovi*. This zinc complex was also tested against bacteria using the disc-diffusion method. The zinc complex exhibited relatively strong activity against *G. stearothermophilus*, showing a zone of inhibition of 16 mm. Chloramphenicol was used as a standard and which showed a zone of inhibition of 19 mm.[38]
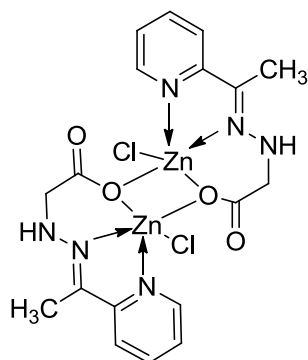
Figure 1.2.5 Structure of *Nenad R. Filipovi*'s zinc complex[38]

Another example of a zinc complex exhibiting antibacterial activity can been found in the work of Ajay K. Singh. Here the zinc complexes were synthesized by reacting zinc acetate with Schiff base ligands. The antibacterial activity of these zinc complexes were measured in three terms: percentage inhibition, minimum inhibitory concentration and zone of inhibition (mm). The most active zinc complex, **Figure 1.2.6**, inhibited 45.4 % growth of *E. coli* at 10 μg/mL; 59.1 % growth at 100 μg/mL and 70.9 % growth of *E.coli* at 200 μg/mL. The paper concluded that the complexation of the zinc with the Schiff base increased the antibacterial activity.[39]
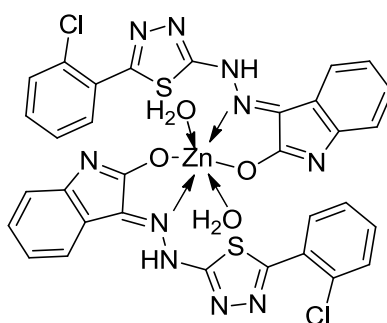
Figure 1.2.6 Structure of Ajay K. Singh's most potent zinc complex[39]

Zinc salts themselves also exhibit excellent antimicrobial activity. Umaira Faiz reported zinc sulfate inhibited the growth of a total of 100 bacterial enteric pathogens (for example, *E.coli*, *Salmonellae*, *Vibrio cholera*, etc) and most of the bacteria were inhibited at a concentration of 0.06 mg/mL to 0.5 mg/mL of zinc.[40]

Other metals are also reported to have antimicrobial activity. Silver containing compounds are very toxic to microorganisms, e.g. Ag(I) complexes of hydroxy-substituted coumarin carboxylates as developed by Bernadette S. Creaven and co-workers at the Institute of Technology, Tallaght. These silver complexes exhibited both antibacterial and antifungal activities against methillin-resistant *Staphylococcus aureus* and *Candida albicans*. Of these silver complexes [Ag(Cca)], **Figure 1.2.7**, is the most potent.[41] These silver complexes mainly act against fungal pathogens by disrupting the cytochrome synthesis, inhibiting respiration, reducing ergosterol biosynthesis and increasing the membrane permeability.[42] Copper containing compounds have also been report to have antimicrobial activity, e.g. copper complexes of N- (butyl(ethyl)carbamothioyl)-4-nitrobenzamide, **Figure 1.2.8**. This copper complex is reported to have high antibacterial activity against the Gram-positive bacteria, *Staphylococcus aureus* and *Staphylococcus epidermidis*.[43]
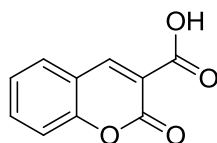
Figure 1.2.7 Structure of the Cca ligand[41]
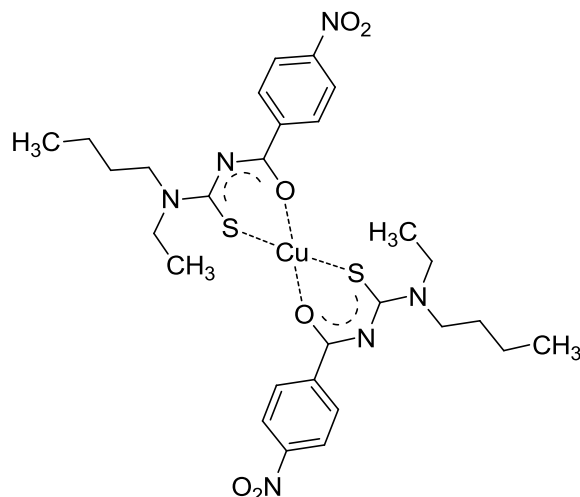
Figure 1.2.8 Structure of copper complex of
N-(butyl(ethyl)carbamothioyl)-4-nitrobenzamide[43]

1.3 The need for novel antimicrobial agents

In recent times the widespread emergence of bacterial resistance to antimicrobial agents, many of which were developed in the twentieth century, is causing great concern particularly when one couples this with the paucity of new antimicrobial drugs. Some scientists have predicted a return to a pre-antibiotic era and a looming medical disaster.[44]

Microorganisms exhibit resistance to antimicrobial agents by four main mechanisms: 1) drug inactivation or modification, 2) alteration of target site, alteration of metabolic pathway, 3) reduced drug accumulation, 4) preventing the penetration of the penicillins into the cell by building a permeability barrier. For example, bacteria build resistance to penicillins by 1) cleavage of the β-lactam ring by β-lactamases or penicillinases, 2) reduce the target affinity to penicillins by alter the PBPs (penicillin binding proteins).[45]

Due to the capacity of bacteria to acquire resistance to antimicrobial agents, some formerly effective antimicrobial agents are no longer useful. For example, most sulfonamides antibiotics are no longer effective as bacteria rapidly acquired resistance to them. Penicillin G was initially effective against *Staphylococcus aureus*, but resistant strains producing penicillinase have developed. The penicillinase-stable penicillin, methicillin, was developed to combat this but soon methicillin-resistant *Staphylococcus aureus* was isolated. Since 1990s,

nosocomial infection or hospital-acquired infection with methicillin-resistant *Staphylococcus aureus* has become a significant problem.

As a result there is a pressing need to discovery new antimicrobial agents to fight this emergence of antimicrobial resistance.

1.4 Project aims for antimicrobial section

This project, in part, aims to 1) synthesize and fully characterize a number of pyrazole/pyrazole-thiourea ligands, 2) use these ligands to generate novel zinc-pyrazole complexes and have them fully characterized; 3) evaluate the antibacterial activity of ligands and the zinc complexes against *E.Coli* (Gram-negative bacteria) and *Staphylococcus aureus* (Gram-positive bacteria).

Chapter 2 Results and Discussion of the synthesis of pyrazole ligands, their metal complexes and the evaluation of their antibacterial activity

2.1 Introduction

We decided to focus our work on pyrazole derivatives for several reasons. They are versatile ligands and can coordinate with many transition metal ions. Furthermore, the nucleophilicity and steric accessibility of pyrazole nitrogens can be altered by appropriate ring substitutions, allowing one to tailor their structure to suit metal complex formation. Pyrazoles are also relatively easy to synthesize and derivatize and have reported antimicrobial activity.[46] We initially focused on zinc as the metal for our complexes as it has reported antimicrobial activity and it is NMR friendly and hence the complexes are easier to characterize (compared to using paramagnetic metals e.g. copper).[35]

2.2 Synthesis of pyrazole ligands and their zinc (II) complexes

The first pyrazole we decided to synthesize was compound **1**, **Figure 2.1.1**.
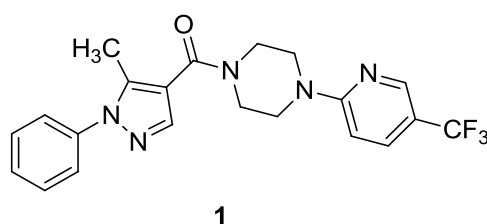
Figure 2.1.1 Structure of **1**

This pyraozle had been made previously in our research group and was relatively easy to synthesize. **1** was prepared following the steps shown in **Figure 2.1.2**.
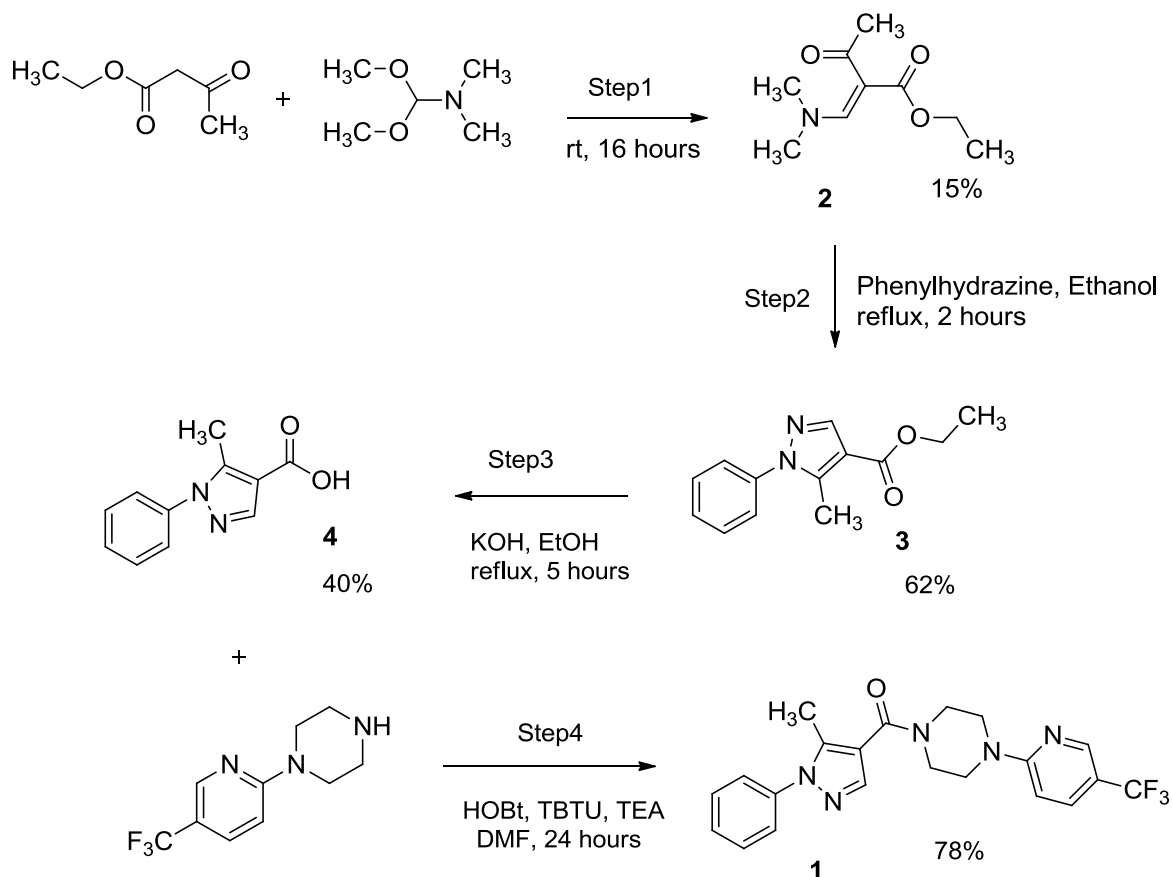
Figure 2.1.2 Synthesis of **1**

In step 1, ethyl acetoacetate and N,N-dimethylformamide dimethylacetal were stirred at room temperature for 16 hours generating **2**. Compound **2** was purified using flash chromatography and its structure confirmed by a singlet with an intergration of 6H at 3.04 ppm in the ^{1}H NMR spectrum, indicating the presence of the (CH_3)$_2$NCHC moiety and a singlet with an intergration of 1H at 7.69 ppm also indicating the presence of the (CH$_3$)$_2$NCHC moiety. The ^{1}H NMR spectrum also shows a quartet at 4.23 ppm and a triplet at 1.32 ppm indicating the presence of the ethyl group. A singlet at 2.33 ppm indicated the presence of the C(O)CH_3 moiety.

In step 2, **2** and phenyl hydrazine were refluxed in ethanol for 2 hours generating **3**. Compound **3** was purified using flash chromatography and its presence was confirmed by a singlet in ^{1}H NMR spectrum at 8.03 ppm indicating the CH of pyrazole. A multiplet in the ^{1}H NMR spectrum at 7.52 – 7.39 ppm, with an intergration for 5H, indicated the presence of the aromatic ring. A triplet in the ^{1}H NMR spectrum at 1.37 ppm and a quartet in the ^{1}H NMR at 4.32 ppm indicated the presence of ethyl group.

In step 3, **3** and potassium hydroxide were refluxed in ethanol for 5 hours generating **4**. Compound **4** was used without further purification and its presence confirmed by the disappearance, in the ^{1}H NMR spectrum, of the triplet at 1.37 ppm and the quartet at 4.32 ppm.

Step 4 required that **4** was treated with 1-(5-trifluoromethyl-2-pyridinyl) piperazine and the coupling reagent HOBT and TBTU, in dry DMF under nitrogen for 24 hours. The structure of the final product **1** was confirmed by a singlet in the ^{1}H NMR spectrum at 8.43 ppm indicating the presence of C*H* of pyrazole, a multiplet with integration of 8H at 3.88 – 3.73 ppm for the piperazine C*H*$_2$. The ^{13}C NMR spectrum CF$_3$ signal at 124.4 ppm showed the expected splitting, quartet, and a coupling constant of 268.5 Hz. The *C*CF$_3$ quartet in the ^{13}C NMR spectrum appeared at 115.9 ppm with a coupling constant of 33.0 Hz. The structure of compound **1** was supported by HRMS and IR spectroscopy, C=O stretch at 1626 cm^{-1}. A proposed mechanism for the generation of **1** is shown in **Figure 2.1.3 (a)** and **(b)**.

Step 1:
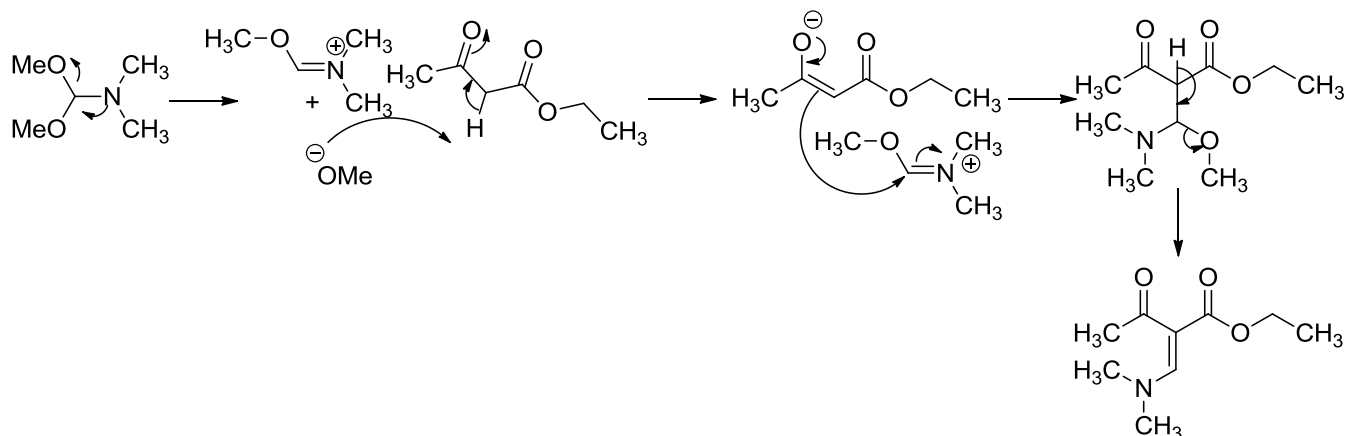
Steps 2 & 3:
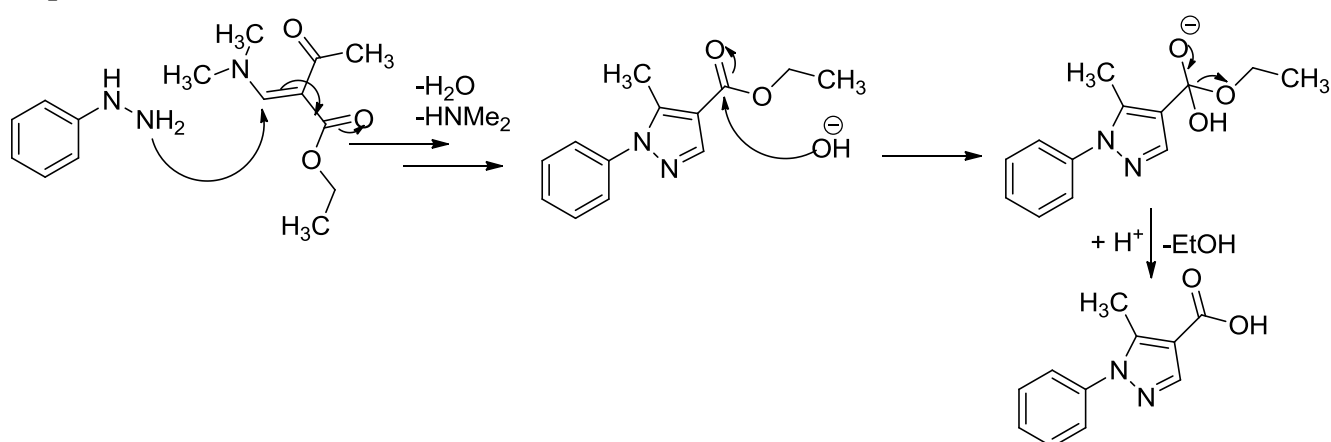
Figure 2.1.3 (a) Proposed mechanism for the generation of **1**, steps 1-3.

Step 4:
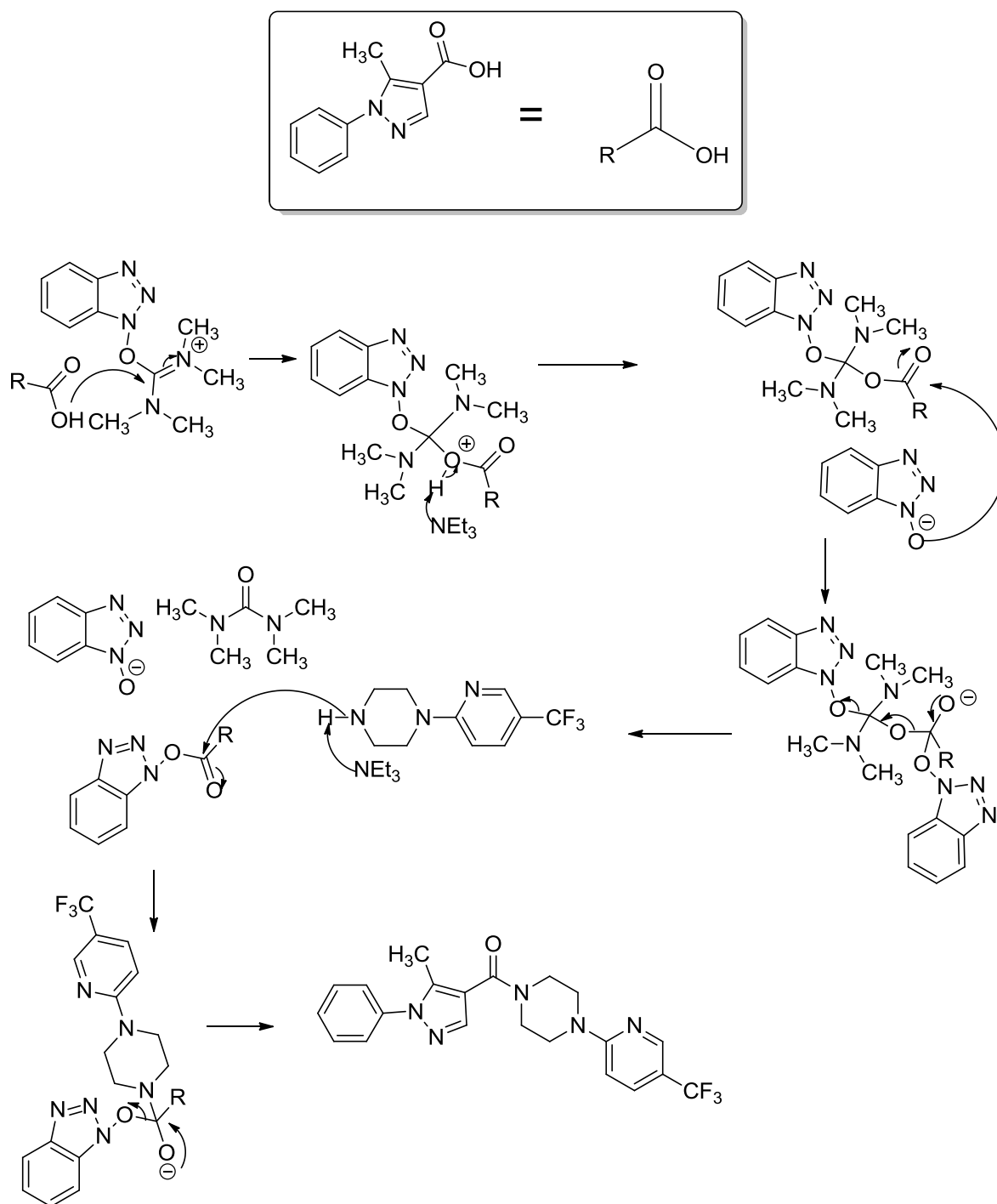
Figure 2.1.3 (b) Proposed mechanism for the generation of **1**, step 4

A family of **1** analogues was then synthesized following the same methodology as used for **1**, **Table 1.1**. The intermediates synthesized during the synthesis of **1** family were shown in

Figure 2.1.4. For example, the ^{1}H NMR spectrum of **6** shows a triplet at 1.11 ppm, integrating to 3H, and a quartet at 2.89 ppm, integrating to 2H, indicating the presence of an ethyl group. The ^{13}C NMR spectrum of **6** shows a quartet at 124.5 ppm, with a coupling constant of 268.8 Hz, indicating the presence of the CF_3 and a quartet at 115.5 ppm, with a coupling constant of 32.5 Hz, indicating the presence of CCF_3. The ^{1}H NMR spectrum of **1** shows a multiplet at 7.70 – 7.66 ppm, with an integration of 3H, and a multiplet at 7.54 – 7.42 ppm, with an integration of 5H, indicating the aromatic systems. The ^{1}H NMR spectrum of **7** (XQ7) shows a multiplet at 7.56 – 7.42 ppm, with an integration of 7H, and a doublet at 6.96 ppm, with an integration of 2H, indicating the aromatic systems. Overall, aromatic proton integration of **1** is 8H while **7** is 9H, indicating the replacement of pyridine ring with the phenyl ring. The ^{1}H NMR spectrum of **8** shows a singlet at 2.42 ppm, integrating to 3H, indicating the presence of CH_3 and a singlet at 3.87 ppm, integrating to 3H, indicating the presence of the OCH_3. The structures of compound **5-9** were supported by HRMS and IR spectroscopy.
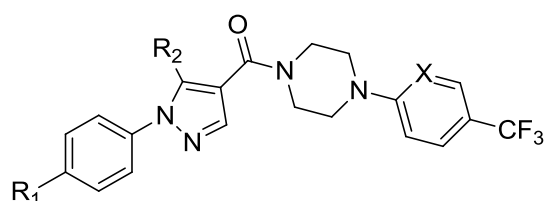
Product	R$_1$	R$_2$	X	Yield (%)*
1	H	CH$_3$	N	78
5	CF$_3$	CH$_3$	N	54
6	H	CH$_2$CH$_3$	N	33
7	H	CH$_3$	CH	60
8	OCH$_3$	CH$_3$	N	54
9	Cl	CH$_3$	N	62

Table 1.1 1-9, * yield of step 4.

10, R$_1$ = CF$_3$ R$_2$ = CH$_3$
11, R$_1$ = H   R$_2$ = CH$_2$CH$_3$
12, R$_1$ = OCH$_3$ R$_2$ = CH$_3$
13, R$_1$ = Cl   R$_2$ = CH$_3$
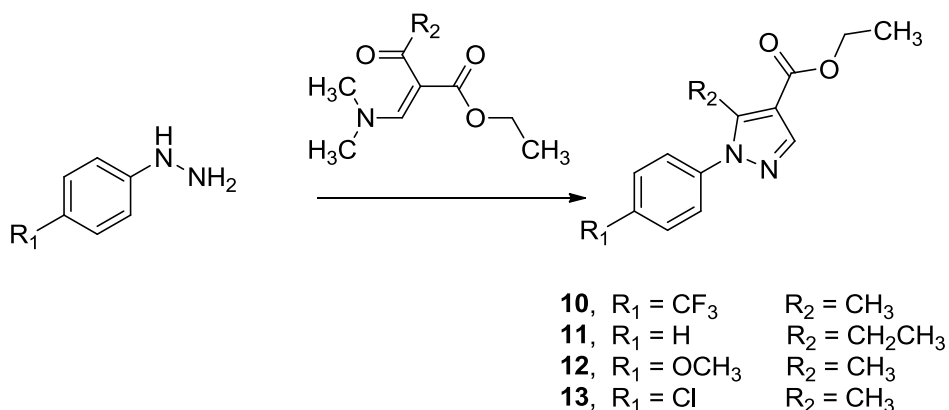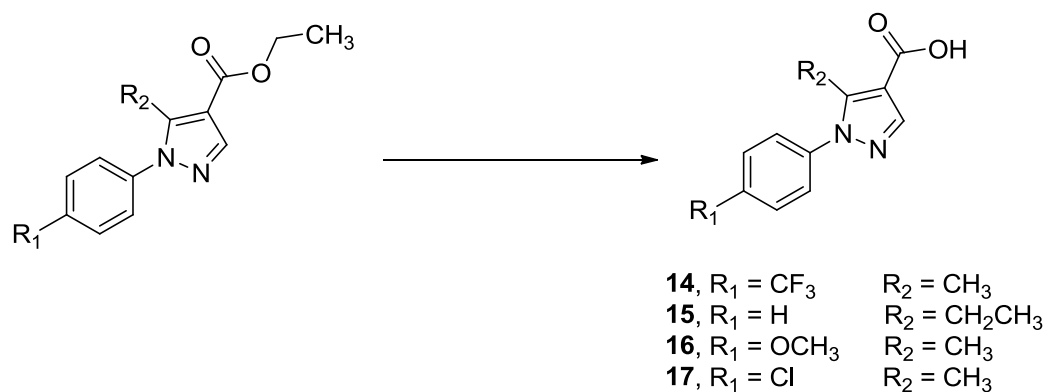
Figure 2.1.4 intermediates synthesized during the synthesis of **1** family

We then attempted to employ **1** and **7** as ligands in the synthesis of zinc complexes. **1** or **7** and zinc chloride were dissolved in methanol and refluxed for 2 hours, **Figure 2.1.5**. To determine whether complexation had occurred we compared the ^{1}H NMR shifts of the parent ligand and the product mixture.
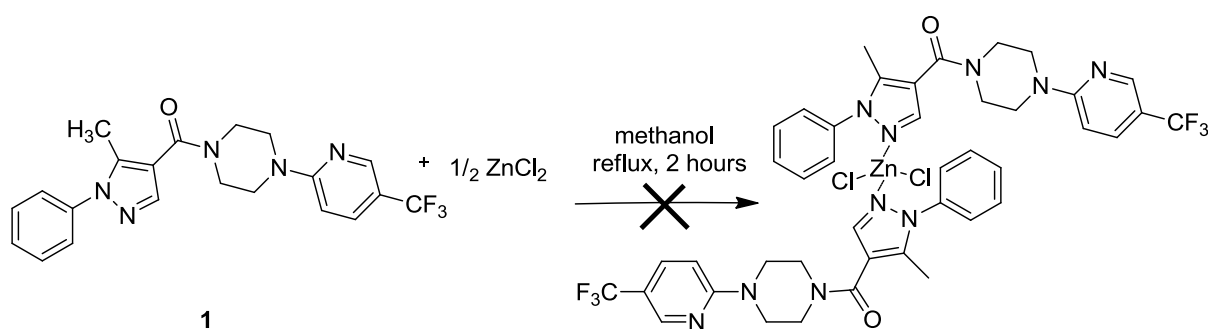
Figure 2.1.5 Attempted synthesis of **1** zinc complex

Unfortunately both **1** and **7** failed to coordinate with zinc, as indicated by the lack of a shift in the ^{1}H NMR spectra. We also attempted the complexation using different reaction times and with zinc acetate in place of $ZnCl_2$, **Table 1.2**. Complexation did not occur for any of the reactions attempted.

Ligand	Metal salt	Solvent	Time (hours)
1	$Zn(Cl)_2$	Methanol	2
7	$Zn(Cl)_2$	Methanol	2
1	$Zn(Cl)_2$	Methanol	5
1	$Zn(Cl)_2$	Methanol	16
1	$Zn(OOCCH_3)_2$	Methanol	2

Table 1.2 Attempted complexation reactions

We considered two reasons that may have contributed to the failed reactions: 1) complexation occurred in solution but the Zn-N bond was too weak to survive work up; 2) steric hindrance (ligand too bulky). We designed several experiments to explore these possible explanations.

1) We monitored the reaction by ^{1}H NMR in order that we could identify complexation if it were occurring in solution but not surviving work up. No evidence for complexation was observed.

2) We explored the steric effect by designing and synthesizing less hindered pyrazole ligands and employed them in complexation reactions with zinc.

A series of less hindered but related pyrazole ligands were designed and synthesized. Compounds **7**, **18**, **19**, **20** and **21** were synthesized using the same methodology as for **1** with one change at step 4, **Figure 2.1.2**. Changing the piperzine/amine in step 4 allowed for the synthesis of the new ligands, **Table 1.3**. Compound **3** had already been prepared during the synthesis of **1**, **Figure 2.1.2**. The structures of the ligands were confirmed using NMR, HRMS and IR spectroscopy. For example, the ^{1}H NMR spectrum of **18** shows two singlets at 2.35 ppm and 2.25 ppm, each integrating to 3H, indicating the presence of two methyl groups and a multiplet at 7.43 – 7.28 ppm indicating the prescence of an aromatic ring. The ^{1}H NMR spectrum of **20** shows a singlet at 3.15 ppm integrating to 6H indicating the presence of the N(CH_3)$_2$ group. The ^{1}H NMR spectrum of **21** shows a quartet at 3.51 ppm, with an integration of 4H, and a triplet at 1.22 ppm, with the integration of 6H, indicating the presence of the two ethyl groups. Additional spectroscopic data can be found in the experimental section. These smaller ligands were then employed in complexation reactions with zinc.

Product	R	Yield (%)*
3	—O—CH₃ (ethyl ester)	64
7	—N N—〈phenyl〉—CF₃	60
18	—N N—CH₃	51
19	—N N—〈phenyl〉	52
20	H₃C—N—CH₃	31
21	H₃C—N—CH₃ (diethylamino)	46

Table 1.3 Ligands synthesized for exploring the steric hindrance during complexation.
* Yield of final step.

The larger ligands **7**, **19** and **21** did not form a zinc complex upon refluxing with $ZnCl_2$ in methanol. Replacing the large phenyl group on **7** with the smaller methyl group produced the smaller ligand **18** and **20**. Both **18** and **20** did form zinc complexes with zinc, upon reaction with $ZnCl_2$ and $Zn(OAc)_2$ respectively, **Table 1.4**. The formation of the zinc complexes **22** (zinc complex of **18**) and **23** (zinc complex of **20**) were confirmed by ^{1}H NMR and CHN microanalysis.

Ligand	Zinc salt	Yield(%)
3	$Zn(Cl)_2$	98
7	$Zn(Cl)_2$, $Zn(OOCCH_3)_2$	0
18	$Zn(Cl)_2$	99
19	$Zn(Cl)_2$	0
20	$Zn(OOCCH_3)_2$	77
21	$Zn(Cl)_2$, $Zn(OOCCH_3)_2$	0

Table 1.4 Complexation reactions

The smaller pyrazole ester ligand **3** also formed a complex **24** with zinc, **Figure 2.1.6**. Again, the formation of this complex was first confirmed by a shift in ^{1}H NMR spectrum, **Figure**

2.1.7. The most obvious shifts are to the CH_3 singlet signals at ~2.5 ppm and to the aromatic multiplet at ~7.5 ppm. The CH pyrazole singlet at ~8 ppm also shows a shift upon complexation.
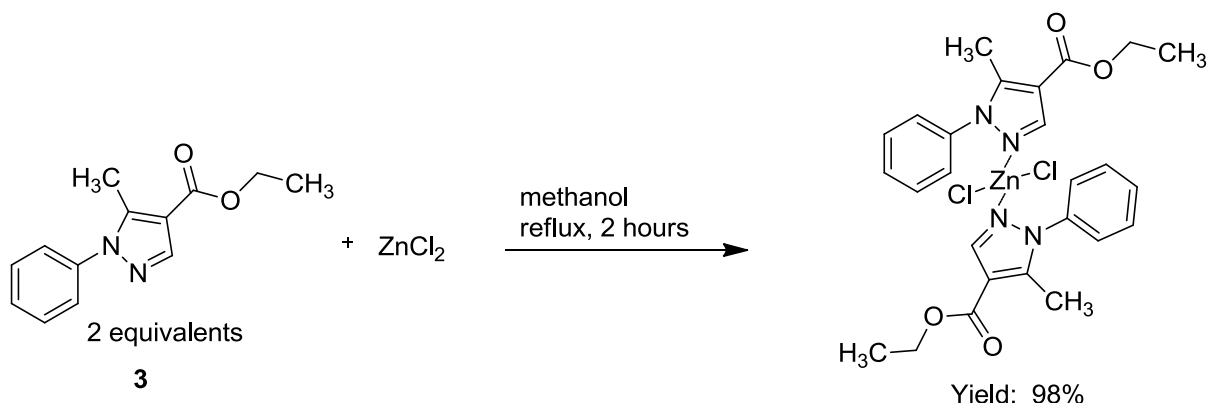
Figure 2.1.6 Synthesis of **24** and proposed structure of **24**

Structure of the predicted zinc complex is in accordance with the Hard and Soft Acid and Base (HSAB) principle, which was reported by Ralph G. Pearson.[47] The ratio of ligand to zinc appears to be determined by the ratio of starting material and is a 2:1, ligand:metal, ratio. Similar zinc(II) complexes have been reported. For example, Jacimovic and co-workers reported the zinc(II) complexes of 4-acetyl-3-amino-5-methyl-pyrazole (aamp) with the molecular formula of $Zn(NCS)_2(aamp)_2$. X-ray crystal structure analysis showed the coordination atoms to be the nitrogen of the two pyrazoles and the ratio of ligand to zinc is 2 : 1, **Figure 2.1.8**.[48] The molecular formula for the **24** was further confirmed by CHN microanalysis, with a calculated result for $C_{26}H_{28}Cl_2N_4O_4Zn$ of C, 52.32; H, 4.73; N, 9.39; and a found result of C, 53.13; H, 4.62; N, 9.26. A crystal of the **24** suitable for x-ray crystal structure determination could not be obtained.
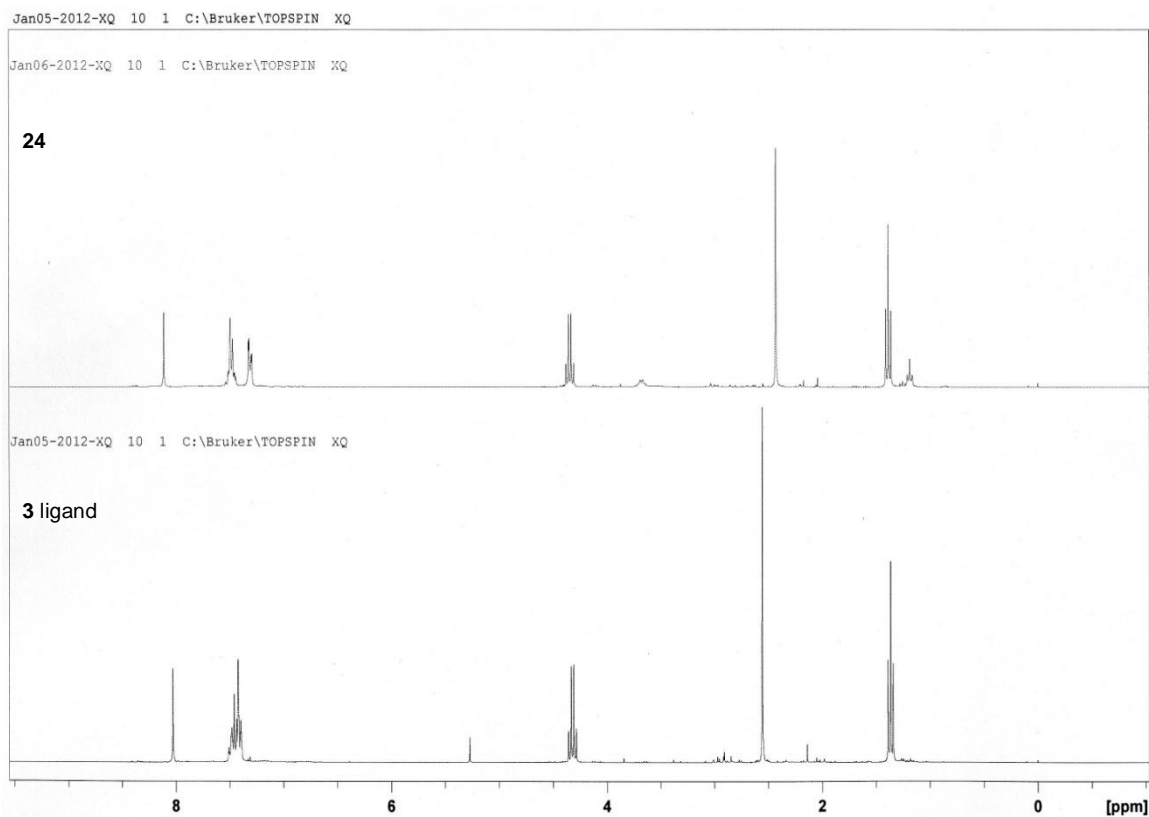
Figure 2.1.7 Comparison of ^{1}H NMR of **3** and its zinc complex **24**
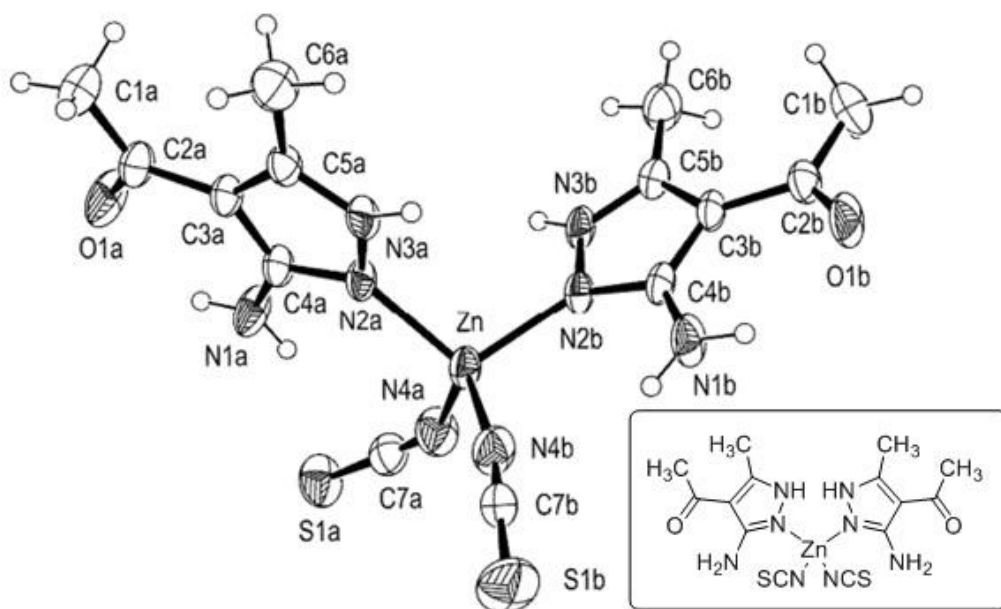
Figure 2.1.8 Structure and x-ray crystal structure of $Zn(NCS)_2(aamp)_2$.[48]

A family of ligands based on **3** were then synthesized **Table 1.5**. **25** to **29** vary in the R^1 substituent and could be accessed using the same synthetic route as used for **3** but with different hydrazines, **Figure 2.1.2**. Compound **29**, with $R^2 = nPr$, was also accessed using the same route but starting from the keto ester 3-oxo-hexanoic acid ethyl ester. The ^1H NMR of **28** shows a singlet at 2.50 ppm, with an integration of 3H, indicating the presence of pyrazole-CH_3 and a singlet at 3.81 ppm, again with an integration of 3H, indicating the presence of OCH_3 group. HRMS confirmed the presence of **28** with a calculated $(M + H^+) = 261.1234$ and a found $(M + H^+) = 261.1225$ (-3.26 ppm difference). For **29** the ^1H NMR of shows a multiplet at 1.64 – 1.51 ppm, integrating to 2H, a triplet at 2.92 ppm, integrating to 2H and a triplet at 0.85 ppm, with an integration of 3H, indicating the presence of propyl group. HRMS confirmed the presence of **29** with a calculated $(2M + Na^+) = 539.2629$ and a found $(2M + Na^+) = 539.2653$ (4.44 ppm difference) The **3** analogues in **Table 1.5** were then employed in subsequent complexation reactions with zinc chloride.
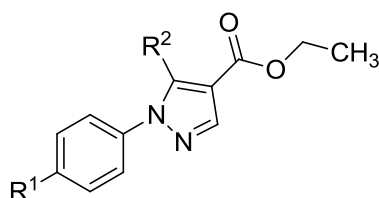
Product	R^1	R^2	Yield (%)*
3	H	CH_3	64
25	F	CH_3	47
26	Cl	CH_3	94
27	CF_3	CH_3	83
28	OCH_3	CH_3	76
29	H	$CH_2CH_2CH_3$	68

Table 1.5 Compound **3** analogues. * Yield of final step.

The complexation reaction was carried out in refluxing methanol using $ZnCl_2$. The successful complexation of **3** analogues with zinc, **Table 1.6**, was confirmed by shifts in the ^1H NMR and by CHN microanalysis. For example, with **26** and its corresponding zinc complex **31** the ^1H NMR spectra show a triplet at 2.92 ppm (CH_2 attached to the pyrazole) shifting to 2.84 ppm upon complexation; a triplet at 1.36 ppm (OCH_2CH_3) shifted to 1.40 ppm upon complexation and a quartet at 4.32 ppm (OCH_2) shifted to 4.35 ppm upon complexation. **31** was further confirmed by CHN microanalysis with a calculated result for $C_{30}H_{36}Cl_2N_4O_4Zn$, C, 55.18; H, 5.56; N, 8.58; and a found result of C, 54.87; H, 5.33; N, 8.25 (calculated for).

Product	Ligand	Zinc salt	Yield (%)*
24	**3**	$Zn(Cl)_2$	98
30	**25**	$Zn(Cl)_2$	71
31	**26**	$Zn(Cl)_2$	100
32	**27**	$Zn(Cl)_2$	67
33	**28**	$Zn(Cl)_2$	52
34	**29**	$Zn(Cl)_2$	80

Table 1.6 Compound **3** analogue zinc complexes. * Isolated yield.

2.3 Synthesis of a pyrazole-thiourea ligand and its zinc(II) complex

Previous research carried out in our group identified certain thiourea containing molecules as having potent antimicrobial activity.[49] As such we became interested in the antimicrobial activity of pyrazole based thiourea compounds and their zinc complexes. A proposed synthetic route to our first pyrazole-thiourea is shown in **Figure 2.1.9**.
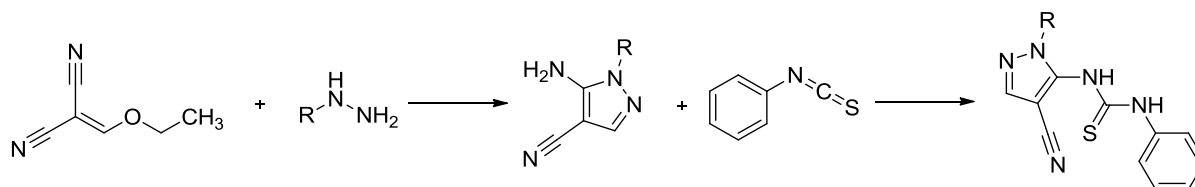
Figure 2.1.9 Proposed synthetic route to a thiourea substituted pyrazole.

We first had to synthesise the amino pyrazoles **35** and **36**. This was achieved by refluxing 2-(ethoxymethylene)malononitrile and hydrazine in ethanol for 30 minutes. The final product was obtained after recrystallization, **Table 1.8**.
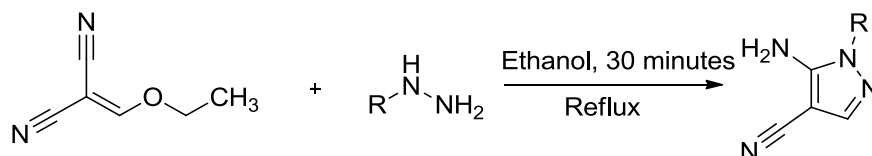
Product	R	Yield (%)*
35	Ph	55
36	H	52

Table 1.8 Synthesis of XQ35 and XQ36. * Isolated yield.

All subsequent attempts to generate a thiourea substituted pyrazole by reacting these amino pyrazoles with phenyl isothiocyanate failed. A complex mixture was obtained in each case, **Table 1.9**.
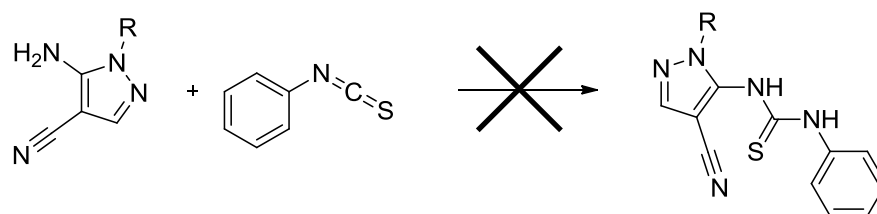
Starting material	Solvent	Base	Temperature (^{o}C)	Time (hours)	Yield (%)
35	Toluene	Potassium tert-butyloxide	80	15	0
35	DMF	Potassium tert-butyloxide	80	24	0
35	Dry DCM	N/A	rt	12	0
35	Dry THF	N/A	rt	24	0
35	Dry DCM	TEA	rt	15	0
35	DMF	NaOH	rt	15	0
36	DMF	N/A	rt	15	0
36	Dry DCM/ DMSO	TEA	rt	15	0

Table 1.9 Attempted synthesis of thiourea substituted pyrazole.

An alternative thiourea substituted pyrazole was needed and we turned our attention to generating as simple a pyrazole as possible, **39**. The successful three step synthetic route to **39** is shown **Figure 2.2.1**.
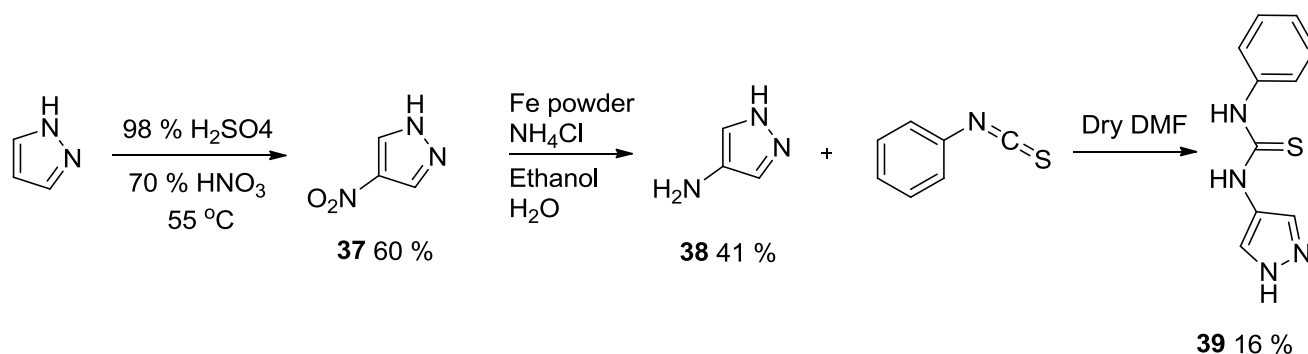
Figure 2.2.1 Synthesis of **39**

In step 1, pyrazole was heated in a mixture of 98 % H_2SO_4 and 70 % HNO_3 to generate the desired product **37**. The structure of **37** was identified by ^{1}H NMR where a singlet at 13.99 ppm for the N*H* was observed along with a singlet at 8.58, with an integration of 2H, for two C*H*s of the pyrazole ring. The presence of **37** was confirmed using HRMS (calculated (M + Na$^+$) = 136.0117, found (M + Na$^+$) = 136.0124 (4.56 ppm)).

In step 2, compound **37**, iron powder and ammonium chloride were heated in an ethanol/H_2O solution at 80 ^oC to give **38**. Compound **38** was confirmed by ^1H NMR where a singlet at 8.58 ppm was observed for the pyrazole C*H* of pyrazole and singlet at 6.99 ppm integrating to 2H observed for the N*H*$_2$.

In step 3, compound **38** and isothiocyanatobenzene were stirred in DMF under nitrogen for 24 hours generating **39**. The singlet at 12.70 ppm on ^1H NMR is identified as a N*H* signal, and the singlet at 9.57 ppm, with an integration of 2H, is identified as the signal for the two pyrazole C*Hs*. A broad singlet at 7.79 ppm is believed to be generated by a second N*H*. The aromatic protons show up as a multiplet with an integration of 5H. The structure of **39** was confirmed using HRMS and IR spectroscopy. Compound **39** was subsequently employed in a complexation reaction with zinc acetate.

Compound **39** were heated in methanol at 40^oC and a methanol solution of zinc acetate added. A precipitate appeared upon addition of the zinc acetate, which was isolated. We believe that complexation has occurred but a sample of sufficient purity could not be obtained and hence the structure of the complex could not be identified. A proposed structure for **39** zinc complex **40** is shown in **Figure 2.2.2**.
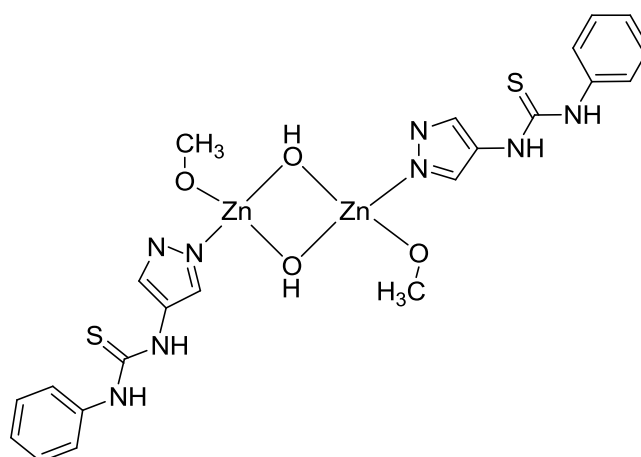
Figure 2.2.2 Possible structure of **40**

Compounds 41 and 42

Compounds **41** and **42** (compound **2** analogues) were also synthesized, as they were requierd as starting materials for the synthesis of compounds **11** and **29** respectively. They were synthesized using the same reaction conditions as described for the synthesis of compound **2**, **Figure 2.2.3**. Similar to compound **2**, the generation of compound **42** was confirmed by the presence of a singlet, with an intergration of 6H, at 2.83 ppm in the ^1H NMR spectrum,

indicating the presence of the (CH_3)$_2$N moiety. In addition, a singlet, with an intergration of 1H, at 7.45 ppm was also present and indicated the presence of the (CH$_3$)$_2$NCH moiety. The ^{1}H NMR spectrum also shows a quartet, with an intergration of 2H, at 4.03 ppm indicating the presence of the OCH_2CH$_3$ moiety and a triplet, with an intergration of 3H, at 1.13 ppm indicating the presence of the OCH$_2$CH_3 moiety. A double of triplets, with an intergration of 2H, at 1.43 ppm indicated the presence of the CH$_2$CH_2CH$_3$ group.

2, R = CH$_3$
41, R = CH$_2$CH$_3$
42, R = CH$_2$CH$_2$CH$_3$
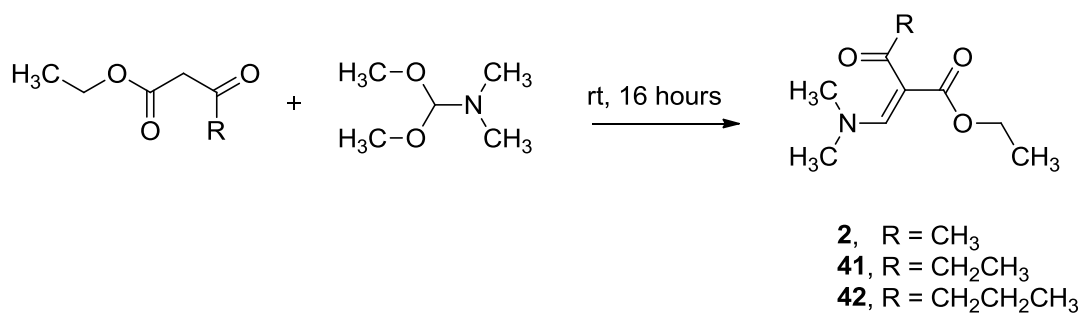
Figure 2.2.3 Synthesis of compound **41** and **42**

2.4 Biological evaluation

Pyrazole derivatives have been reported to have antimicrobial activity against both Gram-positive and Gram-negative bacteria. For example, Rahimizadeh and co-workers reported the biological activity of a series of pyrazole derivatives, with somewhat similar structures to our pyrazole ligands.[50] In this paper N-(4-cyano-1-(2,4-dinitrophenyl) -1H-pyrazol-5-yl)-4-nitrobenzamide, **Figure 2.2.3**, shows a minimum inhibition concentration (100 %) of 25.1 μg/mL aginst methicillin-resistant *S.aureus* (Gram-positive bacteria, Cloxacillin was used as a standard with a minimum inhibition concentration (100%) of 94.0 μg/mL).[50]
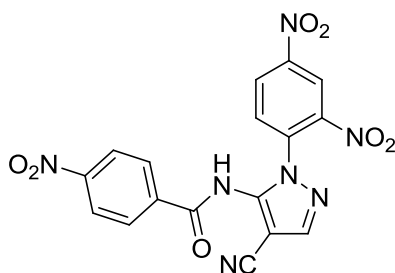
Figure 2.2.3 N-(4-cyano-1-(2,4-dinitrophenyl)-1H-pyrazol-5-yl)-4-nitrobenzamide

Jain and co-workers described the biological activity of 1-phenyl-3-(4-nitrophenyl)-5-(4-(2-ethanoloxy)phenyl) 1H-pyrazole, **Figure 2.2.4**, which was active against *E.coli* (Gram-negative bacteria) with a minimum inhibition concentration (100%) of 0.35 μg/mL.[51] As a result of such publications, we were hopeful that our pyrazole ligands would show inhibition of both Gram-positive and Gram-negative bacteria.
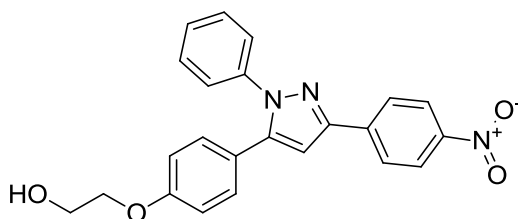
Figure 2.2.4 1-Phenyl-3-(4-nitrophenyl)-5-(4-(2-ethanoloxy)phenyl) 1H-pyrazole

Zinc complexes have been reported to improve the activity of both organic ligands and zinc salts. For example, the zinc complex reported by Johnson and co-workers displayed antimicrobial activity against *P. aeruginosa*.[35] In this case, the zinc complex shows an MIC_{100} of 280 μg/mL while its Schiff-base ligand displayed a higher MIC_{100} of 483 μg/mL, with zinc acetate having an MIC_{100} of 1120 μg/mL. The zinc-complex has improved the antibacterial activity of both the organic ligand and the zinc acetate. Therefore we were again hopeful that

an improvement in the antibacterial activity of our pyrazole ligands and the zinc salts would be observed upon complextaion.

All the ligands synthesized, as well as their zinc-complexes and zinc salts, were tested against *S. aureus,* a Gram-positive bacterium, and *E.coli,* a Gram-negative bacterium. 20 mg of the testing compounds were weighed and first dissolved in 1 mL DMSO. The solutions were then diluted in water. The stock solutions prepared for testing was 20 μg/mL. The susceptibility tests were carried out on 96-well flat-bottom tissue culture plates. The plates from column 12 to column 4 contain test solutions (DMSO/water) of the synthesized compound. The concentration of the test solution is different in each column with column 12 having the highest concentration and column 4 the lowest concentration. Column 3 contains bacteria and media only with column 1 and 2 containing media only. The plates were incubated for 24 hours at 37 $^{\circ}$C. The optical density is then read at 540 nm and growth is quantified as a percentage of the control. The *E.coli* and *S.aureus* strains tested were clinical isolates from patients at St.James Hospital, Dublin. All the results presented are an average from 3 plates for each compound, with a percentage error lower than 10 %. The abbreviations ZC and ZA stands for zinc chloride and zinc acetate, respectively.
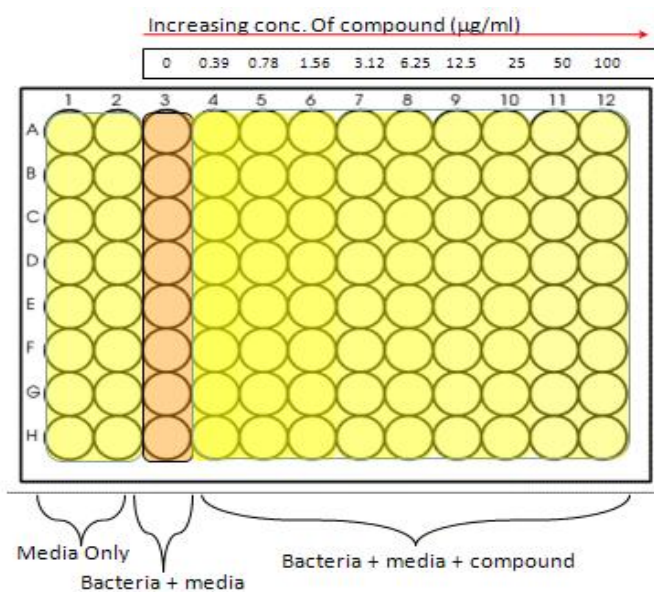
Figure 2.2.5 96-well flat-bottom tissue culture plate

2.4.1 Evaluation of compound 1 and analogues of compound 1 against *E.coli*

Most of the **1** family members were found not to be active against *E.coli*, with the exception of **19**, **Figure 2.2.6**. In comparison with **1**, **19** has replaced the pyridine ring with an unsubstituted phenyl ring. **19** inhibited approximately 40 % of the bacterial growth at 100 µg/mL, 2.89×10^{-4} mmol/mL. The most interesting comparison is between **19** and **7**, as the only difference between the two is the presence or absence of a CF_3 group. **7** has a *p*-CF_3 group on the phenyl ring, and is inactive, where as **19** does not have a CF_3 group and is active, **Table 2.1**. This is a strange phenomenon as many reported antibiotics, like the fluoroquinlones, show improved activity when F atom/atoms are present. A CF_3 group would also increase lipid solubility and hence increase a compounds ability to penetrate the bacterial cell wall.[52]
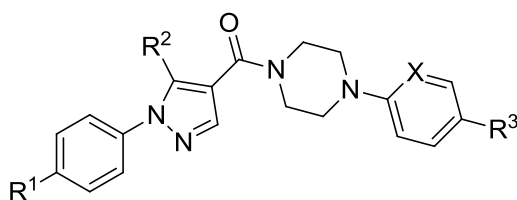
Product	R^1	R^2	X	R^3
1	H	CH_3	N	CF_3
5	CF_3	CH_3	N	CF_3
6	H	CH_2CH_3	N	CF_3
7	H	CH_3	CH	CF_3
8	OCH_3	CH_3	N	CF_3
9	Cl	CH_3	N	CF_3
19	H	CH_3	CH	H

Table 2.1 Compound **1** family
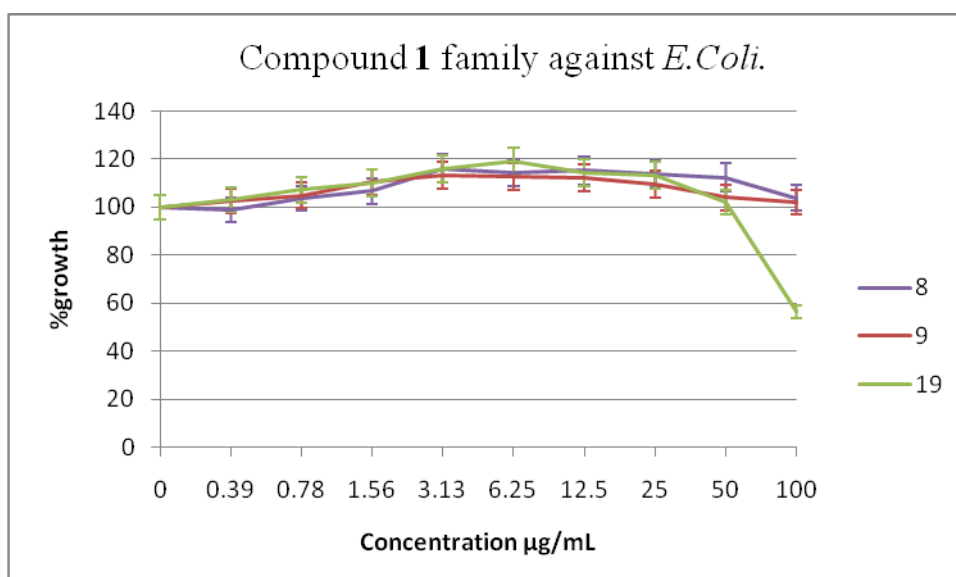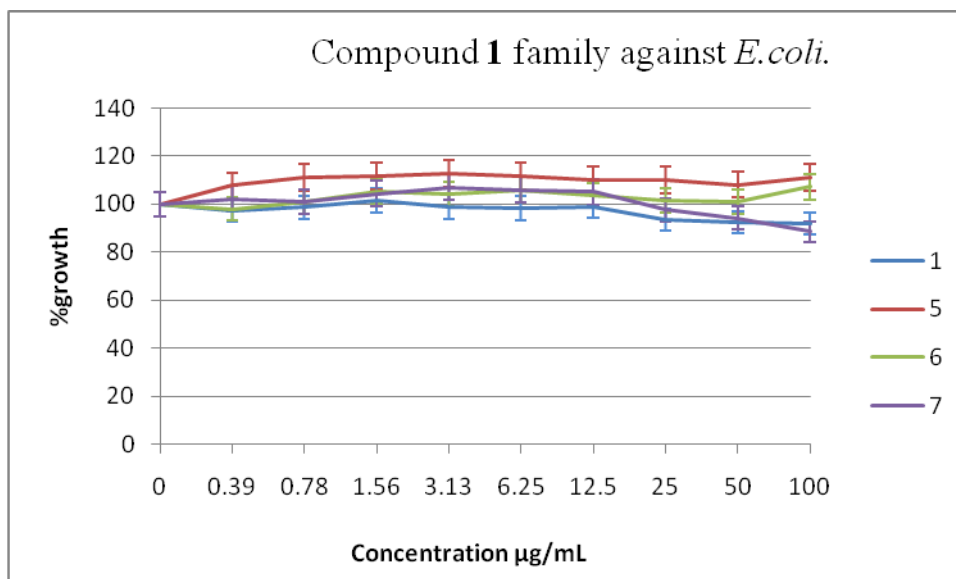
Figure 2.2.6 Compound **1** family against *E.coli*.

2.4.2 Evaluation of 18, 20, 21 and their zinc complexes against *E.coli.*

18, **20** and **21** are structurally smaller than the **1** family, **Table 2.2**. As a result, **18** and **20** were successfully complexed with zinc. **21** did not form a zinc complex and this may be due to its slightly larger size.

Product	R
18	—N(piperazine)N—CH$_3$
20	—N(CH$_3$)$_2$ (H$_3$C–N–CH$_3$)
21	H$_3$C–N–CH$_3$ (H$_3$C-CH$_2$-N-CH$_2$-CH$_3$)
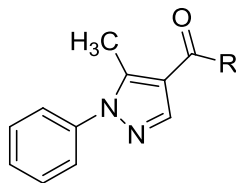
Table 2.2 Structure of **18**, **20** and **21**

Generally, they did not show significant activity against *E.coli*, with **20** and **18** displaying slightly better activity against *E.coli* compared to **21**, **Figure 2.2.7**. The reason for this slightly superior activity is not clear. Perhaps the fact that **18** and **20** could form a zinc complex and **21** could not, may hint that a steric effect may also influence their antibacterial activity. Similar phenomenon have been reported, for example Jiménez-Pérez and co-workers reported the antibacterial activity of N,N'-diaryl-*o*-phenylenediamines, **Figure 2.2.8**, against *S. typhimurium*. Minimal inhibitory concentration (100%) of compound **a1** and **a2** against *S. typhimurium* was reached at 0.35 µg/mL with minimal inhibitory concentration (100%) of compound **a3** reached at 0.75 µg/mL. Jiménez-Pérez suggested that the the steric hindrance effect of the N-aryl groups, on *o*-phenylendiamines, influenced the biological activity.[53]
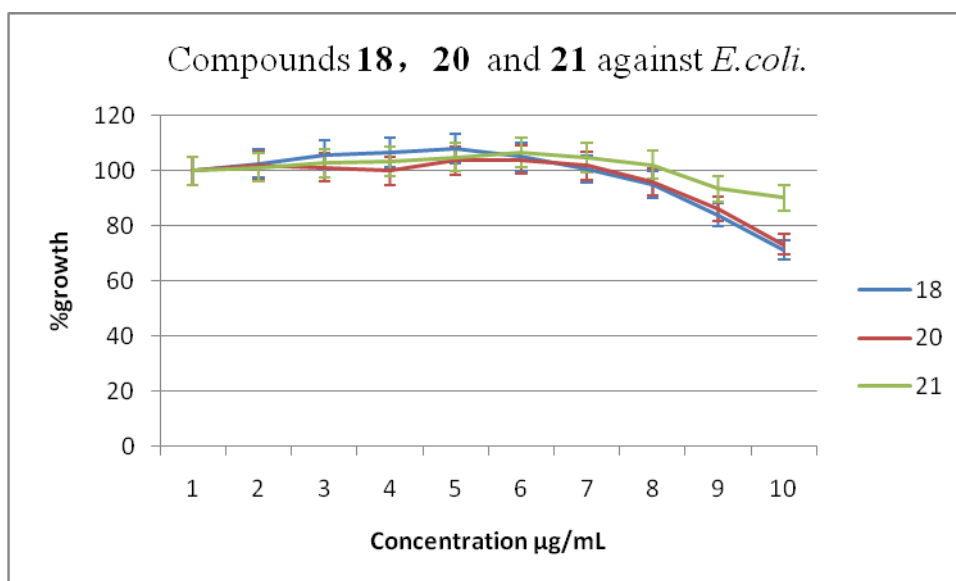
Figure 2.2.7 Compounds **18**, **20** and **21** against *E.coli*
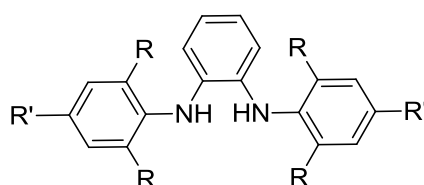
Sample	R	R'
a1	CH₃	H
a2	CH₃	CH₃
a3	*i*Pr	H

Figure 2.2.8 N,N'-diaryl-*o*-phenylenediamines.[53]

E.coli growth was inhibited by approximately 60-70 % by the **18** zinc chloride complex (**22**) and by the **20** zinc acetate complex (**23**), at a concentration of 100 μg/mL, **Figure 2.2.9**. As we had hoped, both **22** (100 μg/mL, 1.42×10^{-4} mmol/mL) and **23** (100 μg/mL, 1.56×10^{-4} mmol/mL) have greatly improved antibacterial activity (about 60-70 % inhibition of *E.coli* growth) compared to the pyrazole ligands **18** (100 μg/mL, 3.52×10^{-4} mmol/mL) and **20** (100 μg/mL, 4.37×10^{-4} mmol/mL) alone (about 20 % inhibition of *E.coli* growth). Zinc chloride (100 μg/mL, 7.35×10^{-4} mmol/mL) inhibited *E.coli* growth by approximately 70-80 % and zinc acetate (100 μg/mL, 5.46×10^{-4} mmol/mL) by approximately 70 % growth. As such, **22** and **23** inhibited nearly the same percentage growth of *E.coli* at much lower concentration compared to zinc salts indicating that the addition of the pyrazole ligands also improved the activity of the zinc salts.
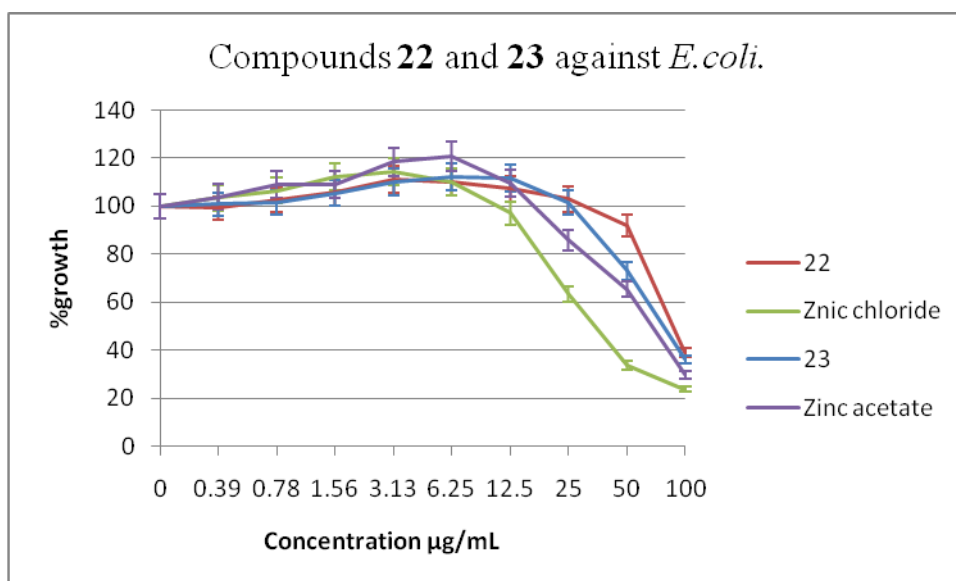
Figure 2.2.9 Compound **22** and **23** against *E.coli*

2.4.3 Evaluation of 3, 3 analogues and their zinc complexes against *E.coli*.

The **3** family, **Table 2.3**, did not show significant activity against *E.coli*, **Figure 2.3.1**. As previously observed with **18** the zinc complexes of the **3** family have significantly improved activity against *E.coli* when compared to the pyrazole ligands, **Figure 2.3.2**. The growth of *E.coli* was inhibited by approximately 70 % when the concentration of **24** was 100 μg/mL, 1.68×10^{-4} mmol/mL and this was the most active complex. Zinc chloride itself inhibited approximately 70-80 % *E. coli* growth at 100 μg/mL, 7.35×10^{-4} mmol/mL. Once again this zinc complex is nearly as active as zinc chloride at much lower concentration and as such the addition of **3** improved the activity of zinc chloride. **32** shows extremely high percentage growth at 25 and 50 μg/mL, possibly due to the precipitation of **32**. During solution preparation **32** was noticeably harder to dissolve than the other complexes. The growth of *E.coli* was inhibited by approximately 20-30% when the concentration of **32** was 100 μg/mL, 1.37×10^{-4} mmol/mL. This inhibition is very low compared to the other **3** family zinc complexes. It may due to the presence of CF_3 substituted on the phenyl ring which appeared to be problematic with previously described pyrazole ligands, in section **2.4.1**, or perhaps it is due to the reduced solubility of **32**.
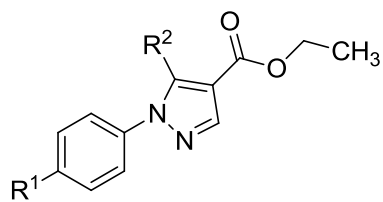
Product	R^1	R^2
3	H	CH$_3$
25	F	CH$_3$
26	Cl	CH$_3$
27	CF$_3$	CH$_3$
28	OCH$_3$	CH$_3$
29	H	CH$_2$CH$_2$CH$_3$

Table 2.3 3 family
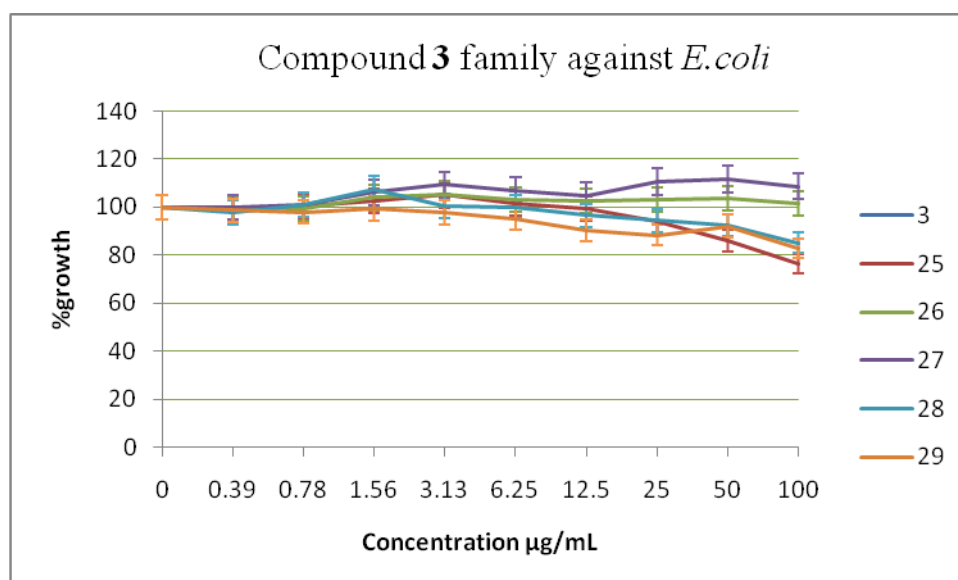
Figure 2.3.1 Compound **3** family against *E.coli*.
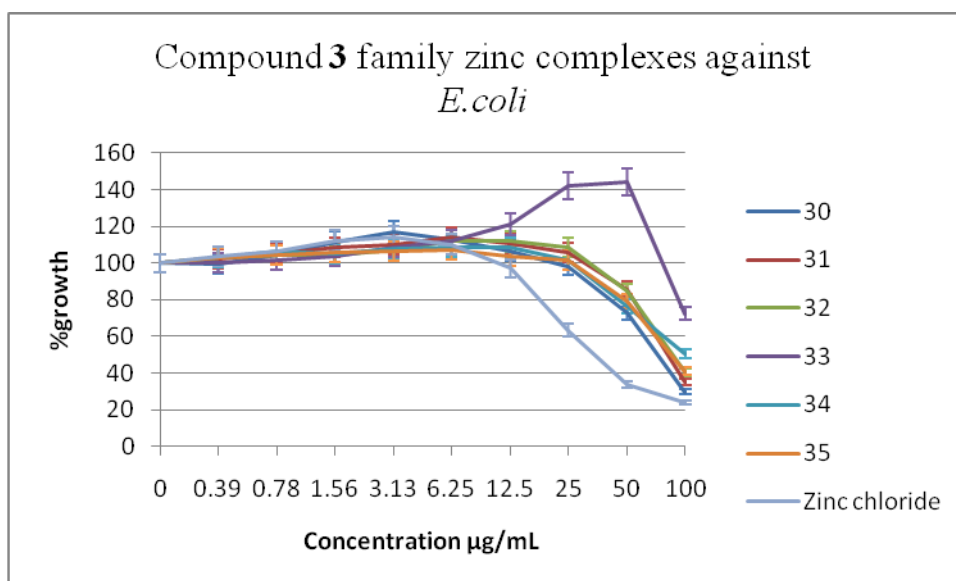
Figure 2.3.2 Compound **3** family zinc complexes againt *E.coli*

2.4.4 Evaluation of 39 and 40 against *E.coli*.

39 is a thiourea substituted pyrazole, **Figure 2.3.3**. Its zinc complex, **40**, could not be isolated with 100% purity but was evaluated against *E. coli* in any case (concentration calculated based on the proposed structure shown in **Figure 2.2.2**). Again we saw that **39** does not show significant antibacterial activity against *E.coli* (approximately 20 % inhibition at 100 μg/mL, 4.59×10^{-4} mmol/mL). However, **40** inhibited approximately 75 % *E.coli* growth at 100 μg/mL, 1.51×10^{-4} mmol/mL. Once again, the zinc complex displayed significantly improved activity against *E.coli* compared to pyrazole ligand. **40** was also observed to slightly increase the activity against *E.coli* at 100 μg/mL, 1.51×10^{-4} mmol/mL when compared to zinc acetate at 100 μg/mL 5.46×10^{-4} mmol/mL, **Figure 2.3.4**. **40** also inhibited approximately 50 % *E. coli* growth at a concentration of 50 μg/mL, 0.76×10^{-4} mmol/mL, where as zinc acetate only inhibited approximately 35 % growth at 50 μg/mL, 2.73×10^{-4} mmol/mL.
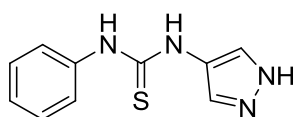
Figure 2.3.3 Structure of **39**
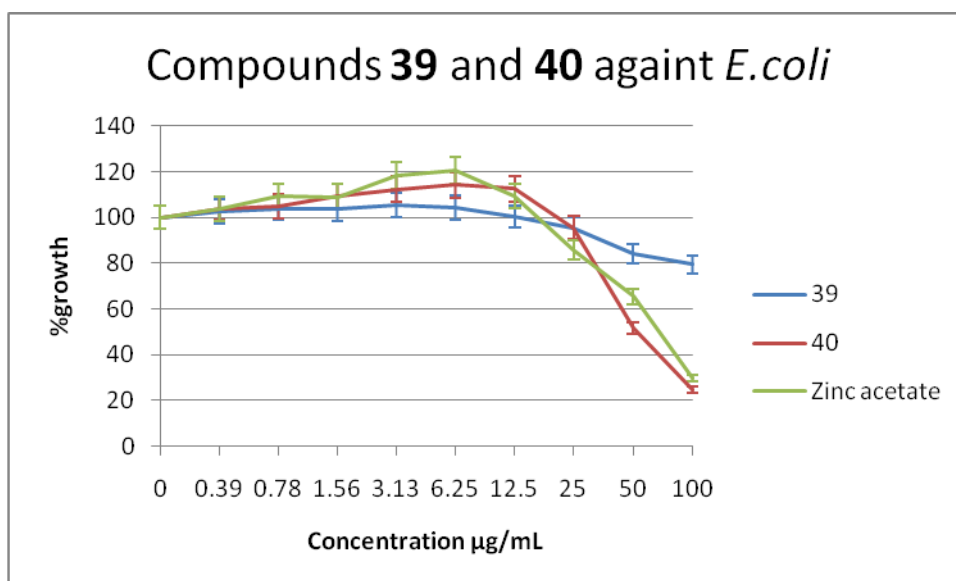
Figure 2.3.4 Compounds **39** and **40** against *E.coli*

2.4.5 Evaluation of the 1 family against *S.aureus*

Generally, the **1** family did not show activity against *S.aureus*, **Figure 2.3.5** and **2.3.6** The structures of the XQ4 family can be seen on **Table 2.1**. XQ14 showed slight activity against *S.aureus* inhibiting growth by approximately 10% at a concentration of 100 µg/mL, 2.89×10^{-4} mmol/mL.
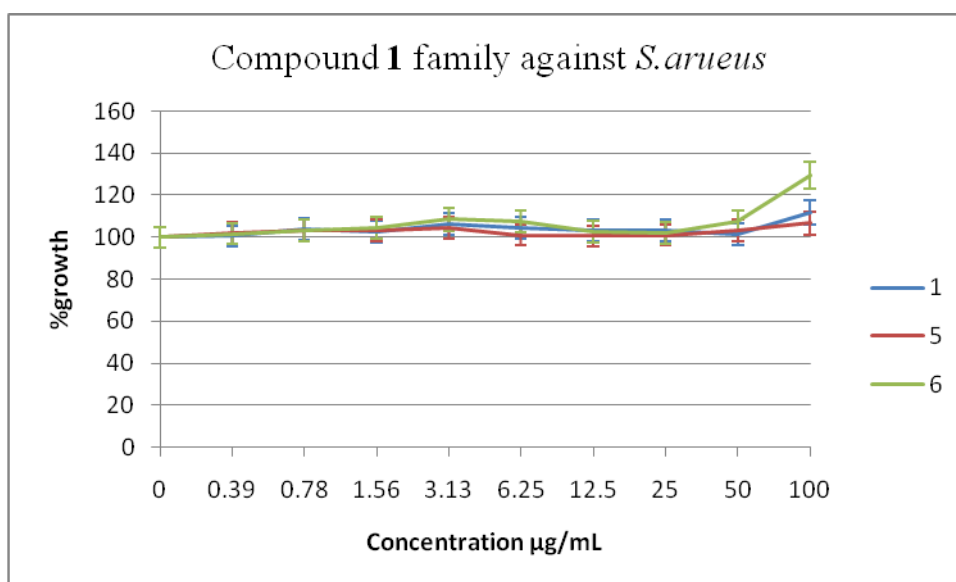
Figure 2.3.5 1 family against *S.aureus*
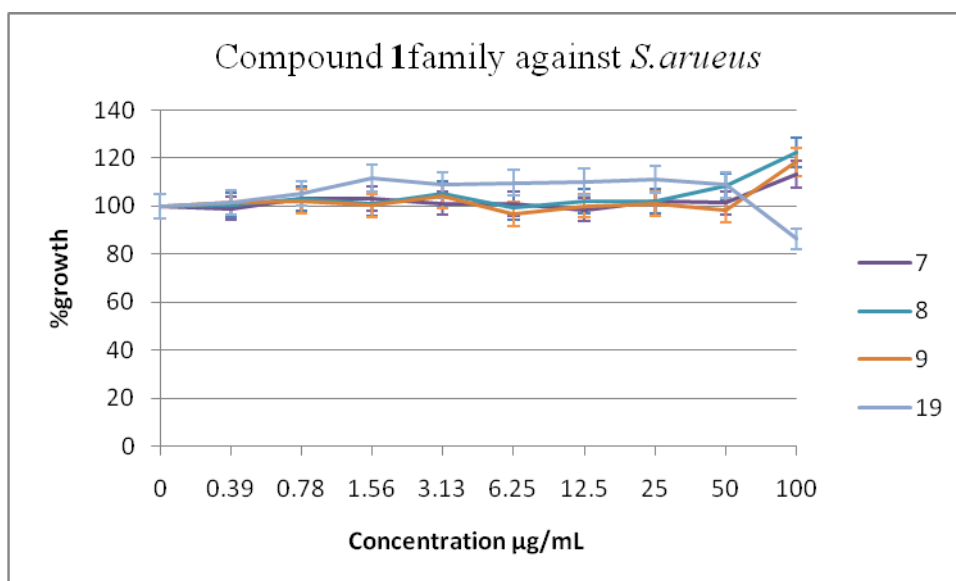
Figure 2.3.6 Compound **1** family against *S.aureus*

2.4.6 Evaluation of compounds 18, 20, 21 and their zinc complexes against *S.aureus*.

The activity of **18** and **21** against *S.aureus* is very low, **Figure 2.3.7**. The structure of these pyrazoles can be found on **Table 2.2**. **20** inhibited approximately 20 % of *S. aureus* growth at 100 μg/mL, 4.37×10^{-4} mmol/mL.
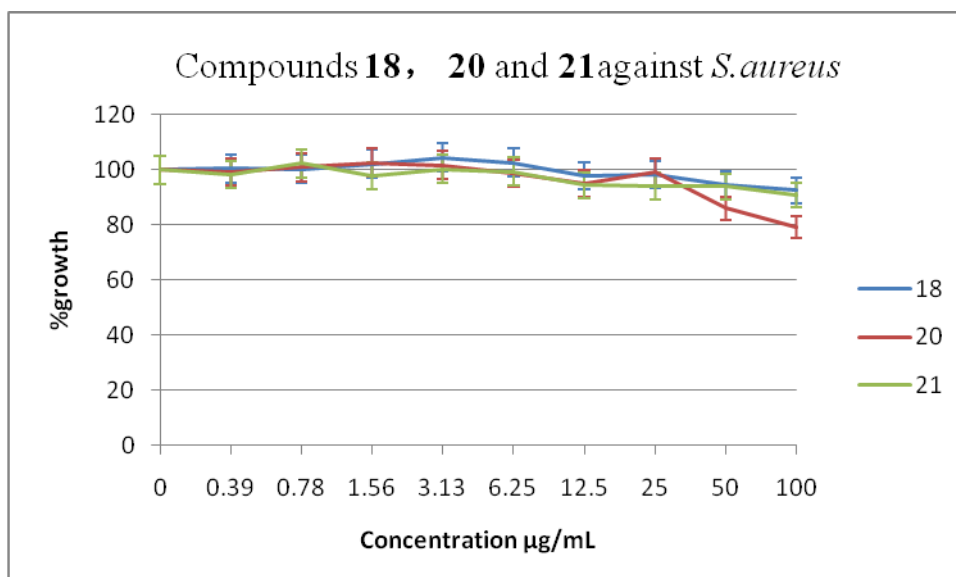
Figure 2.3.7 Compounds **18**, **20** and **21** against *S.aureus*

As with *E. coli*, the zinc complexes **22** and **23** have significantly improved activity against *S. aureus* compared to the pyrazole ligands alone, **Figure 2.3.8**. **21** did not form a zinc complex.

22 (100 µg/mL, 1.42×10^{-4} mmol/mL) inhibited the growth of *S. aureus* by approximately 40 % and XQ25(ZA) (100 µg/mL, 1.56×10^{-4} mmol/mL) by approximately 50 %. Again, we saw that **22** and **23** were inhibited nearly the same percentage growth of *S.aureus* at much lower concentration compared to Zinc chloride (100 µg/mL, 7.35×10^{-4} mmol/mL) and zinc acetate (100 µg/mL, 5.46×10^{-4} mmol/mL) respectively. XQ25(ZA) inhibited the growth of *S. aureus* by approximately 45 % at 50 µg/mL, 0.78×10^{-4} mmol/mL; zinc acetate inhibited approximately 30 % *S. aureus* growth at 50 µg/mL, 2.73×10^{-4} mmol/mL.
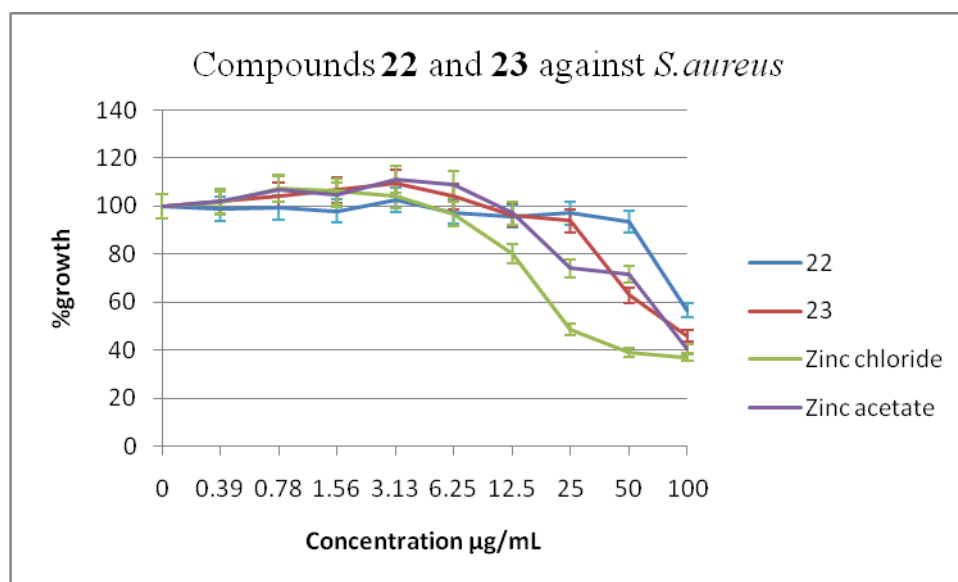
Figure 2.3.8 Compounds **22** and **23** against *S.aureus*.

2.4.7 Evaluation of the 3 family and their zinc complexes against *S.aureus*.

In general the **3** family did not show signification activity against *S.aureus*, **Figure 2.3.9**. The structures of the **3** family can be found on **Table 2.3**. **25** inhibited growth of *S. aureus* by approximately 20 % at 100 µg/mL, 4.03×10^{-4} mmol/mL.
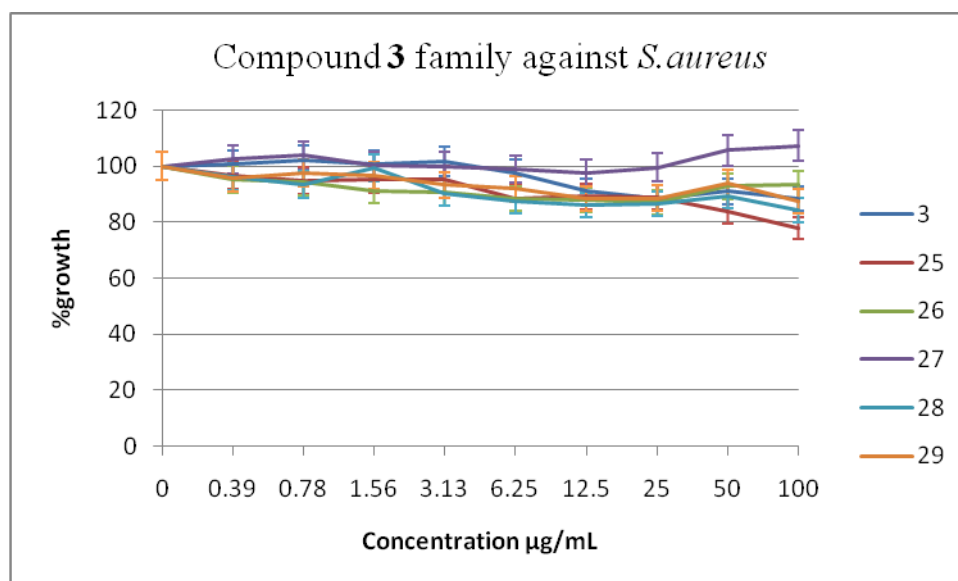
Figure 2.3.9 Compound **3** family against *S.aureus*

Once again, the zinc complexes of **3** family exhibited higher activity than the pyrazole organic ligands. The zinc complex **24** inhibited growth of *S. aureus* by approximately 50 % at a concentration of 100 μg/mL, 1.68 $\times 10^{-4}$ mmol/mL, **Figure 2.4.1**. **30** (100 μg/mL, 1.58 $\times$ 10^{-4} mmol/mL) and **32** (100 μg/mL, 1.37 $\times 10^{-4}$ mmol/mL) were both found to inhibit the growth of *S. aureus* by approximately 40 %. The growth of *S. aureus* at 50 μg/mL of **32** was much higher than 100 % and this is possibly due to an increase in the optical density caused by the precipitation of **32**, as previously discussed in section **2.4.3**. **33** inhibited the growth of *S.aureus* by approximately 50% at a concentration of 100 μg/mL, 1.52 $\times 10^{-4}$ mmol/mL. Zinc chloride inhibited about 60 % growth of *S.aureus* at 100 μg/mL, 7.35 $\times 10^{-4}$ mmol/mL. **31** (100 μg/mL, 1.50 $\times 10^{-4}$ mmol/mL) and **34** (100 μg/mL, 1.53 $\times 10^{-4}$ mmol/mL) exhibited approximately 60-65 % growth inhibition of *S.aureus*. **24**, **31** and **34** were inhibited nearly the same percentage growth of *S.aureus* at much lower concentration compared to zinc chloride. Thus the addition of **3**, **26** and **29** to zinc chloride has improved antimicrobial activity.
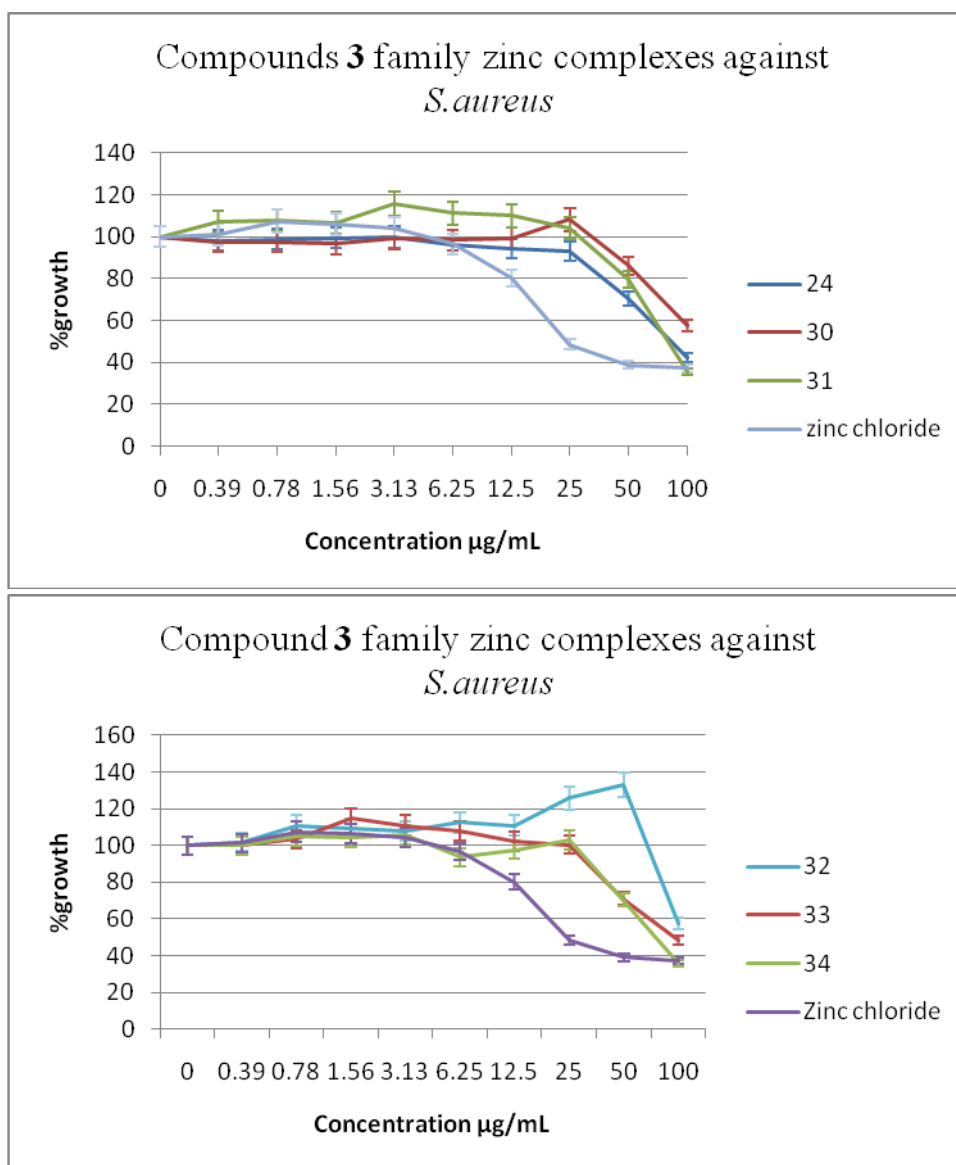
Figure 2.4.1 Compound **3** family zinc complexes against *S.aureus*

2.4.8 Evaluation of 39 and 40 against *S.aureus*.

39 inhibited the growth of *S. aureus* by approximately 10% at a concentration of 100 μg/mL. Its zinc complex, **40**, was found to be significantly more active and showed 60 % growth inhibition at a concentration of 100 μg/mL (1.51×10^{-4} mmol/mL) (concentration calculated based on proposed structure in **Figure 2.4.2**). The activity of **40** against *S. aureus* was slightly superior to zinc acetate at 100 μg/mL and the concentration of **40** (1.51×10^{-4} mmol/mL) is much lower than zinc acetate (5.46×10^{-4} mmol/mL). **40** inhibited *S. aureus* growth by approximately 40 % at 50 μg/mL where as zinc acetate only showed approximately 30 %

inhibition at 50 μg/mL. The addition of **39** to zinc acetate has improved the activity against *S.aureus*.
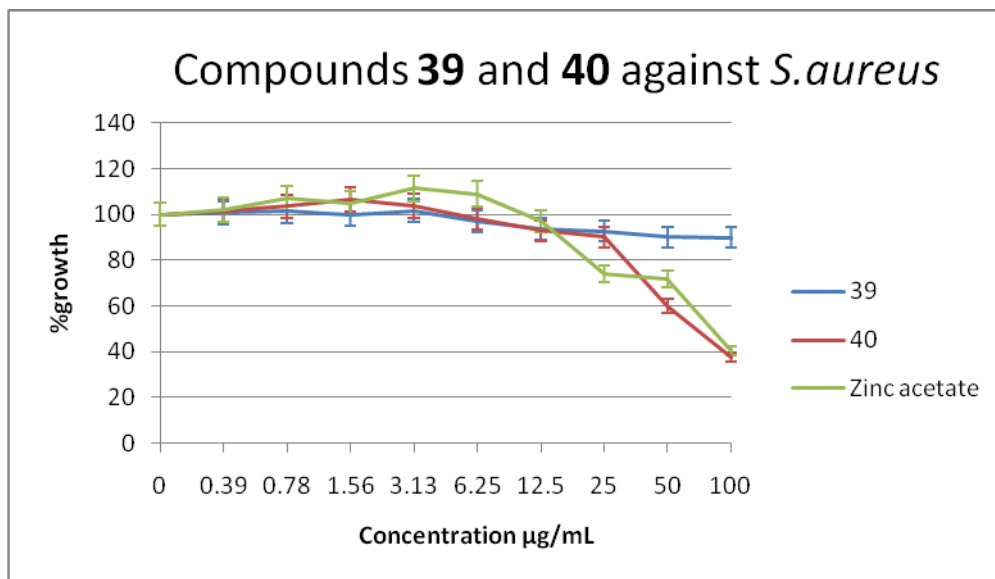
Figure 2.4.2 Compounds **39** and **40** against *S.aureus*

2.4.9 Conclusion

As previously discussed in section **2.4**, we expected the pyrazole ligands and their zinc complexes to exhibit antibacterial activity, with the zinc complexes displaying improved antibacterial activity when compared to either the pyrazole ligands and zinc salts alone. Generally, the susceptibility test results showed that most pyrazole ligands did not exhibit potent activity against either *E. coli* or *S. aureus*. **19** was one of the more potent ligands displaying 40 % inhibition of *E. coli* at 100 μg/mL. All of the zinc complexes exhibited good antibacterial activity against both *E. coli* and *S. aureus* at 100 μg/mL. As we had expected the zinc complexes greatly improved the antibacterial activity of the pyrazole ligands. However, most zinc complexes were as active as the zinc salts alone at 100 μg/mL. But the concentrations of zinc complexes were lower than zinc salts alone. For example, **24** inhibited *E. coli* growth by approximately 70 % at 100 μg/mL (1.68×10^{-4} mmol/mL), **3** inhibited *E. coli* growth by approximately 20 % at 100 μg/mL and zinc chloride inhibited *E. coli* growth by approximately 80 % at 100 μg/mL (7.35×10^{-4} mmol/mL). **40** exhibited better activity against both *E. coli* and *S. aureus* at 50 μg/mL compared to zinc acetate and **39**. The origin of the antimicrobial activity of the pyrazole zinc complexes was not determined. It could arise from the zinc complexes itself, but it may also result from the zinc salt or ion itself after disassociation of the complex upon interaction with the bacterial cell.

Chapter 3 Experimental for the synthesis of pyrazole ligands and their metal complexes

Instrumentation

Reagents were purchased from Sigma-Aldrich, Alfa Aesar, Acros Organics and used without further purification. Anhydrous DMF was purchased from Sigma Aldrich.

All NMR spectra were recorded on a Bruker Avance spectrometer at a probe temperature of 25 °C, unless otherwise stated, operating at 300 MHz for the 1H nucleus and 75 MHz for the 13C nucleus. Proton and carbon signals were assigned with the aid of DEPT experiments for novel compounds. High temperature NMR spectroscopy experiments were carried out by heating the probe. Spectra were recorded in DMSO-d_6, $CDCl_3$ or CD_3OD with Me_4Si used as the internal standard. Chemical shifts are given in ppm downfield form the internal standard and coupling constants are given in Hz.

Melting point analyses were carried out using a Stewart Scientific SMP1 melting point apparatus.

Infrared (IR) spectra were recorded as KBr disks or liquid films between NaCl plates using a Perkin Elmer System 2000 FT-IR spectrometer in the region of 4000-370 cm^{-1}. High resolution mass spectra (HR-MS) were performed on an Agilent-L 1200 Series coupled to a 6210 Agilent Time-of-Flight (TOF) mass spectrometer equipped with an both a positive and negative electrospray source.

Microanalysis was carried out using a Flash EA 1112 Series Elemental Analyser. The sample is burned in oxygen and a helium carrier gas at 900 ^{o}C in a combustion tube.

Flash column chromatography was performed using silica gel 60 (Merck, 0.040-0.063 mm). Analytical thin layer chromatography was carried out on aluminium sheets precoated with Merck TLC Silica gel 60 F254.

3.1 Synthesis of pyrazole ligands of compound 1 family

3.1.1 Synthesis of (5-methyl-1-phenyl-1H-pyrazol-4-yl)-[4-(5-trifluoromethyl-pyridin -2-yl)-piperazin-1-yl]-methanone 1 (XQ4)
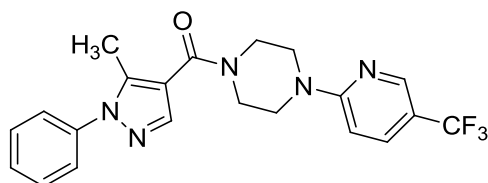
5-Methyl-1-phenyl-1H-pyrazole-4-carboxylic acid **4** (65 mg, 0.32 mmol), HOBt (54 mg, 0.40 mmol), TBTU (130 mg, 0.40 mmol), anhydrous triethylamine (0.09 mL, 0.65 mmol) and dry dimethylformamide (1 mL) were placed in an oven-dried Schlenk tube under a nitrogen atmosphere. The resulting solution was stirred at room temperature for 15 minutes. A second oven-dried Schlenk tube was prepared containing 1-(5-trifluoromethyl-2-pyridinyl) piperazine (92 mg, 0.4 mmol) and dry dimethylformamide (1 mL) under a nitrogen atmosphere. The resulting solution was stirred until complete dissolution of the piperazine had occurred. The piperazine solution was then transferred, *via* a cannula, to the first Schlenk tube containing the carboxylic acid. The resulting solution was stirred for 24 hours under a nitrogen atmosphere, and monitored by TLC. After 24hrs, the dimethylformamide was removed under reduced pressure and the resulting oil was acidified using a 0.1 N aqueous hydrochloric acid solution. The aqueous mixture was extracted with ethyl acetate (20 mL, followed by 4 × 10 mL). The organic extracts were combined and washed with a saturated aqueous sodium bicarbonate solution (3 × 20 mL) and brine (3 × 20 mL). The organic layer was separated and dried over anhydrous magnesium sulphate and evaporated under reduced pressure. The residue was purified using flash chromatography on silica gel eluting with dichloromethane/methanol (95:5) to obtain the desired product as a white solid, 78 % yield (99 mg).

m.p. 186-190 $^{\circ}$C; **^{1}H NMR** (300 MHz, CDCl$_3$) δ 8.43 (s, 1H, C*H* of pyrazole), 7.70 – 7.66 (m, 3H, Ar), 7.54 – 7.42 (m, 5H, Ar), 3.88 – 3.73 (m, 8H, C*H$_2$*), 2.49 (s, 3H, C*H$_3$*); **^{13}C NMR** (75 MHz, CDCl$_3$) δ 164.9 (*C*=O), 160.1 (*C*-2 of pyridine), 145.8 (q, *J* = 4.5 Hz, *C*-6 of pyridine), 141.3 (*C*CH$_3$), 139.0 (Ar*C*), 138.8 (*C*H of pyrazole), 134.7 (q, *J* = 3.0 Hz, *C*-4 of pyridine), 129.3 (Ar*C*H), 128.5 (Ar*C*H), 125.3 (Ar*C*H), 124.4 (q, *J* = 268.5 Hz, *C*F$_3$), 115.9 (q, *J* = 33.0 Hz, *C*CF$_3$), 115.1 (*C*C=O), 105.8 (*C*-3 of pyridine), 44.9 (*C*H$_2$), 11.8 (*C*H$_3$); **IR (KBr)** 3443, 3058, 2868, 1618 (amide), 1556, 1506, 1439, 1316 (tertiary amine), 1273, 1240 (CF$_3$), 1200 (tertiary amine), 1161, 1108, 1006, 944, 873, 808, 770, 698, 634, 476 cm^{-1}; **ESI-MS** C$_{21}$H$_{20}$F$_3$N$_5$O Calc. (M + H$^+$) = 416.1693, found (M + H$^+$) = 416.1705.

3.1.2 Synthesis of ethyl 2-((dimethylamino)methylene)-3-oxobutanoate 2 (XQ1)[54]
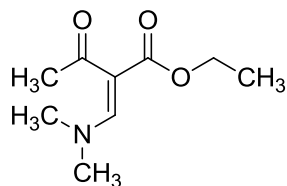
Ethyl acetoacetate (0.2 mL, 1.58 mmol) was stirred at room temperature and N,N-dimethylformamide dimethylacetal (0.252 mL, 1.58 mmol) was added drop wise. The reaction mixture was allowed to stir at room temperature for 16 hours. The resulting solution was evaporated under reduced pressure, then azeotroped with toluene three times (evaporating under reduced pressure) and purified using flash chromatography on silica gel eluting with ethyl acetate/petroleum ether, (80:20) to give a yellow oil, 14.7 % yield (292 mg).

R_f value 0.22 (ethyl acetate/petroleum ether, 80:20). **^{1}H NMR** (300 MHz, CDCl$_3$) δ 7.69 (s, 1H, C*H*=C) 4.23 (q, J = 7.1 Hz, 2H, C*H*$_2$), 3.15 (s, 6H, NC*H*$_3$), 2.33 (s, 3H, C(O)C*H*$_3$), 1.32 (t, J = 7.1 Hz, 3H, CH$_2$C*H*$_3$). Matches known data.[54]

3.1.3 Synthesis of ethyl 5-methyl-1-phenyl-1H-pyrazole-4-carboxylate 3 (XQ2)[55]
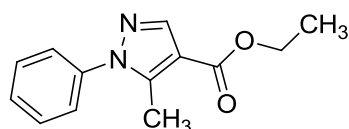
Ethyl 2-((dimethylamino)methylene)-3-oxobutanoate **2** (234 mg, 1.27 mmol) and phenyl hydrazine (0.13 mL, 1.27 mmol) were dissolved in ethanol (5 mL) and refluxed for 2 hours. The mixture was evaporated under reduced pressure and the resulting residue was dissolved in ethyl acetate (40 mL), washed with saturated aqueous sodium bicarbonate (40 mL) and extracted with ethyl acetate (3 × 10 mL). The organic extracts were combined and dried over anhydrous magnesium sulfate, evaporated under reduced pressure and purified using flash chromatography on silica gel eluting with dichloromethane/petroleum ether, (80:20) to give a brown oil, 64 % yield (187 mg).

^{1}H NMR (300 MHz, CDCl$_3$) δ 8.03 (s, 1H, C*H* of pyrazole), 7.52 – 7.39 (m, 5H, Ar), 4.32 (q, J = 7.1 Hz, 2H, C*H*$_2$), 2.56 (s, 3H, C*H*$_3$), 1.37 (t, J = 7.1 Hz, 3H, CH$_2$C*H*$_3$); **ESI-MS** C$_{13}$H$_{14}$N$_2$O$_2$ Calc. (M + H$^+$) = 231.1128, found (M + H$^+$) = 231.1141; Matches known data.[55]

3.1.4 Synthesis of 5-methyl-1-phenyl-1H-pyrazole-4-carboxylic acid 4 (XQ3)[56]
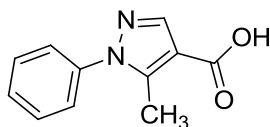
Potassium hydroxide (4.07 mmol, 228 mg) was dissolved in ethanol (2 mL) and added to a solution of ethyl 5-methyl-1-phenyl-1H-pyrazole-4-carboxylate **3** (187 mg, 0.813 mmol) in ethanol (2 mL) and refluxed for 5 hours. The resulting solution was evaporated under reduced pressure and the residue was acidified with a 6 N aqueous hydrochloride solution to a pH of ~ 1. A brown solid separated, which was extracted with ethyl acetate (3 × 10 mL). The organic extracts were combined, dried over anhydrous magnesium sulfate and evaporated under reduced pressure to give a brown solid, 40 % yield (65 mg).

^{1}H NMR (300 MHz, CDCl$_3$) δ 8.13 (s, 1H, C*H* of pyrazole), 7.55 – 7.41 (m, 5H, Ar), 2.59 (s, 3H, C*H*$_3$); **ESI-MS** C$_{11}$H$_{10}$O$_2$N$_2$ Calc. (M + H$^+$) = 203.0815, found (M + H$^+$) = 203.0806; Matches known data.[56]

3.1.5 Synthesis of (5-methyl-1-(4-(trifluoromethyl)phenyl)-1H-pyrazol-4-yl)(4-(5-(trifluoromethyl)pyridin-2-yl)piperazin -1-yl) methanone 5 (XQ5)
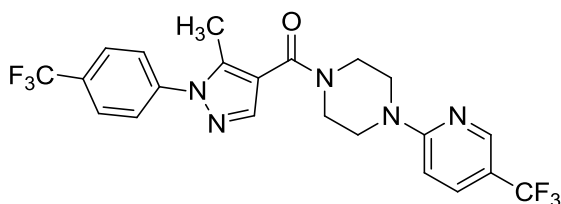
5-Methyl-1-(4-trifluoromethyl-phenyl)-1H-pyrazole-4-carboxylic acid **14** (382 mg, 1.4 mmol), HOBT (246 mg, 1.8 mmol), TBTU (584 mg, 1.8 mmol), anhydrous triethylamine (0.4 mL, 2.5 mmol), and dry dimethylformamide (5 mL) were placed in an oven-dried round bottom flask under a nitrogen atmosphere. The resulting solution was stirred at room temperature for 15 minutes. A second oven-dried round bottom flask was prepared containing 1- (5-trifluoromethyl-2-pyridinyl) piperazine (414 mg, 1.8 mmol) and dry dimethylformamide (5 mL) under a nitrogen atmosphere. The resulting solution was stirred until complete dissolution of the piperazine had occurred. The piperazine solution was then transferred to the first round bottom flask containing the carboxylic acid *via* a syringe. The

resulting solution was stirred for 24 hours, under a nitrogen atmosphere, and monitored by TLC. After 24 hours, the dimethylformamide was removed under reduced pressure and the resulting oil was acidified using a 0.1 N aqueous hydrochloric acid solution. The aqueous mixture was extracted with ethyl acetate (40 mL, followed by 4 × 20 mL). The organic extracts were combined and washed with a saturated aqueous sodium bicarbonate solution (3 × 20 mL) and brine (3 × 20 mL). The organic layer was separated and dried over anhydrous magnesium sulphate and evaporated under reduced pressure. The residue was purified using flash chromatograph on silica gel eluting with dichloromethane/methanol (95:5) to obtain the desired product as a light brown solid, 54 % yield (363 mg).

m.p. 166-170 °C; **^{1}H NMR** (300 MHz, CDCl$_3$) δ 8.43 (s, 1H, C*H* of pyrazole), 7.80 – 7.61 (m, 6H, Ar), 6.70 (d, *J* = 8.9 Hz, 1H, Ar), 3.88 – 3.74 (m, 8H, C*H$_2$*), 2.52 (s, 3H, C*H$_3$*); **^{13}C NMR** (75 MHz, CDCl$_3$) δ 164.5 (*C*=O), 160.1 (*C*-2 of pyridine),145.8 (q, *J* = 12.0 Hz, *C*-6 of pyridine), 141.8 (Ar*C*N), 141.4 (*C*CH$_3$), 139.5 (*C*H of pyrazole), 134.8 (q, *J* = 3 Hz, *C*-4 of pyridine), 130.3 (q, *J* = 33.0 Hz, *C*CF$_3$), 126.5 (q, *J* = 3.7 Hz, Ar*C*H), 125.2 (Ar*C*H), 124.4 (q, *J* = 298.5 Hz, *C*F$_3$), 123.7 (q, *J* = 270.5 Hz, *C*F$_3$), 115.9 (q, *J* = 33.0 Hz, *C*CF$_3$), 116.0 (*C*C=O), 105.8 (*C*-3 of pyridine), 44.8 (*C*H$_2$), 11.9 (*C*H$_3$); **IR (KBr)** 3426, 2869, 1613 (amide), 1559, 1514, 1424, 1325 (tertiary amine), 1242 (CF$_3$), 1170 (tertiary amine), 1130, 1007, 947, 846, 641 cm^{-1}; **ESI-MS** C$_{22}$H$_{19}$F$_6$N$_5$O Calc. (M + H$^+$) = 484.1567, found (M + H$^+$) = 484.1590.

3.1.6 Synthesis of (5-ethyl-1-phenyl-1H-pyrazol-4-yl)-[4-(5-trifluoromethyl-pyridin-2-yl)-piperazin-1-yl]-methanone 6 (XQ6)
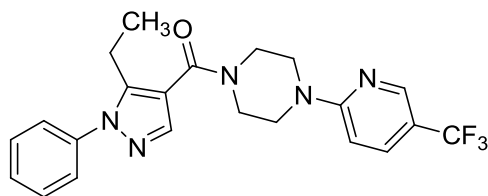
5-Ethyl-1-phenyl-1H-pyrazole-4-carboxylic acid **15** (67 mg, 0.31 mmol), HOBt (53 mg, 0.39 mmol), TBTU (127 mg, 0.39 mmol), anhydrous triethylamine (0.1 ml, 0.72 mmol) and dry dimethylformamide (2 mL) were placed in an oven-dried Schlenk tube under a nitrogen atmosphere. The resulting solution was stirred at room temperature for 15 minutes. A second oven-dried Schlenk tube was prepared containing 1-(5-trifluoromethyl-2-pyridinyl) piperazine (90 mg, 0.39 mmol) and dry dimethylformamide (4 mL) under a nitrogen atmosphere. The resulting solution was stirred until complete dissolution of the piperazine had occurred. The piperazine solution was then transferred, *via* a cannula, to the first Schlenk tube containing the carboxylic acid. The resulting solution was stirred for 24 hours, under a nitrogen atmosphere, and monitored by TLC. After 24 hours, the dimethylformamide was

removed under reduced pressure and the resulting oil was acidified using a 0.1 N aqueous hydrochloric acid solution. The aqueous mixture was extracted with ethyl acetate (40 mL, followed by 4 × 10 mL), the organic extracts were combined and washed with a saturated aqueous sodium bicarbonate solution (3 × 30 mL) and brine (3 × 20 mL). The organic layer was separated, dried over anhydrous magnesium sulphate and evaporated under reduced pressure. The residue was purified using flash chromatograph on silica gel eluting with dichloromethane/methanol (95:5) to give an off white solid, 33 % yield (442 mg).

m.p. 147-149 ^{o}C; **^{1}H NMR** (300 MHz, CDCl$_3$) δ 8.43 (s, 1H, CH of pyrazole), 7.70 – 7.65 (m, 3H Ar), 7.55 – 7.41 (m, 5H, Ar), 3.88 – 3.85 (m, 4H, NCH_2), 3.76 – 3.72 (m, 4H, NCH_2), 2.89 (q, J = 7.5 Hz, 2H, CH_2CH$_3$), 1.11 (t, J = 7.5 Hz, 3H, CH$_2$CH_3); **^{13}C NMR** (75 MHz, CDCl$_3$) δ 164.8 (C=O), 160.1 (C-2 of pyridine), 146.9 (ArC), 145.6 (q, J = 4.5 Hz, C-6 of pyridine), 139.1 (CCH$_2$CH$_3$), 138.5 (CH of pyrazole), 134.5 (q, J = 3.3 Hz, C-4 of pyridine), 129.2 (ArCH), 128.7 (ArCH), 125.7 (ArCH), 124.5 (q, J = 268.8 Hz, CF$_3$), 115.5 (q, J = 32.5 Hz, CCF$_3$), 114.2 (CC=O), 105.8 (C-3 of pyridine), 44.7 (CH$_2$), 18.4 (CH$_2$CH$_3$), 13.7 (CH$_3$); **IR (KBr)** 3454, 2977, 2925, 1610 (amide), 1552, 1505, 1417, 1332 (tertiary amine), 1245 (CF$_3$), 1163(tertiary amine), 1080, 1010, 968, 835, 766, 695, 493 cm^{-1}. **ESI-MS** C$_{22}$H$_{22}$F$_3$N$_5$O Calc. (M + H^{+}) = 430.1849, found (M + H^{+}) = 430.1871.

3.1.7 Synthesis of (5-methyl-1-phenyl-1H-pyrazol-4-yl)-[4-(4-trifluoromethyl-phenyl)-piperazin-1-yl]-methanone 7 (XQ7)
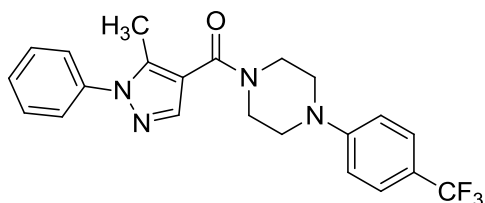
5-Methyl-1-phenyl-1H-pyrazole-4-carboxylic acid **4** (72 mg, 0.36 mmol), HOBT (62 mg, 0.46 mmol), TBTU (150 mg, 0.46 mmol), triethylamine (0.1 mL, 0.6 mmol), and dry dimethylformamide (1 mL) were placed in an oven-heated round bottom flask under a nitrogen atmosphere. The resulting solution was stirred at room temperature for 15 minutes. A second oven-heated round bottom flask was prepared containing (5-methyl-1-phenyl-1H-pyrazol-4-yl)-[4-(4-trifluoromethyl-phenyl)-piperazin-1-yl]-methanone (106 mg, 0.46 mmol) and dry dimethylformamide (1 mL) under a nitrogen atmosphere. The resulting solution was stirred until complete dissolution of the piperazine had occurred. The piperazine solution was then transferred to the first round bottom flask containing the carboxylic acid *via* a syringe. The resulting solution was stirred for 24 hours, under a nitrogen atmosphere, and monitored by TLC. After 24 hours, the dimethylformamide was removed under reduced pressure and the resulting oil was acidified using a 0.1 N aqueous

hydrochloric acid solution. The aqueous mixture was extracted with ethyl acetate (40 mL, followed by 4 × 20 mL), the organic extracts were combined and washed with a saturated aqueous sodium bicarbonate solution (3 × 20 mL) and brine (3 × 20 mL). The organic layer was separated, dried over anhydrous magnesium sulphate and evaporated under reduced pressure. The residue was purified using flash chromatograph on silica gel eluting with dichloromethane/methanol (95:5) to obtain the desired product as a light yellow solid, 60 % yield (89 mg).

m.p. 218-222 °C; **¹H NMR** (300 MHz, CDCl3) δ 7.69 (s, 1H, C*H* of pyrazole), 7.56 – 7.42 (m, 7H, Ar), 6.96 (d, *J* = 8.7 Hz, 2H, Ar), 3.90 (dd, *J* = 6.5, 3.8 Hz, 4H, C*H₂*), 3.35 (dd, *J* = 6.5, 3.8 Hz, 4H, C*H₂*), 2.46 (s, 3H, C*H₃*); **¹³C NMR** (75 MHz, CDCl₃) δ 164.8 (*C*=O), 153.0 (Ar*C*N(CH₂)₂), 141.3 (*C*CH₃), 139.0 (Ar*C*N), 138.9 (*C*H of pyrazole), 129.3 (Ar*C*H), 128.5 (Ar*C*H), 126.5 (q, *J* = 5.8 Hz, *C*HCCF₃), 125.3 (Ar*C*H), 124.6 (q, *J* = 269.0 Hz, *C*F₃), 121.4 (q, *J* = 32.5 Hz, *C*CF₃), 115.1 (Ar*C*H), 48.5 (*C*H₂), 11.8 (*C*H₃); **IR (KBr)** 3418, 2839, 1626 (amide), 1560, 1503, 1426, 1332 (tertiary amine), 1232 (CF₃), 1160 (tertiary amine), 1100, 1065, 1004, 872, 766, 695, 641 cm⁻¹; **ESI-MS** C₂₂H₂₁F₃N₄O Calc. (M + H⁺) = 415.1740, found (M + H⁺) = 415.1756.

3.1.8 Synthesis of [1-(4-methoxy-phenyl)-5-methyl-1H-pyrazol-4-yl]-[4-(5-trifluoromethyl-pyridin-2-yl)-piperazin-1-yl] –methanone 8 (XQ8)
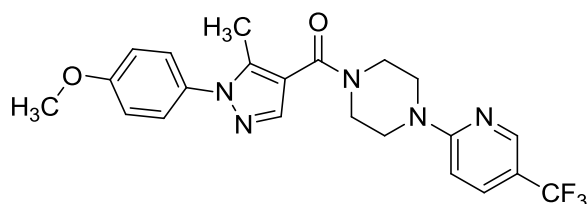
1-(4-Methoxy-phenyl)-5-methyl-1H-pyrazole-4-carboxylic acid **16** (342 mg, 1.47 mmol), HOBT (249 mg, 1.47 mmol), TBTU (597 mg, 1.47 mmol), anhydrous triethylamine (0.5 mL, 3.1 mmol), and dry dimethylformamide (5 mL) were placed in an oven-heated round bottom flask under a nitrogen atmosphere. The resulting solution was stirred at room temperature for 15 minutes. A second oven-heated round bottom flask was prepared containing 1-(5-trifluoromethyl-2-pyridinyl) piperazine (423 mg, 1.8 mmol) and dry dimethylformamide (5 mL) under a nitrogen atmosphere. The resulting solution was stirred until complete dissolution of the piperazine had occurred. The piperazine solution was then transferred to the first round bottom flask containing the carboxylic acid *via* a syringe. The resulting solution was stirred for 24 hours, under nitrogen atmosphere, and monitored by TLC. After 24 hours, the dimethylformamide was removed under reduced pressure and the resulting oil was

acidified using a 0.1 N aqueous hydrochloric acid solution. The aqueous mixture was extracted with ethyl acetate (40 mL, followed by 4 × 20 mL), the organic extracts were combined and washed with a saturated aqueous bicarbonate solution (3 × 20 mL) and brine (3 × 20 mL). The organic layer was separated, dried over magnesium sulphate and evaporated under reduced pressure. The resulting residue was purified using flash chromatograph on silica gel with dichloromethane/methanol (95:5) to obtain the desired product as a white solid, 54 % yield (350 mg).

m.p. 184-188 °C; **^{1}H NMR** (300 MHz, CDCl$_3$) δ 8.43 (s, 1H, C*H* of pyrazole), 7.70 – 7.65 (m, 2H, Ar), 7.35 (dd, *J* = 9.5, 2.8 Hz, 2H, Ar), 7.01 (dd, *J* = 9.5, 2.8 Hz, 2H, Ar), 6.68 (d, *J* = 9.0 Hz, 1H, Ar), 3.87 (s, 3H, OC*H$_3$*), 3.86 – 3.81 (m, 4H, C*H$_2$*), 3.79 – 3.73 (m, 4H, C*H$_2$*), 2.42 (s, 3H, C*H$_3$*); **^{13}C NMR** (75 MHz, CDCl$_3$) δ 165.0 (*C*=O), 160.1 (*C*), 159.6 (*C*), 145.8 (q, *J* = 4.5 Hz, *C*-6 of pyridine), 141.5 (*C*CH$_3$), 138.5 (*C*H of pyrazole), 134.8 (q, *J* = 3.0 Hz, *C*-4 of pyridine), 132.0 (Ar*C*N), 126.8 (Ar*C*H), 124.4 (q, *J* = 273.3 Hz, *C*F$_3$), 116.2 (q, *J* = 33.8 Hz, *C*CF$_3$), 114.7 (*C*C=O), 114.4 (Ar*C*H), 105.8 (*C*-3 of pyridine), 116.2 (*C*-CF$_3$), 55.6 (O-*C*H$_3$), 44.9 (*C*H$_2$), 11.6 (*C*H$_3$); **IR (KBr)** 3482, 3003, 2840, 1606 (amide), 1558, 1519, 1425, 1329 (tertiary amine), 1244 (CF$_3$), 1172 (OCH$_3$), 1115 (tertiary amine), 1036 (OCH$_3$), 1001, 994, 834, 761, 633, 541, 478 cm^{-1}; **ESI-MS** C$_{22}$H$_{22}$F$_3$N$_5$O$_2$ Calc. (M + H$^+$) = 446.1798, found (M + H$^+$) = 446.1819.

3.1.9 Synthesis of

[1-(4-chloro-phenyl)-5-methyl-1H-pyrazol-4-yl]-[4-(5-trifluoromethyl-pyridin-2-yl)-piperazin-1-yl]- methanone 9 (XQ9)
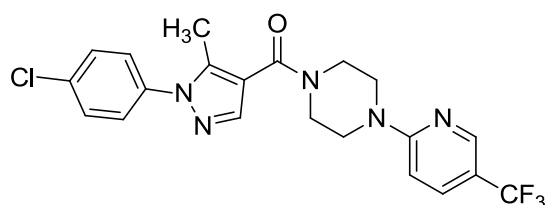
1-(4-Chloro-phenyl)-5-methyl-1H-pyrazole-4-carboxylic acid **17** (542 mg, 2.3 mmol), HOBT (394 mg, 3 mmol), TBTU (952 mg, 3 mmol), anhydrous triethylamine (0.7 mL, 4.6 mmol), and dry dimethylformamide (7 mL) were placed in an oven-heated round bottom flask under a nitrogen atmosphere. The resulting solution was stirred at room temperature for 15 minutes. A second oven-heated round bottom flask was prepared containing 1-(5-trifluoromethyl-2-pyridinyl) piperazine (673 mg, 3 mmol) and dry dimethylformamide (7 mL) under a nitrogen atmosphere. The resulting solution was stirred until complete dissolution of the piperazine had occurred. The piperazine solution was then transferred to the first round bottom flask containing the carboxylic acid *via* a syringe. The resulting solution was stirred for 24 hours, under a nitrogen atmosphere, and monitored by TLC. After 24 hours,

the dimethylformamide was removed under reduced pressure and the resulting oil was acidified using a 0.1 N aqueous hydrochloric acid solution. The aqueous mixture was extracted with ethyl acetate (40 mL, followed by 4 × 20 mL), the organic extracts were combined and washed with a saturated aqueous bicarbonate solution (3 × 20 mL) and brine (3 × 20 mL). The organic layer was separated, dried over anhydrous magnesium sulphate and evaporated under reduced pressure. The resulting residue was purified using flash chromatograph on silica gel with dichloromethane/methanol (95:5) to obtain the desired product as a white solid, 62 % yield (643 mg).

m.p. 186-190 $^{\circ}$C; **^{1}H NMR** (300 MHz, CDCl$_3$) δ 8.42 (s, 1H, C*H* of pyrazole), 7.70 – 7.66 (m, 2H, Ar), 7.50 – 7.38 (m, 4H, Ar), 6.69 (d, *J* = 9.0 Hz, 1H, Ar), 3.88 – 3.83 (m, 4H, C*H*$_2$), 3.77 – 3.73 (m, 4H, C*H*$_2$), 2.46 (s, 3H, C*H*$_3$); **^{13}C NMR** (75 MHz, CDCl$_3$) δ 164.7 (*C*=O), 160.1 (*C*-2 of pyridine), 145.6 (q, *J* = 17 Hz, *C*-6 of pyridine), 141.4 (*C*CH$_3$), 139.1 (*C*H of pyrazole), 137.5 (Ar*C*N), 134.8 (q, *J* = 3.3 Hz, *C*-4 of pyridine), 134.4 (*C*Cl), 129.5 (Ar*C*H), 126.5 (Ar*C*H), 115.5 (*C*C=O), 105.8 (*C*-3 of pyridine), 124.4 (q, *J* = 268.8 Hz, *C*F$_3$), 115.9 (q, *J* = 32.8 Hz, *C*CF$_3$), 44.8 (*C*H$_2$), 11.8 (*C*H$_3$); **IR (KBr)** 3506, 3059, 2912, 1618 (amide), 1558, 1504, 1470, 1422, 1333 (tertiary amine), 1246 (CF$_3$), 1168, 1119 (tertiary amine), 1081, 1003, 947, 814, 749 (Cl), 665, 629, 529, 478 cm^{-1}; **ESI-MS** C$_{21}$H$_{19}$ClF$_3$N$_5$O Calc. (M + H$^+$) = 450.1303, found (M + H$^+$) = 450.1326

3.1.10 Synthesis of ethyl 5-methyl-1-(4-trifluoromethyl-phenyl)-1H-pyrazole-4-carboxylic acid ethyl ester 10 (XQ5b)[57]
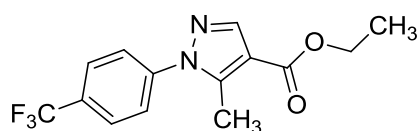
Ethyl 2-((dimethylamino)methylene)-3-oxobutanoate **2** (600 mg, 3.24 mmol) and 4-trifluoromethylphenylhydrazine (570 mg, 3.24 mg) were dissolved in ethanol (20 mL) and refluxed for 2 hours. The mixture was evaporated under reduced pressure and the resulting residue was dissolved in ethyl acetate (20 mL), washed with saturated aqueous sodium bicarbonate solution (20 mL) and extracted with ethyl acetate (3 × 15 mL). The organic extracts were combined, dried over anhydrous magnesium sulfate and evaporated under reduced pressure. The resulting residue was purified using flash chromatography on silica gel eluting with ethyl acetate/petroleum ether (80:20) to obtain the desired product as a brown solid, 32 % yield (309 mg).

m.p. 54-58 $^{\circ}$C; **^{1}H NMR** (300 MHz CDCl$_3$) δ 8.06 (s, 1H, C*H* of pyrazole), 7.79 (d, *J* = 9.0 Hz, 2H, Ar), 7.61 (d, *J* = 9.0 Hz, 2H, Ar), 4.34 (q, *J* = 7.1 Hz, 2H, C*H*$_2$CH$_3$), 2.63 (s, 3H, C*H*$_3$), 1.39 (t, *J* = 7.1 Hz, 3H, CH$_2$C*H*$_3$); **ESI-MS** C$_{14}$H$_{13}$N$_2$O$_2$F$_3$ Calc. (M + H$^+$) = 299.1002, found (M + H$^+$) = 299.1013. Matches known data.[57]

3.1.11 Synthesis of ethyl 5-ethyl-1-phenyl-1H-pyrazole-4-carboxylate 11 (XQ6b) [58]
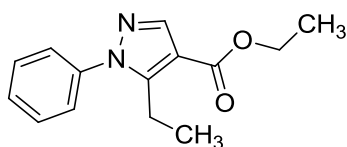
Ethyl 2-((dimethylamino)methylene)-3-oxopentanoate **41** (375 mg, 1.88 mmol), and phenyl hydrazine (0.185 mL, 1.88 mmol) were dissolved in ethanol (10 mL) and refluxed for 2 hours. The mixture was evaporated under reduced pressure and the resulting residue was dissolved in ethyl acetate (20 mL), washed with saturated aqueous sodium bicarbonate solution (20 mL) and extracted with ethyl acetate (3 × 20 mL). The organic extracts were combined and dried over anhydrous magnesium sulfate and evaporated under reduced pressure to give a red oil, 85 % yield (390 mg).

^{1}H NMR (300 MHz, CDCl$_3$) δ 8.03 (s, 1H, C*H* of pyrazole), 7.49 – 7.38 (m, 5H, Ar), 4.33 (q, *J* = 7.1 Hz, 2H, OC*H*$_2$CH$_3$), 2.95 (q, *J* = 7.5 Hz, 2H, C*H*$_2$CH$_3$), 1.37 (t, *J* = 7.1 Hz, 3H, OCH$_2$C*H*$_3$), 1.17 (t, *J* = 7.5 Hz, 3H, CH$_2$C*H*$_3$). Matches know data.[58]

3.1.12 Synthesis of ethyl 1-(4-methoxyphenyl)-5-methyl-1H-pyrazole-4-carboxylate 12 (XQ8b)[55]
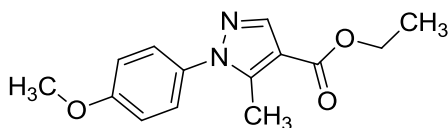
Ethyl 2-((dimethylamino)methylene)-3-oxobutanoate **2** (608 mg, 3.3 mmol) and (4-methoxy-phenyl)-hydrazine (456 mg, 3.3 mmol) were dissolved in ethanol (15 mL) and refluxed for 2 hours. The mixture was evaporated under reduced pressure and the resulting residue was dissolved in ethyl acetate (10 mL), washed with a saturated aqueous sodium bicarbonate solution and extracted with ethyl acetate (3 × 20 mL). The organic extracts were combined, dried over anhydrous magnesium sulfate and evaporated under reduced pressure to

give a yellow oil, 76 % yield (1.1 g).

^{1}H NMR (300 MHz, CDCl$_3$) δ 7.99 (s, 1H, C*H* of pyrazole), 7.30 (d, *J* = 8.9 Hz, 2H, Ar), 6.96 (d, *J* = 8.9 Hz, 2H, Ar), 4.30 (q, *J* = 7.1 Hz, 2H, C*H*$_2$CH$_3$), 3.81 (s, 3H, OC*H*$_3$), 2.50 (s, 3H, C*H*$_3$), 1.35 (t, *J* = 7.1 Hz, 3H, CH$_2$C*H*$_3$); **ESI-MS** C$_{14}$H$_{16}$N$_2$O$_3$ Calc. (M + H$^+$) = 261.1234, found (M + H$^+$) = 261.1225; Matches know data.[55]

3.1.13 Synthesis of ethyl 1-(4-chlorophenyl)-5-methyl-1H-pyrazole-4-carboxylate 13 (XQ9b)[55]
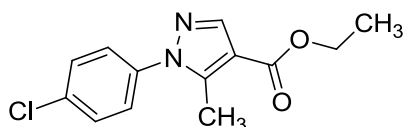
Ethyl 2-((dimethylamino)methylene)-3-oxobutanoate **2** (473 mg, 2.6 mmol) and (4-chloro-phenyl)-hydrazine (465 mg, 2.6 mmol) were dissolved in ethanol (20 mL) and refluxed for 2.5 hours. The resulting solution was evaporated under reduced pressure and the resulting residue was dissolved in ethyl acetate (15 mL), washed with a saturated aqueous sodium bicarbonate solution (3 × 20 mL) and extracted with ethyl acetate (3 × 15 mL). The organic extracts were combined, dried over anhydrous sodium sulfate and evaporated under reduced pressure to give a yellow solid, 94 % yield (647 mg).

m.p. 38-40 $^{\circ}$C; **^{1}H NMR** (300 MHz, CDCl$_3$) δ 8.02 (s, 1H, C*H* of pyrazole), 7.47 (d, *J* = 8.8 Hz, 2H, Ar), 7.38 (d, *J* = 8.8 Hz, 2H, Ar), 4.33 (q, *J* = 7.1 Hz, 2H, *CH*$_2$), 2.57 (s, 3H, C*H*$_3$), 1.37 (t, *J* = 7.1 Hz, 3H, CH$_2$C*H*$_3$); **ESI-MS** C$_{13}$H$_{13}$N$_2$O$_2$Cl Calc. (M + H$^+$) = 265.0738, found (M + H$^+$) = 265.0750. Matches known data.[55]

3.1.14 Synthesis of 5-methyl-1-(4-trifluoromethyl-phenyl)-1H-pyrazole-4-carboxylic acid 14 (XQ5c) [57]
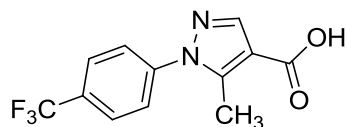
Potassium hydroxide (952 mg, 17 mmol) was dissolved in ethanol (15 mL) and added to a solution of 5-methyl-1-(4-trifluoromethyl-phenyl)-1H-pyrazole-4-carboxylic acid ethyl ester

10 (1.016 g, 3.4 mmol) in ethanol (10 mL) and refluxed for 5 hours. The resulting solution was evaporated under reduced pressure and the residue was acidified with a 6 N aqueous hydrochloride solution to a pH of ~ 1. A brown solid separated, which was extracted by ethyl acetate (3 × 20 mL). The organic extracts were combined, dried over anhydrous magnesium sulfate and evaporated under reduced pressure to give a brown solid, 42 % yield (382 mg).

^{1}H NMR (300 MHz, CDCl$_3$) δ 8.15 (s, 1H, CH of pyrazole), 7.80 (d, J = 8.2 Hz, 2H, Ar), 7.61 (d, J = 8.2 Hz, 2H, Ar), 2.65 (s, 3H, CH_3). Matches known data.[57]

3.1.15 Synthesis of 5-ethyl-1-phenyl-1H-pyrazole-4-carboxylic acid 15 (XQ6c) [56]

Potassium hydroxide (448 mg, 8 mmol) was dissolved in ethanol (15 mL) and added to a solution of ethyl 5-ethyl-1-phenyl-1H-pyrazole-4-carboxylate **11** (390 mg, 1.6 mmol) in ethanol (5 mL), and refluxed for 5 hours. The resulting solution was evaporated under reduced pressure and the residue was acidified with a 6 N aqueous hydrochloride solution to a pH ~ 1. A brown solid separated, which was extracted with ethyl acetate (3 × 20 mL). The organic extracts were combined, dried over anhydrous magnesium sulfate and evaporated under reduced pressure to give a brown solid, 81 % yield (289 mg).

^{1}H NMR (300 MHz, CDCl$_3$) δ 8.13 (s, 1H, CH of pyrazole), 7.55 – 7.40 (m, 5H, Ar), 2.97 (q, J = 7.4 Hz, 2H, CH_2CH$_3$), 1.19 (t, J = 7.4 Hz, 3H, CH$_2$CH_3). Matches known data.[56]

3.1.16 Synthesis of 1-(4-methoxy-phenyl)-5-methyl-1H-pyrazole-4-carboxylic acid 16 (XQ8c)[59]
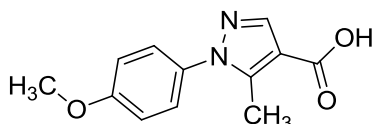
Potassium hydroxide (1.1 g, 20 mmol) was dissolved in ethanol (20 mL) and added to a solution of ethyl 1-(4-methoxyphenyl)-5-methyl-1H-pyrazole-4-carboxylate **12** (1.1 g, 2.5

mmol) in ethanol (5 mL) and refluxed for 5 hours. The resulting solution was evaporated under reduced pressure and the resulting residue was acidified with a 6 N aqueous hydrochloride solution to a pH of ~ 1. A brown solid separated, which was extracted with ethyl acetate (3 ×20 mL). The organic extracts were combined, dried over anhydrous sodium sulfate and evaporated under reduced pressure to give a brown solid, 59 % yield (342 mg).

¹H NMR (300 MHz, CDCl₃) δ 8.09 (s, 1H, C*H* of pyrazole), 7.34 (d, *J* = 8.9 Hz, 2H, Ar), 7.01 (d, *J* = 8.9 Hz, 2H, Ar), 3.87 (s, 3H, OC*H₃*), 2.55 (s, 3H, C*H₃*). Matches known data.[59]

3.1.17 Synthesis of 1-(4-chloro-phenyl)-5-methyl-1H-pyrazole-4-carboxylic acid 17 (XQ9c)[60]
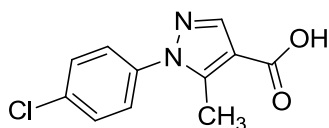
Potassium hydroxide (1.1 g, 19.6 mol) was dissolved in ethanol (15mL) and added to a solution of ethyl 1-(4-chlorophenyl)-5-methyl-1H-pyrazole-4-carboxylate **13** (647 mg, 2.45 mmol) in ethanol (10 mL), and refluxed for 5 hours. The resulting solution was evaporated under reduced pressure and the resulting residue was acidified with a 6 N aqueous hydrochloride solution to a pH of ~ 1. A brown solid separated, which was extracted with ethyl acetate (3 ×20 mL). The organic extracts were combined, dried over anhydrous sodium sulfate and evaporated under reduced pressure to give a brown solid, 94 % yield (542 mg).

¹H NMR (300 MHz, CDCl₃) δ 8.11 (s, 1H, C*H* of pyrazole), 7.44 (dd, *J* = 7.8 Hz, 23.9 Hz, 4H, Ar), 2.59 (s, 3H, C*H₃*). Matches known data.[60]

3.1.18 Synthesis of (5-methyl-1-phenyl-1H-pyrazol-4-yl)-(4-methyl-piperazin-1-yl)-methanone 18 (XQ13)
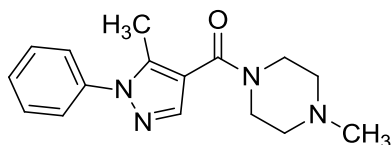
5-Methyl-1-phenyl-1H-pyrazole-4-carboxylic acid **4** (156 mg, 0.8 mmol), HOBT (132 mg, 1.0 mmol), TBTU (316 mg, 1.0 mmol), anhydrous triethylamine (0.22 mL, 1.4 mmol), and dry dimethylformamide (3 mL) were placed in an oven-heated round bottom flask under a nitrogen atmosphere. The resulting solution was stirred at room temperature for 15 minutes.

A second oven-heated round bottom flask was prepared containing 1-methyl-piperazine (0.11 mL, 1.0 mmol) and dry dimethylformamide (2 mL) under a nitrogen atmosphere. The resulting solution was stirred until complete dissolution of the piperazine had occurred. The piperazine solution was then transferred to the first round bottom flask containing the carboxylic acid *via* a syringe. The resulting solution was stirred for 24 hours, under a nitrogen atmosphere, and monitored by TLC. After 24 hours, the dimethylformamide was removed under reduced pressure and the resulting oil was acidified using a 0.1 N aqueous hydrochloric acid solution. The aqueous mixture was extracted with ethyl acetate (40 mL, followed by 4 × 20 mL), the organic extracts were combined and washed with a saturated aqueous bicarbonate solution (3 × 20 mL) and brine (3 × 20 mL). The organic layer was separated, dried over anhydrous magnesium sulphate and evaporated under reduced pressure. The resulting residue was purified using flash chromatograph on silica gel with dichloromethane/methanol (95:5) to obtain the desired product as a brown solid, 51 % yield (112 mg).

m.p. 132-134 $^{\circ}$C; ^{1}**H NMR** (300 MHz, CDCl$_3$) δ 7.65 (s, 1H, C*H* of pyrazole), 7.43 – 7.28 (m, 5H, Ar), 3.67 – 3.64 (m, 4H, C*H$_2$*), 2.39 – 2.36 (m, 4H, C*H$_2$*), 2.35 (s, 3H, C*H$_3$*) 2.25 (s, 3H, C*H$_3$*). ^{13}**C NMR** (75 MHz, CDCl$_3$) δ 164.6 (*C*=O), 140.8 (*C*CH$_3$), 139.1 (Ar*C*), 138.9 (*C*H of pyrazole), 129.2 (Ar*C*H), 128.4 (Ar*C*H), 125.3 (Ar*C*H), 115.6 (*C*C=O), 55.2 (*C*H$_2$), 46.1 (N*C*H$_3$), 11.7 (*C*H$_3$); **IR (KBr)** 3433, 2936, 2790, 1599 (amide), 1558, 1439, 1265, 1200 (tertiary amine), 1149 (tertiary amine), 1008, 939, 899, 878, 767, 696, 658, 600, 511 cm^{-1}; **ESI-MS** C$_{16}$H$_{20}$N$_4$O Calc. (M + H$^+$) = 285.1710, found (M + H$^+$) = 285.1711.

3.1.19 Synthesis of

(5-methyl-1-phenyl-1H-pyrazol-4-yl)-(4-phenyl-piperazin-1-yl)-methanone 19 (XQ14)
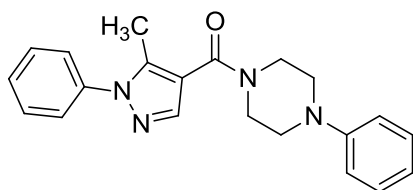
5-Methyl-1-phenyl-1H-pyrazole-4-carboxylic acid **4** (331 mg, 1.4 mmol), HOBT (246 mg, 1.9 mmol), TBTU (591 mg, 1.9 mmol), triethylamine (0.45 mL, 2.8 mmol), dry dimethylformamide (5 mL) were placed in an oven-heated round bottom flask under a nitrogen atmosphere. The resulting solution was stirred at room temperature for 15 minutes. A second oven-heated round bottom flask was prepared containing 1-phenyl-piperazine (0.3 mL, 1.9 mmol) and dry dimethylformamide (2 mL) under a nitrogen atmosphere. The resulting solution was stirred until complete dissolution of the piperazine had occurred. The piperazine solution was then transferred to the first round bottom flask containing the

carboxylic acid *via* a syringe. The resulting solution was stirred for 24 hours, under a nitrogen atmosphere, and monitored by TLC. After 24 hours, the dimethylformamide was removed under reduced pressure and the resulting oil was acidified using a 0.1 N aqueous hydrochloric acid solution. The aqueous mixture was extracted with ethyl acetate (40 mL, followed by 4 × 20 mL), the organic extracts were combined and washed with a saturated aqueous sodium bicarbonate solution (3 × 20 mL) and brine (3 × 20 mL). The organic layer was separated, dried over anhydrous magnesium sulphate and evaporated under reduced pressure. The resulting residue was purified using flash chromatograph on silica gel with dichloromethane/methanol (95:5) to obtain the desired product as a yellow solid, 52 % yield (259 mg).

m.p. 140-144 $^{\circ}$C; **^{1}H NMR** (300 MHz, CDCl$_3$) δ 7.70 (s, 1H, C*H* of pyrazole), 7.54 – 7.41 (m, 5H, Ar), 7.33 – 7.27 (m, 2H, Ar), 6.98 – 6.90 (m, 3H, Ar), 3.91 – 3.88 (m, 4H, C*H$_2$*), 3.26 – 3.23 (m, 4H, C*H$_2$*), 2.45 (s, 3H, C*H$_3$*); **^{13}C NMR** (75 MHz, CDCl$_3$) δ 150.96, 139.0 (*C*H of pyrazole), 129.3 (Ar*C*H), 128.6 (Ar*C*), 125.5 (Ar*C*H), 120.6 (Ar*C*H), 116.7 (Ar*C*H), 115.4 (*C*C=O), 49.9 (*C*H$_2$), 11.7 (*C*H$_3$); **IR (KBr)** 3414, 2836, 1726, 1613 (amide), 1503, 1438, 1228 (tertiary amine), 1156, 1007, 871, 757, 695, 523 cm^{-1}; **ESI-MS** C$_{21}$H$_{23}$N$_4$O (M + H$^+$) = 347.1866, found (M + H$^+$) = 347.1875.

3.1.20 Synthesis of 5-methyl-1-phenyl-1H-pyrazole-4-carboxylic acid dimethylamide 20 (XQ25)
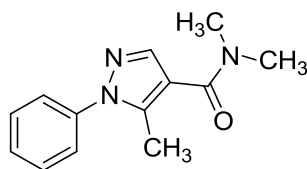
5-Methyl-1-phenyl-1H-pyrazole-4-carboxylic acid **4** (963 mg, 4.8 mmol), HOBT (851 mg, 6.3 mmol), TBTU (2 g, 6.3 mmol), anhydrous triethylamine (0.9 mL, 6.3 mmol), and dry dimethylformamide (10 mL) were placed in an oven-heated round bottom flask under a nitrogen atmosphere. The resulting solution was stirred at room temperature for 15 minutes. Dimethylamine (0.8 mL, 6.3 mmol) was added to the solution *via* a syringe. The resulting solution was stirred for 24 hours under a nitrogen atmosphere, and monitored by TLC. After 24 hours, the dimethylformamide was removed under reduced pressure and the resulting oil was acidified using a 0.1 N aqueous hydrochloric acid solution. The aqueous mixture was extracted with ethylacetate (40 mL, followed by 4 × 20 mL), the organic extracts were combined and washed with a saturated aqueous sodium bicarbonate solution (3 × 20 mL) and brine (3 × 20 mL). The organic layer was separated, dried over anhydrous magnesium sulphate and evaporated under reduced pressure. The residue was purified using flash

chromatograph on silica gel with ethyl acetate/petroleum ether (80:20) to obtain the desired product as a white solid, 31 % yield (240 mg).

m.p. 144-148 ^{o}C; **^{1}H NMR** (300 MHz, CDCl$_3$) δ 7.70 (s, 1H, C*H* of pyrazole), 7.53 − 7.39 (m, 5H, Ar), 3.15 (s, 6H, NC*H$_3$*), 2.45 (s, 3H, C*H$_3$*); **^{13}C NMR** (75 MHz, CDCl$_3$) δ 165.9 (*C*=O), 141.0 (*C*CH$_3$), 139.2 (Ar*C*), 139.1 (*C*H of pyrazole), 129.2 (Ar*C*H), 128.4 (Ar*C*H), 125.3 (Ar*C*H), 77.2 (N(CH$_3$)$_2$), 115.9 (*C*C=O), 11.8 (*C*H$_3$); **IR (KBr)** 3449, 2936, 1563 (amide), 1507, 1496, 1441, 1385, 1264, 1185, 1069, 948, 904, 761, 696, 657, 576, 515 cm^{-1}; **ESI-MS** C$_{13}$H$_{15}$ON$_3$ Calc. (M + H$^+$) = 230.1288, found (M + H$^+$) = 230.1301.

3.1.21 Synthesis of 5-methyl-1-phenyl-1H-pyrazole-4-carboxylic acid diethylamide 21 (XQ27)
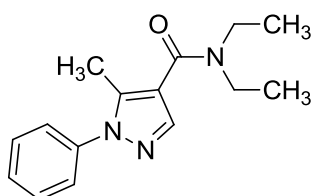
5-Methyl-1-phenyl-1H-pyrazole-4-carboxylic acid **4** (868 mg, 4.3 mmol), HOBT (702 mg, 5.2 mmol), TBTU (1650 mg, 5.2 mmol), anhydrous triethylamine (0.74 mL, 5.2 mmol), and dry dimethylformamide (7 mL) were placed in an oven-dried round bottom flask under a nitrogen atmosphere. The resulting solution was stirred at room temperature for 15 minutes. Diethylamine (0.55 mL, 5.2 mmol) was added to the solution *via* a syringe. The resulting solution was stirred for 24 hours under a nitrogen atmosphere, and monitored by TLC. After 24 hours, the dimethylformamide was removed under reduced pressure and the resulting oil was acidified using a 0.1 N aqueous hydrochloric acid solution. The aqueous mixture was extracted with ethyl acetate (40 mL, followed by 4 × 20 mL), the organic extracts were combined and washed with a saturated aqueous sodium bicarbonate solution (3 × 20 mL) and brine (3 × 20 mL). The organic layer was separated, dried over anhydrous magnesium sulphate and evaporated under reduced pressure. The resulting residue was purified using flash chromatograph on silica gel with ethyl acetate/petroleum ether (80:20) to obtain the desired product as a yellow oil, 46 % yield (503 mg).

R$_f$: 0.45 (ethyl acetate/petroleum ether, 80:20); **^{1}H NMR** (300 MHz, , CDCl$_3$) δ 7.66 (s, 1H, C*H* of pyrazole), 7.52 − 7.35 (m, 5H, Ar), 3.51 (q, *J* = 7.1 Hz, 4H, C*H$_2$*), 2.42 (s, 3H, C*H$_3$*), 1.22 (t, *J* = 7.1 Hz, 6H, CH$_2$C*H$_3$*); **^{13}C NMR** (75 MHz, CDCl$_3$) δ 165.0 (*C*=O), 140.3 (*C*CH$_3$), 139.1 (Ar*C*), 137.8 (*C*H of pyarzole), 129.0 (Ar*C*H), 128.1 (Ar*C*H), 125.1 (Ar*C*H), 116.5 (*C*C=O), 42.9 (*C*H$_2$), 39.8 (*C*H$_2$), 13.8 (CH$_2$*C*H3), 11.6 (*C*H$_3$); **Liquid IR (dichloromethane)** 3441, 2979, 1616 (amide), 1561, 1477, 1432, 1383, 1265, 1084, 736, 448 cm^{-1}; **ESI-MS**

$C_{15}H_{19}ON_3$ Calc. $(M + H^+) = 258.1601$, found $(M + H^+) = 258.1622$.

3.2 Synthesis of zinc complexes of compound 3, 18 and 20

3.2.1 Synthesis of 22 (zinc complex of 18 (XQ13))
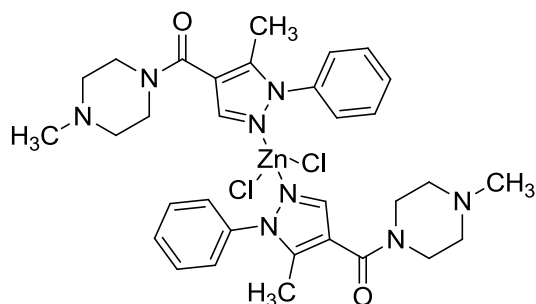
(5-Methyl-1-phenyl-1H-pyrazol-4-yl)-(4-methyl-piperazin-1-yl)-methanone **18** (111 mg, 0.39 mmol) was dissolved in methanol (20 mL). Zinc chloride (28 mg 0.2 mmol) was added and the solution refluxed for 2 hours. The resulting solution was evaporated under reduced pressure, and the resulting residue was dissolved in chloroform. The resulting solution was filtered through a filter paper and the filtrate was evaporated under reduced pressure to give a yellow solid, 99 % yield (137 mg).

m.p. 150-154 ^oC; **^{1}H NMR** (300 MHz, CDCl$_3$) δ 7.65 (s, 2H, C*H* of pyrazole), 7.53 − 7.42 (m, 10H, Ar), 3.84 − 3.81 (m, 8H, C*H*$_2$), 2.47-2.44 (m, 8H, C*H*$_2$), 2.43 (s, 6H, C*H*$_3$) 2.35 (s, 6H, C*H*$_3$); **^{13}C NMR** (75 MHz, CDCl$_3$) δ 164.6 (*C*=O), 141.2 (*C*CH$_3$), 139.0 (*C*H of pyrazole), 138.8 (Ar*C*), 129.3 (Ar*C*H), 128.6 (Ar*C*H), 125.4 (Ar*C*H), 115.1 (*C*C=O), 55.2 (*C*H$_2$), 46.2 (N*C*H$_3$), 11.7 (*C*H$_3$); **IR (KBr)** 3450, 2937, 2794, 1598 (amide), 1558, 1504, 1452, 1396, 1290, 1255, 1233 (tertiary amine), 1142, 1009 (tertiary amine), 938, 877, 765, 698, 658; **Anal. calcd** for $C_{32}H_{40}Cl_2N_8O_2Zn$, C, 54.51; H, 5.72; N, 15.90; found C, 54.39; H, 6.07; N, 15.52.

3.2.2 Synthesis of 23 (zinc complex of 20(XQ25))
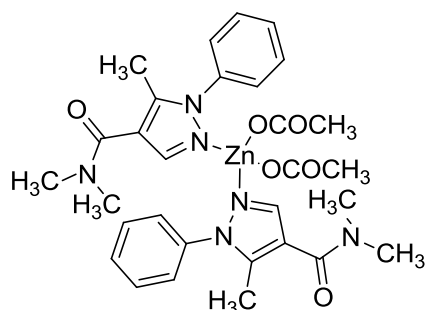
5-Methyl-1-phenyl-1H-pyrazole-4-carboxylic acid dimethylamide **20** (115 mg, 0.5 mmol) was dissolved in methanol (10 mL). Zinc acetate (66 mg, 0.3 mmol) in methanol (5 mL) was added drop wise and the solution was refluxed for 2 hours. The resulting solution was evaporated under reduced pressure and residue recrystallized from methanol to give a white solid, 77 % yield (140 mg).

m.p. 152-154 $^\circ$C (methanol); **^{1}H NMR** (300 MHz, CDCl$_3$) δ 7.71 (s, 2H, C*H* of pyrazole), 7.54 – 7.41 (m, 10H, Ar), 3.47 (s, 6H, C(O)C*H*$_3$), 3.17 (s, 12H, NC*H*$_3$), 2.18 (s, 6H, C*H*$_3$); **^{13}C NMR** (75 MHz, CDCl$_3$) δ 207.5 (*C*(O)CH$_3$), 165.9 (*C*=O), 141.2 (*C*CH$_3$), 139.1 (*C*H of pyrazole), 138.9 (Ar*C*), 129.3 (Ar*C*H), 128.5 (Ar*C*H), 125.4 (Ar*C*H), 115.7 (*C*C=O), 50.6 (N*C*H$_3$), 31.0 (C(O)*C*H$_3$), 11.8 (*C*H$_3$); **IR (KBr)** 3424, 3053, 2936, 2805, 1609 (amide), 1598, 1563, 1507, 1496, 1453, 1392, 1263, 1215, 1185, 1174, 1068, 948, 904, 761, 696, 657, 576, 515 cm^{-1}; **Anal. calcd** for C$_{30}$H$_{36}$N$_6$O$_6$Zn 2H$_2$O, C, 53.14; H, 5.95; N, 12.39; found C, 53.49; H, 5.49; N, 11.88.

3.2.3 Synthesis of 24 (zinc complex of 3 (XQ2))
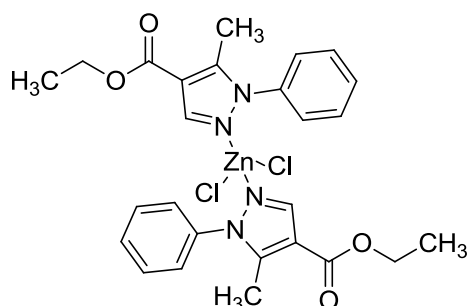
5-Methyl-1-phenyl-1H-pyrazole-4-carboxylic acid ethyl ester **3** (484 mg, 2.10 mmol) was dissolved in methanol (20 mL). Zinc chloride (143 mg 1.05 mmol) was added and the solution refluxed for 2 hours. The resulting solution was evaporated under reduced pressure and the residue recrystallized from chloroform. The desired product was obtained as a brown solid, 98 % yield (607 mg).

m.p. 228-232 $^\circ$C (chloroform); **^{1}H NMR** (300 MHz, CDCl$_3$) δ 8.08 (s, 2H, C*H* of pyrazole), 7.44 – 7.54 (m, 6H, Ar), 7.34 – 7.29 (m, 4H, Ar), 4.38-4.31 (q, *J* = 7.1 Hz, 4H, C*H*$_2$), 2.42 (s, 6H, C*H*$_3$), 1.42-1.37 (t, *J* = 7.1 Hz, 6H, CH$_2$C*H*$_3$); **^{13}C NMR** (75 MHz, CDCl$_3$) δ 162.4 (*C*=O), 146.8 (*C*CH$_3$), 143.5 (*C*H of pyrazole), 135.5 (Ar*C*), 130.7 (Ar*C*H), 129.6 (Ar*C*H), 127.4 (Ar*C*H), 113.1 (*C*C=O), 60.6 (*C*H$_2$), 14.5 (*C*H$_3$), 11.6 (CH$_2$*C*H$_3$); **IR (KBr)** 3423, 2977, 1716 (ester), 1562, 1504, 1401, 1289, 1238 (ester), 1096 (ester), 963, 771, 699, 658, 500 cm^{-1}; **Anal. calcd** for C$_{26}$H$_{28}$Cl$_2$N$_4$O$_4$Zn, C, 52.32; H, 4.73; N, 9.39; found C, 53.13; H, 4.62; N, 9.26.

3.3 Synthesis of pyrazole ligands 25, 29

3.3.1 Synthesis of ethyl 1-(4-fluorophenyl)-5-methyl-1H-pyrazole-4-carboxylate 25 (XQ16)[61]
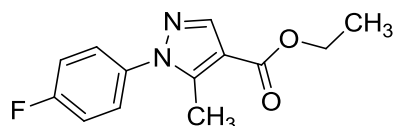
Ethyl 2-((dimethylamino)methylene)-3-oxobutanoate **2** (515 mg, 2.8 mmol) and 4-fluoro-phenyl hydrazine (455 mg, 2.8 mmol) were dissolved in ethanol (20 mL) and refluxed for 2.5 hours. The resulting solution was evaporated under reduced pressure, and the resulting residue was dissolved in ethyl acetate (20 mL), washed with a saturated aqueous sodium bicarbonate solution (3 × 20 mL) and extracted with ethyl acetate (3 ×10 mL). The organic extracts were combined, dried over anhydrous magnesium sulfate and evaporated under reduced pressure to give a brown oil, 47 % yield (353 mg).

^{1}H NMR (300 MHz, CDCl$_3$) δ 8.02 (s, 1H, C*H* of pyrazole), 7.43 – 7.38 (m, 2H, Ar), 7.24 – 7.16 (m, 2H, Ar), 4.33 (q, *J* = 7.1 Hz, 2H, C*H$_2$*), 2.55 (s, 3H, C*H$_3$*), 1,38 (t, *J* = 7.1 Hz, 3H, CH$_2$C*H$_3$*); **ESI-MS** C$_{13}$H$_{13}$O$_2$N$_2$F Calc. (M + H$^+$) = 249.1034, found (M + H$^+$) = 249.1046. Matches known data.[61]

3.3.2 Synthesis of ethyl 1-phenyl-5-propyl-1H-pyrazole-4-carboxylate 29 (XQ23)[56]
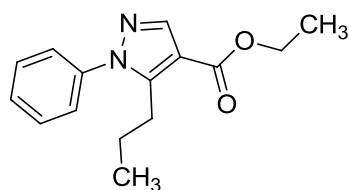
Ethyl 2-((dimethylamino)methylene)-3-oxohexanoate **42** (617 mg, 2.9 mmol) and phenyl hydrazine (0.3 mL, 2.9 mmol) were dissolved in ethanol (20 mL) and refluxed for 2.5 hours. The resulting solution was evaporated under reduced pressure, and the residue was dissolved in ethyl acetate (20 mL), washed with a saturated aqueous sodium bicarbonate solution (3 × 20 mL), and extracted with ethyl acetate (3 × 20 mL). The organic extracts were combined, dried over anhydrous magnesium sulfate and evaporated under reduced pressure to give a light yellow oil, 68 % yield (310 mg).

¹H NMR (300 MHz, CDCl₃) δ 8.04 (s, 1H, C*H* of pyrazole), 7.51 – 7.35 (m, 5H, Ar), 4.32 (q, *J* = 7.1 Hz, 2H, OC*H₂*), 2.92 (t, *J* = 7,8 Hz, 2H, C*H₂*CH₂CH₃), 1.64 – 1.51 (m, 2H, CH₂C*H₂*CH₃), 1.36 (t, *J* = 7.1 Hz, 3H, OCH₂C*H₃*), 0.85 (t, *J* = 7.4 Hz, 3H, CH₂CH₂C*H₃*); **ESI-MS** C₁₅H₁₈N₂O₂ Calc. (2M + Na⁺) = 539.2629, found (2M + Na⁺) = 539.2653. Matches known data.[56]

3.4 Synthesis of zinc complexes of compound 3 family

3.4.1 Synthesis of 30 (zinc complex of 25 (XQ16))
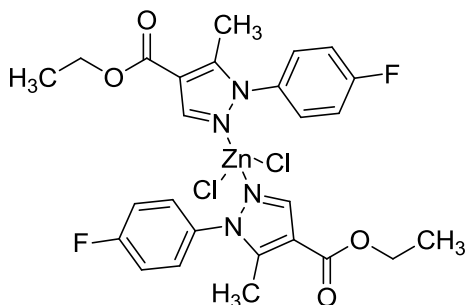
1-(4-Fluoro-phenyl)-5-methyl-1H-pyrazole-4-carboxylic acid ethyl ester **25** (267 mg, 1.07 mmol) was dissolved in methanol (20 mL). Zinc chloride (74 mg, 0.54 mmol) was added and the solution refluxed for 2 hours. The resulting solution was evaporated under reduced pressure and the residue recrystallized from methanol to give a brown solid, 71 % yield (242 mg).

m.p. 58-60 °C (methanol); **¹H NMR** (300 MHz, CDCl₃) δ 8.06 (s, 2H, C*H* of pyrazole), 7.33 – 7.27 (m, 4H, Ar), 7.19 – 7.13 (m, 4H, Ar), 4.35 (q, *J* = 7.2 Hz, 4H, C*H₂*), 2.43 (s, 6H, C*H₃*), 1.39 (t, *J* = 7.1 Hz, 6H, C*H₃*CH₂); **¹³C NMR** (75 MHz, CDCl₃) δ 163.4 (d, *J* = 250.3 Hz, *C*F), 162.3 (*C*=O), 146.9 (*C*CH₃), 143.2 (*C*H of pyrazole), 131.7 (d, *J* = 3.0 Hz, Ar*C*), 129.5 (d, *J* = 9.0 Hz, Ar*C*H), 116.7 (d, *J* = 25.3 Hz, Ar*C*H), 113.2 (*C*C=O), 60.7 (*C*H₂CH₃), 14.3 (CH₂*C*H₃), 11.6 (*C*H₃); **IR (KBr)** 3419, 2984, 1721 (ester), 1563, 1515, 1382, 1293, 1232 (F), 1224 (ester), 1099 (ester), 1011, 845, 777, 629, 579, 514 cm⁻¹; **Anal. calcd for** C₂₆H₂₆Cl₂F₂N₄O₄Zn, C, 49.35; H, 4.14; N, 8.86; found C, 48.56; H, 4.06; N, 8.40.

3.4.2 Synthesis of 31 (zinc complex of 26 (XQ17))
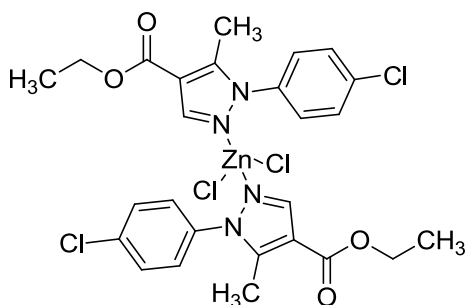
1-(4-Chloro-phenyl)-5-methyl-1H-pyrazole-4-carboxylate **26** (see **13**) (265 mg, 1.1 mmol) was dissolved in methanol (20 mL). Zinc chloride (75 mg, 0.55 mmol) was added and the solution refluxed for 2 hours. The resulting solution was evaporated under reduced pressure to give a pale yellow solid, 100 % yield (340 mg).

m.p. 182-186 $^{\circ}$C; **^{1}H NMR** (300 MHz, CDCl$_3$) δ 8.10 (s, 2H, C*H* of pyrazole), 7.47 – 7.42 (m, 4H, Ar), 7.30 – 7.23 (m, 4H, Ar), 4.35 (q, *J* = 7.1 Hz, 4H, C*H*$_2$CH$_3$), 2.46 (s, 6H, C*H*$_3$), 1.39 (t, *J* = 7.1 Hz, 6H, CH$_2$C*H*$_3$); **^{13}C NMR** (75 MHz, CDCl$_3$) δ 162.4 (*C*=O), 146.5 (*C*CH$_3$), 143.4 (*C*H of pyrazole), 136.6 (Ar*C*), 134.3 (*C*Cl), 129.8 (Ar*C*H), 128.4 (Ar*C*H), 113.4 (*C*C=O), 60.7 (*C*H$_2$), 14.4 (CH$_2$*C*H$_3$), 11.6 (*C*H$_3$); **IR (KBr)** 3412, 3126, 2978, 1717 (ester), 1556, 1501, 1411, 1236 (ester), 1101 (ester), 1010, 963, 836, 777 (Cl), 661, 620, 507; **Anal. calcd** for C$_{26}$H$_{26}$Cl$_4$N$_4$O$_4$Zn, C, 46.91; H, 3.94; N, 8.42; found C, 47.73; H, 3.91; N, 8.34.

3.4.3 Synthesis of 32 (zinc complex of 27 (XQ18))
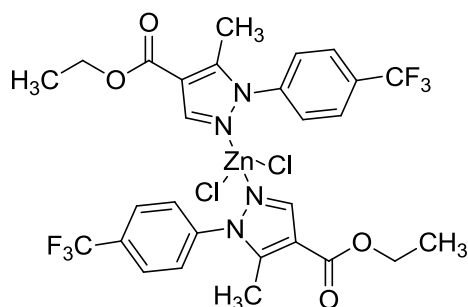
5-Methyl-1-(4-trifluoromethyl-phenyl)-1H-pyrazole-4-carboxylate **27 (**see **10)** (201 mg, 0.56 mmol) was dissolved in methanol (20 mL). Zinc chloride (38 mg, 0.28 mmol) was added and the solution refluxed for 2 hours. The resulting solution was evaporated under reduced pressure and the residue recrystallized from methanol to give a brown solid, 67 % yield (160 mg).

m.p. 150-154 $^{\circ}$C (methanol); **^{1}H NMR** (300 MHz, CDCl$_3$) δ 8.16 (s, 2H, C*H* of pyrazole), 7.78 (d, *J* = 8.2 Hz, 4H, Ar), 7.54 (d, *J* = 8.2 Hz, 4H, Ar), 4.35 (q, *J* = 7.1 Hz, 4H, C*H*$_2$), 2.54 (s, 6H, C*H*$_3$), 1.39 (t, *J* = 7.1 Hz, 6H, CH$_2$C*H*$_3$); **^{13}C NMR** (75 MHz, CDCl$_3$) δ 162.1 (*C*=O), 146.7 (Ar*C*), 143.5 (*C*H of pyrazole), 138.6 (*C*CH$_3$), 132.1 (q, *J* = 33.0 Hz, *C*CF$_3$), 127.7 (Ar*C*H), 126.7 (q, *J* = 3.7 Hz, Ar*C*H), 123.3 (q, *J* = 270.8 Hz, *C*F$_3$), 113.7 (*C*C=O), 60.7 (*C*H$_2$), 14.1 (CH$_2$*C*H$_3$), 11.6 (*C*H$_3$), **IR (KBr)** 3429, 2986, 1722 (ester), 1617, 1561, 1400, 1326 (CF$_3$), 1246 (ester), 1132, 1100 (ester), 1067, 1010, 961, 851, 777, 663, 613, 515 cm^{-1}; **Anal. calcd** for C$_{28}$H$_{26}$Cl$_2$F$_6$N$_4$O$_4$Zn, C, 45.89; H, 3.58; N, 7.65; found C, 46.42; H, 3.79; N, 7.37.

3.4.4 Synthesis of 33 (zinc complex of 28(XQ19))
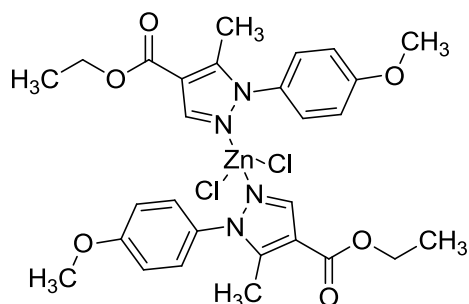
Ethyl 1-(4-methoxyphenyl)-5-methyl-1H-pyrazole-4-carboxylate **28** (see **12**) (213 mg, 0.82 mmol) was dissolved in methanol (20 mL). Zinc chloride (56 mg, 0.41 mmol) was added and the solution refluxed for 2 hours. The resulting solution was evaporated under reduced pressure and the residue recrystallized from chloroform to give a pale brown solid, 52 % yield (140mg).

m.p. 210-214 ^{o}C (chloroform); **^{1}H NMR** (300 MHz, CDCl$_3$) δ 8.09 (s, 2H, C*H* of pyrazole), 7.20 – 7.15 (m, 4H, Ar), 6,94 – 6.89 (m, 4H, Ar), 4.33 (q, *J* = 7.1 Hz, 4H, C*H$_2$*), 3.85 (s, 6H, OC*H$_3$*), 2.39 (s, 6H, C*H$_3$*), 1.38 (t, *J* = 7.1 Hz, 6H, CH$_2$C*H$_3$*); **^{13}C NMR** (75 MHz, CDCl$_3$) δ 162.4 (*C*=O), 161.1 (*C*OCH$_3$), 147.1 (*C*CH$_3$), 143.2 (*C*H of pyrazole), 128.8 (Ar*C*), 127.9 (*C*C=O), 114.5 (Ar*C*H), 112.8 (Ar*C*H), 60.6 (*C*H$_2$), 55.6 (O*C*H$_3$), 14.4 (*C*H$_3$CH$_2$), 11.6 (*C*H$_3$); **IR (KBr)** 3415, 2984, 1724 (ester), 1514, 1382, 1258 (ester), 1229 (ether), 1105 (ester), 1019, 963, 836, 772, 637, 590, 526; **Anal. calcd** for C$_{28}$H$_{32}$Cl$_2$N$_4$O$_6$Zn 2H$_2$O, C, 48.54; H, 5.24; N, 8.09; found C, 48.84; H, 4.30; N, 8.21.

3.4.5 Synthesis of 34 (zinc complex of 29 (XQ23))
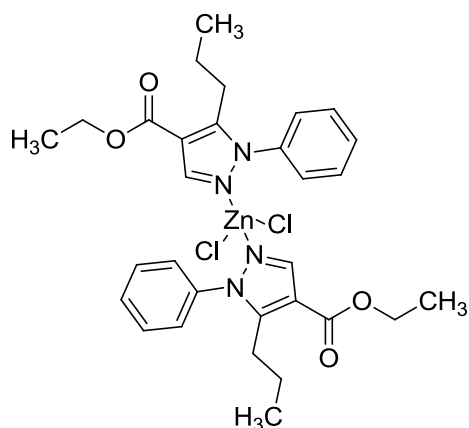
1-Phenyl-5-propyl-1H-pyrazole-4-carboxylate **29** (310 mg, 1.20 mmol) was dissolved in methanol (20 mL). Zinc chloride (83 mg, 0.6 mmol) was added and the solution refluxed for

2 hours. The resulting solution was evaporated under reduced pressure and the residue recrystallized from chloroform to give a white solid, 80 % yield (314 mg).

m.p. 200-204 $^{\circ}$C (chloroform); **^{1}H NMR** (300 MHz, CDCl$_3$) δ 8.05 (s, 2H, C*H* of pyrazole), 7.56 – 7.42 (m, 6H, Ar), 7.31 – 7.23 (m, 4H, Ar), 4.35 (q, *J* = 7.1 Hz, 4H, OC*H*$_2$CH$_3$), 2.84 (t, *J* = 7.8 Hz, 4H, C*H*$_2$CH$_2$CH$_3$), 1.56 – 1.46 (m, 4H, CH$_2$C*H*$_2$CH$_3$), 1.40 (t, *J* = 7.1 Hz, 6H, OCH$_2$C*H*$_3$), 0.84 (t, *J* = 7.4 Hz, 6H, C*H*$_3$CH$_2$CH$_2$); **^{13}C NMR** (75 MHz, CDCl$_3$) δ 162.1 (*C*=O), 150.9 (Ar*C*), 143.6 (*C*H of pyrazole), 135.6 (*C*CH$_2$CH$_3$), 130.7 (Ar*C*H), 129.5 (Ar*C*H), 127.7 (Ar*C*H), 112.5 (*C*C=O), 60.5 (O*C*H$_2$CH$_3$), 26.7 (*C*H$_2$CH$_2$CH$_3$), 22.3 (CH$_2$*C*H$_2$CH$_3$), 14.4 (OCH$_2$*C*H$_3$), 13.8 (CH$_2$CH$_2$*C*H$_3$); **IR (KBr)** 3427, 2971, 1725 (ester), 1555, 1502, 1455, 1380, 1297, 1253 (ester), 1215, 1101 (ester), 979, 765, 694, 646, 510 cm^{-1}; **Anal. calcd** for C$_{30}$H$_{36}$Cl$_2$N$_4$O$_4$Zn, C, 55.18; H, 5.56; N, 8.58; found C, 54.87; H, 5.33; N, 8.25.

3.5   Synthesis of a thiourea substituted pyrazole and its zinc complex

3.5.1 Synthesis of 4-nitro-1H-pyrazole 37 (XQ43)[62]
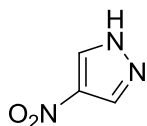
Pyrazole (533 mg, 7.83 mmol) was added in portions to concentrated sulfuric acid (4 mL) while keeping the temperature below 40 $^{\circ}$C using an ice bath. Nitric acid (70 % aqueous solution, 0.55 mL) was added dropwise while maintaining the temperature below 55 $^{\circ}$C, the mixture was then heated at 55 $^{\circ}$C for 5 hours. The resulting solution was slowly poured onto ice and neutralized with 50 % aqueous sodium hydroxide. The resulting slurry was diluted with ethyl acetate (30 mL) and the mixture filtered. The filtrate was washed with distilled water (30 mL), brine (30 mL), dried over anhydrous sodium sulfate, and evaporated under reduced pressure to give a white solid, 60 % yield (534 mg).

^{1}H NMR (300 MHz, DMSO-d_6) δ 13.99 (s, 1H, N*H*), 8.58 (s, 2H, C*H*C); **^{13}C NMR** (75 MHz, DMSO-d_6) δ 135.32 (*C*NO$_2$), 132.32 (*C*HC); **ESI-MS** C$_3$H$_3$N$_3$O$_2$ Calc. (M + Na$^+$) = 136.0117, found (M + Na$^+$) = 136.0124. Matches known data.[62]

3.5.2 Synthesis of 1H-pyrazol-4-ylamine 38 (XQ44)[62]
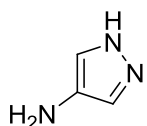
A stirred mixture of iron (773 mg, 13.8 mmol), ammonium chloride (247 mg, 4.6 mmol),

water (1.5 mL) and ethanol (7 mL) was heated to 80 $^{\circ}$C. 4-Nitro-1H-pyrazole **37** (520 mg, 4.6 mmol) was added in portions. The mixture was stirred at 80 $^{\circ}$C for 2 hours after which it was allowed to cool to room temperature. The reaction mixture was diluted with ethyl acetate (30 × 3mL), the resultant mixture was filtered through a pad of celite and the filtrate was evaporated under reduced pressure. In order to remove residual water, the residue was diluted with ethyl acetate (30 mL), dried over anhydrous sodium sulfate, and evaporated under reduced pressure to give a purple red oil, 41 % yield (155 mg).

^{1}H NMR (300 MHz, DMSO-d_6) δ 8.58 (s, 2H, C*H*), 6.99 (s, 2H, N*H*); Matches known data.[62]

3.5.3 Synthesis of 1-phenyl-3-(1H-pyrazol-4-yl)-thiourea 39 (XQ45)
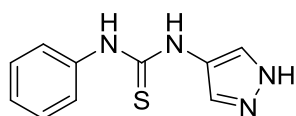
To a solution of 1H-pyrazol-4-ylamine **38** (196 mg, 2.4 mmol) in anhydrous dimethylformamide (8 mL), isothiocyanatobenzene (0.36 mL, 3 mmol) was added under a nitrogen atmosphere. The resulting solution was stirred for 24 hours under a nitrogen atmosphere and then evaporated under reduced pressure and diluted with ethyl acetate (30 mL). The mixture was filtered and the solid obtained was dried to give a grey solid, 16 % yield (82 mg).

m.p. 174-176 $^{\circ}$C; **^{1}H NMR** (300 MHz, DMSO-d_6) δ 12.70 (s, 1H, N*H*-N), 9.57 (s, 2H, C*H* of pyrazole), 7.79 (br, 2H, N*H*C=S), 7.47 – 7.44 (m, 2H, Ar), 7.34 – 7.29 (m, 2H, Ar), 7.14 – 7.09 (m, 1H, Ar); **^{13}C NMR** (75 MHz, DMSO-d_6) δ 179.1 (*C*=S), 139.5 (Ar*C*), 128.3 (*C* of pyrazole), 124.3 (Ar*C*H), 123.7 (Ar*C*H), 79.1 (*C*H of pyrazole); **IR (KBr)** 3448, 3325 (secondary amine), 3225, 2977, 1589, 1549, 1496 (secondary amine), 1370 (C=S), 1309 (secondary amine), 1279 (secondary amine), 1011, 953, 698, 608 cm^{-1}; **ESI-MS** $C_{10}H_{10}N_4S$ Calc. (M + H$^+$) = 219.0699, found 219.0706.

3.5.4 Synthesis of 40 (zinc complex of 39 (XQ45))
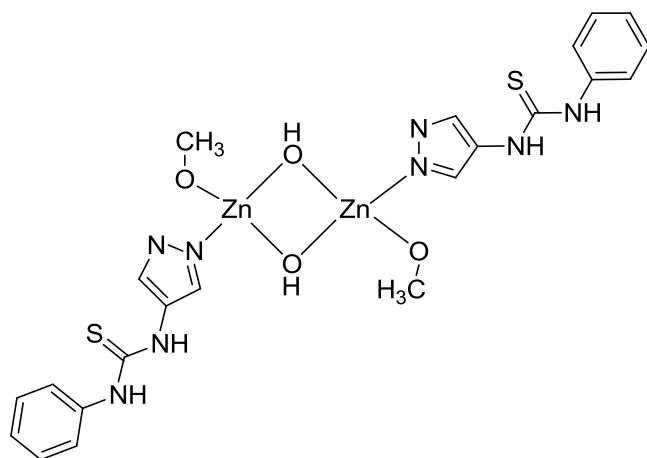
1-Phenyl-3-(1H-pyrazol-4-yl)-thiourea **39** (97 mg, 0.445 mmol) was dissolved in methanol (10 mL) and the solution was heated to 40 ^{o}C to give a clear solution. Zinc acetate (49 mg, 0.223 mmol) was dissolved in methanol (5 mL) and this solution was added drop wise to the thiourea solution. A solid precipitated was generated, which was filtered and dried to give a grey solid, 54 % yield (40 mg).

m.p. > 300 ^{o}C; **^{1}H NMR** (300 MHz, DMSO-d_6) δ 9.97 (br, 2H, NNH), 7.80 (s, 4H, CH of pyrazole), 7.57 – 7.46 (m, 4H, Ar), 7.36 – 7.27 (m, 4H, Ar), 7.11 – 7.06 (m, 2H, Ar), 1.87 (s, 6H, OCH_3); **^{13}C NMR** (75 MHz, DMSO-d_6) δ 139.86 (ArC), 128.20 (C of pyrazole), 123.90 (ArCH), 123.38 (ArCH), 79.12 (CH of pyrazole), 22.80 (OCH$_3$); **IR (KBr)** 3252 (secondary amine), 1592, 1537, 1496 (secondary amine), 1389 (C=S), 1337 (secondary amine), 1198, 1144 (secondary amine), 1071, 1013, 924, 886, 847, 754, 693, 623, 546, 489 cm^{-1}. **Anal. calcd** for $C_{22}H_{28}N_8O_4S_2Zn_2$, C, 39.83; H, 4.25; N, 16.89; found C, 39.81; H, 2.86; N, 17.80.

3.6.1 Synthesis of ethyl 2-((dimethylamino)methylene)-3-oxopentanoate 41 (XQ6a)[56]
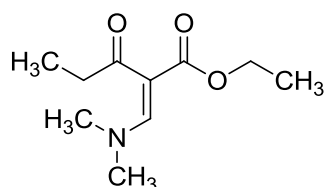
3-Oxo-pentanoic acid ethyl ester (0.6 mL, 4.74 mmol) was stirred at room temperature and dimethoxymethyl-dimethyl-amine (0.76 mL, 4.74 mmol) was added drop wise. The resulting solution was allowed to stir at room temperature for 16 hours. The resulting solution was evaporated under reduced pressure and azetroped with toluene three times (evaporating under reduced pressure) to give a yellow oil, 51 % yield (471 mg). The crude product was used without further purification.

^{1}H NMR (300 MHz, CDCl$_3$) δ 7.57 (s, 1H, C=CH), 4.14 (q, J = 7.1 Hz, 2H, OCH_2), 2.95 (s, 6H, NCH_3), 2.59 (q, J =7.4 Hz, 2H, C(O)CH_2), 1.24 (t, 3H, J = 7.1 Hz, OCH$_2$CH_3), 1.01 (t, 3H, J = 7.4 Hz, CH$_2$CH_3). Matches known data.[56]

3.6.2 Synthesis of ethyl 2-((dimethylamino)methylene)-3-oxohexanoate 42 (XQ22)[54]
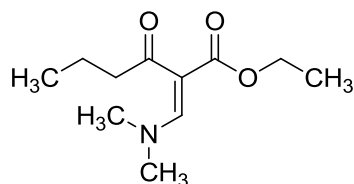
3-Oxo-hexanoic acid ethyl ester (0.4 mL, 2.5 mmol) was stirred at room temperature and dimethoxymethyl–dimethyl–amine (0.42 mL, 3.12 mmol) was added drop wise. The reaction mixture was allowed to stir at room temperature for 16 hours. The resulting solution was evaporated under reduced pressure and then azotroped with toluene three times (evaporating under reduced pressure) to give a yellow oil, 80 % yield (427 mg). The crude product was used without further purification.

R_f value: 0.42 (ethyl acetate/petroleum ether, 80 : 20); **^{1}H NMR** (300 MHz, CDCl$_3$) δ 7.45 (s, 1H, C*H*=C), 4.03 (q, *J* = 7.1 Hz, 2H, OC*H$_2$*CH$_3$), 2.83 (s, 6H, NC*H$_3$*), 2.44 (t, *J* = 7.5 Hz, 2H, C*H$_2$*CH$_2$CH$_3$), 1.43 (dt, *J* = 7.4 Hz, 2H, C(O)CH$_2$C*H$_2$*CH$_3$), 1.13 (t, *J* = 7.1 Hz, 3H, OCH$_2$C*H$_3$*), 0.73 (t, *J* = 7.4 Hz, 3H, C(O)CH$_2$CH$_2$C*H$_3$*). Matches know data.[54]

Chapter 4: Introduction to the synthesis of biphenyl sulfones and their fluorescent properties

4.1 Fluorescence

Fluorescence is a particular case of luminescence. Energy is supplied in the form of electromagnetic radiation resulting in excitation of the molecule from a lower energy state into a higher energy state. We then see decay back to a lower energy state with the release of the energy in the form of light.

In 1819 Edward D. Clarke described fluorescence in fluorites (a halide mineral composed of calcium fluoride).[63] Sir David Brewster described the fluorescence of chlorophyll (a green pigment found in cyanobacteria and the chloroplasts of algae and plants) in 1833[64] and Sir John Herschel described fluorescence of quinine sulfate in 1845.[65] In 1852, George Gabriel Stokes described the ability of fluorites and uranium glass to change invisible light beyond the violet end of the visible light into blue light. "Fluorescence" was named in his seminal paper on the wavelength change of light.[66] Since then fluorescence spectroscopy was developed significantly and been applied to many areas e.g. biochemistry, medicine and analytical chemistry.[70,71] An interesting case is that of the fluorescence reported by Nicolás Monardes in 1565.[67] This fluorescence was observed in an infusion from a medicinal wood called *lignum nephriticum*. Monardes did not know the chemical compound responsible for the fluorescence at that time. It was subsequently found to be matlaline, but this only reported by A. Ulises Acuña in 2009, **Figure 4.1.1**.[68]
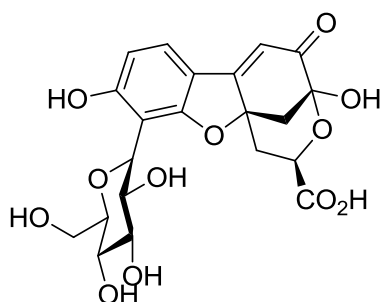
Figure 4.1.1 Structure of matlaline

4.2 Fluorophores

As discussed on previous page, fluorescence has been applied to various areas including biochemistry, medicine and analytical chemistry. Some organic fluorescent dyes have proved to be efficient fluorescent probes and sensors in photochemistry and photobiology. For example, the photo-induced intramolecular charge transfer in donor-acceptor biphenyls was shown to be very useful in sensing hydrogen bonds as well as pH.[69] Fluorescence probes represent the most important area of fluorescence spectroscopy. Organic fluorescent markers for the labeling of amino acids, peptides, proteins, DNA, and other biomolecules are common.[70] They are more generally covalently bonded to macromolecules as markers for bioactive reagents. There are two major classes of fluorophores, intrinsic and extrinsic. Intrinsic fluorophores are natural occurring fluorophores which including NADH (Nicotinamide adenine dinucleotide), flavins, aromatic amino acids, derivatives of pyridoxyl and chlorophyll. Extrinsic fluorophores either provide fluorescence activity to the sample when none exists or change the spectral properties of the sample after its addition.[71]

4.2.1 Intrinsic fluorophores

NADH (Nicotinamide adenine dinucleotide) is an enzyme cofactor found in all living cells. NADH is highly fluorescent, where as in its oxidized form NAD^+ is non-fluorescent, **Figure 4.1.2**. NADH has a maximum absorption at 340 nm, and a maximum emission at 460 nm. It partially quenches (decreases in intensity of fluorescence) in solution due to the collision and stacking of the adenine moiety. Once bound to a protein, the fluorescence activity of NADH will change, and depending on the protein, the fluorescence will either increase or decrease. The lifetime of NADH is increased in aqueous buffer,[71] lifetimes as long as 5 ns have been reported for NADH bound to horse liver alcohol dehydrogenase [72] and octopine dehydrogenase.[73]

Flavins including riboflavin, FMN (flavin mononucleotide), and FAD (flavin adenine dinucleotide) have fluorescent activity in their oxidized form, whereas their reduced forms are non-fluorescent. This is in contrast to NADH. The fluorescent activity of FAD is quenched due to complex formation between the flavin and the adenosine units, **Figure 4.1.2**.[74] The typical lifetime for FAD is 2.3 ns. Flavins have maximum absorption around 425 nm (visible range), and maximum emission around 525 nm. Once bound to proteins, flavins are generally weakly fluorescent or non-fluorescent.[71]

Aromatic amino acids including tryptophan, tyrosine and phenylalanine, **Figure 4.1.2**, are the origin of intrinsic fluorescence in proteins.[75] Here tryptophan is taken as an example. Tryptophan is often used as a reporter group for protein conformational changes, because its emission is highly sensitive to its environment. Tryptophan has a maximum absorption around 295 nm, and a maximum emission around 353 nm. The indole groups of tryptophan

residues are the dominant sources of emission in proteins. They can be quenched by a nearby electron deficient group, such as a carboxylic acids and protonated histidine residues, amongst others.[71]
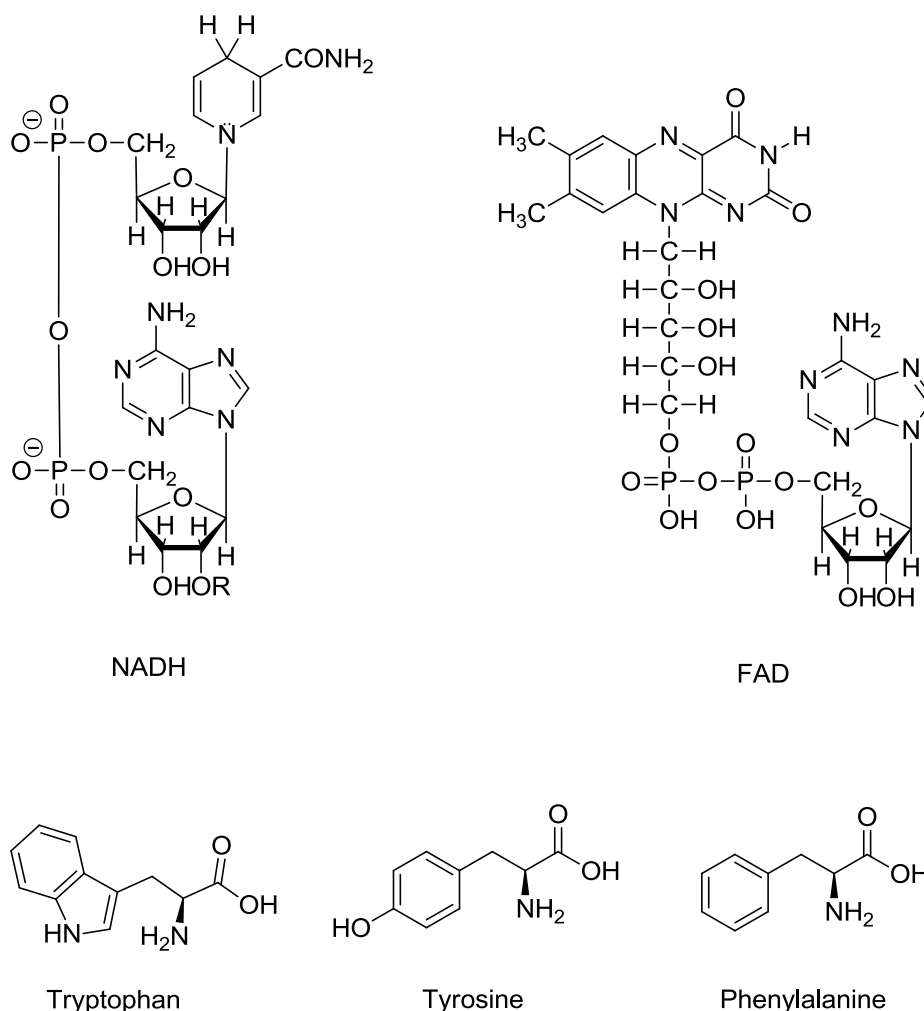
Figure 4.1.2 Structures of some intrinsic fluorophores

4.2.2 Extrinsic fluorophores

Numerous extrinsic fluorophores have been developed during the past decade due to the inadequacy of intrinsic fluorophores for certain purposes. For example, extrinsic fluorophores with a longer wavelength of emission and excitation were developed for labeling proteins. Extrinsic fluorophores have also been developed for the labeling of lipids and DNA.[69]

4.2.3 Protein labeling fluorophores

Fluorophores used for the labeling of proteins can be attached *via* covalent bonds or *via* non-covalent interactions.

There are a number of fluorophores used to covalently label proteins, e.g. dansyl chloride, fluorescein and rhodamine. These fluorophores are some of the most widely used. Dansyl chloride, **Figure 4.1.3**, was originally described by Gregorio Weber,[76] and it is widely used to label proteins. Its emission wavelength is highly sensitive to the solvent polarity. Dansyl chloride has a maximum emission around 520 nm and a maximum absorption at 350 nm, a wavelength at which intrinsic fluorophores in proteins cannot be excited. Fluoresceins and rhodamines, **Figure 4.1.3**, have maximum emission from 510 to 615 nm and have maximum absorption around 480 and 600 nm, respectively. Unlike dansyl chloride, fluoresceins and rhodamines are not sensitive to solvent polarity; but they have high molar extinction coefficients. As well as the labeling of proteins they have also been used for the labeling of antibodies.[71]

Dansyl chloride   Fluorescein   Rhodamine
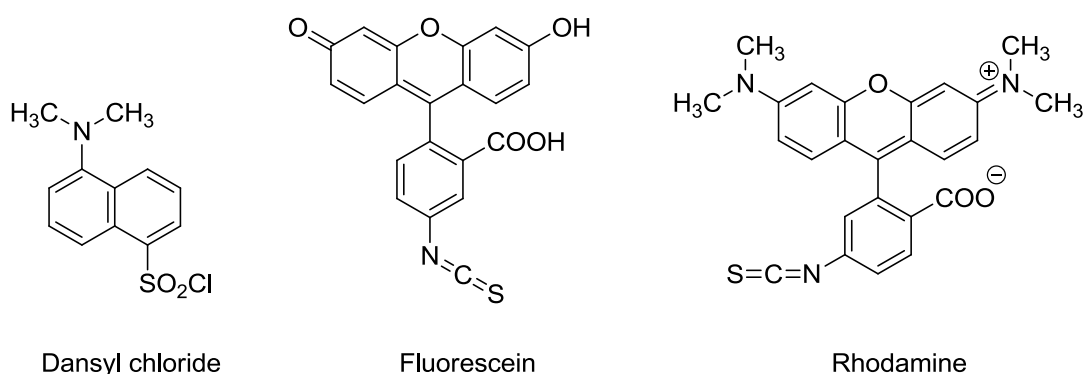
Figure 4.1.3 Structures of some fluorophores used to covalently label proteins

There are a number of fluorophores used for non-covalent protein labeling. ANS (1-anilinonaphthalene-6-sulfonic acid) and TNS (2-(p-toluidinyl)naphthalene-6-sulfonic acid) are the commonly used fluorophores. They belong to the family of non-covalent protein labeling fluorophores, naphthylamine sulfonic acids, **Figure 4.1.4**. Here ANS is taken as an example. Emission from ANS is insignificant when dissolved in buffer, but it is highly fluorescence when bound to proteins.[77] For example, when ANS is added to BSA (bovine serum albumin), the ANS emission increases and tryptophan emission from BSA decreases. The maximum emission of ANS bound to BSA occurs at $\approx$ 470 nm (280 nm excitation).[71]

ANS

TNS

Figure 4.1.4 Structures of fluorophores used for the non-covalent labeling of proteins

4.2.4 Membrane labeling fluorophores

Membranes have been labeled by the covalent attachment of fluorophores to lipids. For example, pyrene has been attached to lipids (pyrene-lipid) to estimate the diffusive process in membranes by the extent of excimer formation, **Figure 4.1.5**. The maximum emission of pyrene-PC (pyrene-phosphatidylcholine) is at $\approx$ 470 nm and its intensity is highly dependent on the temperature. The unstructured emission at higher temperatures is due to excimer formation between the pyrene groups.[78]

Pyrenyl-PC

Figure 4.1.5 Structure of pyrenyl-PC

4.2.5 DNA labeling flourophores

DNA can be made fluorescent through the use of fluorescent DNA base analogues. For example, IXP (isoxanthopterin), an analogue of guanine, **Figure 4.1.6**, has a maximum emission at around 420 nm when part of a dinucleotide or oligonucleotide. IXP fluorescence quenches when part of a double-helical DNA oligonucleotide, but it is more fluorescent when part of a dinucleotide.[79] IXP has found use in an assay for the HIV integrase protein, due to its dependence on the DNA structure.[80]
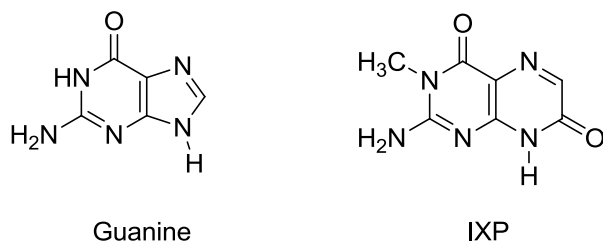
Figure 4.1.6 Structures of guanine and IXP

4.3 Fluorescence spectroscopy

Fluorescence spectroscopy is concerned with measuring/detecting transitions between electronic states and vibrational states of a given molecule. Molecules being examined have a ground electronic state of low energy and an excited electronic state of higher energy. Each of these electronic states has various vibrational states.

Fluorescent molecules are able to absorb and emit photons of lights, which contain energy proportional to their frequency. The higher the frequency of the light then the higher energy the photons carry.

In fluorescence spectroscopy, a molecule is excited by absorbing a photon and moves from its ground electronic state to one of the various vibrational states of its excited electronic state. The molecule will reach its lowest vibrational state by collision with other molecules, losing vibrational energy through these collisions, and then emit a photon and returning to its ground electronic state. As the molecules could drop down to any one of the various vibrational states of its ground electronic state, the photons emitted could be of different amounts of energy. Therefore the light emitted could have different frequencies. Fluorescence spectroscopy analyses the different frequencies of light emitted to determine the nature/energies of the different energy levels. The fluorometer measures different frequencies of fluorescent light emitted from the sample with the excitation light held constant, giving an emission spectrum. For an excitation spectrum, the excitation lights were

scanned through different wavelengths using monochrometer and recorded with the emission light held a constant wavelength.[81]

4.4 Electrocyclic reaction

An electrocyclic reaction is an intramolecular reaction in which a new σ bond is formed between the ends of conjugated π system. There are two kinds of electrocyclic reactions and they differ in terms of their reaction conditions, thermal and photochemical conditions, which give opposite configurations.

(2*E*,4*Z*,6*E*)-octatriene   *cis*-5,6-dimethyl-1,3-cyclohexadiene

(2*E*,4*Z*,6*E*)-octatriene   *trans*-5,6-dimethyl-1,3-cyclohexadiene
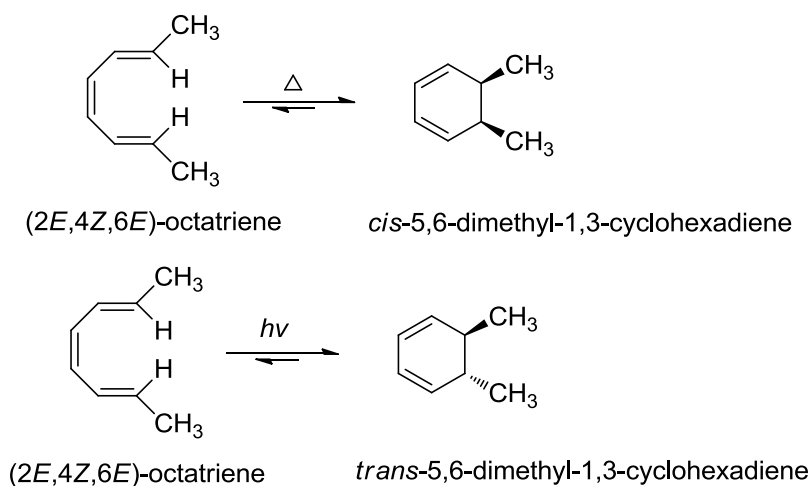
Figure 4.1.7 Examples of electrocyclic reactions

To form the new σ bond, the p orbital at the end of the conjugate system must rotate. There are two ways of this can occur. If the HOMO (highest occupied molecular orbital) is asymmetric, then the conrotatory ring-closure is symmetry allowed. If the HOMO is symmetric, then the disrotatory ring-closure is symmetry allowed.

HOMO is asymmetric   **HOMO is symmetric**
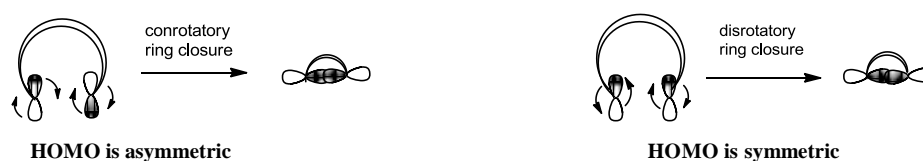
Figure 4.1.8 Conrotatory and disrotatory ring closures

4.4.1 Woodward-Hoffmann rules

The Woodward-Hoffmann rules are a set of rules in organic chemistry predicting the energy barrier heights of pericyclic reactions and are based on the conservation of orbital symmetry. Hoffmann was awarded the Nobel Prize in chemistry in 1981.

Number of conjugated π bonds	Reaction conditions	Allowed mode of ring closure
Even number	Thermal	Conrotatory
	Photochemical	Disrotatroy
Odd number	Thermal	Disrotatory
	Photochemical	Conrotatory

Figure 4.1.9 Summary of Woodward-Hoffmann rules for electrocyclic Reaction

Looking at the ring closure of (2*E*,4*Z*,6*E*)-octatriene as an example of a three conjugated π bonds system:

The ground-state HOMO of a compound with three conjugated π bonds is symmetric, and hence under thermal condition, the ring closure of (2*E*,4*Z*,6*E*)-octatriene is disrotatory, **Figure 4.2.1**, and the *cis* conformation of the product is obtained.
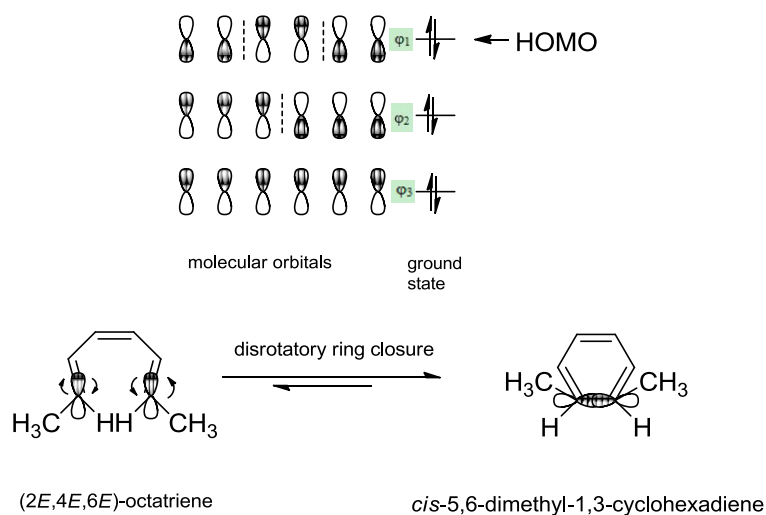
Figure 4.2.1 Thermal ring closure of (2*E*, 4*E*, 6*E*)-octatriene

Under photochemical conditions, the excited state HOMO must be considered. The new HOMO prodcued of the triene, under the photochemical conditions, is asymmetric, therefore the ring closure of (2*E*,4*Z*,6*E*)-octatriene is conrotatory, **Figure 4.2.2**, and the *trans* conformation of the product is obtained.

molecular orbitals   ground state   excited state

(2*E*,4*E*,6*E*)-octatriene   *trans*-5,6-dimethyl-1,3-cyclohexadiene

conrotatory ring closure
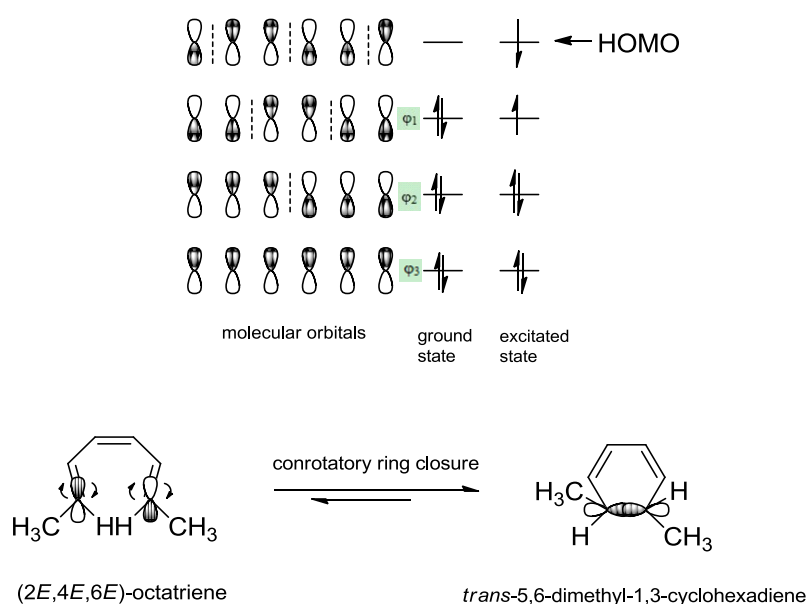
Figure 4.2.2 Photochemical ring closure of (2*E*, 4*E*, 6*E*)-octatriene

4.4.2 Some typical examples of electrocyclic reaction

Electrocyclic reactions have been frequently found in biological system, e.g. biosynthesis of natural products. Classical examples of an electrocyclic reaction in biosynthesis include the biosynthesis of endiandric acid or vitamin D. Here the biosynthesis of vitamin D_3 is taken as an example. The first step is a conrotatory ring opening of 7-dehydrocholesterol under photochemical conditions, to form pre vitamin D_3. A [1,7]-hydride shift then followed to form vitamin D_3, **Figure 4.2.3**.[82] Another example of an electrocyclic reaction in a biological system was the thermal rearrangement of benzonorcaradiene diterpenoid to the benzocycloheptatriene diterpenoid isosalvipuberlin, **Figure 4.2.4**.[83] This transformation can be considered as a thermal disrotatory electrocyclic reaction.
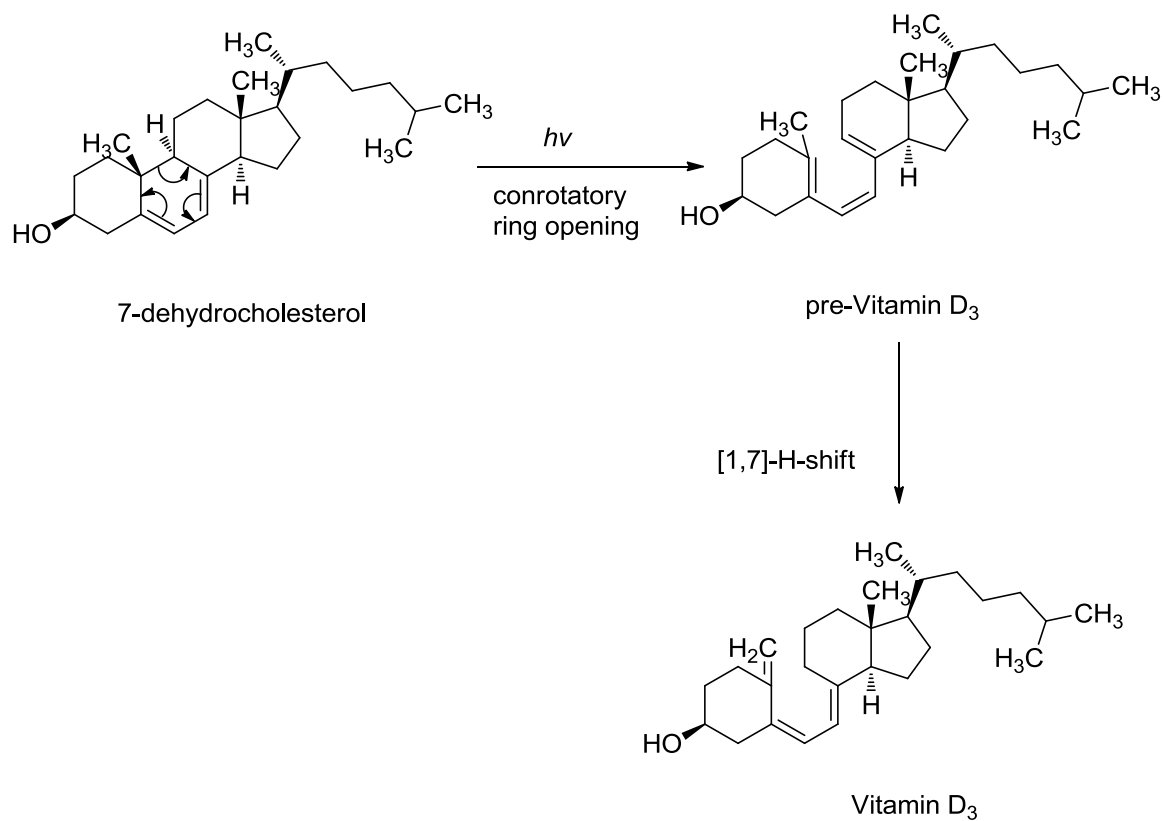
Figure 4.2.3 Vitamin D$_3$ formation
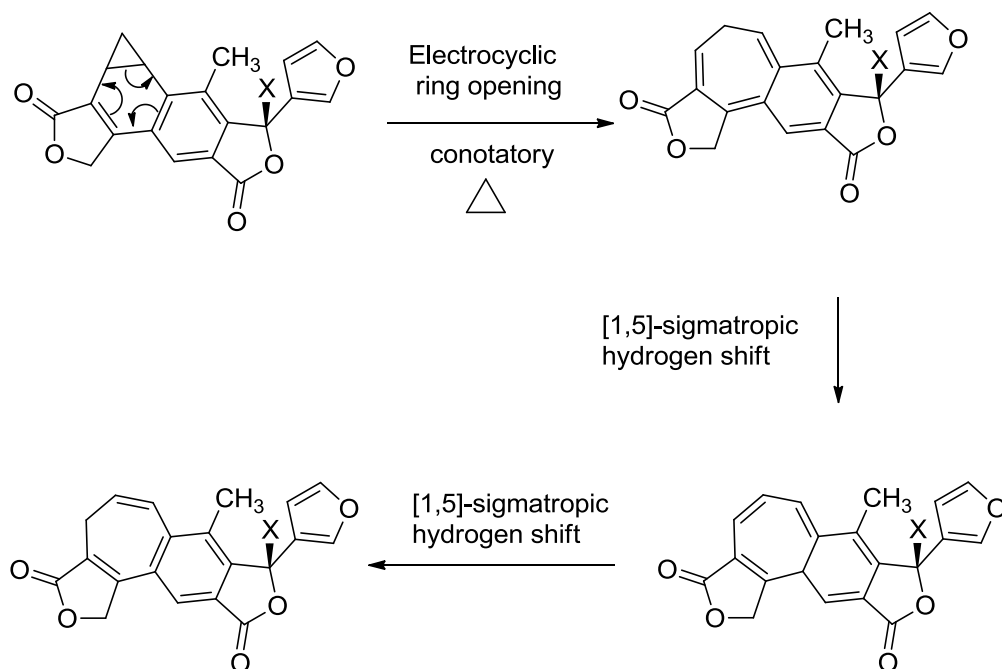
Figure 4.2.4 Benzocycloheptatriene diterpenoid isosalvipuberlin formation

Electrocyclic reactions are also often found in organic synthesis. One well studied example is the conrotatory thermal ring-opening of benzocyclobutane. The resulting product is a very unstable ortho-quinodimethene, which can be trapped in an *endo* Diels Alder addition with a strong dienophile such as maleic anhydride, **Figure 4.2.5**.[84]
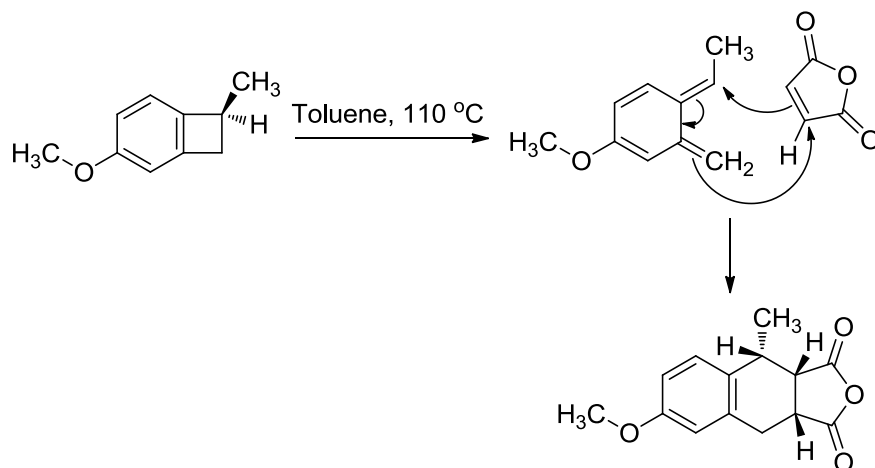
Figure 4.2.5 An electrocyclic ring opening and subsequent Diels Alder cycloaddition.

4.5 Project aims for biphenyl sulfone section

This project, in part, aims to 1) synthesize and characterize a family of bis-sulfonyl trienes that are potential substrates for electrocyclisation reactions, 2) use the trienes to generate, and characterize, a family of biphenyl sulfones *via* an electrocyclisation reaction, 3) the biphenyl sulfones are expected to be fluorescent in nature and as such their fluorescence will be evaluated and characterized.

Chapter 5 Results and discussion of the synthesis of biphenyl sulfones and their fluorescent properties

Preliminary research carried out by the Stephens group discovered that a bissulfonyl triene can undergo a thermally driven rearrangement to give a biphenyl sulfone, albeit in a low yield, **Figure 5.1.1**.[87] This was an intriguing result and one we decided to investigate further. We were also curious to see if a fluorescent biphenyl would result, particularly if we added an electron donating group, e.g. dimethylamino, on the biphenyl and para to the sulfone.[93]
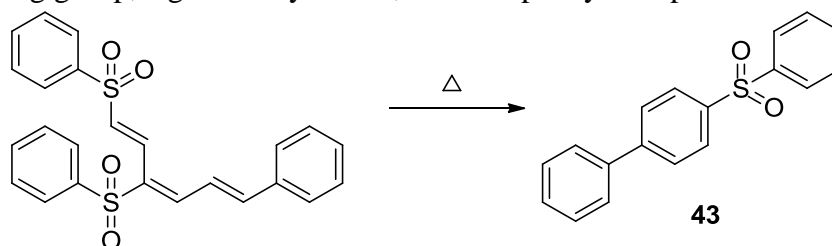
Figure 5.1.1 Thermal generation of 4-(phenylsulfonyl)-1,1'-biphenyl **43**

A traditional method for preparing 4-(phenylsulfonyl)-1,1'-biphenyl is using a Suzuki-Miyaura coupling[85] or Friedel-Crafts reaction.[86] For example, Su-Dong Cho reported a synthetic route using Suzuki-Miyaura coupling. Here Su-Dong employed phenylboronic acid and 1-chloro-4-(phenylsulfonyl)benzene as starting materials with 2 equivalents of Cs_2CO_3 as base, 10 mol% of a bulky electron-rich monoaryl phosphine ligand, **Figure 5.1.2**, and 1 mol% $Pd_2(dba)_3$. The reaction mixture was refluxed in 1,4-dioxane for 12 hours to afford the bisphenyl sulfone product in a 97 % yield.[85]
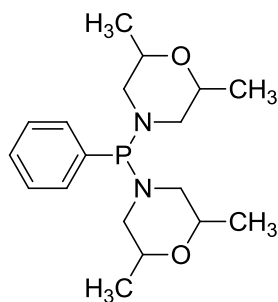
Figure 5.1.2 Phosphine ligand used in the Suzuki-Miyaura coupling[85]

Tongshou Jin and co-workers reported a Friedel-Crafts synthetic route for synthesizing 4-(phenylsulfonyl)-1,1'-biphenyl, **Figure 5.1.3**. The reaction was catalyzed using $Fe(OH)_3$ and stirred at 140 ^{o}C to give the bisphenyl sulfone in 80% yield.[86]
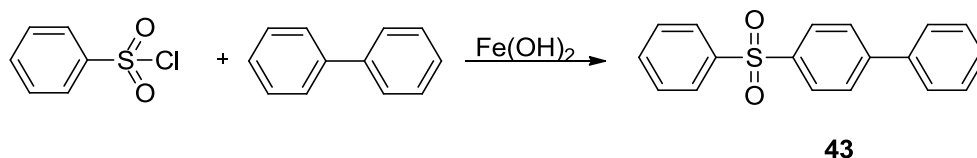
Figure 5.1.3 Friedel-Crafts generation of 4-(phenylsulfonyl)-1,1'-biphenyl **43**[86]

5.1 Synthesis of bissulfonyl trienes

In order to optimize the thermal generation of the bisphenyl sulfones we first had to generate the corresponding bissulfonyl trienes. The trienes in question could be prepared using the previous developed methodology of the Stephens group. Triene **44** was synthesised in one step from the commercial available *trans*-cinnamaldehyde and bis-phenylsulfonyl propene, a stock of which was previously made by Stephens group, with aluminium oxide as the catalyst **Figure 5.1.4**. The bis-phenylsulfonyl propene was made by treating allyl phenylsulfone with elemental bromine and TEA. The resulting bromo-phenylsulfonyl propene was treated with benzenesulfinic acid sodium salt to generate the desired product.[87]

Bis-phenylsulfonyl propene   **44**
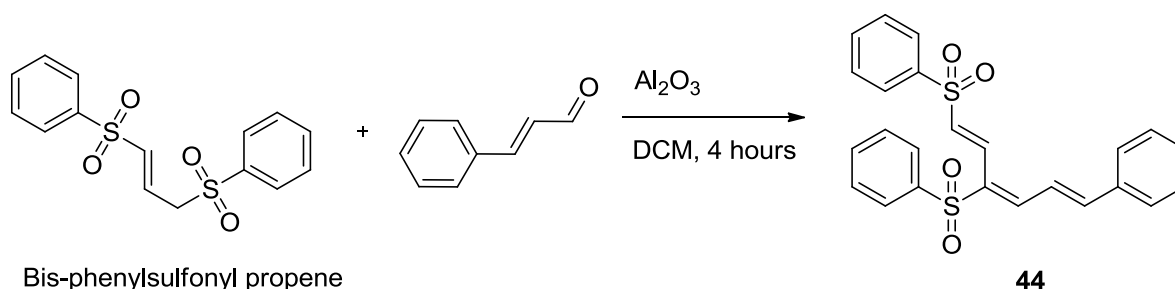
Figure 5.1.4 Triene **44** synthesis

A family of novel trienes were synthesized using this methodology, **Table 5.1**. The triene derivatives were choosen to synthesis with the aim of exploring the effect of adding the electron donating or electron withdrawing groups to the biphenyl sulfones. The trienes were characterized using NMR, IR, HRMS and CHN microanalysis. For example, the ^{1}H and ^{13}C NMR spectra for triene **44** generated the expected multitude of signals in the aromatic reagion. Seventeen distinct signals were found in the ^{13}C NMR spectrum, four of which were identified as tertiary carbons using a DEPT 135 spectrum (as expected). CHN microanalysis and HRMS for triene **44** confirmed its identity, calculated for [$C_{24}H_{20}O_4S_2$] C, 66.03; H, 4.62; found C, 66.19; H, 4.66 and HRMS calc. (M + H$^+$) = 437.0876, found (M + H$^+$) = 437.0871 (-1.17 ppm). The IR spectrum also showed the SO$_2$ group with bands at 1310 and 1145 cm^{-1}. ^{1}H NMR of triene **50** shows a singlet at 3.87 ppm with an integration of 3H indicating the presence of OCH$_3$ group. ^{1}H NMR of triene **53** shows a singlet at 2.41 ppm indicating the

presence of CH$_3$ group. ^{13}C NMR of triene **3** exhibited twenty one distinct signals due to the unsymmetrical of the ortho substituted phenyl ring. CHN microanalysis of the triene **46** confirmed its identity, calculated for [C$_{25}$H$_{22}$O$_5$S] C, 64.36; H, 4.75; found C, 64.56; H, 4.55. ^{1}H NMR of triene **48** shows a singlet at 3.08 ppm with an integration of 6H indicating the presence of N(CH$_3$)$_2$ group. ^{1}H NMR of triene **52** shows a singlet at 3.95 ppm with an integration of 3H indicating the presence of C(O)OCH$_3$ group. CHN microanalysis of the triene **52** confirmed its identity, calculated for [2(C$_{26}$H$_{22}$O$_6$S$_2$)H$_2$O] C, 62.01; H, 4.60; found C, 62.20; H, 5.08. The ^{1}H NMR spectrum of triene **44** is shown in **Figure 5.1.5**.
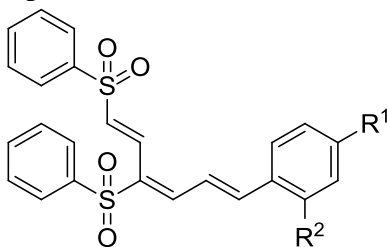
Product	R^1	R^2	Yield (%)
Triene **44**	H	H	57
4-Nitro triene **45**	NO$_2$	H	57
2-OMe triene **46**	H	OCH$_3$	62
2-Nitro triene **47**	H	NO$_2$	46
4-Dimethylamino triene **48**	N(CH$_3$)$_2$	H	77
4-Chloro triene **49**	Cl	H	43
4-OMe triene **50**	OCH$_3$	H	37
4-Cyano triene **51**	CN	H	29
4-MeO$_2$C triene **52**	C(O)OCH$_3$	H	32
4-Methyl triene **53**	CH$_3$	H	26

Table 5.1 Triene synthesis
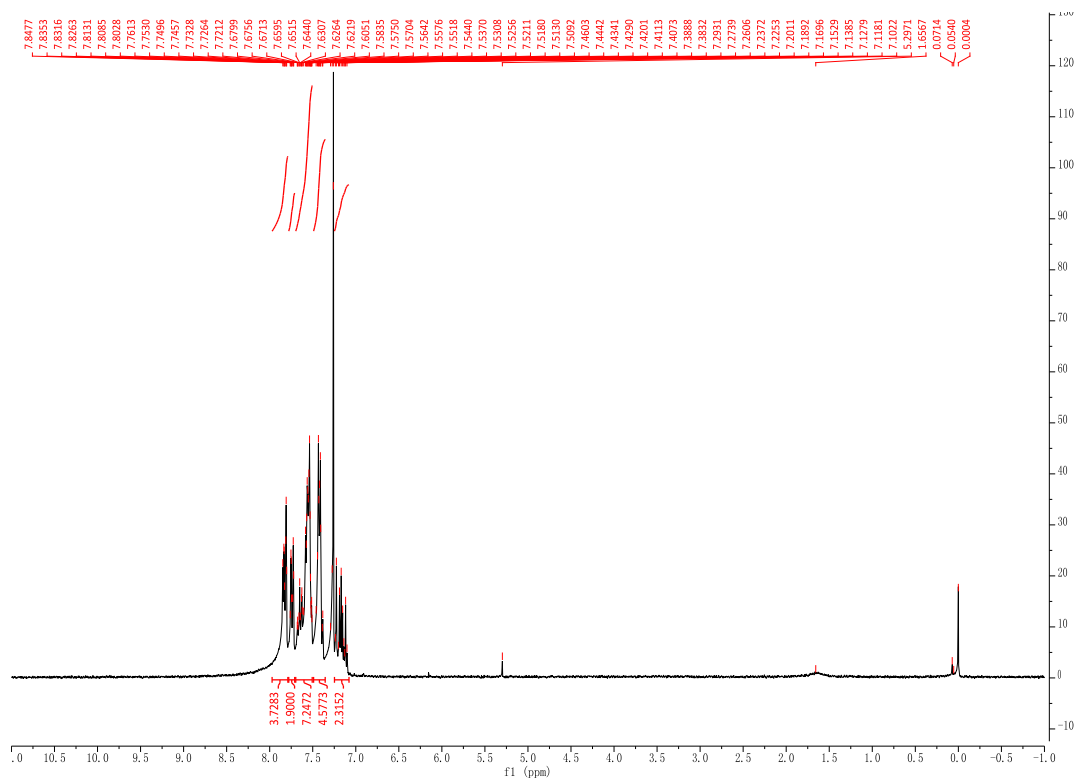
Figure 5.1.5 ^{1}H NMR of triene **44**

X-ray crystal structures of triene **45** and triene **50** were obtained with our collaborator Prof Pat McArdle (NUI Galway), **Figure 5.1.6** and **5.1.7**. (for X-ray data, see **Appendix table 0.1-0.2**)
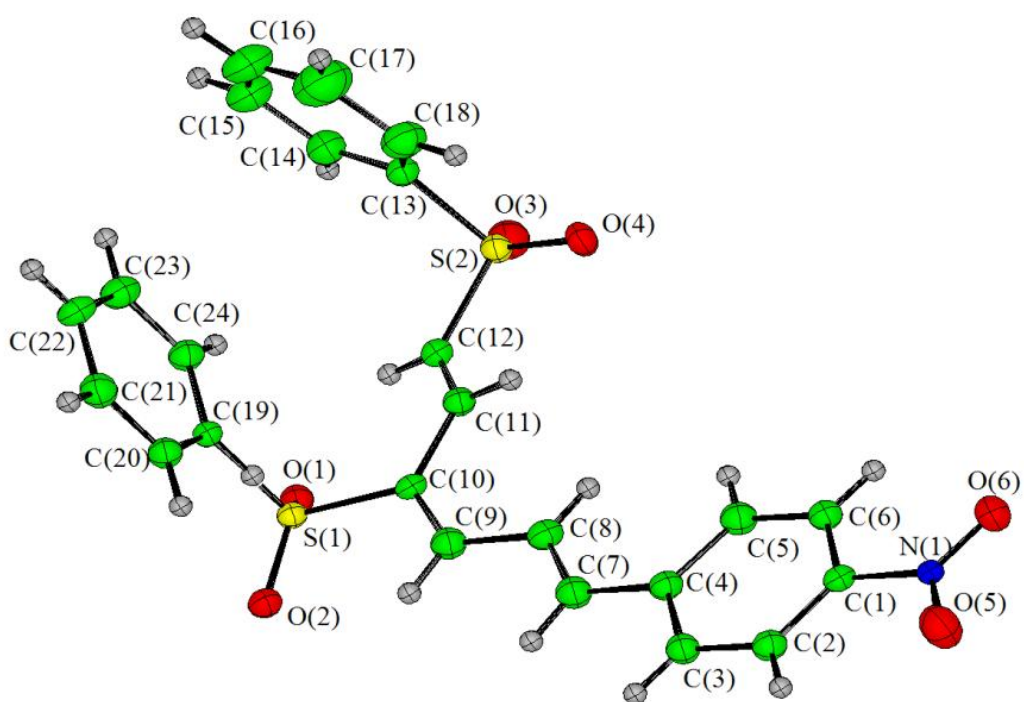
Figure 5.1.6 X-ray crystal structure of
1-[(1*E*,3*E*,5*E*)-4,6-bis(phenylsulfonyl)hexa-1,3,5-trien-1-yl]-4-nitrobenzene **45**
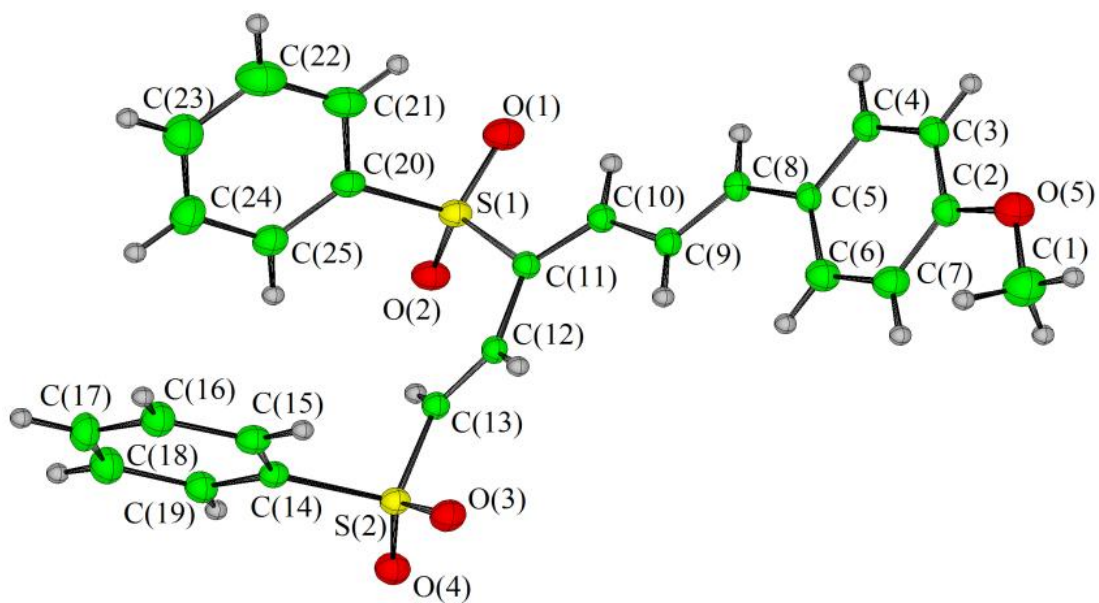
Figure 5.1.7 X-ray crystal structure of
((1*E*,3*E*,5*E*)-6-(4-methoxyphenyl)hexa-1,3,5-triene-1,3diyldisulfonyl)dibenzene **50**

The starting cinnamaldehydes for some trienes were not commercially available and had to be synthesized as a result. The triene **51** is taken as an example. 4-Cyano cinnamaldehyde **54** was prepared by refluxing 4-formylbenzonitrile in THF with (triphenylphosphoranylidene) acetaldehyde for 24 hours, **Figure 5.1.8**. The final product was purified using flash chromatography. The product obtained was a mixture of *trans* and *cis* isomers (*trans* predominately), and used without further purification.[99] The product was confirmed by ^{1}H NMR, with a doublet doublet at 6.8 ppm for CH=C*H*C(O)H, and HRMS, $C_{10}H_7NO$ calc. $(M + H^+) = 158.0600$, found $(M + H^+) = 158.0604$ (2.17 ppm). The mechanism of this reaction is shown in **Figure 5.1.9**.
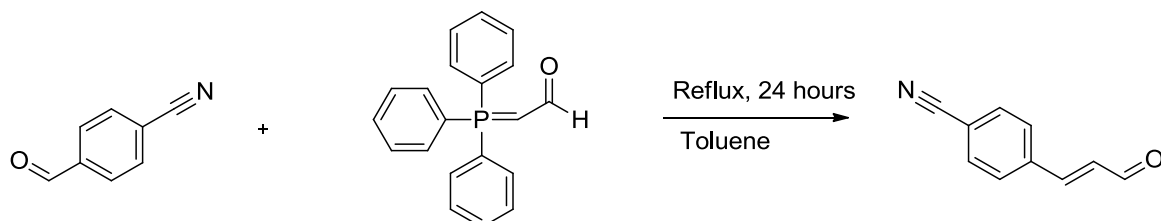
Figure 5.1.8 Synthesis of 4-cyano cinnamaldehyde **54**
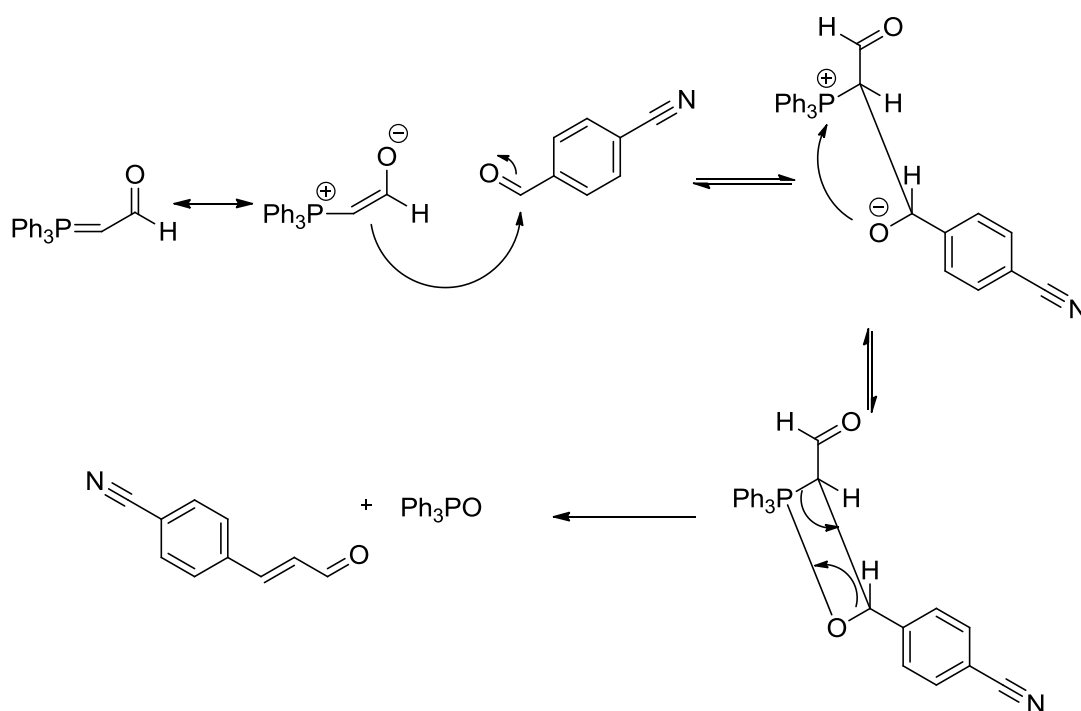
Figure 5.1.9 Proposed mechanism for synthesis of 4-cyano cinnamaldehyde **54**

5.2 Synthesis of the biphenyl sulfone family

A number of different reaction conditions were explored in order to develop an effective methodology for the synthesis of bisphenyl sulfones, **Table 5.2**. The synthesis of 4-(phenylsulfonyl)-1,1'-biphenyl **43** was used as the test reaction. The first conditions we explored used microwave irradiation. Microwaves would be able to heat the triene directly and as a result we thought tha this method may produce a fast and high yielding transformation. We dissolved triene **44** in different solvents e.g. toluene, NMP, and heated the solution at various temperature under microwave irradiation. The microwave reaction conditions found to work best employed NMP as the solvent and heated at 170 ^{o}C for 1 hour under microwave. However, the isolated yield was only 45 % yield for this reaction. We were keen to try a solvent free reaction but were concerned about generating super heated hot spots (due directly heating solids) under microwave conditions. As a result we explored heating the neat compound in an oil bath. This proved to be an excellent approach and after some optimization the 4-(phenylsulfonyl) -1,1'-biphenyl **43** was obtained in a 96 % yield after heating for 1 hour at 170 ^{o}C. All the reactions attempted are shown in **Table 5.2**. The structure of desired products was confirmed ^{1}H and ^{13}C NMR, HRMS and CHN microanalysis, **Figure 5.2.1**.

Concentration /amount	Solvent	Temperature (^{o}C)	Time	microwave	Yield (%)
14 mg	neat	115	5 hours	No	small
10mg/3mL	Toluene	110	15 mins	yes	N/A
10mg/3mL	Toluene	130	15 min	yes	N/A
10mg/3mL	DMF	120	15 mins	yes	N/A
14mg	neat	115	10 hours	no	small
15mg/1mL	Toluene	133	15 mins	yes	N/A
15mg/1mL	NMP	200	15 mins	yes	small
14mg/0.5mL	NMP	200	1 hours	yes	small
62mg	neat	170	1 hours	no	96
58mg	neat	150	1 hours	no	61
71mg	neat	130	1 hours	no	N/A
59mg/2mL	NMP	170	1 hours	yes	45
57mg	neat	170	45 mins	no	78

Table 5.2 Attempted reactions for the synthesis of 4-(phenylsulfonyl)-1,1'-biphenyl **43**
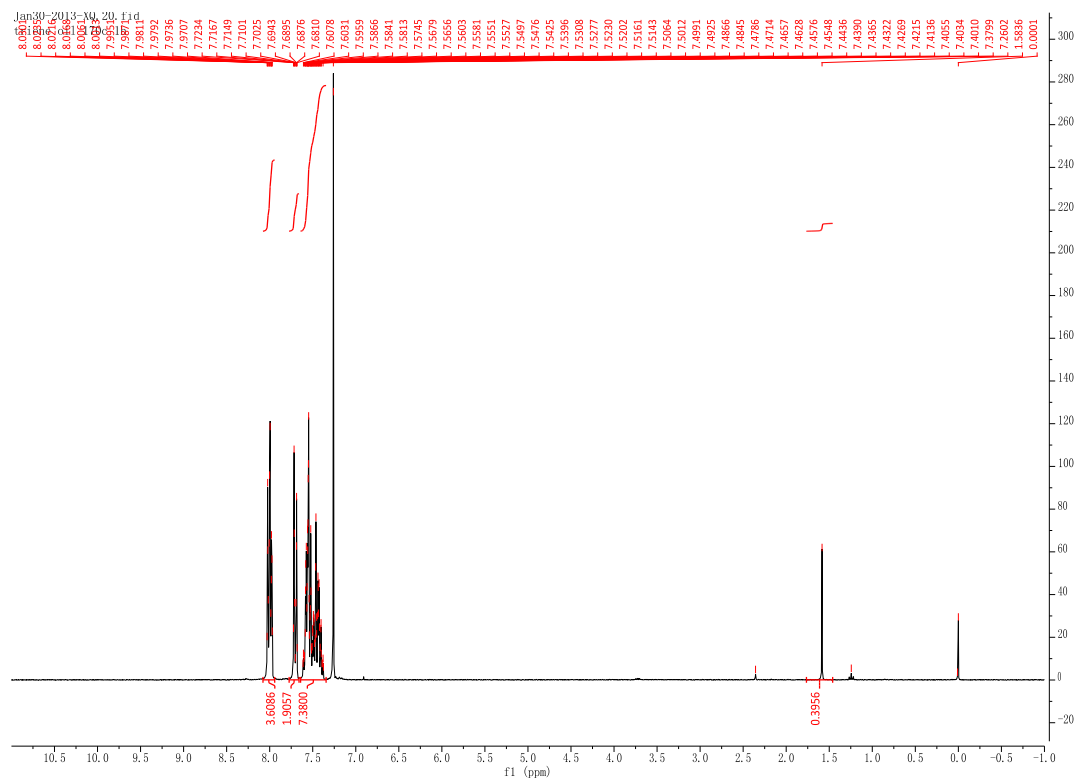
Figure 5.2.1 ^{1}H NMR of 4-(phenylsulfonyl)-1,1'-biphenyl **43**

An x-ray crystal structure of the biphenyl **43** was obtained with our collaborator Prof Pat McArdle (NUI Galway), **Figure 5.2.2**.[87]
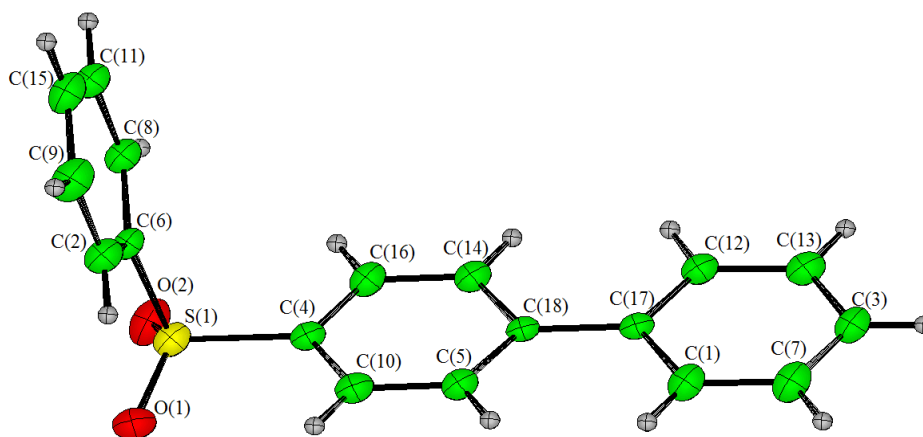
Figure 5.2.2 X-ray crystal structure of 4-(phenylsulfonyl)-1,1'-biphenyl **43**[87]

We consider the thermal generation of the biphenyl sulfones to be a thermal electrocyclic reaction, whose proposed mechanism is shown in **Figure 5.2.3**. A disrotatory overlap of the HOMO orbitals was assigned, **Figure 5.2.4**, based on the analysis of frontier molecular

orbitals of triene **44**. This predicts the syn-diastereomer of intermediate diene according to the Woodward-Hoffman rules (see introduction on electrocyclic reactions).
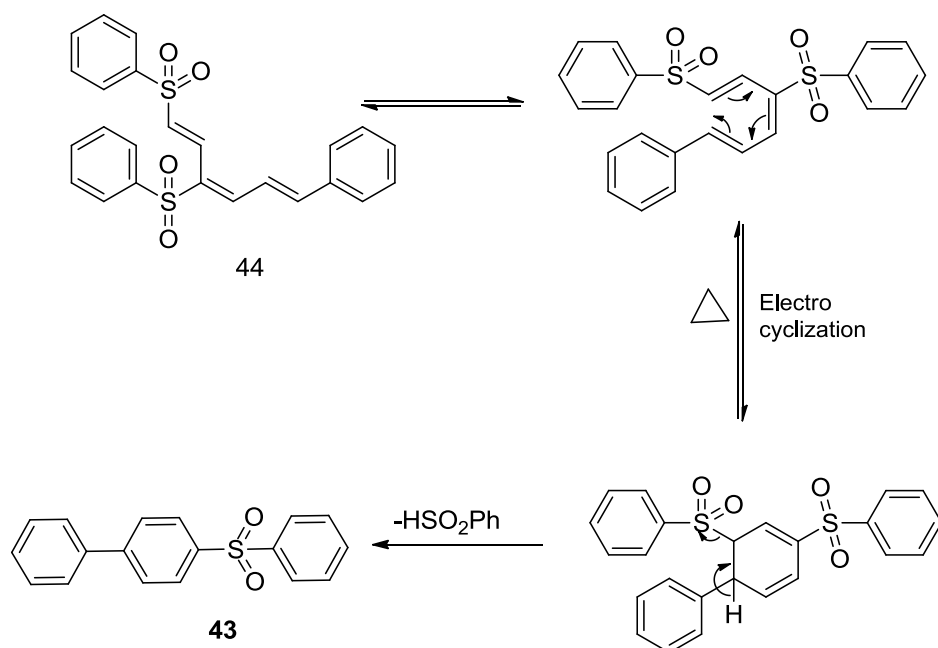
Figure 5.2.3 Proposed reaction mechanism for the generation of the bisphenyl sulfones.
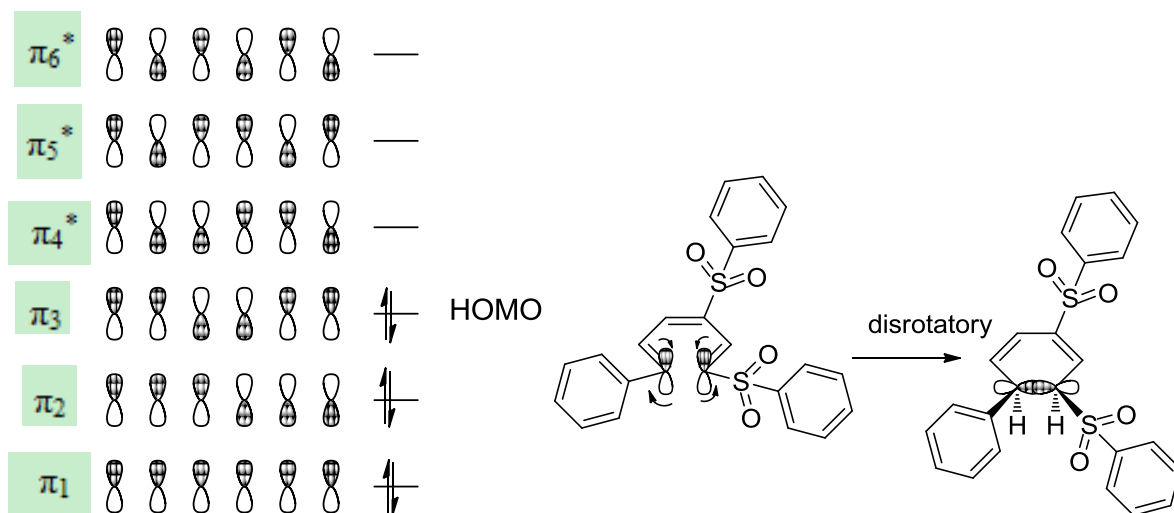
Figure 5.2.4 Analysis of molecular orbitals of the thermal electrocyclic reaction.

A family of biphenyls was synthesized using this methodology. Their structures and yields are given in **Table 5.3**. The structure of the biphenyl derivatives were confirmed by ^{1}H and ^{13}C NMR, HRMS and CHN microanalysis. The ^{1}H NMR spectrum of 4-dimethylamino

biphenyl **55** showed a singlet at 3.01 ppm, with an integration of 6H, indicating the presence of $N(CH_3)_2$ group. Its HRMS analysis generated a found $(M + H^+) = 338.1210$ (calculated for $C_{20}H_{19}NO_2S$ $(M + H^+) = 338.1209$, 0.16 ppm difference). CHN microanalysis calculated for $[3(C_{20}H_{19}NO_2S) \cdot H_2O]$ C, 69.94; H, 5.77; N, 4.08; found C, 70.19; H, 6.28; N, 3.39. The calibration of H_2O is based on the ^1H NMR of dimethylamino biphenyl, **Figure 5.2.5**, which shows a 3:1 ratio of biphenyl:H_2O.
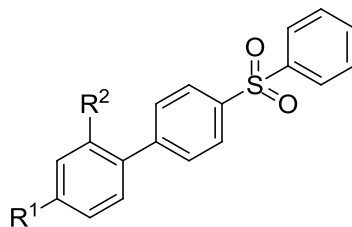
Product	R^1	R^2	Yield (%)
Biphenyl **43**	H	H	96
4-Dimethylamino biphenyl **55**	$N(CH_3)_2$	H	42
4-Methyl biphenyl **56**	NO_2	H	35
4-MeO$_2$C biphenyl **57**	Cl	H	60
4-OMe biphenyl **58**	$C(O)OCH_3$	H	62
4-Chloro biphenyl **59**	CN	H	50
4-Cyano biphenyl **60**	OCH_3	H	31
2-OMe biphenyl **61**	H	OCH_3	39
2-Nitro biphenyl **62**	H	NO_2	31
4-Nitrobiphenyl **63**	CH_3	H	40

Table 5.3 Biphenyl compounds synthesized
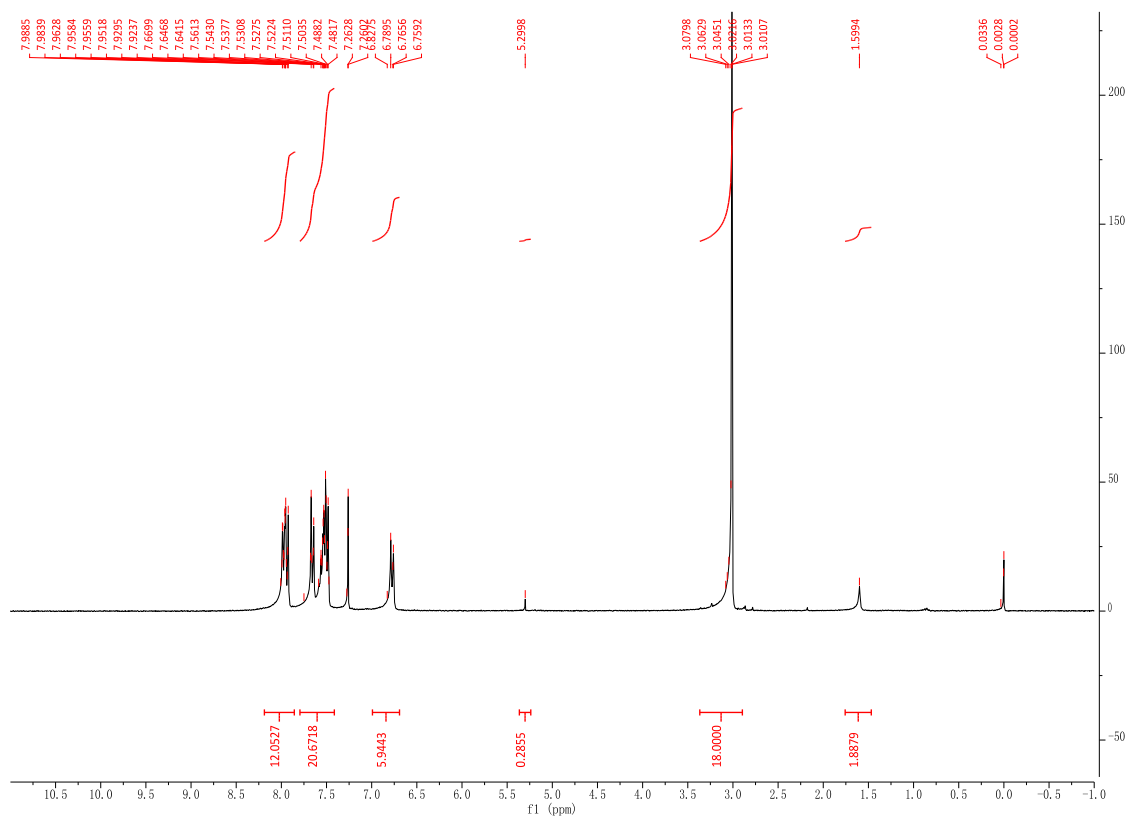
Figure 5.2.5 ^{1}H NMR of dimethylamino biphenyl **55**

An x-ray crystal structure of the biphenyl **63** and biphenyl **58** were obtained with our collaborator Prof Pat McArdle (NUI Galway), **Figure 5.2.6** and **5.2.7**. (for X-ray data, see **Appendix table 0.1-0.2**)
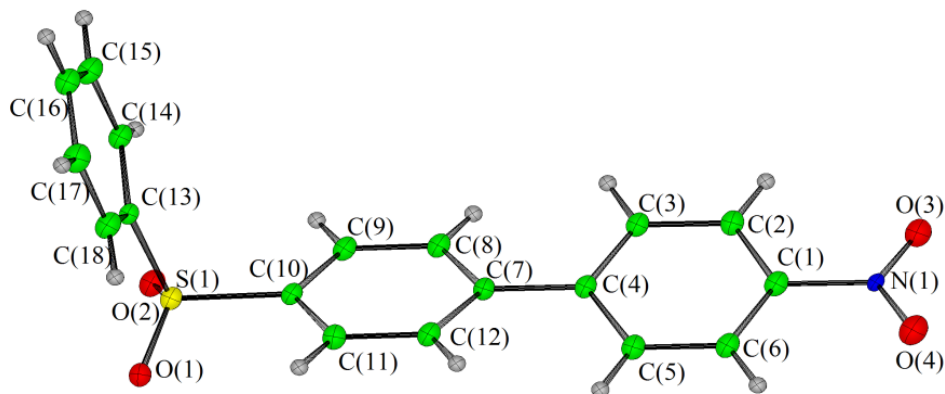
Figure 5.2.6 X-ray crystal structure of 4-nitro-4'-(phenylsulfonyl)-1,1'-biphenyl **63**
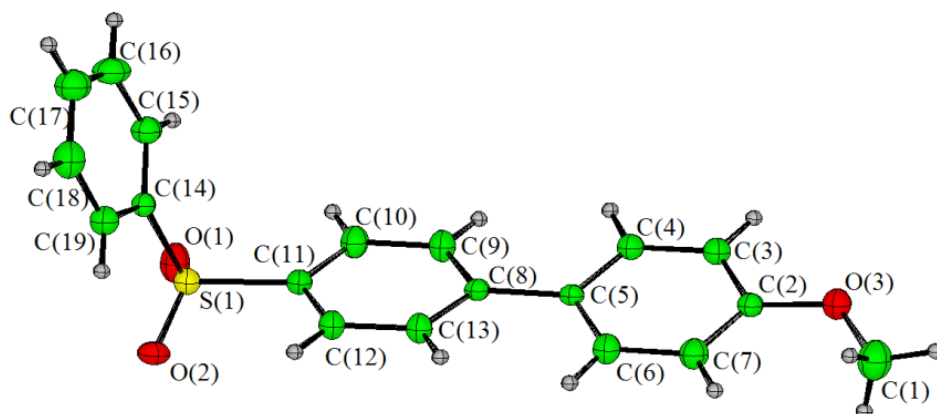
Figure 5.2.7 X-ray crystal structure of 4-methoxy-4'-(phenylsulfonyl)-1,1'-biphenyl **58**

The ^{1}H NMR spectrum of biphenyl **61** showed two poorly separated singlets at 3.78 ppm that together integrated to 3H, **Figure 5.2.8**. This suggested that two isomers or perhaps two rotamers for biphenyl **61** were formed.
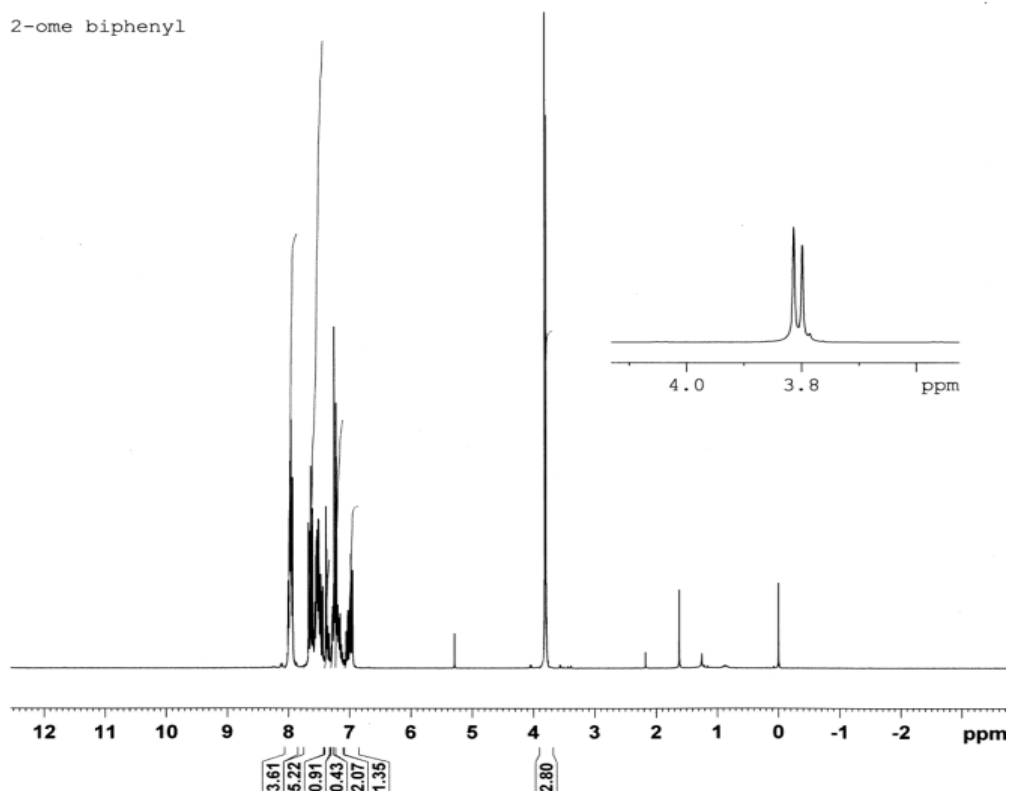
Figure 5.2.8 ^{1}H NMR of biphenyl **61**

HRMS analysis generated a found (M + H$^+$) = 325.0905 for biphenyl **61** (calculated for C$_{19}$H$_{16}$O$_3$S, (M + H$^+$) = 325.0893, 3.6 ppm difference). CHN microanalysis found C, 69.58; H, 5.48; calculated for [4(C$_{19}$H$_{16}$O$_3$S) H$_2$O] C, 69.38; H, 5.06. In order to investigate if two rotamers were present, which might be expected to interconvert rapidly at higher temperatures, we recorded the ^{1}H NMR in CDCl$_3$ at 25 $^{\circ}$C and 50 $^{\circ}$C and in DMSO-d_6 at 25 $^{\circ}$C and 111 $^{\circ}$C. In all cases the two singlets did not change and did not turn into single singlet (i.e. an average signal of two rapidly interconverting rotamers). The ^{13}C NMR and DEPT 135 spectra revealed ten tertiary carbons. The structure of biphenyl **61** contains five tertiary carbons, furthermore two signals at 55.78 and 55.54 ppm were obtained indicating two OCH$_3$ groups. As such, the ^{13}C NMR data supported our two isomers theory. DFT calculations carried out by our colaborator Dr Elisa Fadda, NUI Maynooth (details are described in section **5.3.9**) found two isomers of equal stablity in the gas phase, **Figure 5.2.9 and 5.3.1**, which again supported our theory.
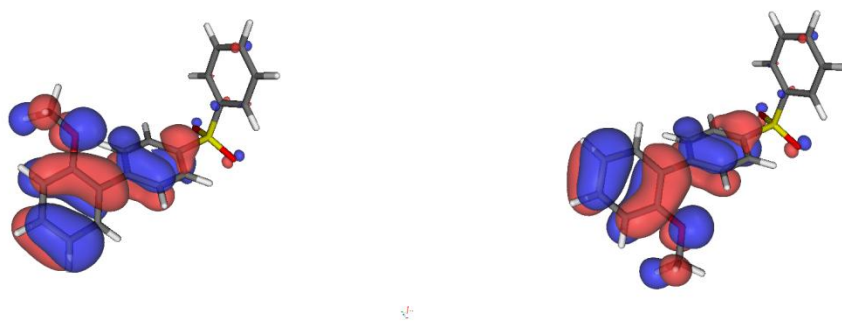
Figure 5.2.9 Molecular orbital plots of the two biphenyl **61** isomers (HOMO)
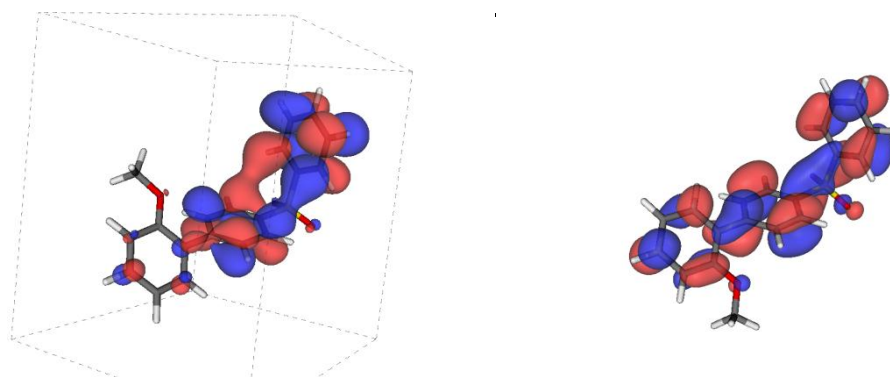
Figure 5.3.1 Molecular orbital plots of the two biphenyl **61** isomers (LUMO)

We believe that the existence of a partial double bond between the biphenyl aromatic rings stops the rotation of the biphenyl system resulting in two stable isomers, see **Figure 5.3.2**.

The related biphenyl **62** exists as single isomer as the NO_2 substituent on the phenyl ring is strongly electron withdrawing (as opposed to electron donating) and therefore does not generate a partial double bond in the biphenyl system. The general synthesis of triene and biphenyl compounds were shown in **Figure 5.3.3**.
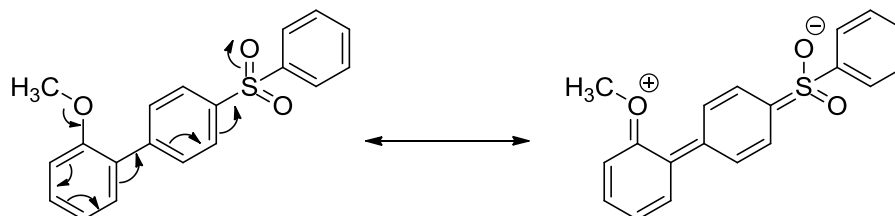
Figure 5.3.2 Partial double bond in biphenyl system of biphenyl **61**
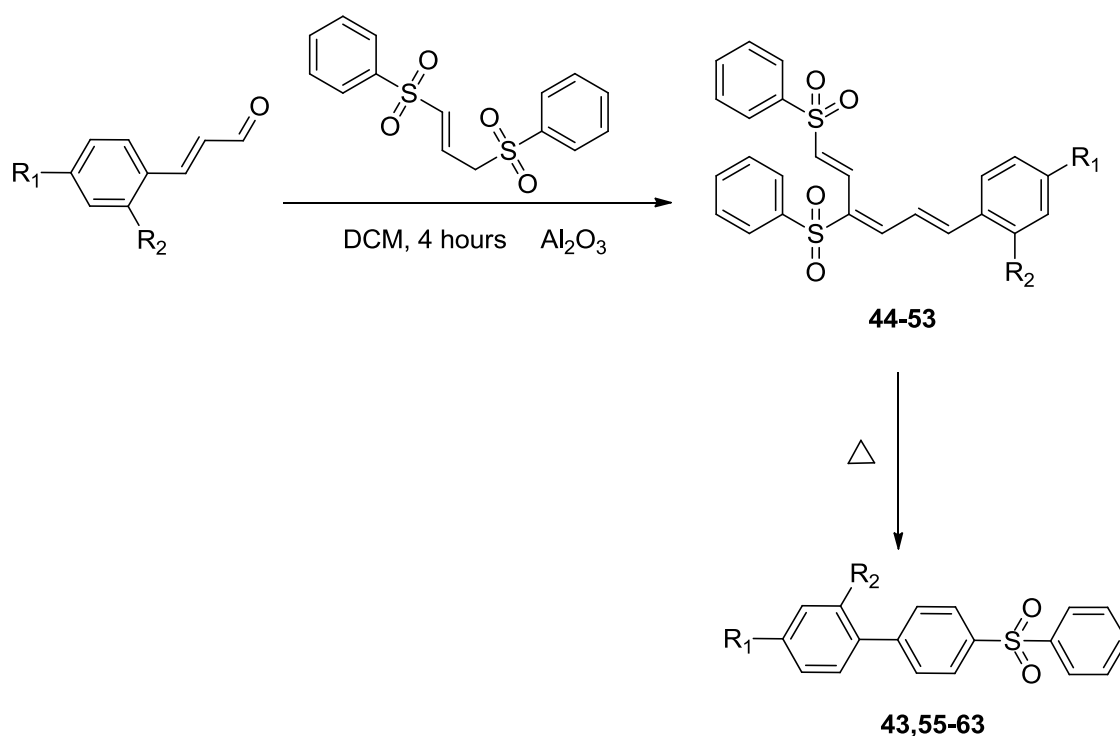
44, R_1 = H,	R_2 = H		**43**, R_1 = H,	R_2 = H
45, R_1 = NO_2,	R_2 = H		**55**, R_1 = $N(CH_3)_2$,	R_2 = H
46, R_1 = H,	R_2 = OCH_3		**56**, R_1 = NO_2,	R_2 = H
47, R_1 = H,	R_2 = NO_2		**57**, R_1 = Cl,	R_2 = H
48, R_1 = $N(CH_3)_2$,	R_2 = H		**58**, R_1 = $C(O)OCH_3$,	R_2 = H
49, R_1 = Cl,	R_2 = H		**59**, R_1 = CN,	R_2 = H
50, R_1 = OCH_3,	R_2 = H		**60**, R_1 = OCH_3,	R_2 = H
51, R_1 = CN,	R_2 = H		**61**, R_1 = H,	R_2 = OCH_3
52, R_1 = $C(O)OCH_3$,	R_2 = H		**62**, R_1 = H,	R_2 = NO_2
53, R_1 = CH_3,	R_2 = H		**63**, R_1 = CH_3,	R_2 = H

Figure 5.3.3 The general synthesis of triene and biphenyl compounds

5.3 Fluorescent properties of the biphenyl sulfone family

The substituted biphenyls were found exhibiting fluorescent properties, and as a result they underwent a fluorescence study. The substituted biphenyl compounds **55-63 Table 5.4**, were examined for fluorescent activity. The procedure for fluorescent study were described in experimental section. Compound **55** was of particular interest to us as we believed that a "push-pull" effect would exist due to the presence of the electron donating dimethylamino group and the electron withdrawing sulfone group. This, we believed, would manifest itself through a twisted intramolecular charge transfer (TICT) mechanism of fluorescence.[91] As such, compound **55** was employed in the generation of a UV-absorption spectrum, emission spectrum and excitation spectrum in several solvents (chloroform, methanol, toluene, ethylene glycol, acetic acid, n-hexane, dichloromethane and acetonitrile). Compounds **56-63** were also studied and their UV-absorption spectrum, emission spectrum, and excitation spectrum generated in two solvents (chloroform and methanol). UV-absorption spectrums were recorded using a Unicam UV 500 spectrometer, emission and excitation spectrums were recorded using a JASCO FP-6300 spectrofluorometer.
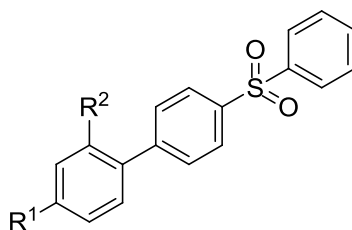
Product	R^1	R^2
Biphenyl **55**	$N(CH_3)_2$	H
Biphenyl **56**	CH_3	H
Biphenyl **57**	$C(O)OCH_3$	H
Biphenyl **58**	OCH_3	H
Biphenyl **59**	Cl	H
Biphenyl **60**	CN	H
Biphenyl **61**	H	OCH_3
Biphenyl **62**	H	NO_2
Biphenyl **63**	NO_2	H

Table 5.4 Biphenyl compounds

5.3.1 Absorption spectrum of 55

Compound **55** was studied in eight solvents and summary of its UV-absorption spectra is

given in **Table 5.5**. The UV-absorption spectra shown in **Figure 5.3.4**, **Figure 5.3.5** and **Figure 5.3.6** were recorded at a higher concentration (This was only for present the bands clearly, not for calculating quantum yield). The UV-absorption spectra were also recorded at a lower concentration (0.712×10^{-3} mM) as this was required for quantum yield calculation, see in **appendix** (**Figure 0.1-0.6**).

Solvent	λ_{abs}[a]
Chloroform	343
Methanol	339
Toluene	340
Acetic acid	277[b]
Ethylene glycol	348
Dichloromethane	348
n-Hexane	336
Acetonitrile	344

Table 5.5 UV absorption maxima for compound **55**. [a] λ_{abs} are reported at the maximum absorbance wavelength in nm (concentration of sample, 0.712×10^{-3} mM). [b] Shoulder at 324 nm.
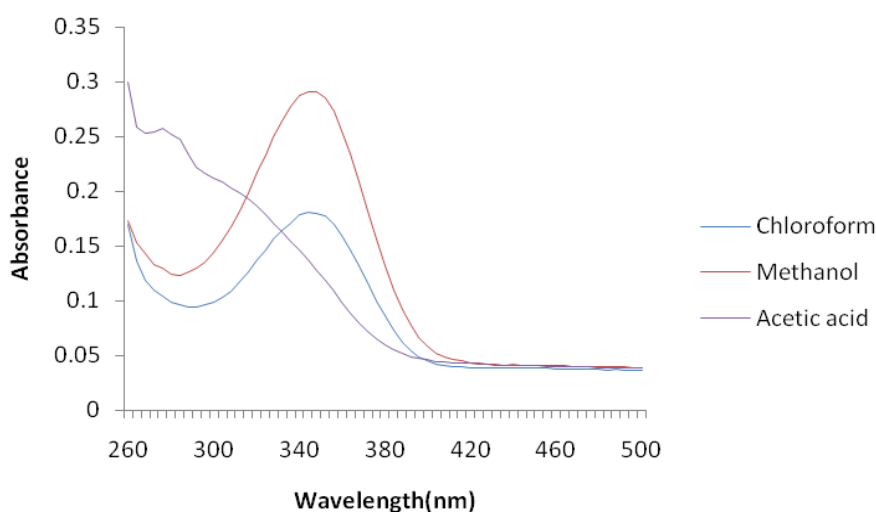
Figure 5.3.4 Absorption spectrum of **55** (in CHCl$_3$, MeOH and acetic acid)
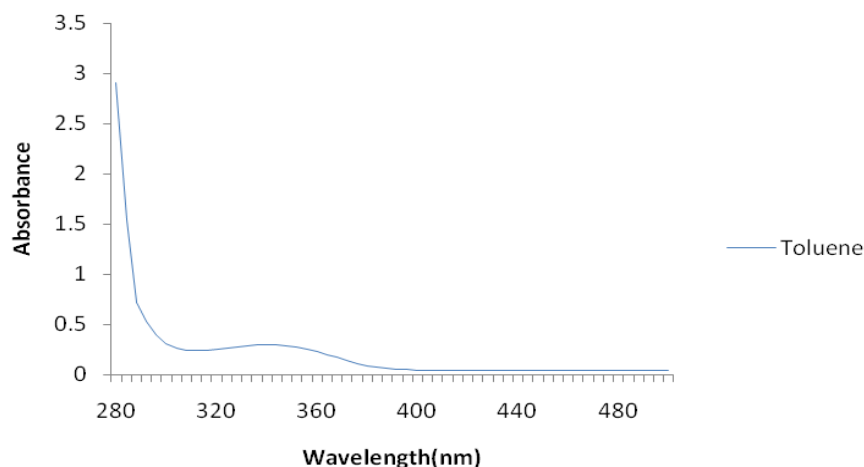
Figure 5.3.5 Absorption spectrum of **55** (in toluene)
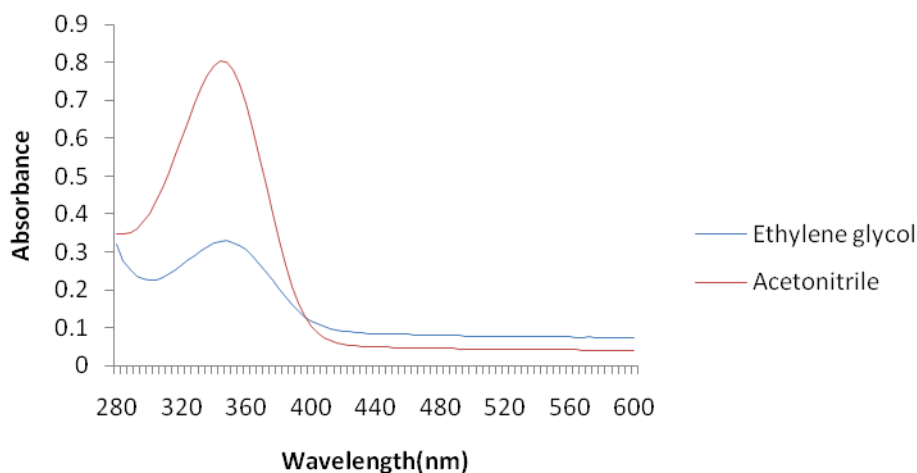
Figure 5.3.6 Absorption spectrum of **55** (in ethylene glycol and MeCN)

5.3.2 Emission spectrum of 55

The absorption maximum from the UV spectrum was used as an excitation parameter to generate the emission spectra. After excitation at 340 nm, a single emission band for compound **55** was found in all solvents (except n-hexane), **Table 5.6**. The emission spectra are show in **Figure 5.3.7** and **Figure 5.3.8**.

Solvent	λ_{em} [a]
Chloroform	433
Methanol	483
Toluene	412
Acetic acid	463
Ethylene glycol	486
Dichloromethane	450
n-Hexane	374[b]
Acetonitrile	475

Table 5.6 Maximum emission bands for compound **55** after excitation at 340 nm. [a] λ_{em} in nm.
[b] A second emission band was observed at 390 nm (concentration of sample, 0.712×10^{-3} mM).
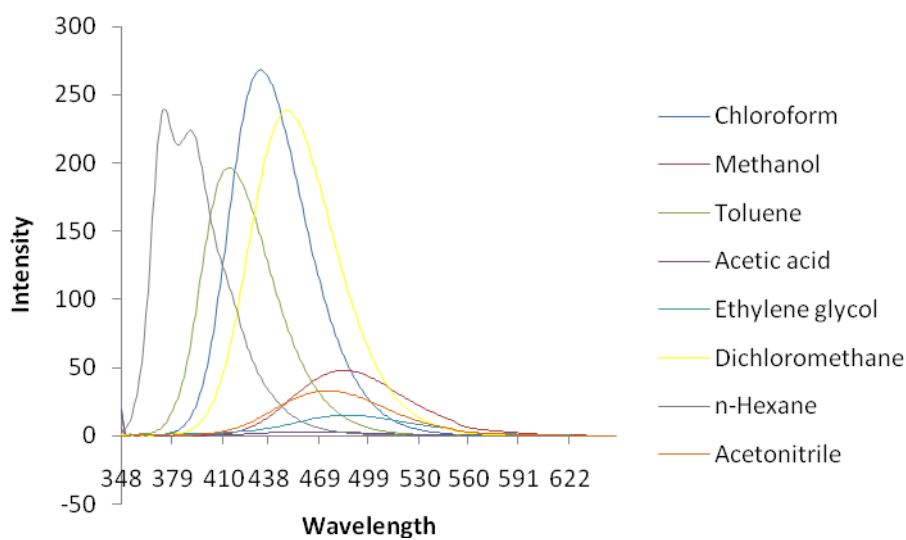
Figure 5.3.7 Emission spectra of **55** in different solvents (concentration of sample, 0.712×10^{-3} mM)
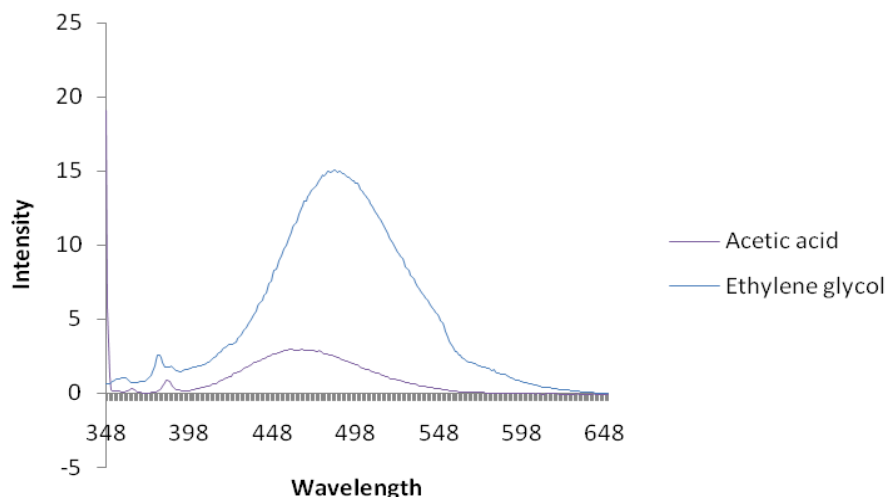
Figure 5.3.8 Zoomed in emission spectra of **55** in acetic acid and ethylene glycol (concentration of sample, 0.712×10^{-3} mM)

In order to better understand the nature of the emission our colleague, Dean St. Mart, fitted the emission band of **55** in chloroform using a Gaussian calculation, **Figure 5.3.9**. Two single bands were obtained indicating two possible deactivation pathways/processes. The intensity ratio of the two bands was 1.3: 1. We propose that the major band could be from the deactivation of S_1 (1st excited state) to S_0 (ground state), as it requires less energy for the molecule to be excited to S_1, and the minor band was from the deactivation from S_2 (2nd excited state) to S_1.

Data: fluoresce_normCHCl3
Model: Gauss
Equation: y=y0 + (A/(w*sqrt(PI/2)))*exp(-2*((x-xc)/w)^2)
Weighting:
y   No weighting

Chi^2/DoF   = 0.00003
R^2   = 0.99971

y0	0	±0
xc1	22391.35333	±76.14949
w1	2545.39522	±35.68031
A1	1716.37283	±135.73588
xc2	23388.58877	±10.63839
w2	1847.04077	±35.51398
A2	1323.7513	±134.56587
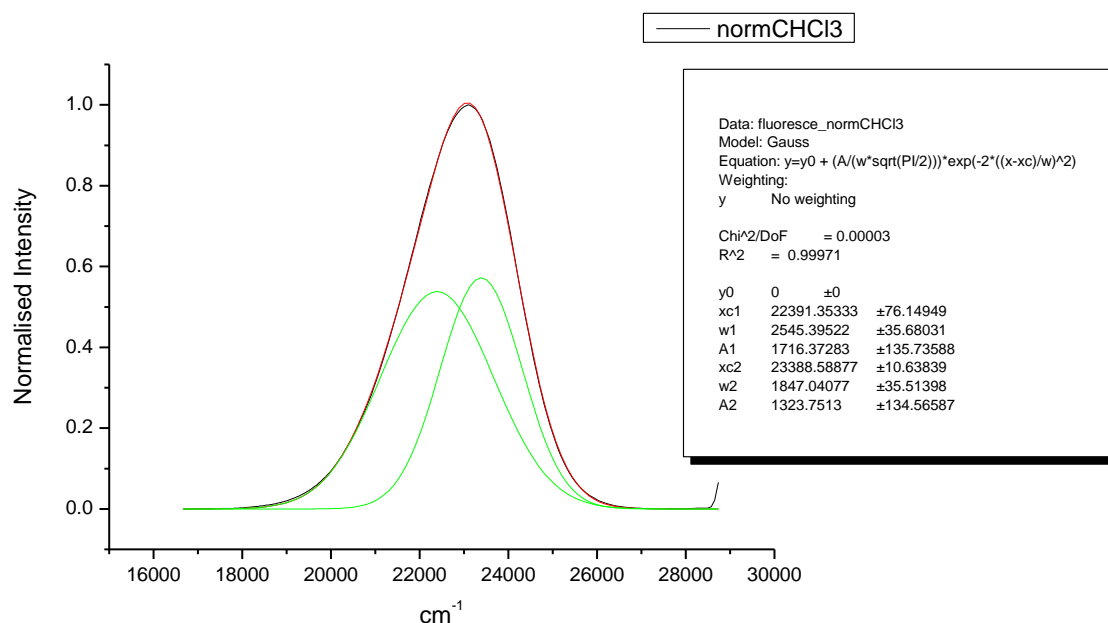
```
                Chi^2/DoF        3.16951E-5
                R^2                  0.99971
    Peak            Area     Center    Width    Height

    ------------------------------------------------------------------

     1              1716.4   22391    2545.4   0.53802
     2              1323.8   23389    1847.0   0.57183

    ------------------------------------------------------------------

                Yoffset = 0
```

Figure 5.3.9 Gaussian normalised fit for compound **55** in chloroform

5.3.3 Excitation spectrum of 55

Emission maximum values were used as an emission parameter to generate the excitation spectra for compound **55**. Excitation bands for compound **55** are summarized in **Table 5.7**. The excitation spectra are show in **Figure 5.4.1**, **Figure 5.4.2** and **Figure 5.4.3**.

Solvent	λ_{em}[a]	λ_{ex}[b]
Chloroform	433	346
Methanol	483	345
Toluene	412	346
Acetic acid	463	327
Ethylene glycol	486	347
Dichloromethane	450	346
n-Hexane	374	336
Acetonitrile	475	342

Table 5.7 Excitation bands for compound **55**. [a] λ_{em} in nm. [b] λ_{ex} in nm (concentration of sample, 0.712×10^{-3} mM).
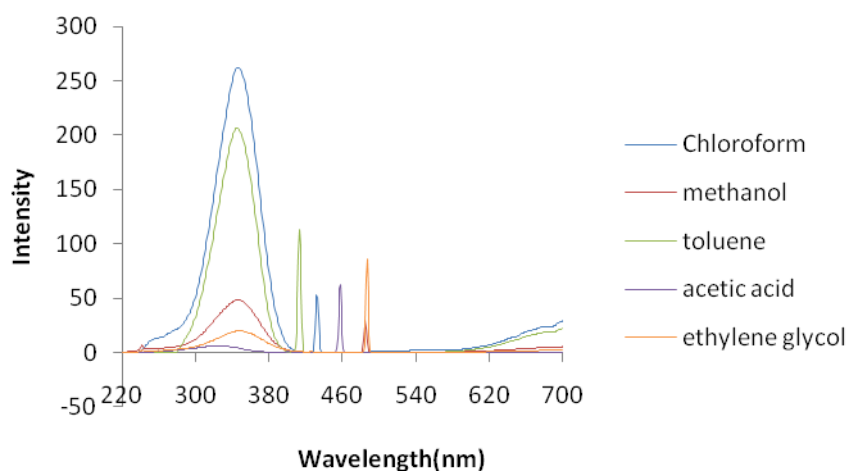
Figure 5.4.1 Excitation spectrum of **55** in different solvents (concentration of sample, 0.712 $\times 10^{-3}$ mM).
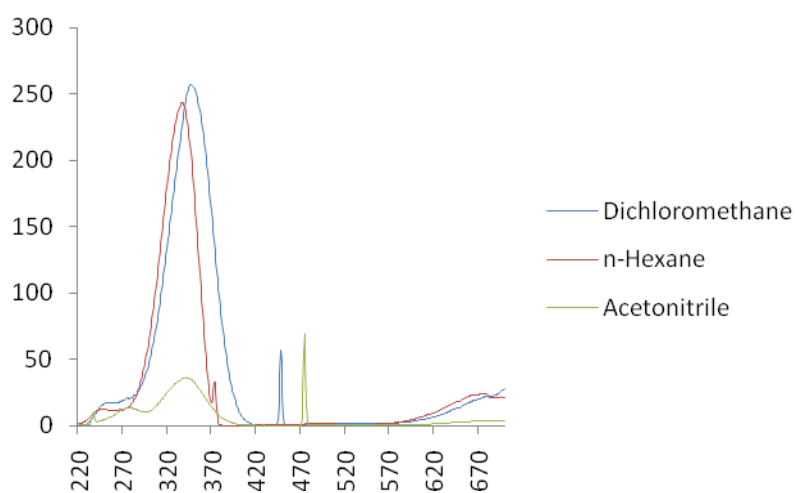
Figure 5.4.2 Excitation spectrum of **55** in different solvents (concentration of sample, 0.712 $\times 10^{-3}$ mM).
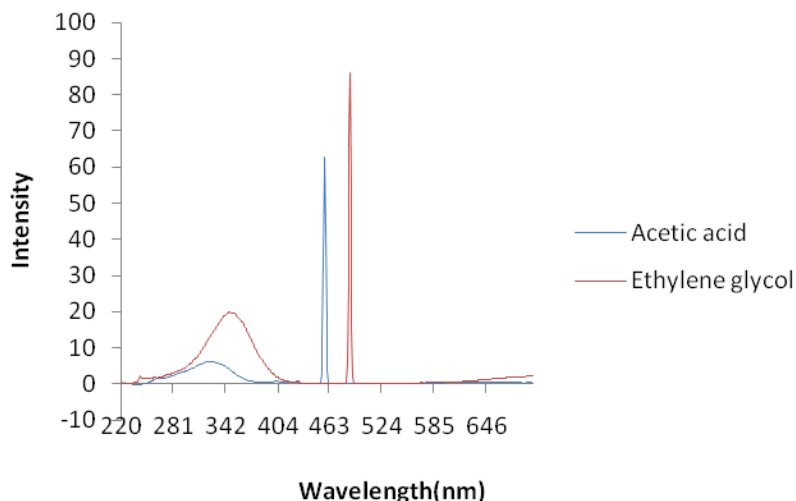
Figure 5.4.3 Zoomed in excitation spectrum of **55** in acetic acid and ethylene glycol (concentration of sample, 0.712×10^{-3} mM).

5.3.4 Absorption spectra of compounds 56-61

The biphenyl sulfones **56-61** were studied in chloroform and methanol and a summary of their UV-absorption spectra is given in **Table 5.8**. The UV-absorption spectra are shown in **Figure 5.4.4**, **Figure 5.4.5** and **Figure 5.4.6**.

Compound	λ_{abs} in CHCl$_3$[a]	λ_{abs} in MeOH[a]
56	291	284
57	280	281
58	295	299
59	281	279
60	280	276
61	285	284

Table 5.8 UV absorption maxima for compounds **56-61**. [a] λ_{abs} are reported at the maximum absorbance wavelength in nm (**56** at 1.1×10^{-3} mM; **57** at 0.60×10^{-3} mM; **58** at 0.88×10^{-3} mM; **59** at 0.96×10^{-3} mM; **60** at 0.35×10^{-3} mM; **61** at 0.86×10^{-3} mM)
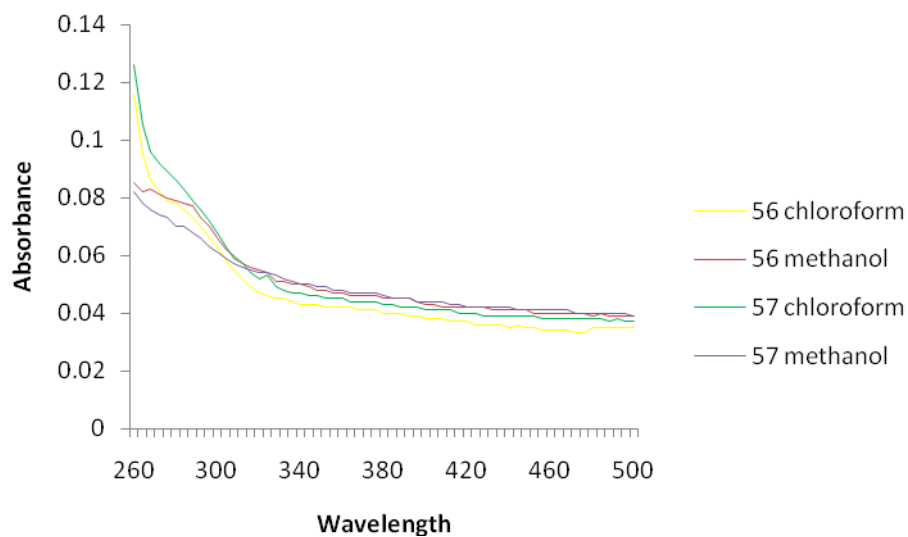
Figure 5.4.4 Absorption spectrum of **56-57** in chloroform and methanol (**56** at 1.1×10^{-3} mM;
57 at 0.60×10^{-3} mM).
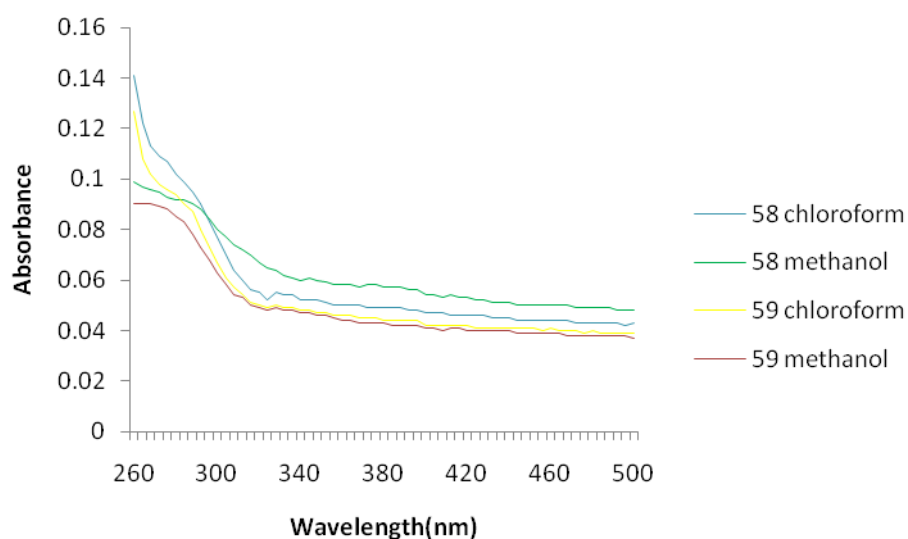
Figure 5.4.5 Absorption spectrum of **58-59** in chloroform and methanol (**58** at 0.88×10^{-3} mM; **59** at 0.96×10^{-3} mM).
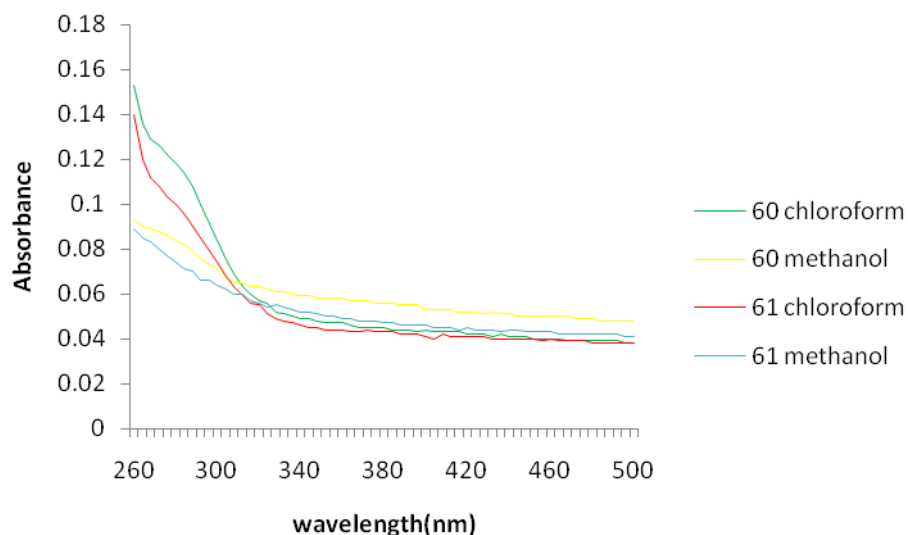
Figure 5.4.6 Absorption spectrum of **60-61** in chloroform and methanol (**60** at 0.35×10^{-3} mM; **61** at 0.86×10^{-3} mM).

5.3.5 Emission spectra of 56-61

The absorption maximum from the UV spectrum was used as an excitation parameter to generate the emission spectra. Compounds **56-61** were excited at 285 nm and a summary of their emission bands are given in **Table 5.9**. The emission spectra are show in **Figure 5.4.7**, **5.4.8** and **Figure 5.4.9**.

Compound	λ_{em} in CHCl$_3$[a]	λ_{em} in MeOH[a]
56	340	348
57	332[b]	332[c]
58	359	389
59	335	345
60	329[d]	327[e]
61	362[f]	406[g]

Table 5.9 Maximum emission bands for compounds **56-61** after excitation at 285 nm. [a] λ_{em} in nm. [b] two shoulders at 320 nm and 347 nm. [c] two shoulders at 319 nm and 342 nm. [d] two shoulders at 316 nm and 341 nm. [e] two shoulders at 315 nm and 339 nm. [f] one shoulder at 418 nm. [g] an unsymmetrical emission band.
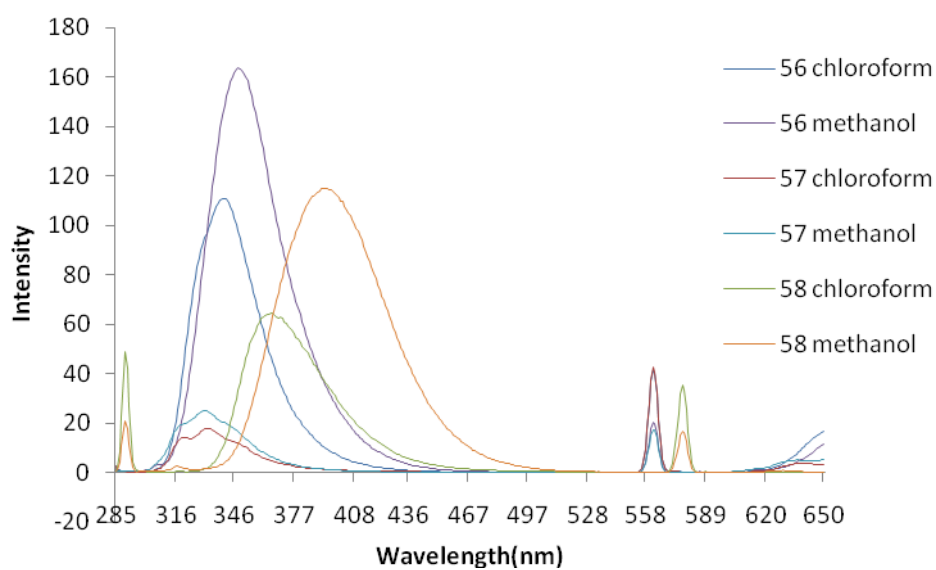
Figure 5.4.7 Emission spectra of compounds **56-58** in chloroform and methanol (**56** at 1.1×10^{-3} mM; **57** at 0.60×10^{-3} mM; **58** at 0.88×10^{-3} mM).
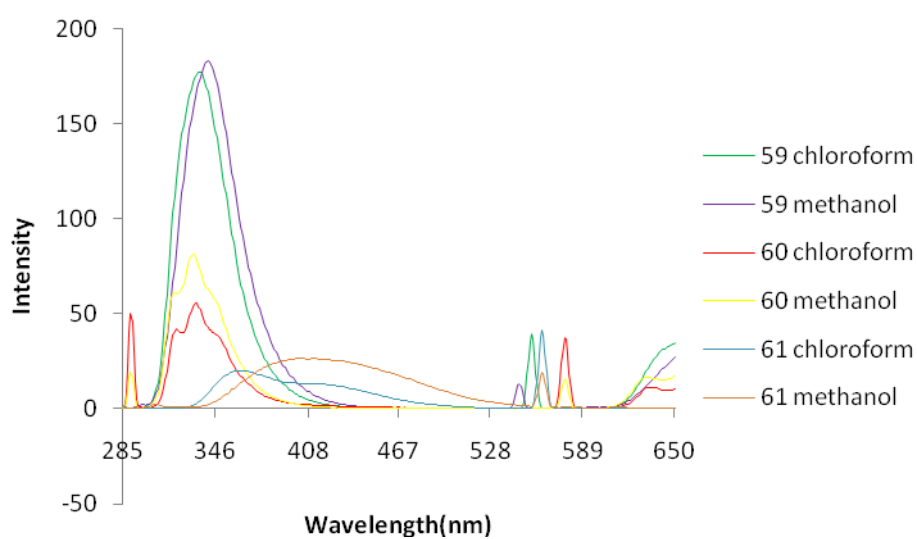
Figure 5.4.8 Emission spectrum of **59-61** in chloroform and methanol (**59** at 0.96×10^{-3} mM; **60** at 0.35×10^{-3} mM; **61** at 0.86×10^{-3} mM).
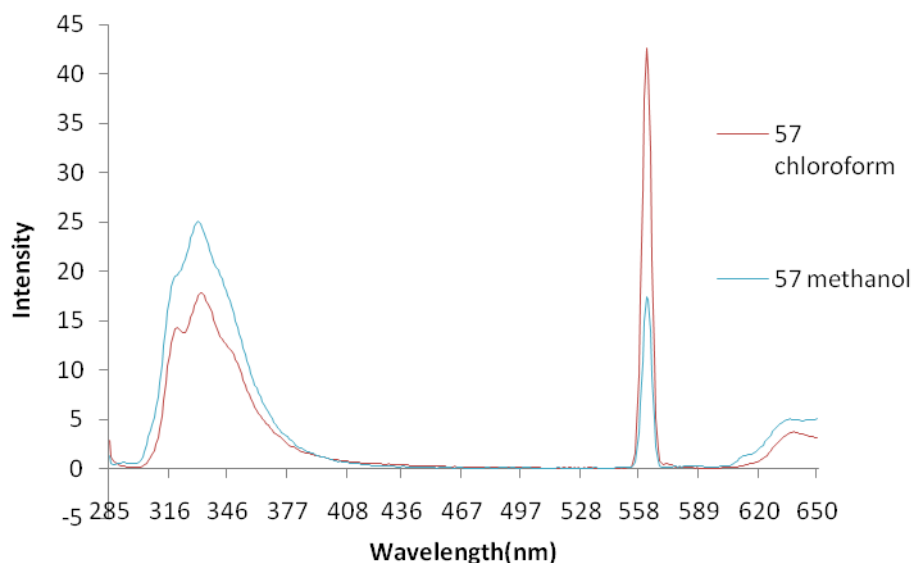
Figure 5.4.9 Zoomed in emission spectrum of **57** in chloroform and methanol

5.3.6 Excitation spectrum of 56-61

Emission maximum values were used as an emission parameter to generate the excitation spectra for compounds **56-61**. Excitation bands for compound **56-61** are summarized in **Table 5.10**. The excitation spectra are show in **Figure 5.4.10** and **Figure 5.5.1**.

Compound	λ_{em} in CHCl$_3$[a]	λ_{ex} in CHCl$_3$[a]	λ_{em} in MeOH[a]	λ_{ex} in MeOH[a]
56	340	288	348	287
57	332	286	332	286
58	359	299	389	299
59	335	284	345	284
60	329	284	327	283
61	362	301[b]	406	301[b]

Table 5.10 Excitation bands for compound **56-61**. [a] λ_{em} and λ_{ex} in nm. [b] Shoulder observed at

273 nm.
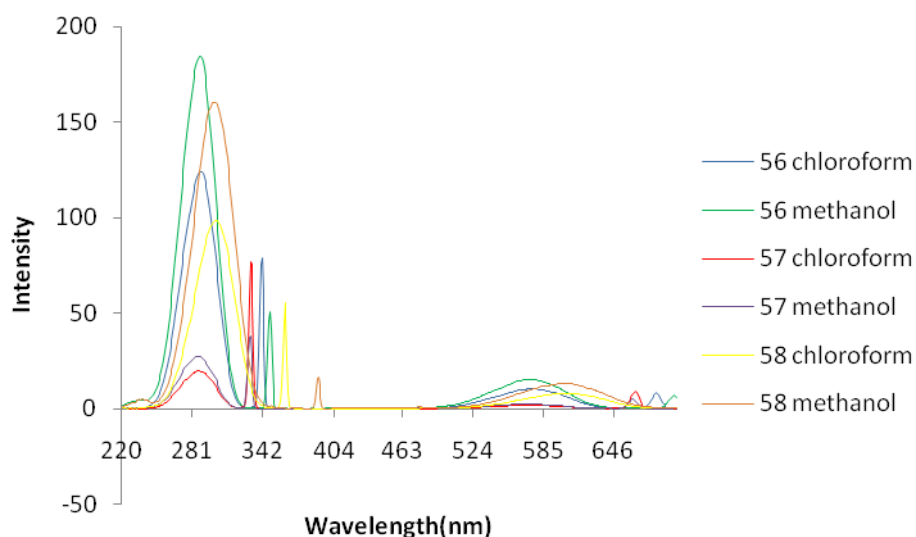
Figure 5.4.10 Excitation spectra of **56-58** in chloroform and methanol (**56** at 1.1×10^{-3} mM; **57** at 0.60×10^{-3} mM; **58** at 0.88×10^{-3} mM).
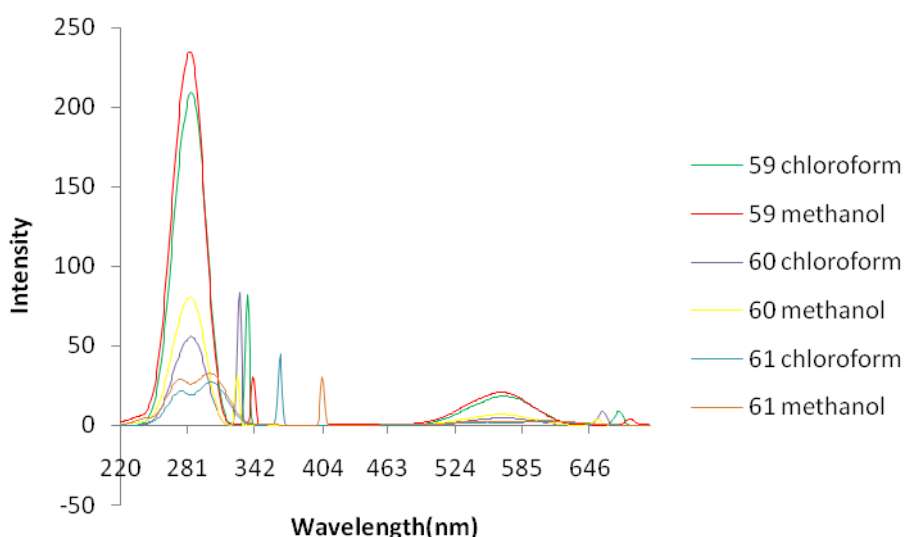
Figure 5.5.1 Excitation spectra of **59-61** in chloroform and methanol (**59** at 0.96×10^{-3} mM; **60** at 0.35×10^{-3} mM; **61** at 0.86×10^{-3} mM).

Compound **62** and **63** did not exhibit any fluorescent properties, **Figure 5.5.2**. This is possibly due to the strong electron-withdrawing nature of NO_2 group, the resultant existence of a low-lying n to π^* transition and an efficient intersystem crossing process.[88] Thus most NO_2 substituted aromatic compounds are not fluorescent. The absence of detectable fluorescence is possibly due to a high rate of S_1 (1st excited state) to S_0 (ground state) internal conversion, non-radiative decay.[88]
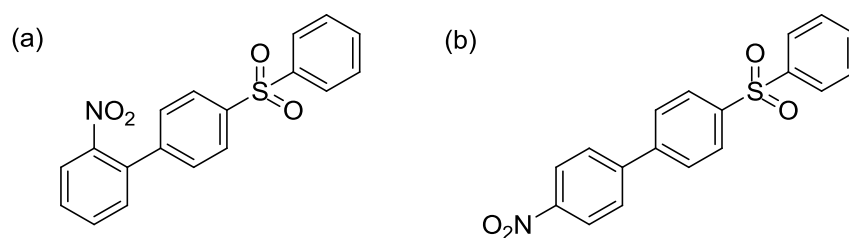
Figure 5.5.2 Structure of (a) **62** and (b) **63**

5.3.7 Photophysics of 55-61

The absorption, emission and excitation spectra of compounds **55-61** were analyzed, and their corresponding photophysical data listed in **Table 5.11**.

Compound	Solvent	λ_{abs}	λ_{em}	Stokes (nm)	$\varepsilon \ (\times 10^4$ $M^{-1}cm^{-1})$	Φ
55	Chloroform	284/343	433	90	2.47	0.71
	Methanol	339	483	144	2.89	0.18
	Toluene	340	412	72	4.18	0.88
	Acetic acid	277/324	463	139	4.72	0.02
	Ethylene glycol	348	486	138	8.43	0.23
	Dichloromethane	348	450	102	3.16	0.88
	n-Hexane	336	374/390	38/54	3.51	0.70
	Acetonitrile	344	475	131	2.67	0.12
56	Chloroform	291	340	49	4.00	0.31
	Methanol	284	348	64	3.57	0.39
57	Chloroform	280	332	52	5.08	0.09
	Methanol	281	332	51	3.29	0.07
58	Chloroform	295	359	64	5.83	0.25
	Methanol	299	389	90	7.00	0.57
59	Chloroform	281	335	54	4.99	0.55
	Methanol	279	345	66	4.71	0.48
60	Chloroform	280	329	49	15.6	0.71
	Methanol	276	327	51	7.14	0.40
61	Chloroform	285	362/418	77/133	6.14	0.20
	Methanol	284	406	122	3.25	0.16

Table 5.11 Photophysical data for the biphenyl sulfones

The Stokes shifts were calculated using Stokes shift = λ_{em} - λ_{abs}, where λ_{em} is the wavelength

of maximum emission from the emission spectrum and λ_{abs} is the wavelength of absorbance, which corresponding to the maximum emission, in UV-absorption spectrum.

Molar extinction coefficient e was obtained from the Beer Lamber law and calculated using $e = 1 / l * c$, where c is the concentration of the examed solution, l is the path length of the cuvette and l is the corrected maximum absorbance.

Quantum yields Q were calculated using $Q = Q_R(I/I_R)(OD_R/OD)(n^2/n^2_R)$[71] where the "$Q$" is quantum yield; "$I$" is the integrated intensity of emission spectrum; "OD" is the optical density i.e. the corrected absorbance which corresponds to the maximum emission in UV-absorption spectrum (base line corrected using "origin" software before being applied to the quantum yield calculation.); "n" is the refractive index of the solvent; subscript "R" refers to the reference fluorophore of known quantum yield. Quinine sulfate in 0.1 M H_2SO_4 was chosen as the standard for calculating quantum yield of compound **55** and was prepared at the same concentration as compound **55**. UV-absorption spectrum of quinine sulfate in 0.1 M H_2SO_4 was obtained along with the emission spectrum after excitation at 340 nm (same wavelength as used for compound **55**). 2-Aminopyridine in 0.1 N H_2SO_4 was chosen as the standard for calculating the quantum yields of compounds **56-61** and was prepared at different concentrations (1.1×10^{-6} M; 0.88×10^{-6} M; 0.66×10^{-6} M; 0.35×10^{-6} M) to match the concentrations of compounds **56-61**. UV-absorption spectrum of 2-aminopyridine in 0.1 N H_2SO_4 was obtained; emission spectrum was obtained after excitation at 285 nm (same wavelength as used for compounds **56-61**).

Compound **55** was found to have a Stokes shift in all solvents (from 90 nm in chloroform to 144 nm in methanol). Compound **55** had a very high quantum yield in toluene and dichloroform (Φ close to 0.9), a high quantum yield in chloroform and n-hexane ($\Phi > 0.7$) and a high molar extinction coefficient in ethylene glycol ($\varepsilon > 80\,000$ $M^{-1}cm^{-1}$). Compound **56-61** all generated relatively large Stokes shifts (from 49 nm for compound **56** in chloroform to 122 nm for compound **61** in methanol). The quantum yield varied across compounds **56-61** (from a low of $\Phi = 0.07$ for compound **57** in methanol to $\Phi = 0.71$ for compound **60** in chloroform). As we previously discussed on **page 101**, compound **61** was a mixture of two isomers and may explain the two large Stokes shifts obtained in chloroform (77 nm and 133 nm). A single large Stokes shift was obtained for compound **61** in methanol (122 nm).

5.3.8 Solvatochromic analysis, compound 55

Solvatochromism was termed by Hantzschlater. It is a phenomenon that UV/vis/near-IR absorption spectra of chemical coumpounds may be influenced by the surrounding medium and that solvents can bring about a change in the position, intensity and shape of absorption bands.[89] An initial observation of compound **55** in two solvents, chloroform and methanol, suggested that compound **55** may be highly solvatochromic. Subsequent quantum yield calculations confirmed what we had observed, namely a marked difference in quantum yield for compound **55** in the two solvents ($\Phi = 0.71$ in chloroform and $\Phi = 0.18$ in methanol).

As a result compound **55** underwent a solvatochromic study where it's UV-absorption and fluorescence was examined in eight solvents. Photophysical data for compound **55** (Stokes shifts, quantum yield and extinction coefficient, **Table 5.11**) in different solvents were plotted against solvent polarity, **Table 5.12**.

Solvent	E_T^{30}(kcal mol^{-1})错误！未定义书签。
Chloroform	39.1
Methanol	55.4
Toluene	33.9
Acetic acid	55.2
Ethylene glycol	56.3
Dichloromethane	40.7
n-Hexane	31.0
Acetonitrile	45.6

Table 5.12 Solvent polarity, E_T^{30}

The maximum absorbance for compound **55** was found to be insensitive to solvent polarity, (E_T^{30}).[89]

The Stokes shifts were plotted against Reichardt's solvent polarity parameter (E_T^{30})[89] to give an excellent linear correlation ($R^2 = 0.8941$, **Figure 5.5.3**). The Stokes shifts were found to be highly solvatochromic, to solvent polarity, generating a large slope of 3.35 nm/kcal mol^{-1}. The changes in Stokes shift resulted from changes of its emission wavelength in the different solvents. For example, the Stokes shift of **55** increased from 72 nm in toluene ($\lambda_{em} = 412$ nm) to 144 nm in methanol ($\lambda_{em} = 483$ nm).
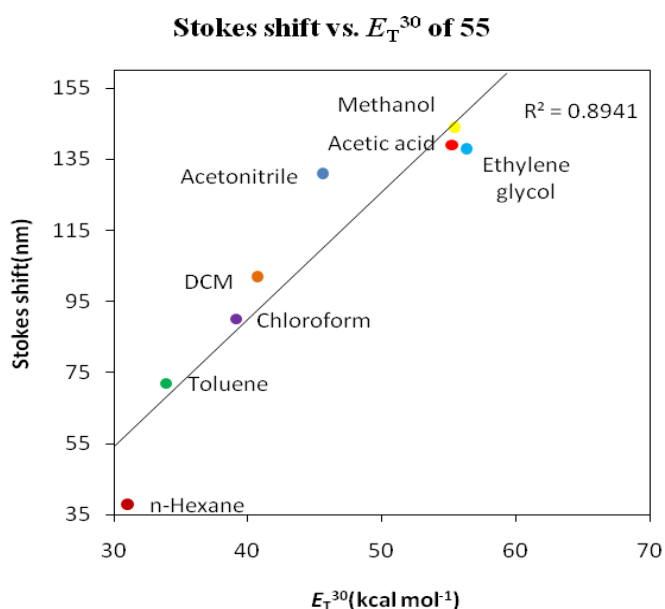
Figure 5.5.3 Plot of Stokes shift versus E_T^{30} value for compound **55**

The quantum yields of **55**, in different solvents, were plotted against Reichardt's solvent polarity parameter (E_T^{30}) to give a relatively linear correlation ($R^2 = 0.7121$, **Figure 5.5.4**). The quantum yield was found to be highly sensitive to solvent polarity with a slope of -0.033 mol kcal^{-1} and ranging from from $\Phi = 0.88$ in toluene to $\Phi = 0.18$ in methanol. The quantum yield of **55** was very low ($\Phi = 0.02$) in acetic acid, even when compared to the protic solvent methanol ($\Phi = 0.18$). This is probably due to the acetic acid (pK_a = 4.7) protonating the dimethylamino group (pK_{aH} ~ 10) which inhibits the intramolecular charge transfer (ICT) and hence quenches the fluorescence. The result in acetic acid is in fact supportive of an intramolecular charge transfer mechanism for fluorescence.

Quantum yield vs. E_T^{30} of 55
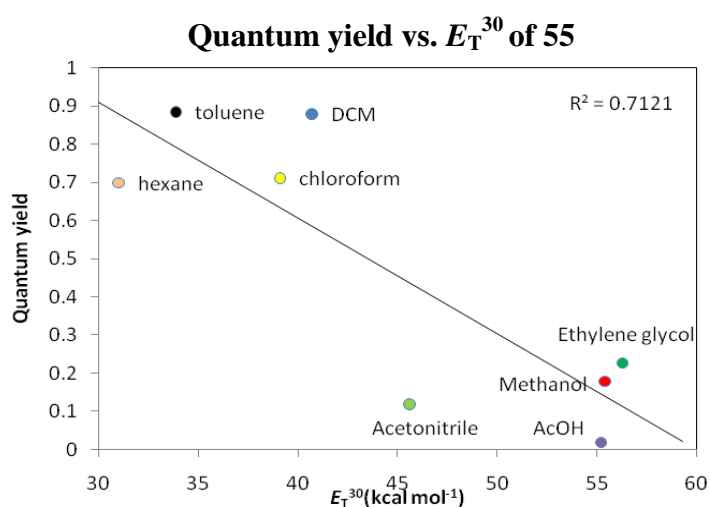
Figure 5.5.4 Plot of quantum yield versus E_T^{30} value for compound **55**

5.3.9 Mechanism of fluorescence

The mechanism of fluorescence for these biphenyls is most likely *via* a twisted intramolecular charge transfer (TICT) process. Lippert and co-workers reported that *p*-(dimethylamino)-benzonitrile (DMABN) showed one emission band at around 360 nm in non-polar solvent and two emission bands in polar solvent with an extra band at around 450-500 nm.[90] This phenomenon was explained by the concept of TICT.[91] TICT suggests that the donor dialkylamino transfers an electron to the acceptor cyanobenzene, and the donor undergoes a twist simultaneously. The donor orbital become orthogonal to the acceptor orbital which ensures complete electron transfer due to this twist process, **Figure 5.5.5**. The resulting state is polar and known as TICT state.[91]
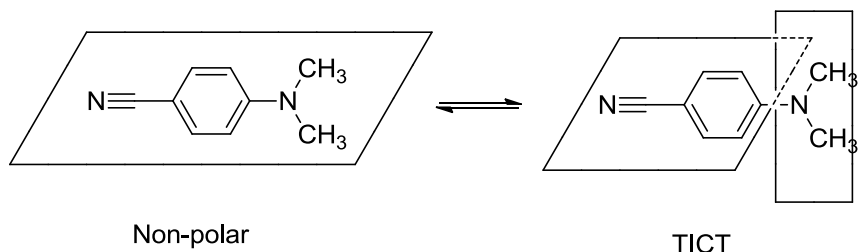
Figure 5.5.5 TICT process of DMABN[91]

2,4-Dichloro-6-[p-(N,N-diethylamino)biphenylyl]-1,3,5-triazine, **Figure 5.5.6**, is a fluorescent dye reported by Yan Ma and co-workers. It has a diethyl amino (electron donor) and triazine (electron acceptor) joined by the twistable aromatic chain and as a result exhibits intramolecular charge transfer character.[92]
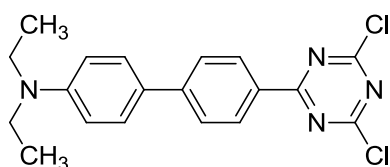
Figue 5.5.6 Structure of 2,4-Dichloro-6-[p-(N,N-diethylamino)biphenylyl]-1,3,5-triazine[92]

Michael Maus and co-workers reported a series of biphenyls with dimethylamino (electron donor) and cyano group (electron acceptor) joined by the twistable biphenyl chain, **Figure 5.5.7**.[93] These compounds are similar in structure to our biphenyl sulfones where we have a dimethylamino donor and a sulfone acceptor linked by a biphenyl, compound **55**.

Figure 5.5.7 Structure of biphenyls as reported by Michael Maus[93]

DFT calculations of compounds **55-63** were performed on request by our colleague Dr Elisa Fadda using the following method: All molecules were built with version 9.4 of Maestro (Academic License);[94] their geometry was optimized with version 6.5 of TURBOMOLE[95] at the b97d//def2-SVP level of theory[96], within the resolution of the identity approximation and in redundant internal coordinates. b97d represents the b97 GGA functional[97] augmented with Grimme dispersion contribution.[96] The molecular orbitals images have been produced with version 4.5.0 of the MOLEKEL software package.[98] These DFT calculations generated HOMO and LUMO energies for compounds **55-63**.

The DFT calculations of compound **55** indicate charge transfer from the dimethylamino group to the phenylsulfone group upon going from HOMO to LUMO, **Figure 5.5.8**. DFT calculations of compound **56-63** were shown in the **appendix**. These results suggest the existing of a push-pull system where the dimethylamino group acts as an electron donor and phenylsulfone group acts as an electron acceptor in the excited state. The calculated HOMO-LUMO gaps (**55 < 58 < 59 < 57 < 60 < 56**) were inversely correlated with the Stokes shifts (in chloroform), **Table 5.13**.

HOMO (-0.170532 au)

LUMO (-0.0768876 au)
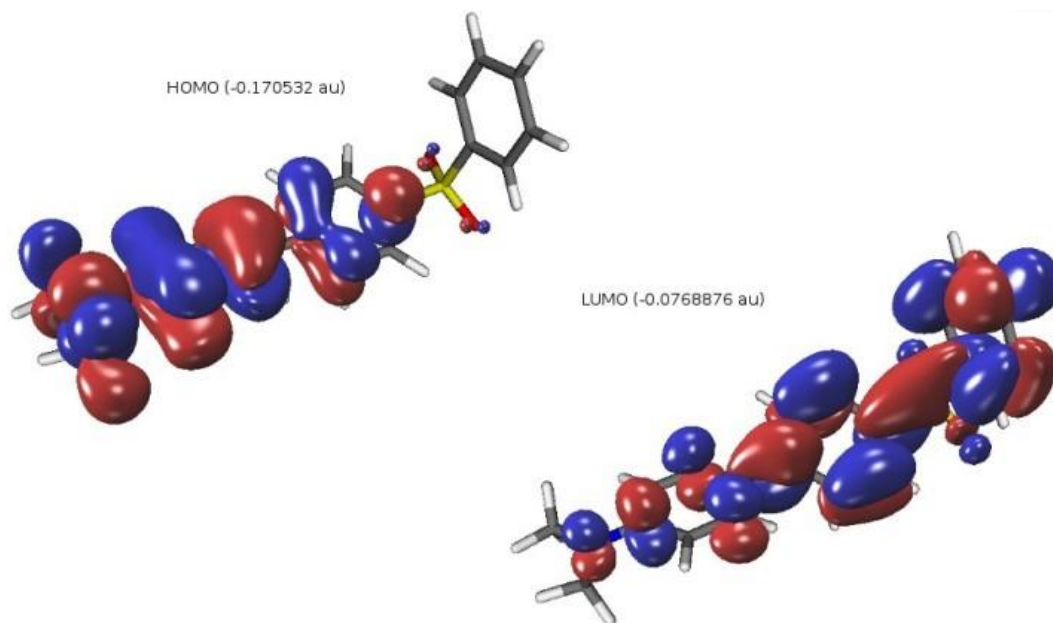
Figure 5.5.8 Molecular orbital plot of compound **55**

Compound	HOMO-LUMO gaps (au)	Stokes shifts (nm)[a]
55	0.094	90
58	0.112	64
59	0.120	54
57	0.121	52
60	0.122	49
56	0.123	49

Table 5.13 Comparison of HOMO-LUMO gap and Stokes shift. [a] In chloroform.

Increasing the electron donating ability of the electron donor was accompanied by a decrease in the HOMO-LUMO gap. These results are consistent with our prediction that these biphenyl compounds exhibit fluorescence *via* a twisted intramolecular charge transfer (TICT). Compound **55** is taken as an example, the donor (dimethylamino) group transfers an electron to the acceptor (phenylsulfone) and undergoes a twist simultaneously. The donor (dimethylamino) group orbital becomes orthogonal to the acceptor (phenylsulfone) orbital

which ensures complete electron transfer due to this twist process, **Figure 5.5.9**.
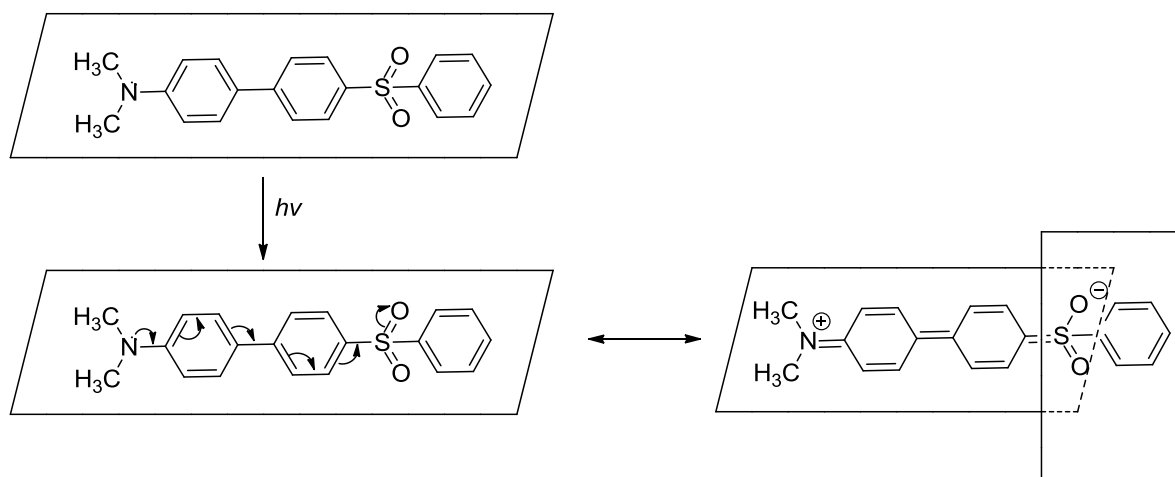
Figure 5.5.9 Proposed TICT mechanism for compound **55**

As previously mentioned in section **5.3.9**, the calculated HOMO-LUMO gaps for **55-60** were inversely correlation to their Stokes shift. The HOMO-LUMO gaps of compound **55-60** were plotted against their Stokes shifts (in chloroform) giving an excellent linear correlation ($R^2 = 0.9978$, **Figure 5.6.1**). These results suggested that the underlying photophysical processes are similar for **55-60**, where stronger electron donating groups generate smaller HOMO-LUMO gaps and red-shifted emissions, as compared to weaker electron donating groups. Therefore, it may be possible for us to tailor the biphenyl system so as to further decrease the HOMO-LUMO gap with the aim of causing a red-shift in emission.
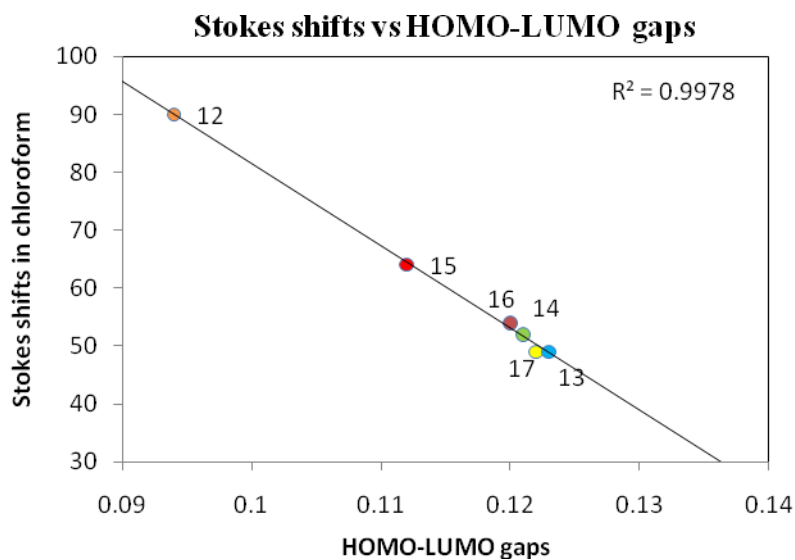
Figure 5.6.1 Plot of Stokes shifts (in chloroform) versus HOMO-LUMO gaps

5.4.1 Conclusion

We have developed a novel solvent-free methodology for synthesizing fluorescent biphenyl sulfones with a relatively short reaction time and in good yields. This methodology exploits an interesting electrocyclisation of bissulfonyl trienes. A new family of substituted biphenyl sulfones resulted. UV-absorption, emission and excitation spectra were generated for the family of biphenyl sulfones and their photophysical characterisitics studied (e.g. Stokes shift, quantum yield, molar extinction coefficients). The biphenyl sulfones with NO_2 substituents did not exhibit fluorescence due to the strong electron withdrawing nature of the NO_2 group. Other substituted biphenyl sulfones exhibited highly solvatochromic emissions from twisted intramolecular charge transfer (TICT) states. Of these substituted biphenyls, compound **55** was found to show a very high quantum yield in toluene and dichloromethane (Φ close to 0.9) and high quantum yield in chloroform and n-hexane ($\Phi > 0.7$). Compound **55** also exhibited large Stokes shifts (90 nm in chloroform; 144 nm in methanol; 139 nm in acetic acid; 138 nm in ethylene glycol; 102 nm in dichloromethane; 131 nm in acetonitrile) and high molar extinction coefficient in ethylene glycol ($\varepsilon > 80\ 000\ M^{-1}cm^{-1}$). The HOMO-LUMO gaps of the biphenyl sulfones (compounds **55-60)** were plotted against their Stokes shifts (in chloroform) giving an excellent linear correlation ($R^2 = 0.9978$). These results suggested that the underlying photophysical processes are similar for **55-60**, where stronger electron donating groups generate smaller HOMO-LUMO gaps and red-shifted emissions, as compared to weaker electron donating groups. In future work, it may be possible to tailor the electronics of this biphenyl system to further decrease the HOMO-LUMO gap with the aim of causing a red-shift in emission. These biphenyl systems also have potential as probes for reporting changes in microenvironmental polarity.

Chapter 6 Experimental for the synthesis of biphenyl sulfones

Instrumentation

Reagents were purchased from Sigma-Aldrich, Alfa Aesar, Acros Organics and used without further purification. Anhydrous DMF was purchased from Sigma Aldrich.

All NMR spectra were recorded on a Bruker Avance spectrometer at a probe temperature of 25 °C, unless otherwise stated, operating at 300 MHz for the 1H nucleus and 75 MHz for the 13C nucleus. Proton and carbon signals were assigned with the aid of DEPT experiments for novel compounds. High temperature NMR spectroscopy experiments were carried out by heating the probe. Spectra were recorded in DMSO-d_6, CDCl$_3$ or CD$_3$OD with Me$_4$Si used as the internal standard. Chemical shifts are given in ppm downfield form the internal standard and coupling constants are given in Hz.

Melting point analyses were carried out using a Stewart Scientific SMP1 melting point apparatus.

Infrared (IR) spectra were recorded as KBr disks or liquid films between NaCl plates using a Perkin Elmer System 2000 FT-IR spectrometer in the region of 4000-370 cm^{-1}. High resolution mass spectra (HR-MS) were performed on an Agilent-L 1200 Series coupled to a 6210 Agilent Time-of-Flight (TOF) mass spectrometer equipped with an both a positive and negative electrospray source.

Microanalysis was carried out using a Flash EA 1112 Series Elemental Analyser. The sample is burned in oxygen and a helium carrier gas at 900 ^{o}C in a combustion tube.

Flash column chromatography was performed using silica gel 60 (Merck, 0.040-0.063 mm). Analytical thin layer chromatography was carried out on aluminium sheets precoated with Merck TLC Silica gel 60 F254.

UV-vis spectra were recorded using a Unicam UV 540 spectrometer. Excitation and emission spectra were recorded on a JASCO FP-6300 spectrofluorometer.

6.1 Attempted procedures for the synthesis of 4-(phenylsulfonyl)-1,1'-biphenyl 43 (Biphenyl 11)

1-[(1E,3E,5E)-4,6-Bis(phenylsulfonyl)hexa-1,3,5-trien-1-yl]-4-benzene **44** (10 mg, 0.023 mmol) was dissolved in toluene (3 mL). The solution was heated under microwave conditions at 110 ^{o}C for 15 minutes. The resulting solution was purified using flash chromatograph on silica gel with ethyl acetate/petroleum ether (50 : 50). The ^{1}H NMR of the elutent showed no reaction.

1-[(1E,3E,5E)-4,6-Bis(phenylsulfonyl)hexa-1,3,5-trien-1-yl]-4-benzene **44** (10 mg, 0.023 mmol) was dissolved in toluene (3 mL). The solution was heated under microwave conditions at 130 ^{o}C for 15 minutes. The resulting solution was purified using flash chromatograph on silica gel with ethyl acetate/petroleum ether (50 : 50). The ^{1}H NMR of the elutent showed no reaction.

1-[(1E,3E,5E)-4,6-Bis(phenylsulfonyl)hexa-1,3,5-trien-1-yl]-4-benzene **44** (15 mg, 0.034 mmol) was dissolved in toluene (1 mL). The solution was heated under microwave conditions at 130 ^{o}C for 15 minutes. The resulting solution was purified using flash chromatograph on silica gel with ethyl acetate/petroleum ether (50 : 50). The ^{1}H NMR of the elutent showed no reaction.

1-[(1E,3E,5E)-4,6-Bis(phenylsulfonyl)hexa-1,3,5-trien-1-yl]-4-benzene **44** (10 mg, 0.023 mmol) was dissolved in dimethylformamide (3 mL). The solution was heated under microwave conditions at 120 ^{o}C for 15 minutes. The resulting solution was purified using flash chromatograph on silica gel with ethyl acetate/petroleum ether (50 : 50). The ^{1}H NMR of the elutent showed no reaction.

1-[(1E,3E,5E)-4,6-Bis(phenylsulfonyl)hexa-1,3,5-trien-1-yl]-4-benzene **44** (15 mg, 0.034 mmol) was dissolved in NMP (1 mL). The solution was heated under microwave conditions at 200 ^{o}C for 15 minutes. The resulting solution was purified using flash chromatograph on silica gel with ethyl acetate/petroleum ether (50 : 50) to give a pale yellow solid. The yield was too low to be isolated.

1-[(1*E*,3*E*,5*E*)-4,6-Bis(phenylsulfonyl)hexa-1,3,5-trien-1-yl]-4-benzene **44** (14 mg, 0.032 mmol) was dissolved in NMP (0.5 mL). The solution was heated under microwave conditions at 200 ^{o}C for 1 hour. The resulting solution was purified using flash chromatograph on silica gel with ethyl acetate/petroleum ether (50 : 50) to give a pale yellow solid. The yield was too low to be isolated.

Neat 1-[(1*E*,3*E*,5*E*)-4,6-bis(phenylsulfonyl)hexa-1,3,5-trien-1-yl]-4-benzene **44** (14 mg, 0.032 mmol) was heated at 115 ^{o}C for 5 hours and purified using flash chromatograph on silica gel with ethyl acetate/petroleum ether (50:50) to give a pale yellow solid. The yield was too low to be isolated.

Neat 1-[(1*E*,3*E*,5*E*)-4,6-bis(phenylsulfonyl)hexa-1,3,5-trien-1-yl]-4-benzene **44** (14 mg, 0.032 mmol) was heated 115 ^{o}C for 10 hours and purified using flash chromatograph on silica gel with ethyl acetate/petroleum ether (50:50) to give a pale yellow solid. The yield was too low to be isolated.

Neat 1-[(1*E*,3*E*,5*E*)-4,6-bis(phenylsulfonyl)hexa-1,3,5-trien-1-yl]-4-benzene **44** (62 mg, 0.142 mmol) was heated at 170 ^{o}C for 1 hour and purified using flash chromatograph on silica gel with ethyl acetate/petroleum ether (50:50) to give a pale yellow solid, 96 % yield (40 mg).

Neat 1-[(1*E*,3*E*,5*E*)-4,6-bis(phenylsulfonyl)hexa-1,3,5-trien-1-yl]-4-benzene **44** (58 mg, 0.133 mmol) was heated at 150 ^{o}C for 1 hour and purified using flash chromatograph on silica gel with ethyl acetate/petroleum ether (50:50) to give a pale yellow solid, 61 % yield (24 mg).

Neat 1-[(1*E*,3*E*,5*E*)-4,6-bis(phenylsulfonyl)hexa-1,3,5-trien-1-yl]-4-benzene **44** (71 mg, 0.163 mmol) was heated at 130 ^{o}C for 1 hour and purified using flash chromatograph on silica gel with ethyl acetate/petroleum ether (50:50). The ^{1}H NMR of elutent showed no reaction.

1-[(1*E*,3*E*,5*E*)-4,6-Bis(phenylsulfonyl)hexa-1,3,5-trien-1-yl]-4-benzene **44** (59 mg, 0.135 mmol) was dissolved in NMP (2 mL). The solution was heated under microwave at 170 ^{o}C for 1 hour. The resulting solution was purified using flash chromatograph on silica gel with ethyl acetate/petroleum ether (50 : 50) to give a pale yellow solid, 45 % yield (18 mg).

Neat 1-[(1*E*,3*E*,5*E*)-4,6-bis(phenylsulfonyl)hexa-1,3,5-trien-1-yl]-4-benzene **44** (57 mg, 0.131 mmol) was heated at 170 ^{o}C for 45 minutes and purified using flash chromatograph on silica gel with ethyl acetate/petroleum ether (50:50) to give a pale yellow solid, 78 % yield (30 mg).

6.1.1 Synthesis of 4-(phenylsulfonyl)-1,1'-biphenyl under microwave conditions 43 (Biphenyl 11)
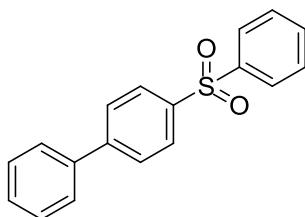
1-[(1E,3E,5E)-4,6-Bis(phenylsulfonyl)hexa-1,3,5-trien-1-yl]-4-benzene **44** (59 mg, 0.2 mmol) was dissolved in NMP, and heated under microwave conditions at 170 ^{o}C for 1 hour. The resulting solution was purified using flash chromatograph on silica gel with ethyl acetate/petroleum ether (50:50) to give a pale yellow solid, 45 % yield (18 mg).

m.p. 150-154 ^{o}C; **^{1}H NMR** (300 MHz, CDCl$_3$) δ 8.03 − 7.97 (m, 4H), 7.72 − 7.68 (m, 2H), 7.61 − 7.38 (m, 8H); **^{13}C NMR** (75 MHz, CDCl$_3$) δ 146.2 (*C*), 141.7 (SO$_2$*C*), 140.1 (SO$_2$*C*), 139.2 (*C*), 133.2 , 129.4, 129.1, 128.6, 128.2, 128.0, 127.7, 127.4; **IR (KBr)** 3430, 3059, 2917, 1726, 1446, 1395, 1308 (SO$_2$), 1155 (SO$_2$), 1108, 1072, 843, 724, 595, 567 (SO$_2$) cm^{-1}; **ESI-MS** C$_{18}$H$_{14}$O$_2$S Calc. (M + H$^+$) = 295.0787, found (M + H$^+$) = 295.0792; **Anal. calcd** for [C$_{18}$H$_{14}$O$_2$S] C,73.44; H, 4.79; found C, 73.49; H, 4.68.

6.1.2 Synthesis of 4-(phenylsulfonyl)-1,1'-biphenyl under neat condition 43 (Biphenyl 11)
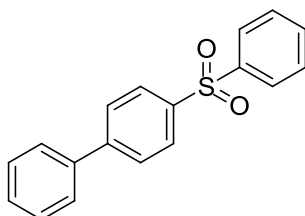
Neat 1-[(1E,3E,5E)-4,6-bis(phenylsulfonyl)hexa-1,3,5-trien-1-yl]-4-benzene **44** (62 mg, 0.14 mmol) was heated at 170 ^{o}C for 1 hour. The resulting brown oil was cooled to room temperature and purified using flash chromatography on silica gel with ethyl acetate/petroleum ether (50:50) to give a pale yellow solid, 96 % yield (40 mg).

m.p. 150-154 ^{o}C; **^{1}H NMR** (300 MHz, CDCl$_3$) δ 8.03 − 7.97 (m, 4H), 7.72 − 7.68 (m, 2H), 7.61 − 7.38 (m, 8H); **^{13}C NMR** (75 MHz, CDCl$_3$) δ 146.2 (*C*), 141.7 (SO$_2$*C*), 140.1 (SO$_2$*C*), 139.2 (*C*), 133.2 , 129.4, 129.1, 128.6, 128.2, 128.0, 127.7, 127.4; **IR (KBr)** 3430, 3059, 2917, 1726, 1446, 1395, 1308 (SO$_2$), 1155 (SO$_2$), 1108, 1072, 843, 724, 595, 567 (SO$_2$) cm^{-1};

ESI-MS $C_{18}H_{14}O_2S$ Calc. $(M + H^+)$ = 295.0787, found $(M + H^+)$ = 295.0792; **Anal. calcd** for $[C_{18}H_{14}O_2S]$ C,73.44; H, 4.79; found C, 73.49; H, 4.68.

6.2 Synthesis of Trienes

6.2.1 Synthesis of 1-[(1*E*,3*E*,5*E*)-4,6-bis(phenylsulfonyl)hexa-1,3,5-trien-1-yl]-4-benzene 44 (Triene 1)
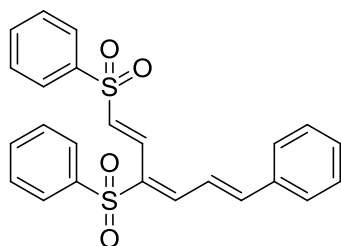
1,3-Bisphenylsulfonyl propene (644 mg, 2 mmol), *trans*-cinnamaldehyde (0.25 mL, 2 mmol) and aluminium oxide (6.732 g, 66 mmol) were stirred in dichloromethane (5 mL) for 4 hours at room temperature. The resulting suspension was filtered through a pad of celite and extracted with dichloromethane (40 mL). The resulting solution was evaporated under reduced pressure and purified using flash chromatograph on silica gel with ethyl acetate/petroleum ether (50:50) to give a green solid, 57 % yield (495 mg).

m.p.164-166 ^{o}C; **^{1}H NMR** (300 MHz, CDCl$_3$) δ 7.78 − 7.88 (m, 3H), 7.71 − 7.78 (m, 2H), 7.61 − 7.70 (m, 1H), 7.50 − 7.61 (m, 6H), 7.36 − 7.48 (m, 5H), 7.08 − 7.24 (m, 3H); **^{13}C NMR** (75 MHz, CDCl$_3$) δ 147.8, 145.5, 139.9 (SO$_2$Ar*C*), 139.7 (SO$_2$Ar*C*), 135.0 (Ar*C*), 133.7, 133.6, 132.9, 132.2 (*C*), 130.8, 129.4, 129.3, 129.1, 128.3, 127.7, 127.5, 120.3; **IR (KBr)** 3077, 3057, 3031, 1590, 1446, 1310 (SO$_2$), 1213, 1178, 1145 (SO$_2$), 1072, 976, 848, 719, 545 cm^{-1}; **ESI-MS** Calc. $(M + H^+)$ = 437.0876, found $(M + H^+)$ = 437.0871; **Anal. calcd** for $[C_{24}H_{20}O_4S_2]$ C, 66.03; H, 4.62; found C, 66.19; H, 4.66.

6.2.2 Synthesis of 1-[(1*E*,3*E*,5*E*)-4,6-bis(phenylsulfonyl)hexa-1,3,5-trien-1-yl]-4-nitrobenzene 45 (Triene 2)
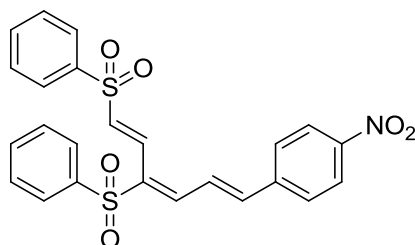
1,3-Bisphenylsulfonyl propene (96 mg, 0.3 mmol), 4-nitrocinnamaldehyde (54 mg, 0.3 mmol) and aluminium oxide (1009 mg, 9.9 mmol) were stirred in dichloromethane (1 mL) for 4 hours at room temperature. The resulting suspension was filtered through a pad of celite and extracted with dichloromethane (40 mL). The resulting solution was evaporated under reduced pressure and purified using flash chromatograph on silica gel with ethyl acetate/petroleum ether (50:50) to give a green solid, 57 % yield (82 mg).

m.p. 166-170 $^{\circ}$C; **^{1}H NMR** (300 MHz, CDCl$_3$) δ 8.29 – 8.25 (m, 2H), 7.84 – 7.80 (m, 3H), 7.75 – 7.64 (m, 6H), 7.61 – 7.50 (m, 4H), 7.44 – 7.39 (m, 2H), 7.26 – 7.18 (m, 2H); **^{13}C NMR** (75 MHz, CDCl$_3$) δ 148.4 (NO$_2$Ar*C*), 143.9, 143.5, 140.8 (Ar*C*), 139.5 (SO$_2$Ar*C*), 139.1 (SO$_2$Ar*C*), 135.1 (*C*), 134.4, 133.9, 133.9, 129.5, 129.4, 128.6, 128.5, 127.8, 127.7, 124.4, 124.1; **IR (KBr)** 3429, 3068, 1602, 1517 (NO$_2$), 1446, 1342 (NO$_2$), 1306 (SO$_2$), 1144 (SO$_2$), 1086, 989, 831, 746, 686, 601, 585 (NO$_2$), 548 (SO$_2$) cm^{-1}; **ESI-MS** C$_{24}$H$_{19}$NO$_6$S$_2$ Calc. (M + H$^+$) = 482.0727, found 482.0730.

6.2.3 Synthesis of

((1*E*,3*E*,5*E*)-6-(2-methoxyphenyl)hexa-1,3,5-triene-1,3-diyldisulfonyl)dibenzene 46

(Triene 3)
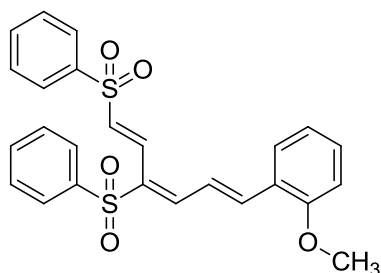
1,3-Bisphenylsulfonyl propene (96 mg, 0.3 mmol), 2-methoxy cinnamaldehyde (49 mg, 0.3 mmol), and aluminium oxide (1009 mg, 9.9 mmol) were stirred in dichloromethane (1 mL) for 4 hours at room temperature. The resulting suspension was filtered through a pad of celite and extracted with dichloromethane (40 mL). The resulting solution was evaporated under reduced pressure and recrystallized from dichloromethane and petroleum ether, to give a yellow solid, 62 % yield (87 mg).

m.p. 162-166 $^{\circ}$C (dichloromethane/petroleum ether); **^{1}H NMR** (300 MHz, CDCl$_3$) δ 7.88 – 7.80 (m, 3H), 7.76 – 7.73 (m, 2H), 7.65 – 7.51 (m, 7H), 7.43 – 7.36 (m, 3H), 7.33 – 7.28 (m, 1H), 7.24 – 7.09 (m, 1H), 7.04 – 6.93 (m, 2H), 3.93 (s, 3H, OC*H*$_3$). **^{13}C NMR** (75 MHz, CDCl$_3$) δ 158.4 (*C*OCH$_3$), 147.0, 143.5, 140.0 (SO$_2$Ar*C*), 139.9 (SO$_2$Ar*C*), 133.6, 133.5, 132.3, 132.1, 131.0 (*C*), 129.6, 129.4, 129.2, 128.8, 127.7, 127.5, 123.9 (Ar*C*), 121.0, 121.0, 111.3, 55.7 (*C*H$_3$); **IR (KBr)** 3436, 3008, 1585, 1481, 1309 (SO$_2$), 1149 (SO$_2$), 1185 (OCH$_3$),

1085 (OCH$_3$), 985, 844, 753, 687, 597, 544 (SO$_2$) cm^{-1}; **ESI-MS** C$_{25}$H$_{22}$O$_5$S$_2$ Calc. (M + H$^+$) = 467.0981, found (M + H$^+$) = 467.0978; **Anal. calcd** for [C$_{25}$H$_{22}$O$_5$S] C, 64.36; H, 4.75; found C, 64.56; H, 4.55.

6.2.4 Synthesis of

((1*E*,3*E*,5*E*)-6-(2-nitrophenyl)hexa-1,3,5-triene-1,3-diyldisulfonyl)dibenzene 47 (Triene 4)
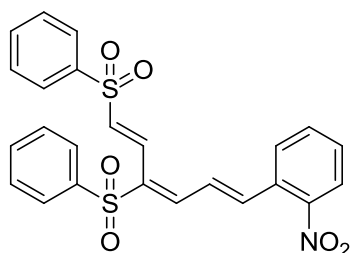
1,3-Bisphenylsulfonyl propene (96 mg, 0.3 mmol), 2-nitro cinnamaldehyde (54 mg, 0.3 mmol), and aluminium oxide (1009 mg, 9.9 mmol) were stirred in dichloromethane (1 mL) for 4 hours at room temperature. The resulting suspension was filtered through a pad of celite and extracted with dichloromethane (40 mL). The resulting solution was evaporated under reduced pressure and recrystallized from dichloromethane and petroleum ether to give a yellow solid, 46 % yield (67 mg).

m.p. 170-174 ^{o}C (dichloromethane/petroleum ether); **^{1}H NMR** (300 MHz, CDCl$_3$) δ 8.09 – 8.06 (m, 1H), 7.86 – 7.78 (m, 4H), 7.76 – 7.64 (m, 5H), 7.62 – 7.49 (m, 5H), 7.46 – 7.39 (m, 2H), 7.22 – 7.03 (m, 2H). **^{13}C NMR** (75 MHz, CDCl$_3$) δ 148.0 (NO$_2$Ar*C*), 143.9, 141.8, 139.5 (SO$_2$Ar*C*), 139.2 (SO$_2$Ar*C*), 134.9 (Ar*C*), 134.2, 133.9, 133.8, 133.8, 130.8 (*C*), 130.6, 129.5, 129.4, 129.1, 128.7, 127.8, 127.7, 125.3, 124.8; **IR (KBr)** 3429, 3062, 1608, 1523 (NO$_2$), 1446, 1349 (NO$_2$), 1304 (SO$_2$), 1147 (SO$_2$), 1082, 952, 746, 595 (NO$_2$), 542 (SO$_2$) cm^{-1}; **ESI-MS** C$_{24}$H$_{19}$NO$_6$S$_2$ Calc. (M + H$^+$) = 482.0727, found (M + H$^+$) = 482.0718.

6.2.5 Synthesis of

4-((1*E*,3*E*,5*E*)-4,6-bis(phenylsulfonyl)hexa-1,3,5-trien-1-yl)-N,N-dimethylaniline 48 (Triene 5)
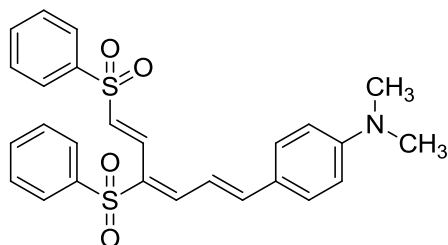
1,3-Bisphenylsulfonyl propene (96 mg, 0.3 mmol), 4-dimethylamino cinnamaldehyde (54 mg, 0.3 mmol), and aluminium oxide (1009 mg, 9.9 mmol) were stirred in dichloromethane (1 mL) for 4 hours at room temperature. The resulting suspension was filtered through a pad of celite and extracted with dichloromethane (40 mL). The resulting solution was evaporated under reduced pressure and recrystallized from dichloromethane and petroleum ether to give a red solid, 77 % yield (111 mg).

m.p. 168-172 $^{\circ}$C (dichloromethane/petroleum ether); **^{1}H NMR** (300 MHz, CDCl$_3$) δ 7.85 – 7.79 (m, 3H), 7.76 – 7.72 (m, 2H), 7.65 – 7.46 (m, 8H), 7.41 – 7.36 (m, 2H), 7.21 – 7.16 (m, 1H), 7.03 – 6.93 (m, 2H), 6.71 – 6.67 (m, 2H), 3.08 (s, 6H, NC*H*$_3$); **^{13}C NMR** (75 MHz, CDCl$_3$) δ 152.2 (*C*N), 149.6, 147.9, 140.4 (SO$_2$Ar*C*), 140.4 (*C*), 133.4, 133.2, 130.6, 129.9, 129.7, 129.3, 129.1, 127.6, 127.2, 122.8 (Ar*C*), 115.1, 111.9, 40.1 (NCH$_3$); **IR (KBr)** 3430, 2914, 1572, 1446, 1372 (N(CH$_3$)$_2$), 1306 (SO$_2$), 1166 (SO$_2$) 1147 (N(CH$_3$)$_2$), 1084, 978, 841, 752, 601 (SO$_2$) cm^{-1}; **ESI-MS** C$_{26}$H$_{25}$NO$_4$S$_2$ Calc. (M + H$^+$) = 480.1298, found (M + H$^+$) = 480.1322.

6.2.6 Synthesis of

((1*E*,3*E*,5*E*)-6-(4-chlorophenyl)hexa-1,3,5-triene-1,3-diyldisulfonyl)dibenzene 49 (Triene 6)
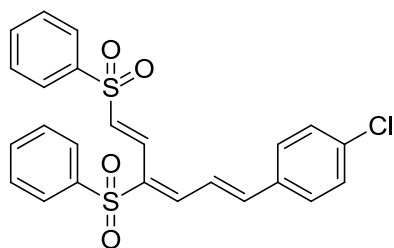
1,3-Bisphenylsulfonyl propene (96 mg, 0.3 mmol), 4-chlorocinnamaldehyde (50 mg, 0.3 mmol), and aluminium oxide (1009 mg, 9.9 mmol) were stirred in dichloromethane (1 mL) for 4 hours at room temperature. The resulting suspension was filtered through a pad of celite and extracted with dichloromethane (40 mL). The resulting solution was evaporated under reduced pressure and recrystallized from dichloromethane and petroleum ether to give a green/yellow solid, 43 % yield (61 mg).

m.p. 128-132 $^{\circ}$C (dichloromethane/petroleum ether); **^{1}H NMR** (300 MHz, CDCl$_3$) δ 7.83 – 7.79 (m, 3H), 7.74 – 7.64 (m, 3H), 7.61 – 7.48 (m, 6H), 7.44 – 7.39 (m, 4H), 7.22 – 7.07 (m, 3H); **^{13}C NMR** (75 MHz, CDCl$_3$) δ 146.2, 145.1, 139.8 (SO$_2$Ar*C*), 139.5 (SO$_2$Ar*C*), 136.8 (*C*Cl,), 133.8, 133.6, 133.4 (Ar*C*), 133.1, 132.6 (*C*), 129.5, 129.5, 129.4, 129.3, 128.9, 127.7, 127.5, 120.7; **IR (KBr)** 3426, 1602, 1308 (SO$_2$), 1145 (SO$_2$), 1085, 843, 752 (Cl), 601 (SO$_2$) cm^{-1}; **ESI-MS** C$_{24}$H$_{19}$ClO$_4$S$_2$ Calc. (M + H$^+$) = 471.0486, found (M + H$^+$) = 471.0490; **Anal. calcd** for [2(C$_{24}$H$_{19}$ClO$_4$S$_2$) ·H$_2$O] C, 60.05; H, 4.20; found C, 60.08; H, 3.65. Calibration of H$_2$O is based on the ^{1}H NMR.

6.2.7 Synthesis of

((1*E*,3*E*,5*E*)-6-(4-methoxyphenyl)hexa-1,3,5-triene-1,3-diyldisulfonyl)dibenzene 50

(Triene 7)
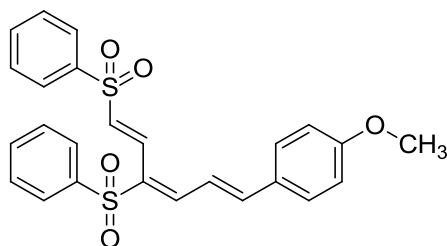
1,3-Bisphenylsulfonyl propene (96 mg, 0.3 mmol), 4-methoxycinnamaldehyde (49 mg, 0.3 mmol), and aluminium oxide (1009 mg, 9.9 mmol) were stirred in dichloromethane (1 mL) for 4 hours at room temperature. The resulting suspension was filtered through a pad of celite and extracted with dichloromethane (40 mL). The resulting solution was evaporated under reduced pressure and recrystallized from dichloromethane and petroleum ether to give a yellow/green solid, 37 % yield (52 mg).

m.p. 166-170 ^{o}C (dichloromethane/petroleum ether); **^{1}H NMR** (300 MHz, CDCl$_3$) δ 7.87 – 7.80 (m, 3H), 7.76 – 7.72 (m, 2H), 7.68 – 7.51 (m, 7H), 7.44 – 7.37 (m, 2H), 7.24 – 7.15 (m, 2H), 7.10 – 7.04 (m, 1H), 7.00 – 6.92 (m, 2H), 3.87 (s, 3H, OC*H*$_3$); **^{13}C NMR** (75 MHz, CDCl$_3$) δ 162.0 (*C*OCH$_3$), 148.0, 146.5, 140.0 (SO$_2$Ar*C*), 139.9 (SO$_2$Ar*C*), 133.6, 133.5, 131.7, 130.3 (*C*), 130.2, 129.4, 129.3, 129.2, 127.8 (Ar*C*), 127.7, 127.4, 118.0, 114.7; **IR (KBr)** 3438, 3066, 1588, 1307 (SO$_2$), 1257 (OCH$_3$), 1149 (SO$_2$), 1085 (OCH$_3$), 851, 740, 602 (SO$_2$) cm^{-1}; **ESI-MS** C$_{25}$H$_{22}$O$_5$S$_2$ Calc. (M + H$^+$) = 467.0981, found (M + H$^+$) = 467.0987; **Anal. calcd** for [3(C$_{25}$H$_{22}$O$_5$S$_2$) · H$_2$O] C, 63.54; H, 4.83; found C, 63.09; H, 4.37. Calibration of H$_2$O is based on the ^{1}H NMR.

6.2.8 Synthesis of

4-((1*E*,3*E*,5*E*)-4,6-bis(phenylsulfonyl)hexa-1,3,5-trien-1-yl)benzonitrile 51 (Triene 8)
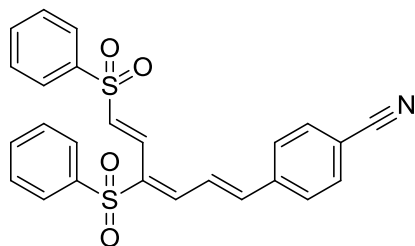
1,3-Bisphenylsulfonyl propene (139 mg, 0.43 mmol), 4-cyanocinnamaldehyde **54** (68 mg, 0.43 mmol), and aluminium oxide (1458 mg, 14.3 mmol) were stirred in dichloromethane (2 mL) for 4 hours at room temperature. The resulting suspension was filtered through a pad of celite and extracted with dichloromethane (40 mL). The resulting solution was evaporated

under reduced pressure and recrystallized from dichloromethane and petroleum ether to give a pale green solid, 29 % yield (58 mg).

m.p. 156-160 °C (dichloromethane/petroleum ether); **^{1}H NMR** (300 MHz, CDCl$_3$) δ 7.88 – 7.79 (m, 3H), 7.74 – 7.68 (m, 5H), 7.66 – 7.62 (m, 2H), 7.60 – 7.50 (m, 4H), 7.44 – 7.39 (m, 2H), 7.22 – 7.16 (m, 3H); **^{13}C NMR** (75 MHz, CDCl$_3$) δ 144.5, 143.7, 139.5 (SO$_2$ArC), 139.2 (SO$_2$ArC), 139.0 (ArC), 134.7 (C), 134.2, 133.9 , 133.9, 132.8, 129.5, 129.4, 128.6, 128.4, 127.8, 127.7, 123.5, 118.3 (CN), 113.6 (CCN); **IR (KBr)** 3414, 3069, 2223 (CN), 1605, 1445 1307 (SO$_2$), 1287, 1145 (SO$_2$), 1085, 972, 846, 718, 684, 585, 545 (SO$_2$) cm^{-1}; **ESI-MS** C$_{25}$H$_{19}$NO$_4$S$_2$ Calc. (M + H$^+$) = 462.0828, found (M + H$^+$) = 462.0832.

6.2.9 Synthesis of methyl

4-((1E,3E,5E)-4,6-bis(phenylsulfonyl)hexa-1,3,5-trien-1-yl)benzoate 52 (Triene 9)
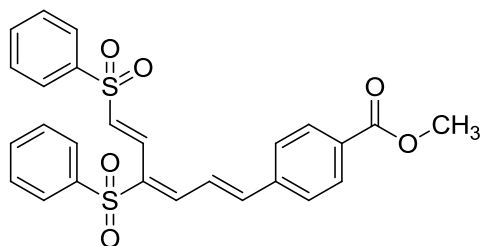
1,3-Bisphenylsulfonyl propene (96 mg, 0.3 mmol), 4-(3-oxo-propenyl)-benzoic acid methyl ester **64** (57 mg, 0.3 mmol), and aluminium oxide (1009 mg, 9.9 mmol) were stirred in dichloromethane (2 mL) for 4 hours at room temperature. The resulting suspension was filtered through a pad of celite and extracted with dichloromethane (40 mL). The resulting solution was evaporated under reduced pressure and recrystallized from dichloromethane and petroleum ether to give a yellow/green solid, 32 % yield (48 mg).

m.p. 168-172 °C (dichloromethane/petroleum ether); **^{1}H NMR** (300 MHz, CDCl$_3$) δ 8.11 – 8.07 (m, 2H), 7.85 – 7.81 (m, 3H), 7.76 – 7.72 (m, 2H), 7.70 – 7.53 (m, 7H), 7.67 – 7.39 (m, 2H), 7.25 – 7.15 (m, 3H), 3.95 (s, 3H, OCH_3); **^{13}C NMR** (75 MHz, CDCl$_3$) δ 166.3 (C=O), 145.9, 144.5, 139.7 (SO$_2$ArC), 139.4 (SO$_2$ArC), 139.0 (CC(O)OCH$_3$), 133.8, 133.7, 133.6 (C), 133.6, 131.6 (ArC), 130.3, 129.5, 129.3, 128.8, 128.0, 127.8, 127.6, 122.4, 52.4 (CH$_3$); **IR (KBr)** 3430, 3004, 2813, 1718 (C(O)OCH$_3$), 1683, 1425, 1316 (SO$_2$), 1288 (C(O)OCH$_3$), 1128 (SO$_2$), 1107 (C(O)OCH$_3$), 982, 760, 691, 584 (SO$_2$) cm^{-1}; **ESI-MS** C$_{26}$H$_{22}$O$_6$S$_2$ Calc. (M + H$^+$) = 495.0931, found (M + H$^+$) = 495.0920; **Anal. calcd** for [2(C$_{26}$H$_{22}$O$_6$S$_2$) ·H$_2$O] C, 62.01; H, 4.60; found C, 62.20; H, 5.08. The calibration of H$_2$O is based on the ^{1}H NMR.

6.2.10 Synthesis of ((1*E*,3*E*,5*E*)-6-(p-tolyl)hexa-1,3,5-triene-1,3-diyldisulfonyl)dibenzene 53 (Triene 10)
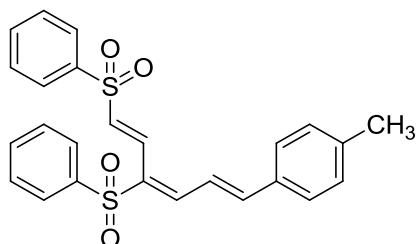
3-p-Tolyl-propenal **65** (72 mg, 0.49 mmol), 1,3-bisphenylsulfonyl propene (128 mg, 0.4 mmol) and aluminium oxide (1346 mg, 13.2 mmol) were stirred in dichloromethane (3 mL) for 4 hours at room temperature. The resulting suspension was filtered through a pad of celite and extracted with dichloromethane (40 mL). The resulting solution was evaporated under reduced pressure and recrystallized from dichloromethane and petroleum ether to give a yellow solid, 26 % yield (47 mg).

m.p. 148-152 $^{\circ}$C (dichloromethane/petroleum ether); **^{1}H NMR** (300 MHz, CDCl$_3$) δ 7.84 – 7.80 (m, 3H), 7.74 – 7.72 (m, 2H), 7.67 – 7.63 (m, 2H), 7.61 – 7.51 (m, 4H), 7.47 – 7.38 (m, 4H), 7.25 – 7.20 (m, 2H), 7.15 – 7.07 (m, 2H), 2.41 (s, 3H, C*H*$_3$); **^{13}C NMR** (75 MHz, CDCl$_3$) δ 148.2, 146.2, 141.7 (*C*), 139.9 (SO$_2$Ar*C*), 139.7 (SO$_2$Ar*C*), 133.7, 133.5, 132.3, 131.3 (Ar*C*), 129.9, 129.5, 129.3, 129.2, 128.4, 127.7, 127.5, 119.3, 21.7 (*C*H$_3$); **IR (KBr)** 3425, 3067, 1591, 1446 (CH$_3$), 1308 (SO$_2$), 1143 (SO$_2$), 1084, 988, 846, 740, 687, 602, 566 (SO$_2$) cm^{-1}; **ESI-MS** C$_{25}$H$_{22}$O$_4$S$_2$ Calc. (M + H$^+$) = 451.1032, found (M + H$^+$) = 451.1022.

6.2.11 Synthesis of 4-cyanocinnamaldehyde 54 [99]
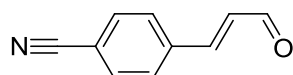
A solution of 4-formylbenzonitrile (255 mg, 1.95 mmol) and (triphenylphosphoranylidene) acetaldehyde (550 mg, 1.73 mmol) in tetrahydrofuran (10 mL) was refluxed for 24 hours. The resulting solution was evaporated under reduced pressure and purified using flash chromatograph on silica gel eluting with ethyl acetate/petroleum ether (10:90–30:70) to give a white solid, 47 % yield (128 mg).

^{1}H NMR (300 MHz, CDCl$_3$) δ 9.78 (d, *J* = 7.5 Hz, 1H, C(O)H), 7.77 – 7.70 (m, 4H, Ar), 7.54 (d, *J* = 16.1 Hz, 1H, PhC*H*=CH), 6.80 (dd, *J* = 16.1, 7.5 Hz, 1H, CH=C*H*C(O)H); **ESI-MS** C$_{10}$H$_7$NO Calc. (M + H$^+$) = 158.0600, found (M + H$^+$) = 158.0604. Matches known data.[99]

6.3 Synthesis of biphenyl sulfones

6.3.1 Synthesis of N,N-dimethyl-4'-(phenylsulfonyl)-[1,1'-biphenyl]-4-amine 55 (Biphenyl 12)
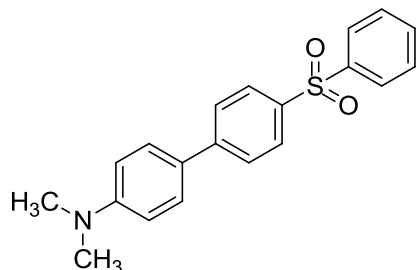
Neat 4-((1E,3E,5E)-4,6-bis(phenylsulfonyl)hexa-1,3,5-trien-1-yl)-N,N-dimethylaniline **48** (61 mg, 0.13 mmol) was stirred at 170 ^{o}C for 1 hour. The resulting brown oil was cooled to room temperature and purified using flash chromatography on silica gel with ethyl acetate/petroleum ether (50:50) and recrystallized from dichloromethane and petroleum ether to give a pale yellow solid, 42 % yield (18 mg).

m.p. 204-208 ^{o}C (dichloromethane/petroleum ether); **^{1}H NMR** (300 MHz, CDCl$_3$) δ 7.99 – 7.92 (m, 4H), 7.68 – 7.64 (m, 2H), 7.59 – 7.43 (m, 5H), 6.83 – 6.76 (m, 2H), 3.01 (s, 6H, NCH_3); **^{13}C NMR** (75 MHz, CDCl$_3$) δ 150.7 (CH$_3$NC), 146.2 (SO$_2$ArC), 142.1 (SO$_2$ArC), 138.2 (ArC), 133.0, 129.3, 128.2, 128.0, 127.5, 126.5, 112.5, 40.4 (CH$_3$); **IR (KBr)** 3415, 2922, 1612, 1588, 1446, 1369 (N(CH$_3$)$_2$), 1307 (SO$_2$), 1261 (N(CH$_3$)$_2$), 1153 (SO$_2$), 807, 739, 621, 576 (SO$_2$) cm^{-1}; **ESI-MS** C$_{20}$H$_{19}$NO$_2$S Calc. (M + H$^+$) = 338.1209, found 338.1210.

6.3.2 Synthesis of 4-methyl-4'-(phenylsulfonyl)-1,1'-biphenyl 56 (Biphenyl 13)
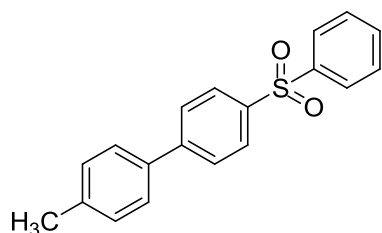
Neat ((1E,3E,5E)-6-(p-tolyl)hexa-1,3,5-triene-1,3-diyldisulfonyl)dibenzene **53** (34 mg, 0.075 mmol) was stirred at 170 ^{o}C for 1 hour. The resulting brown oil was cooled to room temperature and purified using flash chromatography on silica gel with dichloromethane and recrystallized from dichloromethane and petroleum ether to give a white solid 35 % (8 mg).

m.p. 154-158 ^{o}C (dichloromethane/petroleum ether); **^{1}H NMR** (300 MHz, CDCl$_3$) δ 8.04 – 7.97 (m, 3H), 7.73 – 7.66 (m, 2H), 7.61 – 7.45 (m, 5H), 7.28 – 7.25 (m, 3H), 2.40 (s, 3H,

CH_3); ^{13}**C NMR** (75 MHz, CDCl$_3$) δ 146.1 (*C*), 141.8 (SO$_2$*C*), 139.7 (SO$_2$*C*), 138.7 (*C*), 136.2 (CH$_3$*C*), 133.2, 129.8, 129.3, 128.2, 127.7, 127.6, 127.2, 21.2 (*C*H$_3$); **IR (KBr)** 3431, 3025, 1594, 1448 (CH$_3$), 1393 (CH$_3$), 1321, 1308 (SO$_2$), 1155 (SO$_2$), 1108, 805, 749, 630, 580, 562 (SO$_2$) cm^{-1}; **ESI-MS** C$_{19}$H$_{16}$O$_2$S Calc. (M + H$^+$) = 309.0944, found (M + H$^+$) = 309.0945 **Anal. calcd** for [3(C$_{19}$H$_{16}$O$_2$S) ·H$_2$O] C, 72.58; H, 5.34; found C, 73.05; H, 4.94. The calibration of H$_2$O is based on the ^{1}H NMR.

6.3.3 Synthesis of methyl 4'-(phenylsulfonyl)-[1,1'-biphenyl]-4-carboxylate 57 (Biphenyl 14)
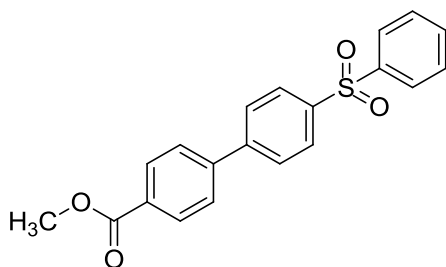
Neat methyl 4-((1*E*,3*E*,5*E*)-4,6-bis(phenylsulfonyl)hexa-1,3,5-trien-1-yl)benzoate **52** (42 mg, 0.085 mmol) was stirred at 170 ^{o}C for 1 hour. The resulting brown oil was cooled to room temperature and purified using flash chromatography on silica gel with dichloromethane and recrystallized from dichloromethane and petroleum ether to give a white solid 60 % yield (14 mg).

m.p. 204-208 ^{o}C (dichloromethane/petroleum ether); ^{1}**H NMR** (300 MHz, CDCl$_3$) δ 8.14 – 8.11 (m, 2H), 8.06 – 7.97 (m, 4H), 7.75 – 7.72 (m, 2H), 7.65 – 7.50 (m, 5H), 3.95 (s, 3H, OCH_3); ^{13}**C NMR** (75 MHz, CDCl$_3$) δ 165.6 (*C*=O), 143.9 (Ar*C*), 142.4 (Ar*C*), 140.5 (SO$_2$Ar*C*), 134.0 (SO$_2$Ar*C*), 132.3, 129.3, 129.1 (*C*C=O), 128.4, 127.3, 127.1, 126.7, 126.3, 52.3 (*C*H$_3$); **IR (KBr)** 3433, 3065, 1714 (C(O)OCH$_3$), 1609, 1431, 1321 (SO$_2$), 1280 (C(O)OCH$_3$), 1157 (SO$_2$), 1108 (C(O)OCH$_3$), 1073, 834, 771, 732, 603, 544 (SO$_2$) cm^{-1}; **ESI-MS** C$_{20}$H$_{16}$O$_4$S Calc. (M + H$^+$) = 353.0842, found (M + H$^+$) = 353.0825; **Anal. calcd** for [2(C$_{20}$H$_{16}$O$_4$S) 3H$_2$O] C, 63.31; H, 5.05; found C, 62.81; H, 4.66. Calibration of H$_2$O is base on the ^{1}H NMR.

6.3.4 Synthesis of 4-methoxy-4'-(phenylsulfonyl)-1,1'-biphenyl 58 (Biphenyl 15)
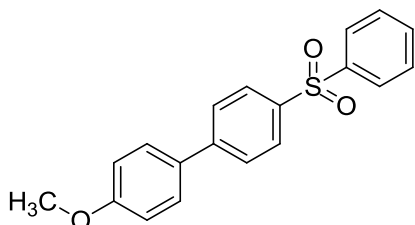
Neat ((1*E*,3*E*,5*E*)-6-(4-methoxyphenyl)hexa-1,3,5-triene-1,3-diyldisulfonyl)dibenzene **50** (46 mg, 0.099 mmol) was stirred at 170 °C for 1 hour. The resulting brown oil was cooled to room temperature and purified using flash chromatography on silica gel with dichloromethane and recrystallized from dichloromethane and petroleum ether to give a white solid 62 % (20 mg).

m.p. 170-174 °C (dichloromethane/petroleum ether); **^{1}H NMR** (300 MHz, CDCl$_3$) δ 8.00 – 7.95 (m, 4H), 7.68 – 7.64 (m, 2H), 7.60 – 7.48 (m, 5H), 7.01 – 6.96 (m, 2H), 3.86 (s, 3H, OC*H$_3$*); **^{13}C NMR** (75 MHz, CDCl$_3$) δ 160.2 (CH$_3$O*C*), 145.8 (*C*), 141.8 (*C*), 139.3 (*C*), 133.2, 131.5 (*C*), 129.3, 128.5, 128.2, 127.6, 127.3, 114.5, 55.4 (*C*H$_3$); **IR (KBr)** 3425, 3066, 1605, 1589, 1485, 1448, 1392, 1307 (SO$_2$), 1255 (OCH$_3$), 1152 (SO$_2$), 1107, 1033 (OCH$_3$), 825, 747, 629, 583, 563 (SO$_2$) cm^{-1}; **ESI-MS** C$_{19}$H$_{16}$O$_3$S Calc. (M + H$^+$) = 325.0893, found (M + H$^+$) = 325.0896; **Anal. calcd** for [2(C$_{19}$H$_{16}$O$_3$S) H$_2$O] C, 68.45; H, 5.08; found C, 68.11; H, 4.94. The calibration of H$_2$O is based on ^{1}H NMR.

6.3.5 Synthesis of 4-chloro-4'-(phenylsulfonyl)-1,1'-biphenyl 59 (Biphenyl 16)
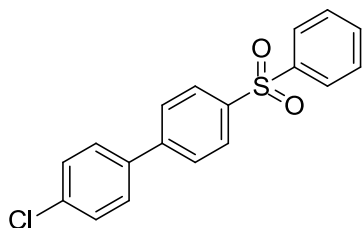
Neat ((1*E*,3*E*,5*E*)-6-(4-chlorophenyl)hexa-1,3,5-triene-1,3-diyldisulfonyl)dibenzene **49** (53 mg, 0.11 mmol) was stirred at 170 °C for 1 hour. The resulting brown oil was cooled to room temperature and purified using flash chromatography on silica gel with ethyl acetate/petroleum ether (50:50) and recrystallized from dichloromethane and petroleum ether to give a pale yellow solid, 50 % yield (18 mg).

m.p. 162-166 °C (dichloromethane/petroleum); **^{1}H NMR** (300 MHz, CDCl$_3$) δ 8.04 – 7.97 (m, 4H), 7.74 – 7.64 (m, 2H), 7.61 – 7.40 (m, 7H); **^{13}C NMR** (75 MHz, CDCl$_3$) δ 144.9 (Cl*C*), 141.6 (SO$_2$Ar*C*), 140.5 (SO$_2$Ar*C*), 137.6 (Ar*C*), 134.9 (Ar*C*), 133.3, 129.4, 129.3, 128.6, 128.3, 127.8, 127.7; **IR (KBr)** 3429, 3063, 1593, 1477, 1389, 1318 (SO$_2$), 1158 (SO$_2$), 1107, 1002, 816, 781, 718 (Cl), 604, 572 (SO$_2$) cm^{-1}; **ESI-MS** C$_{18}$H$_{13}$ClO$_2$S Calc. (M + H$^+$) = 329.0398, found (M + H$^+$) = 329.0395.

6.3.6 Synthesis of 4'-(phenylsulfonyl)-[1,1'-biphenyl]-4-carbonitrile 60 (Biphenyl 17)
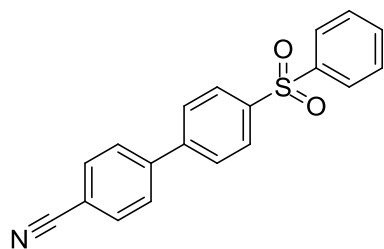
Neat 4-((1*E*,3*E*,5*E*)-4,6-bis(phenylsulfonyl)hexa-1,3,5-trien-1-yl)benzonitrile **51** (60 mg, 0.13 mmol) was stirred at 170 °C for 1 hour. The resulting brown oil was cooled to room temperature and purified using flash chromatography on silica gel with dichloromethane and recrystallized from dichloromethane and petroleum ether to give a white solid 31 % yield (13 mg).

m.p. 186-190 °C (dichloromethane/petroleum ether), **^{1}H NMR** (300 MHz, CDCl$_3$) δ 8.08 – 7.97 (m, 3H), 7.78 – 7.45 (m, 9H), 7.19 – 7.08 (m, 1H); **^{13}C NMR** (75 MHz, CDCl$_3$) δ 144.0 (Ar*C*), 143.6 (Ar*C*), 141.6 (SO$_2$Ar*C*), 141.3 (SO$_2$Ar*C*), 133.5, 132.9, 129.5, 128.5, 128.2, 128.1, 127.8, 118.5 (*C*N), 112.3 (NC*C*); **IR (KBr)** 3429, 2227 (CN), 1592, 1391, 1308 (SO$_2$), 1156 (SO$_2$), 823, 745, 616, 562 (SO$_2$) cm^{-1}; **ESI-MS** C$_{19}$H$_{13}$NO$_2$S Calc. (M + Na$^+$) = 342.0559, found (M + Na$^+$) = 342.0570.

6.3.7 Synthesis of 2-methoxy-4'-(phenylsulfonyl)-1,1'-biphenyl 61 (Biphenyl 18)
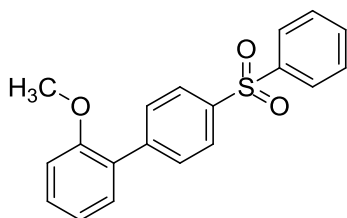
Neat ((1*E*,3*E*,5*E*)-6-(2-methoxyphenyl)hexa-1,3,5-triene-1,3-diyldisulfonyl)dibenzene **46** (77 mg, 0.165 mmol), was stirred at 170 °C for 1 hour. The resulting brown oil was cooled to room temperature and purified using flash chromatography on silica gel with ethyl acetate/petroleum ether (30:70) to give a white solid, 39 % yield (21 mg).

m.p. 22-26 °C; **^{1}H NMR** (300 MHz, CDCl$_3$) δ 8.01 – 7.93 (m, 4H), 7.67 – 7.44 (m, 5H), 7.40 – 7.38 (m, 1H), 7.25 – 7.15 (m, 2H), 7.05 – 6.95 (m, 1H), 3.78 (s, 3H, OC*H$_3$*). **^{13}C NMR** (75 MHz, CDCl$_3$) δ 156.4 (*C*OCH$_3$), 156.3 (*C*OCH$_3$), 143.8 (SO$_2$Ar*C*), 142.8 (SO$_2$Ar*C*), 141.8 (SO$_2$Ar*C*), 141.7 (SO$_2$Ar*C*), 140.0 (Ar*C*), 139.6 (Ar*C*), 137.7 (Ar*C*), 135.7, 135.0, 133.2, 133.2, 130.8, 130.4, 130.3, 129.9, 129.3, 129.3, 129.1, 128.8, 127.8, 127.7, 127.4, 127.4,

126.2, 125.5 (ArC), 121.1, 112.3, 111.3, 55.8 (OCH_3), 55.5 (OCH_3); **IR (KBr)** 3438, 3008, 1596, 1478, 1383, 1319 (SO$_2$), 1264 (OCH_3), 1156 (SO$_2$), 1106, 1023 (OCH_3), 839, 751, 687, 598 (SO$_2$) cm^{-1}; **ESI-MS** C$_{19}$H$_{16}$O$_3$S Calc. (M + H$^+$) = 325.0893, found (M + H$^+$) = 325.0905; **Anal. calcd** for [4(C$_{19}$H$_{16}$O$_3$S) H$_2$O] C, 69.38; H, 5.06; found C, 69.58; H, 5.48. Calculation of H$_2$O is based on ^{1}H NMR.

6.3.8 Synthesis of 2-nitro-4'-(phenylsulfonyl)-1,1'-biphenyl 62 (Biphenyl 19)
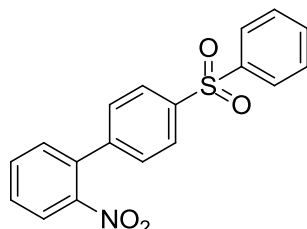
Neat ((1E,3E,5E)-6-(2-nitrophenyl)hexa-1,3,5-triene-1,3-diyldisulfonyl)dibenzene **47** (45 mg, 0.0936 mmol) was stirred at 170 ^{o}C for 1 hour. The resulting brown oil was cooled to room temperature and purified using flash chromatography on silica gel with dichloromethane and recrystallized from dichloromethane and petroleum ether to give a white solid 31 % yield (10 mg).

m.p. 118-122 ^{o}C (dichloromethane/petroleum ether); **^{1}H NMR** (300 MHz, CDCl$_3$) δ 8.10 – 7.94 (m, 5H), 7.81 – 7.52 (m, 5H), 7.49 – 7.34 (m, 3H); **^{13}C NMR** (75 MHz, CDCl$_3$) δ 148.6 (NO$_2$$C$), 142.8 (NO$_2CC$), 141.3 (SO$_2$$C$), 141.2 (SO$_2$$C$), 134.8 (NO$_2CCC$), 133.5, 132.9, 131.9, 129.5, 129.3, 128.9, 128.0, 127.8, 124.6; **IR (KBr)** 3430, 1632, 1525 (NO$_2$), 1351 (SO$_2$), 1317 (NO$_2$), 1156 (SO$_2$), 1107, 735, 595 (NO$_2$), 565 (SO$_2$) cm^{-1}; **ESI-MS** C$_{18}$H$_{13}$NO$_4$S Calc. (M + H$^+$) = 340.0638, found (M + H$^+$) = 340.0645; **Anal. calcd** for [2(C$_{18}$H$_{13}$NO$_4$S) ·H$_2$O] C, 62.06; H, 4.05; N, 4.02; found C, 62.17; H, 3.71; N, 3.89. The calibration is based on the ^{1}H NMR.

6.3.9 Synthesis of 4-nitro-4'-(phenylsulfonyl)-1,1'-biphenyl 63 (Biphenyl 20)
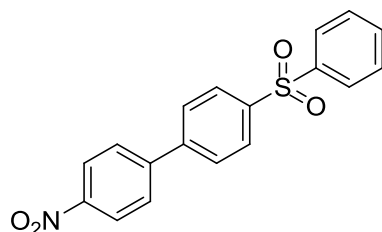
Neat 1-[(1E,3E,5E)-4,6-bis(phenylsulfonyl)hexa-1,3,5-trien-1-yl]-4-nitrobenzene **45** (58 mg, 0.12 mmol) was stirred at 170 ^{o}C for 1 hour. The resulting brown oil was cooled to room temperature and purified using flash chromatography on silica gel with ethyl acetate/petroleum ether (20:80–50:50) and recrystallized from dichloromethane and petroleum ether to give a white solid, 40 % yield (21 mg).

m.p. 198-202 $^{\circ}$C (dichloromethane/petroleum ether); **^{1}H NMR** (300 MHz, CDCl$_3$) δ 8.35 – 8.30 (m, 2H), 8.11 – 7.98 (m, 4H), 7.84 – 7.70 (m, 4H), 7.65 – 7.51 (m, 3H); **^{13}C NMR** (75 MHz, CDCl$_3$) δ 147.8 (NO$_2$*C*), 145.4 (NO$_2$C*C*HCH*C*), 143.6 (SO$_2$Ar*C*), 141.8 (SO$_2$Ar*C*), 141.3 (SO$_2$*C*CHCH*C*), 133.5, 129.4, 128.5, 128.3, 128.3, 127.7, 124.3; **IR (KBr)** 3420, 3071, 1592, 1518 (NO$_2$), 1338 (NO$_2$), 1315 (SO$_2$), 1155 (SO$_2$), 1107, 832, 730, 601 (NO$_2$), 571 (SO$_2$) cm^{-1}; **ESI-MS** C$_{18}$H$_{13}$NO$_4$S (M + H$^+$) = 340.0638, found (M + H$^+$) = 340.0645.

6.4.1 Synthesis of 4-(3-oxo-propenyl)-benzoic acid methyl ester 64 [99]
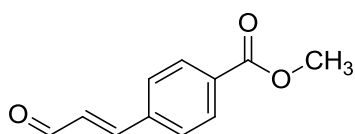
4-Formyl-benzoic acid methyl ester (338 mg, 2.05 mmol) and (triphenylphosphoranylidene) acetaldehyde (625 mg, 2.05 mmol) were refluxed in toluene (7 mL) for 24 hours. The resulting solution was evaporated under reduced pressure and purified using flash chromatography on silica gel with ethyl acetate/petroleum ether (100:20) to give a light green solid, 34 % yield (134 mg).

^{1}H NMR (300 MHz, CDCl$_3$) δ 9.75 (d, *J* = 7.6 Hz, 1H, C(O)H), 8.11 – 8.08 (m, 2H, Ar), 7.65 – 7.62 (m, 2H, Ar), 7.51 (d, *J* = 16.0 Hz, 1H, PhC*H*=CH), 6.78 (dd, *J* = 16.0, 7.6 Hz, 1H, CH=C*H*C(O)H), 3.94 (s, 3H, CH$_3$); **ESI-MS** C$_{11}$H$_{10}$O$_3$ Calc. (M + H$^+$) = 191.0703 found (M + H$^+$) = 191.0706. Matches known data.[99]

6.4.2 Synthesis of 3-p-tolyl-propenal 65[99]
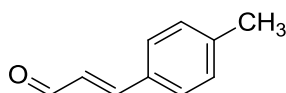
4-Methyl-benzaldehyde (0.18 mL, 1.5 mmol) and (triphenylphosphoranylidene)acetaldehyde (456 mg, 1.5 mmol) were dissolved in toluene and refluxed for 24 hours. The resulting solution was evaporated under reduced pressure and purified using flash chromatography on silica gel with ethyl acetate/petroleum ether (100:20) to give a yellow oil, 64 % yield (142 mg).

^{1}H NMR (300 MHz, CDCl$_3$) δ 9,63 (d, *J* = 7.8 Hz, 1H, C(O)H), 7.42 (d, *J* = 3.5 Hz, 1H, PhC*H*=CH), 7.33 (d, *J* = 7.9 Hz, 2H, Ar), 7.27 (d, *J* = 7.9 Hz, 2H, Ar), 6.64 (dd, *J* = 16.0, 7.8

Hz, 1H, CH=C*H*C(O)H), 2.35 (s, 3H, C*H*$_3$); **ESI-MS** $C_{10}H_{10}O$ Calc. $(M + H^+) = 147.0804$, found $(M + H^+) = 147.0810$. Matches known data.[100]

6.3 General method for the fluorescence study of biphenyl compounds

6.3.1 Preparation of solutions

Biphenyl **55** (2.4 mg) was weighed out and dissolved in chloroform (100 mL) using a 100 mL volumetric flask. The resulting solution, solution **A,** was stored in dark as a parent solution. Solution **A** (1 mL) was transferred to another 100 mL volumertric flask and made up to 100 mL using chloroform. The resulting solution **B** was then examined in the fluorescence study.

Solution **A** (0.1 mL) was transferred to a 10 mL volumetric flask and gently blown dry. Methanol (10 mL) was added to the volumetric flask and shaken to ensure complete dissolution of biphenyl **55**. The resulting solution was then examined in the fluorescence study.

Solutions of biphenyl **55** were prepared in different solvents at same concentration (0.00024 mg/mL, 0.712×10^{-3} mM) using this method. This method was applied in the preparation of biphenyl **55** solutions in toluene, acetic acid, ethylene glycol, dichloromethane, n-hexane and acetonitrile and also to all biphenyls (**56-61**) in chloroform and methanol.

6.3.2 Fluorescence study

A UV-vis spectrum of solution **B** of biphenyl **55** (in chloroform) was obtained using a Unicam UV 540 spectrometer. The UV-vis spectrum was recorded with a maximum absorption at 340 nm. The fluorescence (excitation and emission spectra) for solution **B** was obtained using a JASCO FP-6300 spectrofluorometer. The maximum absorption of 340 nm for solution **B** was used as an excitation parameter to generate the emission spectrum. Emission maximum of solution **B** was recorded at 433 nm. This emission maximum of 433 nm for solution **B** was then used as an emission parameter to generate the excitation spectrum, with a maximum at 346 nm. This method was applied to solutions of biphenyl **55** in methanol toluene, acetic acid, ethylene glycol, dichloromethane, n-hexane and acetonitrile and also to all biphenyls (**56-61**) in chloroform and methanol.

Quantum yields Q were calculated using $Q = Q_R(I/I_R)(OD_R/OD)(n^2/n^2_R)$ where the "Q" is quantum yield; "I" is the integrated intensity of emission spectrum (which was calculated using "origin" software); "OD" is the optical density, it is the corrected absorbance which corresponds to the maximum emission in UV-absorption spectrum (base line corrected using "origin" software before being applied to the quantum yield calculation.); "n" is the refractive index of the solvent; subscript "R" refers to the reference fluorophore of known quantum yield.

The intergrated intensity of solution **B** was calculated 15784.32109; "OD" of solution **B** is 0.01757; n^2 of solution **B** is 1.4458^2.

Quinine sulfate in 0.1 M H_2SO_4 was chosen as the reference for calculating quantum yield of biphenyl **55** and was prepared at the same concentration as solution **B** and called solution **C**. UV-absorption spectrum of solution **C** was obtained along with the emission spectrum after excitation at 340 nm (same wavelength as used for biphenyl **55**). The integrated intensity of solution **C** was calculated 5754.789124; "OD_R" of solution **C** is 0.0445; n^2_R of solution **C** is 1.355^2; quantum yield Q_R was 0.577. Therefore the quantum yield of solution **B** was calculated $= (15784.32\ 109/\ 5754.789124) \times (0.01757\ /\ 0.0445) \times (1.4458^2\ /\ 1.355^2) \times 0.58 = 0.71$.

The reference material should have maximum absorption (excitation parameter) close to sample at the same temperature as the reference material was excited at the same wavelength as the sample.

Bibliography

1 Tomoo, S.; Keizo, Y. *Jpn. Med. Assoc. J.* **2009**, *52* (2), 103-108.

2 Kuiling, D.; Shaoxu, H. *Bull. Chin. Acad. Sci*. **2011**, *26* (1), 20-30.

3 Chain, E.; Florey, H. W. *Lancet* **1940**, *239*, 226-228.

4 Graham, D. *Intellectual property rights and the life science industries: past, present and future*; World Scientific, **2009**.

5 Comroe, J. H. Jr. *Am. Rev. Respir. Dis.* **1978**, *117* (4), 773–781.

6 Emmerson, A. M.; Jones, A. M. *J. Antimicrob. Chemother.* **2003**, *51* (1), 13–20.

7 Podolsky, M. L. *Cures Out of Chaos: How Unexpected Discoveries Led to Breakthroughs in Medicine and Health*; Harwood Academic Publishers, **1998**.

8 Andre, B. *Antimicrobial agents: antibacterials and antifungals*; ASM Press: Washington, DC, **2005**.

9 Demchick, P. K. *J. Bacteriol.* **1996**, *178* (3), 768–773.

10 Van, H. J. *Glycobiology* **2001**, *11* (3), 25R – 36R.

11 Hakenbeck, R.; Coyette, J. *Cell Mol Life Sci*, **1998**, *54*, 332–340.

12 Richard, L. S.; Ronald, S. G.. *Infectious Diseases of the Female Genital Tract*; Lippincott Williams & Wilkins, **2009**.

13 PRIMAXIN (Brand Name Drug) FDA Application No. (NDA) 050587 Drug Details, Drugs@FDA

14 Smith, S. *Deadly bacteria's foothold spurs study: Mass. specialists try to halt spread*; The Boston Globe, **2010**.

15 Livermore, D. M; Woodford, N. *Curr. Opin. Microbiol.* **2000**, *3* (5), 489–495.

16 Hellinger, W. C.; Brewer, N. S. *Mayo. Clin. Proc.* **1999**, *74* (4), 420-434.

17 Roberta, J. W.; Christian, M. *ACS Med. Chem. Lett.* **2012**, *3* (5), 357–361.

18 Livermore, D. M.; Williams, J. D. *J. Antimicrob. Chemother.* **1981**, *8*, 29-37.

[19] Lim, S. M.; Webb, S. A. *Anaesthesia* **2005**, *60* (9), 887-902.

[20] Shnayerson, M.; Plotkin, M. *The Killers Within: The Deadly Rise of Drug-Resistant Bacteria*; Back Bay Books, **2003**.

[21] Sharma, D.; Cukras, A. R.; Rogers, E. J.; Southworth, D. R.; Green, R. *J. Mol. Biol*. **2007**, *374* (4), 1065-76.

[22] Walsh, C. *Antibiotics: actions, origins, resistance*; American Society for Microbiology Press: Washington DC, **2003**.

[23] Zuckerman, J. *Infect. Dis. Clin. N. Am.* **2004**, *18*, 621–649.

[24] Ackermann, G.; Rodloff, A. C. *J. Antimicrob. Chemother.* **2003**, *51* (3), 497-511.

[25] Chopra, I.; Roberts, M. *Microbiol. Mol. Biol. Rev*. **2001**, *65* (2), 232-260.

[26] Jukes; Thomas, H. *Rev. Infect. Dis.* **1985**, *7* (5), 702-707.

[27] Goldstein, E. J. *Am. J. Med.* **1987**, *82* (6B), 3-17.

[28] King, D.E.; Malone, R.; Lilley, S. H. *Am. Fam. Phys.* **2000**, *61* (9), 2741–2748.

[29] Pozniak, A. L.; Miller, R. *AIDS* **1999**, *13* (4), 435–45.

[30] Finch, R. G.; Greenwood, D.; Norrby, S. R.; Whitley, R. J. *Antibiotic and chemotherapy: anti-infective agents and their use in therapy;* 8th ed.; An imprint of Elsevier Science Limited: United Kingdom, **2003**.

[31] Bermingham, A.; Derrick, J. P. *Bioessays* **2002**, *24* (7), 637-648.

[32] Richey, D. P.; Brown, G. M. *J. Biol. Chem.* **1969**, *244* (6), 1582-1592.

[33] Lacey, R. W. *J. Antimicrob. Chemother*. **1979**, *5* (B), 75-83.

[34] Garg, S.K.; Ghosh, S.S.; Mathur, V. S. *Int. J. Clin. Pharmacool. Ther. Toxicol.* **1986**, *24* (1), 23–25.

[35] Neil, P.; Matthew, D.; Geraldine, M.; Luis, D.; Nicholas, W.; Alex, G.; Shard, S. S.; A. Tobias A. Jenkins; Andrew, L. J. *New J. Chem.* **2011**, *35*, 1477.

[36] McDevitt, C. A. *PLoS Pathog.* **2011**, *7*, e1002357.

[37] Tariq, M.; Rabia, R.; Aqsa, G.; Amina, K.; Jamil, A.; Umer, S.; Waheed, Z.; Muhammad, S. *Arabian J. Chem.* **2010**, *3*, 219–224.

[38] Nenad, R.; Filipovi ć, Ivanka, M.; Dragana, M.; Natalija, P.; Miloˇs, M.; Marija, D.; Maja, J.; Milena, S.; Miomir, N.; Katarina, A.; Tamara, T. *J. Biochem. Molecular toxicology* **2014**, *28* (3), 99-110.

[39] Ajay, K.; Singh, O. P.; Pandey, S. K.; Sengupta. *Spectrochim. Acta, Part A: Mol. Biomol.Spectrosc.* **2013**, *113*, 393-399.

[40] Umaira, F.; Tariq, B.; Luqman, S.; Wajid, H.; Faisal, Hanif. *J Ayub Med Coll Abbottabad* **2011**, *23* (2), 18-21.

[41] Bernadette, S. C.; Denise, A. E.; Kevin, K.; Malachy, M.; Andy, N.; Bhumika, T.; Maureen, W. *Inorg. Chim. Acta* **2006**, *359* (12), 3976–3984.

[42] Bhumika, T.; Andy, N.; Raymond, R.; Bernadette, S. C.; Maureen, W.; Malachy, M.; Denise, E.; Kevin, K.; *Toxicol. in Vitro* **2007**, *21*, 801–808.

[43] Sohail, S.; Naghmana, R.; Muhammad, A.; Rizwan, H.; *Eur. J. Chem.* **2010**, *1* (3), 200-205.

[44] Ian, C. *J. Antimicrob. Chemother.* **2013**, *68*, 496-505.

[45] Quale, J.; Bratu, S.; Landman, D.; Heddurshetti, R.; *Clin. Infect. Dis.* **2003**, *37*, 214-220.

[46] Naveen, V. K.; Vidyanand, K. R. *J. Coord. Chem.* **2011**, *64*, 725-741.

[47] a) Pearson, R. G. *J. Am. Chem. Soc.* **1963**, *85*, 3533.
b) Pearson, R. G. *J. Chem. Educ.* **1987**, *64*, 561.

[48] Zeljko, K.; Jacimovic, G.; Bogdanovic, A.; Berta, H.; Vukadin, M.; Leovac; Katalin, M. S. *J. Serb. Chem. Soc.* **2009**, *74* (11), 1259–1271.

[49] Niamh, D. Ph.D. thesis, National University of Ireland, Maynooth, October 2013.

[50] Mohammad, R.; Mehdi, P.; Mehdi, B.; Shima, R.; Ali, S. *World J Microbiol Biotechnol.* **2010**, *26*, 317–321

[51] Anju, G.; Neelam, J.; Sandeep, J. *Orient. J. Chem.* **2013**, *29* (2), 553-558.

[52] Carmen, L.; Mariana, C. C. *Int J Mol Sci.* **2011**, *12* (10), 6432–6444.

[53] V ćtor, M.; Jim énez, P.; Marisol, I.; Blanca, M. M.; Alberto, G.; Rosa, S.; Eugenio, H. F.; Sylvain, B.; Noemi, W.; Rosalba, R. D. *J. Mol. Struct.* **2013**, *1031*, 168–174.

[54] Bach, P.; Bostrom, J.; Brickmann, K.; Cheng, L.; Giordanetto, F.; Groneberg, R. D.;

Harvey, D. M.; O'sullivan, M. F.; Zetterberg, F.; Osterlund, K. Novel Pyridine Compounds. Patent WO200673361 A1, 2006.

[55] Heshmatollah, A. *J. Fluorine Chem.* **2011**, *132*, 995–1000.

[56] Giulia, M.; Luisa, M.; Pietro, S. *J. Heterocycl. Chem.* **1987**, *24*, 1669 – 1676.

[57] Bartroli, J.; Turmo, E.; Anguita, M. New Carboxamides With Antifungal Activity. Patent WO199705131, 1997.

[58] Kim, G. T.; Koh, J. S.; Han, H.O.; Kim, S. H.; Kim, K.; Chung, H.; Kim, Y. C.; Kim, M.; Koo, K. D.; Yim, H. J.; Hur, G.; Lee, S. H.; Lee, C.; Woo, S. H. Novel Compounds As Agonist For Ppar Gamma And Ppar Alpha, Method For Preparation Of The Same, And Pharmaceutical Composition Containing The Same. Patent WO2005040127, 2005.

[59] Ushio, H.; Hamada, M.; Watanabe, M.; Numata, A.; Fujie, N.; Takashima, T.; Furukawa, H.; Ando, J. Amide Derivative And Use Thereof. Patent WO2012050159 A1, 2012.

[60] Andrij, D.; Andreas, S. *Eur. J. Org. Chem.* **2010**, *22*, 4296-4305.

[61] Ushio, H.; Ishibuchi, S.; Naito, Y.; Sugiyama, N.; Kawaguchi, T.; Chiba, K.; Ohtsuki, M.; Naka, Y. Amide Compounds And Medicinal Use Thereof. Patent EP 1176140A1, 2002.

[62] Charvat, T.; Hu, C.; Jin, J.; Li, Y.; Melikian, A.; Pennell, A. M. K.; Punna, S.; Ungashe, S.; Zeng, Y. Triazolyl Pyridyl Benzenesulfonamides. Patent WO2008008375, 2008.

[63] Edward, D. C. Account of a newly discovered variety of green fluor spar, of very uncommon beauty, and with remarkable properties of colour and phosphorescence. In *The Annals of Philosophy*; **1819**; 14 : 34 - 36; from page 35: "The finer crystals are perfectly transparent. Their colour by transmitted light is an intense *emerald green*; but by reflected light, the colour is a deep *sapphire blue*; "

[64] David, B. *Trans. R. Soc. Edinburgh* **1834**, *12*, 538-545.

[65] Herschel, J. F. W. *Phil. Trans.* **1945**, 143–145 & 147–153.

[66] Stokes, G. G. *Philosophical Transactions of the Royal Society of London* **1852**, *142*, 463–562.

[67] (a) Ulises, A. A.; Francisco, A.; Purificación, M.; Marta, L.; Benjamín, R. *Org. Lett.* **2009**, *11* (14), 3020–3023. (b) Monardes, N.; Dos Libros/El Vno trata de todas las cosas que traen de nuestras Indias occidentales que sirVen al uso de Medicina. . . , en casa de Sebastian Trugillo, Seville, **1565**.

[68] Ulises, A. A.; Francisco, A.; Purificació n, M.; Marta, L.; Benjam ń, R. *Org. Lett.* **2009**, *11* (14), 3020–3023.

[69] Maus, M.; Rurack, K. *New J. Chem.* **2000**, *24*, 677.

[70] Sameriro, M.; Goncalves, T. *Chem.Rev.* **2009**, *109*, 190-212.

[71] Joseph, R. L. *Principles of Fluorescence Spectroscopy*; 3 rd ed.; Springer Science+Business Media, LLC: New York , **2006**

[72] Gafni, A.; Brand, L. *Biochem.* **1976**, *15* (15), 3165–3171.

[73] Brochon, J. C.; Wahl, P.; Monneuse-Doublet, M.; Olomucki, A. *Biochem.* **1977**, *16* (21), 4594–4599.

[74] Visser, A. J. W. G. *Photochem Photobiol* **1984**, *40* (6), 703–706.

[75] Permyakov, E. A. *Luminescent spectroscopy of proteins*; CRC Press: London, **1993**.

[76] Weber, G. *Biochem J* **1951**, *51*, 155–167.

[77] Daniel, E.; Weber, G. *Biochem.* **1966**, *5* (6), 1893–1900.

[78] Kinnunen, P. K. J.; Koiv, A.; Mustonen, P. Pyrene-labeled lipids as fluorescent probes in studies on biomembranes and membrane mod-els. In *Fluorescence spectroscopy: new methods and applications*; Springer-Verlag: New York, **1993**.

[79] Hawkins, M. E.; Wolfgang, P.; Abhijit, M.; Yves, G. P.; Frank, M. B. *Nucleic Acids Res* **1995**, *23* (15), 2872–2880.

[80] Kulkosky, J.; Skalka, A. M. *J Acquired Immune Def Synd* **1990**, *3*, 839–851.

[81] Skoog, D. A. *Principles of Instrumental Analysis*; 6 th ed.; Thomson Brooks/Cole, **2007**.

[82] Christopher, M. B.; Jeremiah, P. M.; Dirk, T.; *Chem. Rev.* **2005**, *105* (12), 4757-4778.

[83] Arnason, J. T.; Rachel, M.; John, T. R. *Phytochemistry of Medicinal Plant*; 2 nd ed.; Springer Plenum Press: New York, **1995**.

[84] Yuji, M.; Noriko, O.; Hideo, N. *J. Am. Chem. Soc.* **2006**, *128* (2), 412 – 413.

[85] Su-Dong, C.; Ho-Kyun, K.; Heung-seop, Y.; Mi-Ra, K.; Jin-Kook, L.; Jeum-Jong, K.; Yong-Jin, Y. *Tetrahedron* **2007**, *63* (6), 1345-1352.

[86] Tongshou, J.; Ying, Z.; Yanran, M.; Tongshuang, L. *Indian J. Chem.* **2005**, 2183-2185.

[87] John, J. M. Studies in Synthesis and Organocatalysis: (i) Design and Synthesis of Novel Electro Deficient Dienes and their Application in the first Enamine Activated Organocatalytic 1,6-Conjugate Addition. (ii) The Development of a New Organocatalytic Methodolgy through the combination of DNA-Based Catalysis and Organocatalysis. Ph.D. Thesis, National University of Ireland, Maynooth, October 2012**.**

[88] Bernard, V. *Molecular Fluorescence: Principles and Applications*; WILEY-VCH Verlag GmbH: 69469 Weinheim (Federal Republic of Germany), **2002**.

[89] Reichardt, C. *Chem. Rev.* **1994**, *94*, 2319.

[90] (a) Lippert, E. Z. *Naturforsch.* **1955**, *1011*, 541. (b) Lippert, E.; Luder, W.; Boos, H. *In Aduances in Molecular Spectroscopy*; Mangini, A., Ed.; Pergamon: New York, **1962**, p 443.

[91] Kankan, B.; Mihir, C. *Chem. Rev.* **1993**, *93*, 507-535.

[92] Yan, M.; Rui, H.; Guangsheng, S.; Yuan, W. *J. Phys. Chem.* **2009**, *113*, 5066–5072.

[93] Maus, M.; Retting, W. *Chem. Phys.* **1997**, *218*, 151-162

[94] Schrödinger Release 2013-1: Maestro, version 9.4, Schrödinger, LLC, New York, NY, 2013.

[95] TURBOMOLE v. 6.5 2013, a development of the University of Karlsruhe and Forschungszentrum Karlsruhe GmbH, 1989-2007, TURBOMOLE GmbH, since 2007; available from www.turbomole.com

[96] Becke, A.D. *J. Chem. Phys.* **1997**, *107* (20), 8554-8560.

[97] Grimme, S. *J. Comp. Chem.* **2006**, *27* (15), 1787-1799.

[98] Varetto, U. MOLEKEL 5.4.0; Swiss National Supercomputing Centre: Lugano (Switzerland).

[99] Sumei, R.; Paul, M. *Label Compd. Radiopharm* **2009**, *52*, 316-323.

[100] Bellassoued, M.; Majidi, A. *J.* Org. Chem. **1993**, *58*, 2517-2522.

Presentations

The Design and Synthesis of a Series of Pyrazole Heterocycles and their Zinc Complexes

Poster presentation at The Irish Institute for Metal-Based Drugs Conference, 2012 (17/12/2012).

Appendix

Selected spectra

Spectra 1: ^{1}H NMR of ((1*E*,3*E*,5*E*)-6-(2-Nitrophenyl)hexa-1,3,5-triene-1,3-diyldisulfonyl)dibenzene **47**
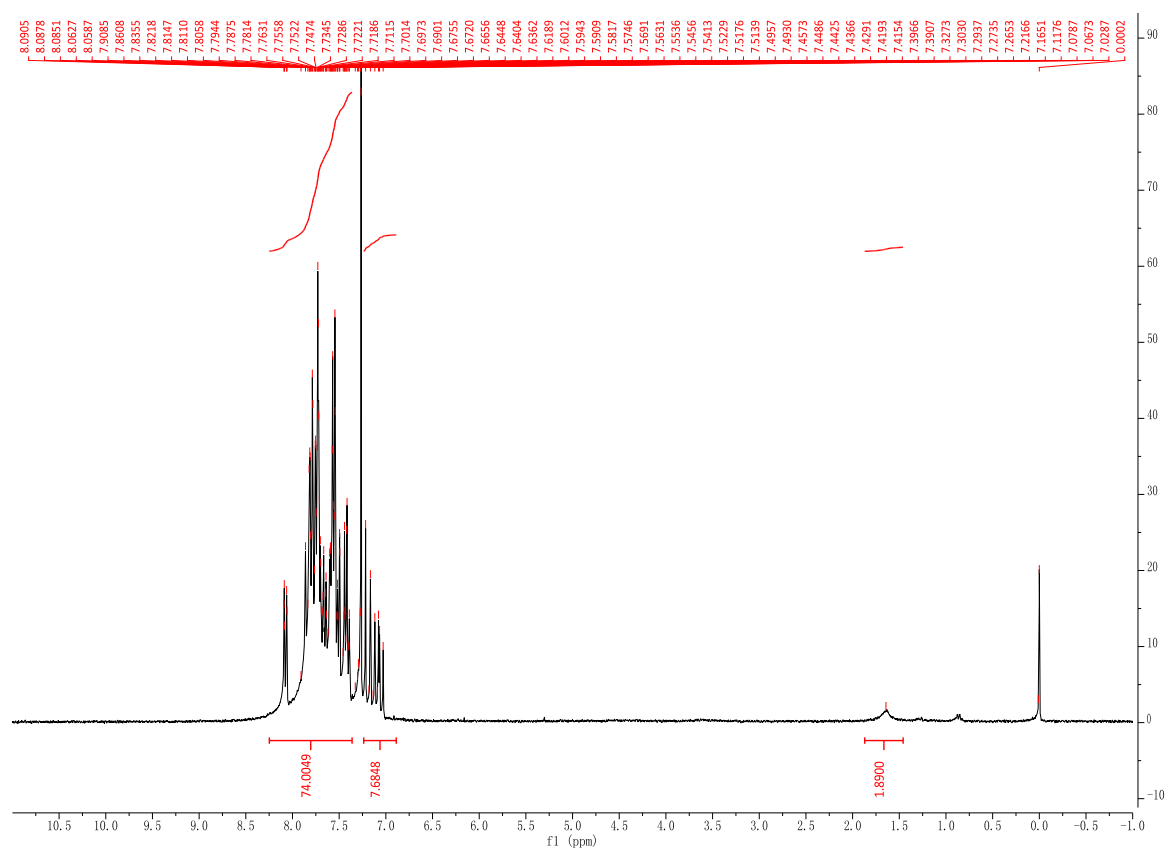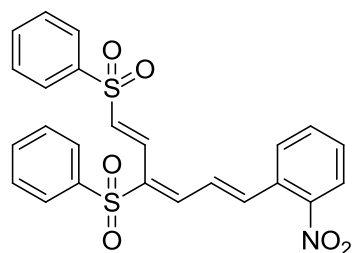
Spectra 2: [^1]H NMR of 4-((1*E*,3*E*,5*E*)-4,6-Bis(phenylsulfonyl)hexa-1,3,5-trien-1-yl)-N,N-dimethylaniline **48**
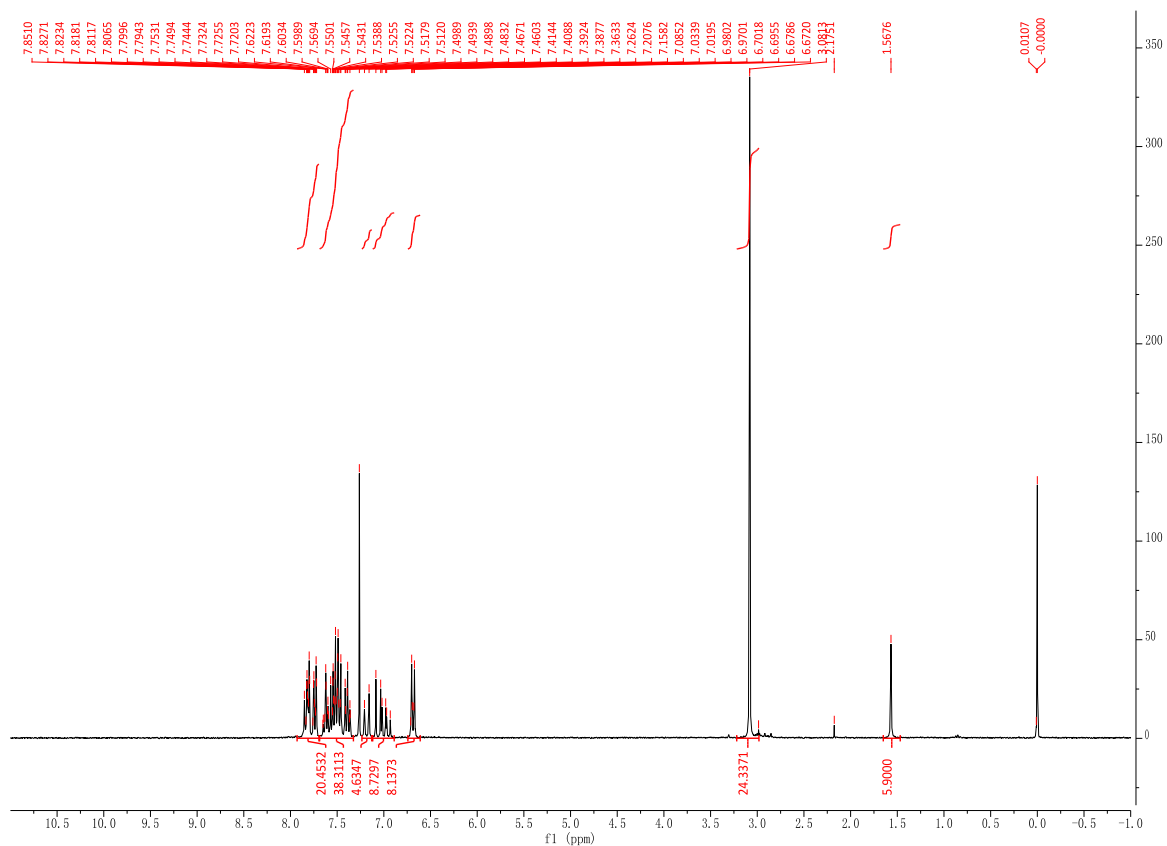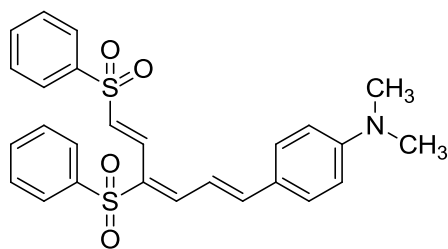
Spectra 3: ^{1}H NMR of ((1E,3E,5E)-6-(4-Chlorophenyl)hexa-1,3,5-triene-1,3-diyldisulfonyl)dibenzene **49**
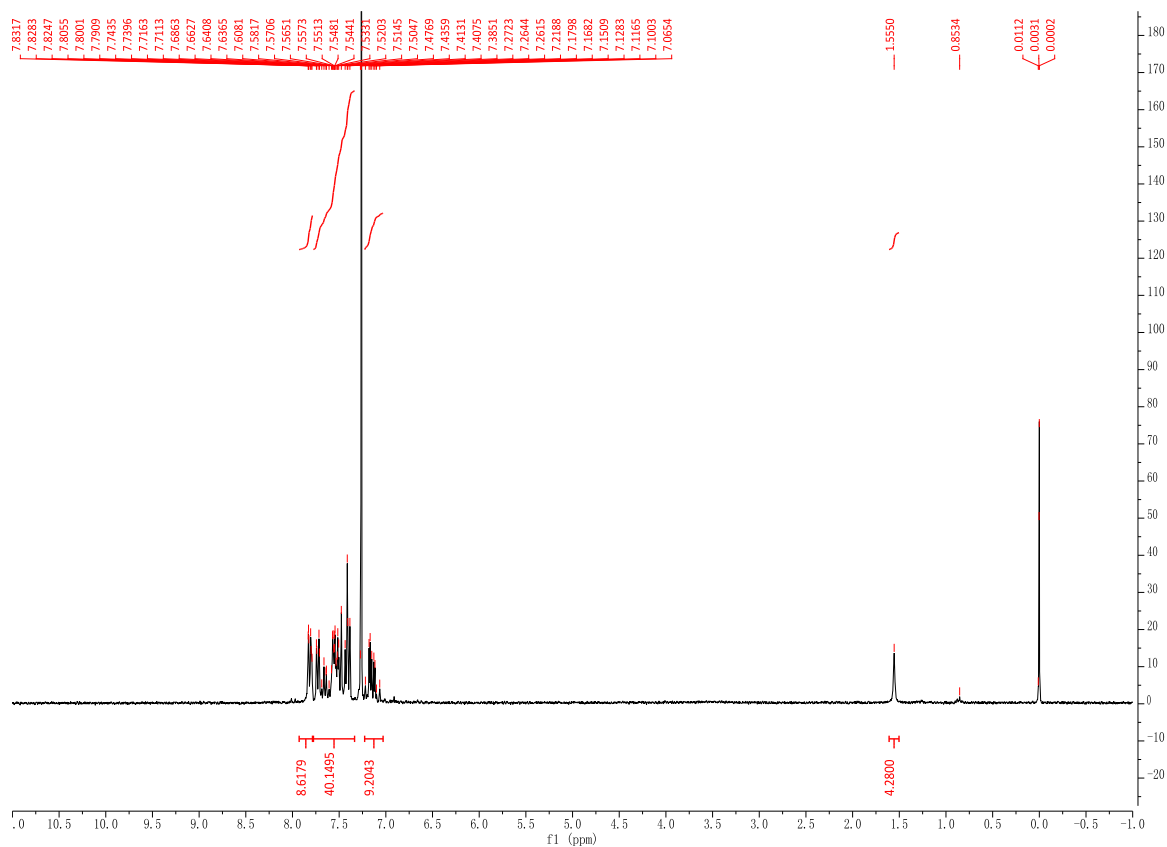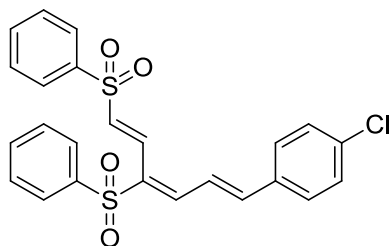
Spectra 4: ^{1}H NMR of ((1*E*,3*E*,5*E*)-6-(4-Methoxyphenyl)hexa-1,3,5-triene-1,3-diyldisulfonyl)dibenzene **50**
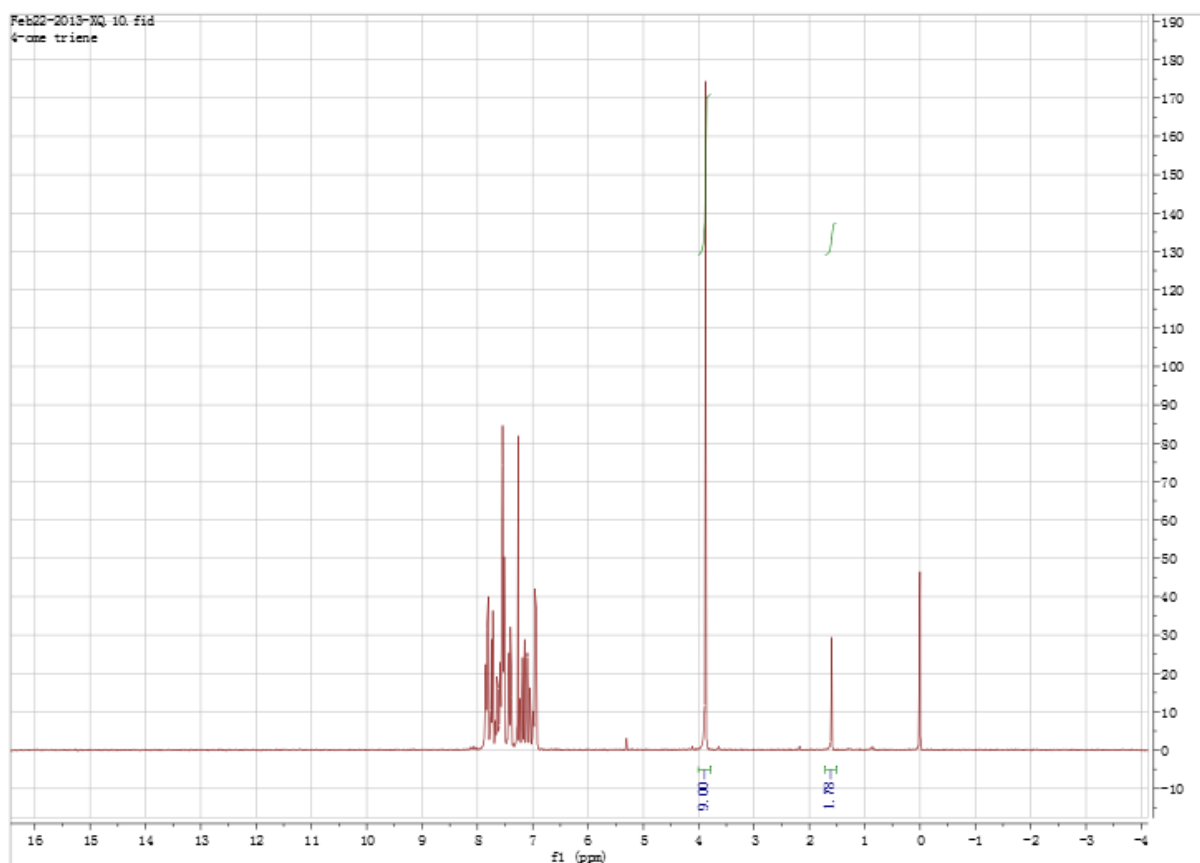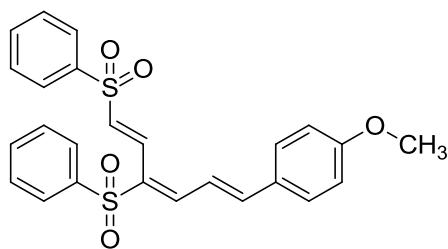
Spectra 5: ^{1}H NMR of 4-((1*E*,3*E*,5*E*)-4,6-Bis(phenylsulfonyl)hexa-1,3,5-trien-1-yl)benzonitrile **51**
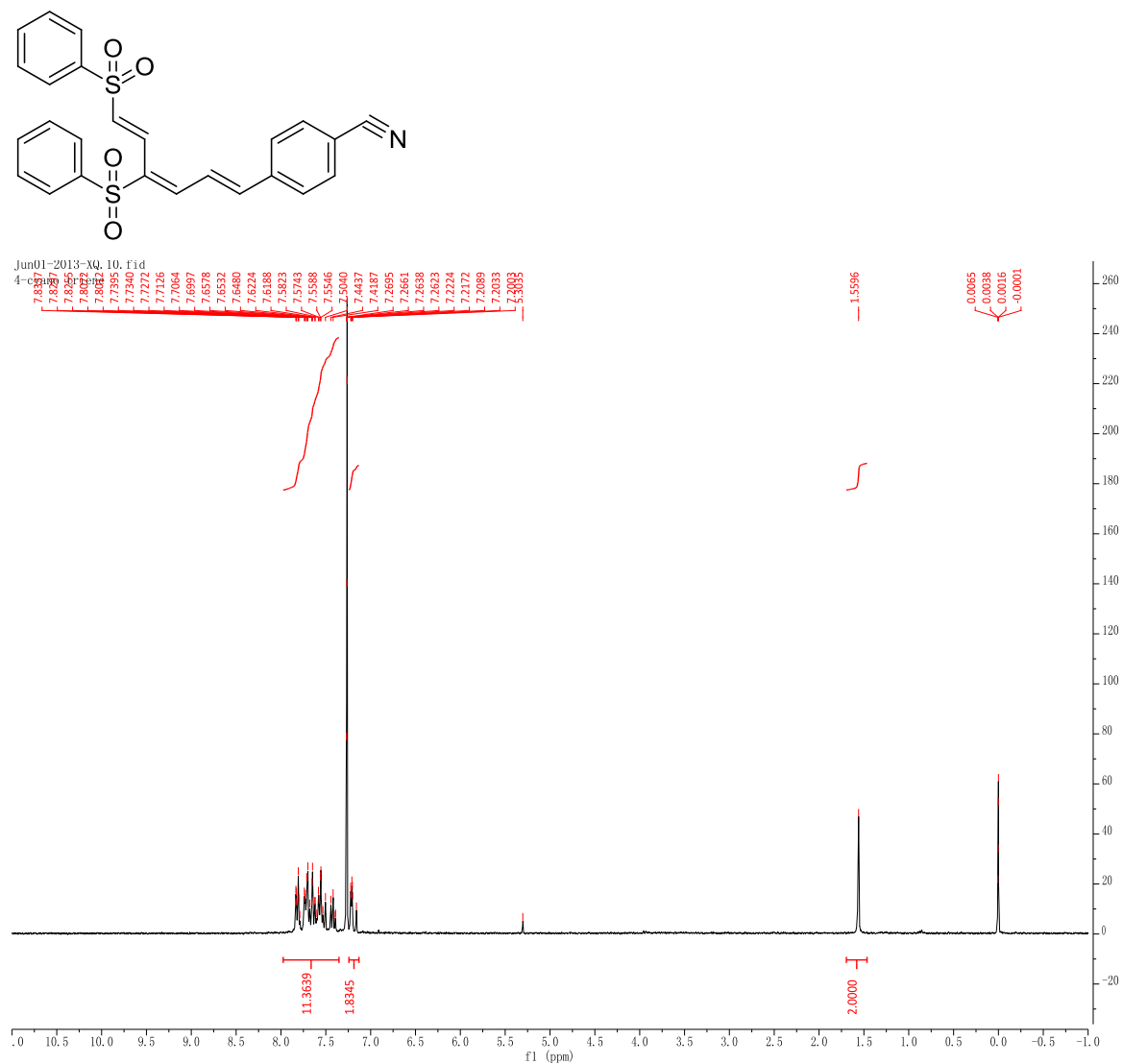
Spectra 6: ^{1}H NMR of Methyl 4-((1*E*,3*E*,5*E*)-4,6-bis(phenylsulfonyl)hexa-1,3,5-trien-1-yl)benzoate **52**
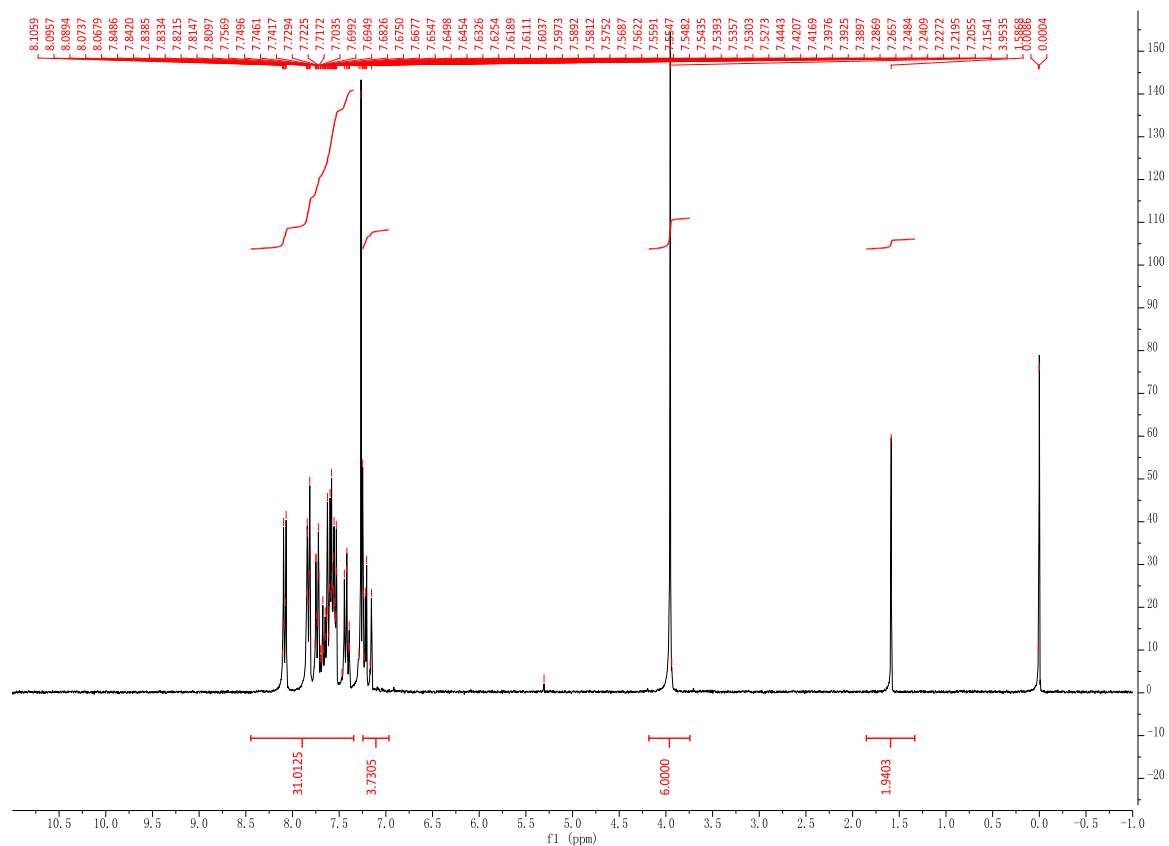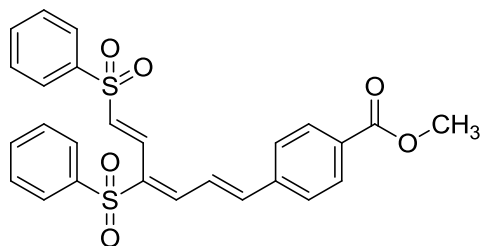
Spectra 7: ^{1}H NMR of ((1*E*,3*E*,5*E*)-6-(p-Tolyl)hexa-1,3,5-triene-1,3-diyldisulfonyl)dibenzene **53**
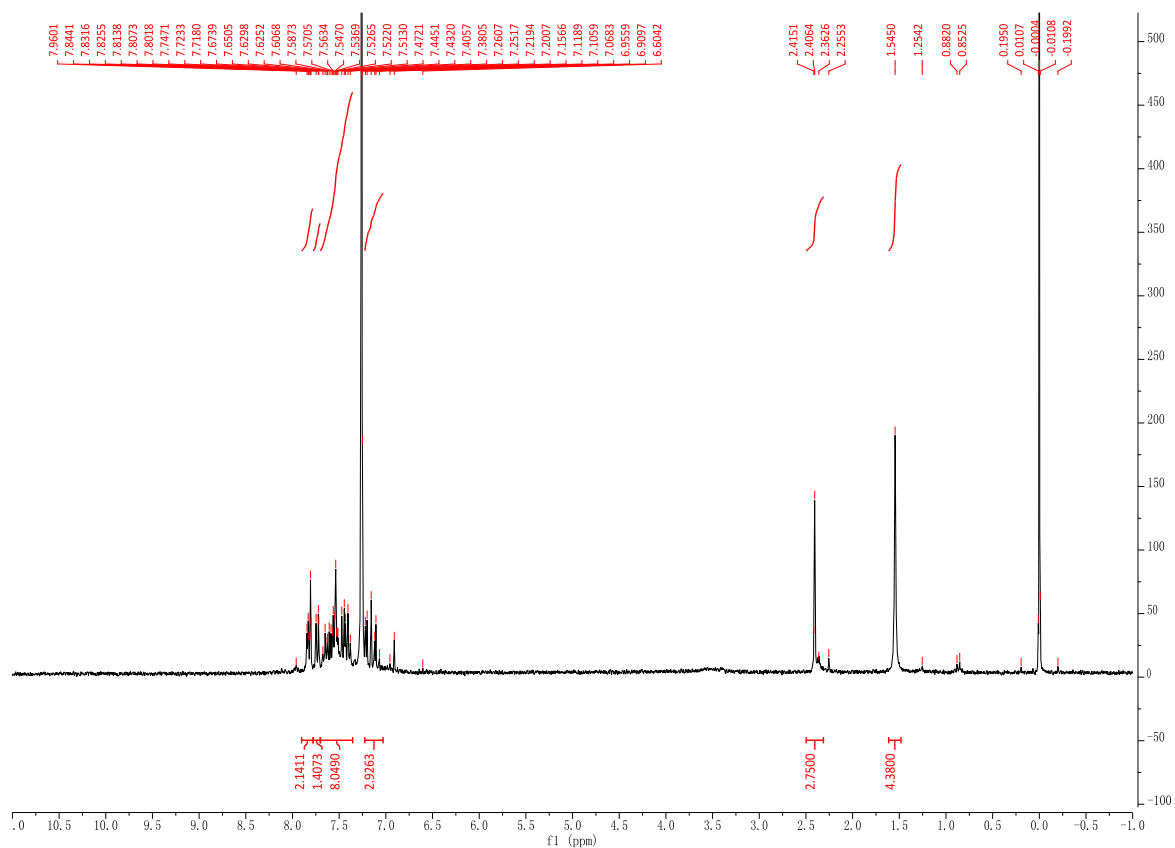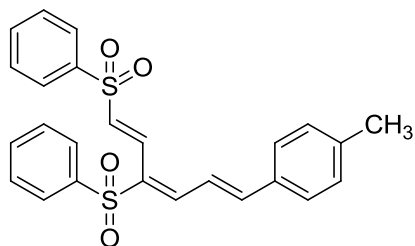
Spectra 8: ^{1}H NMR of N,N-dimethyl-4'-(phenylsulfonyl)-[1,1'-biphenyl]-4-amine **55**
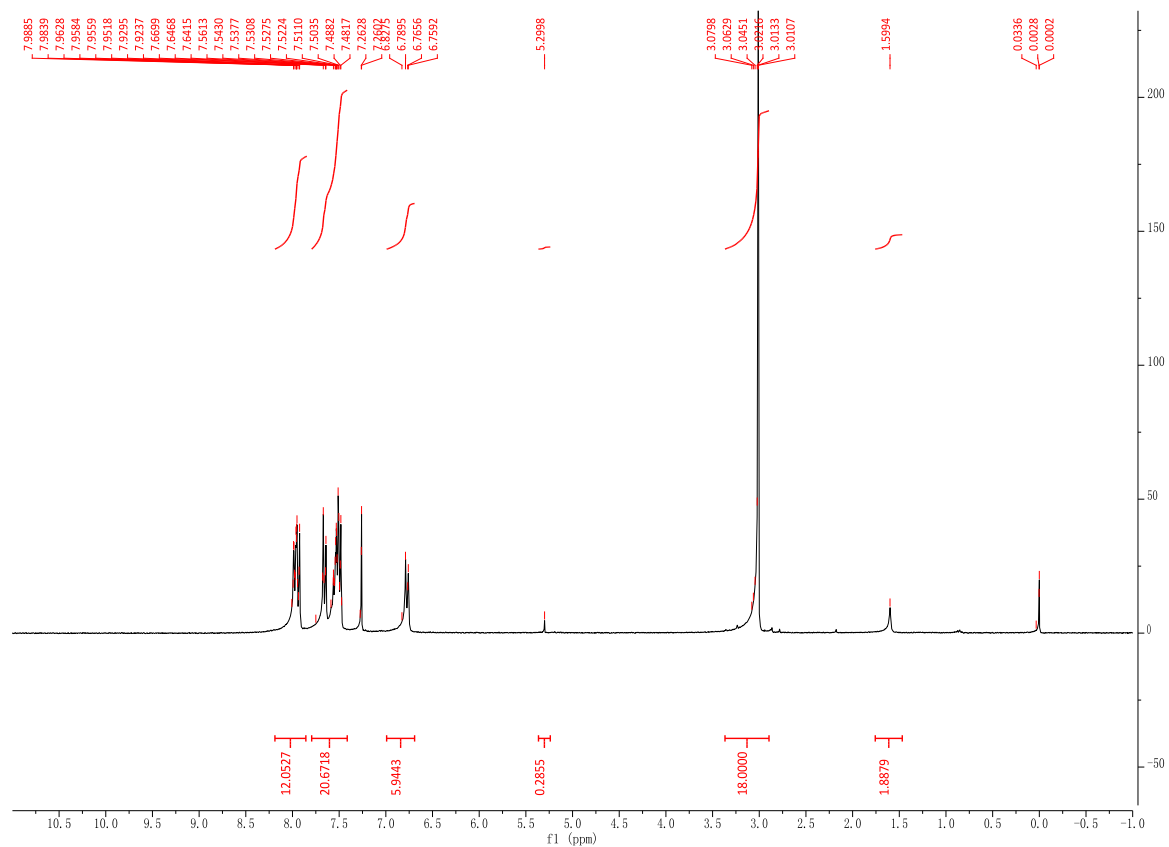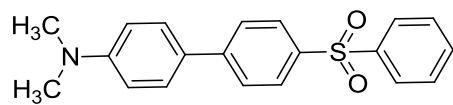
Spectra 9: ^{1}H NMR of 4-Methyl-4'-(phenylsulfonyl)-1,1'-biphenyl **56**
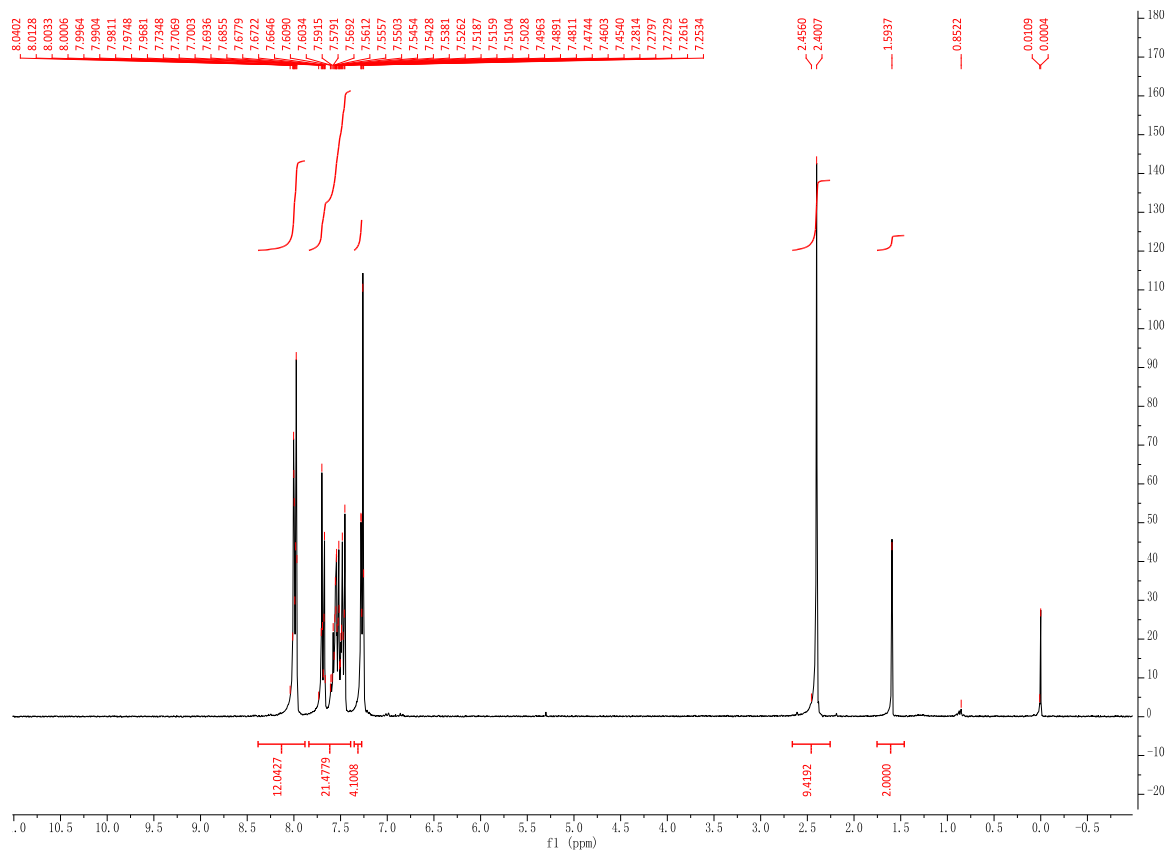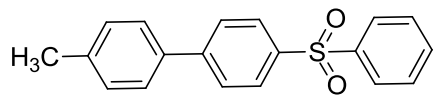
Spectra 10: ^{1}H NMR of Methyl 4'-(phenylsulfonyl)-[1,1'-biphenyl]-4-carboxylate **57**
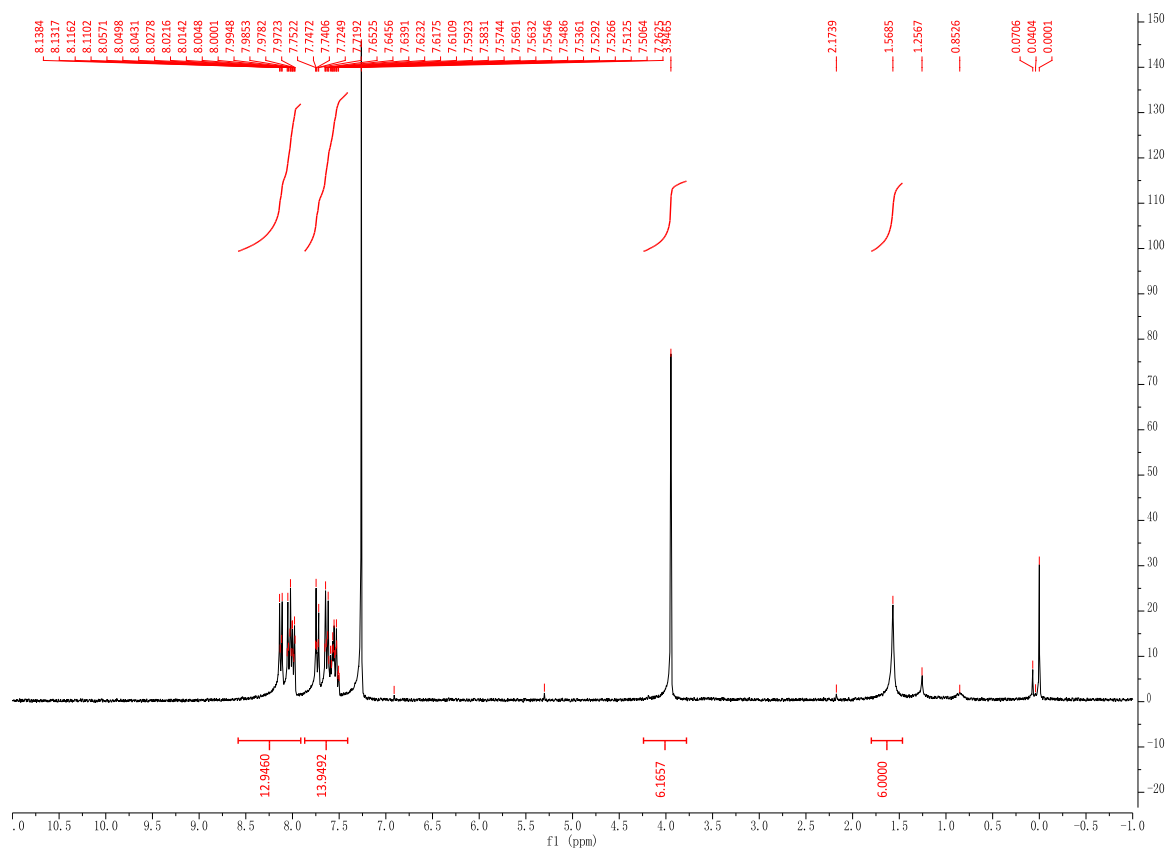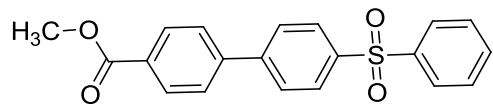
Spectra 11: ^{1}H NMR of ^{1}H NMR of 4-Methoxy-4'-(phenylsulfonyl)-1,1'-biphenyl **58**
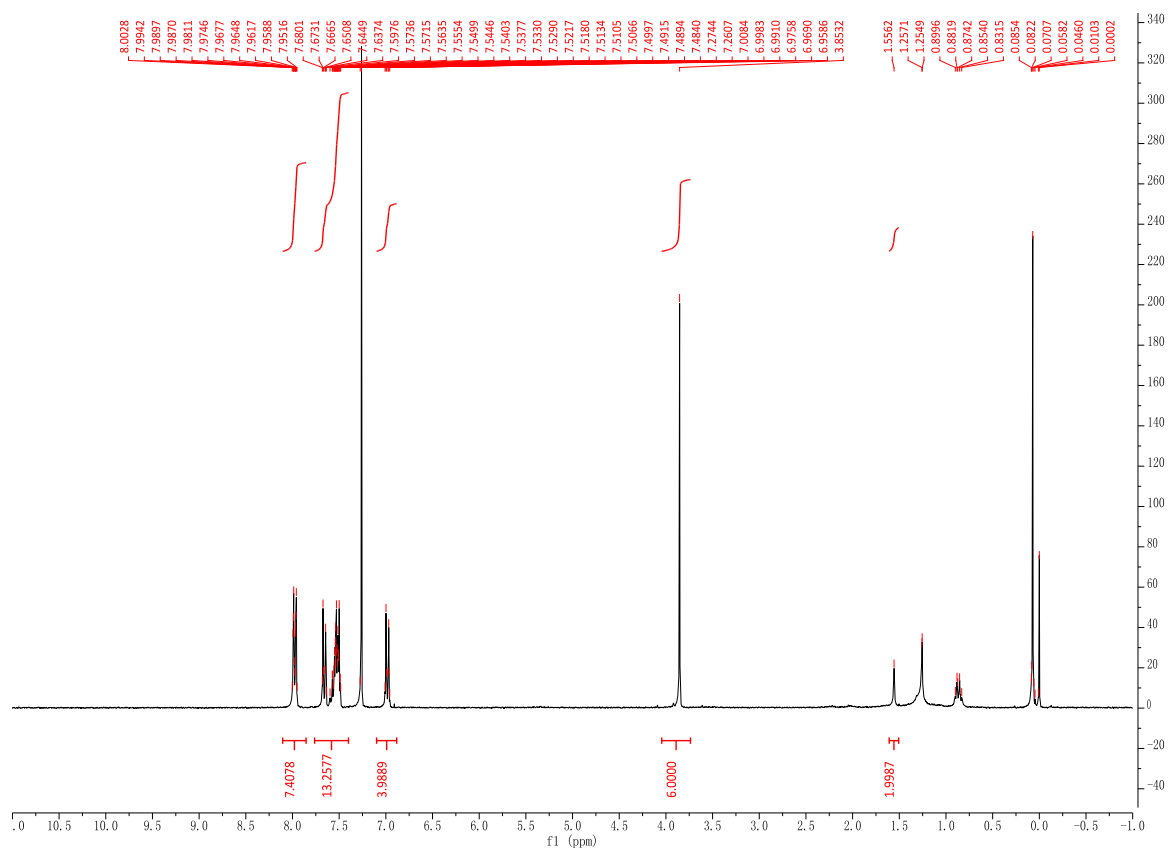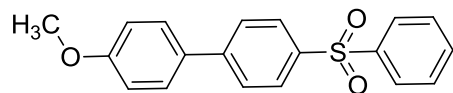
Spectra 12: ^{1}H NMR of 4'-(Phenylsulfonyl)-[1,1'-biphenyl]-4-carbonitrile **60**
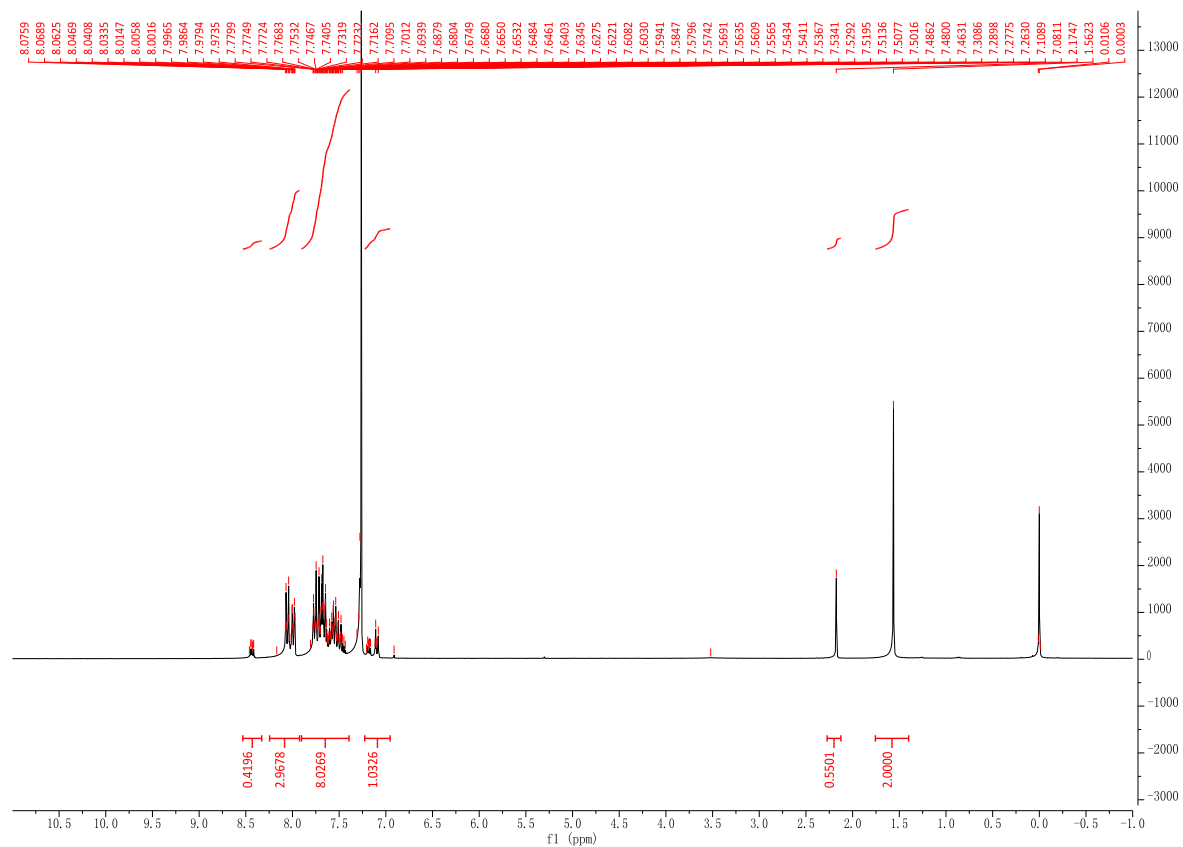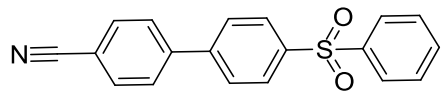
Spectra 13: ^{1}H NMR of 2-methoxy-4'-(phenylsulfonyl)-1,1'-biphenyl **61**
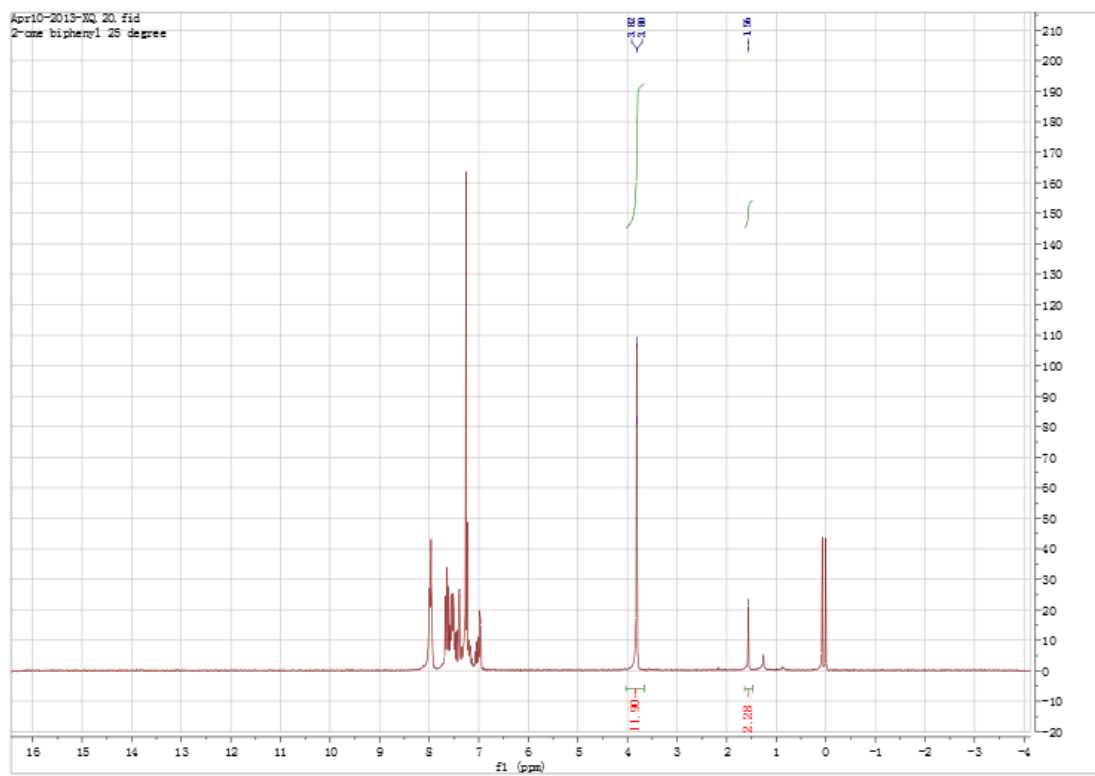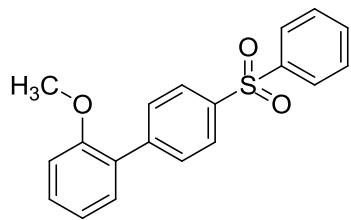
Spectra 14: ^{1}H NMR of 2-Nitro-4'-(phenylsulfonyl)-1,1'-biphenyl **62**
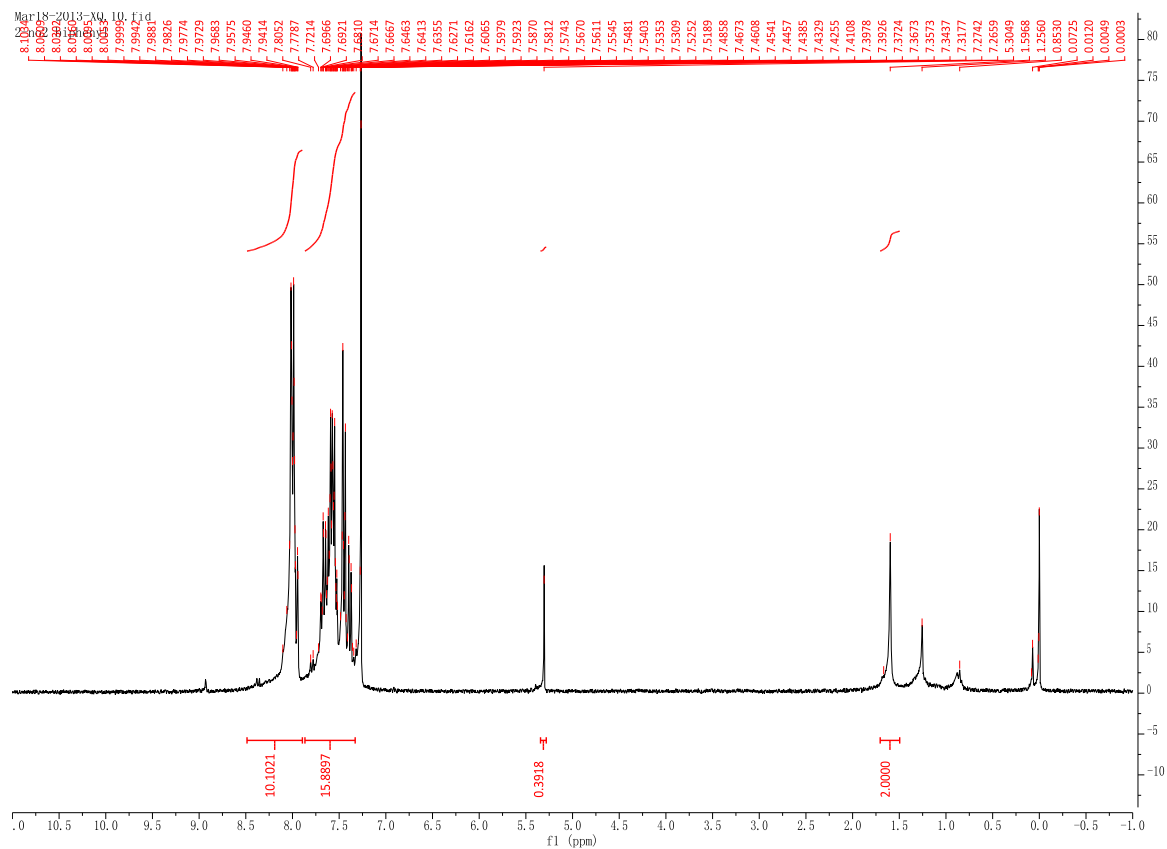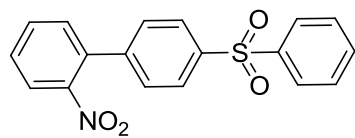
Spectra 15: ¹H NMR of 4-Nitro-4'-(phenylsulfonyl)-1,1'-biphenyl **63**
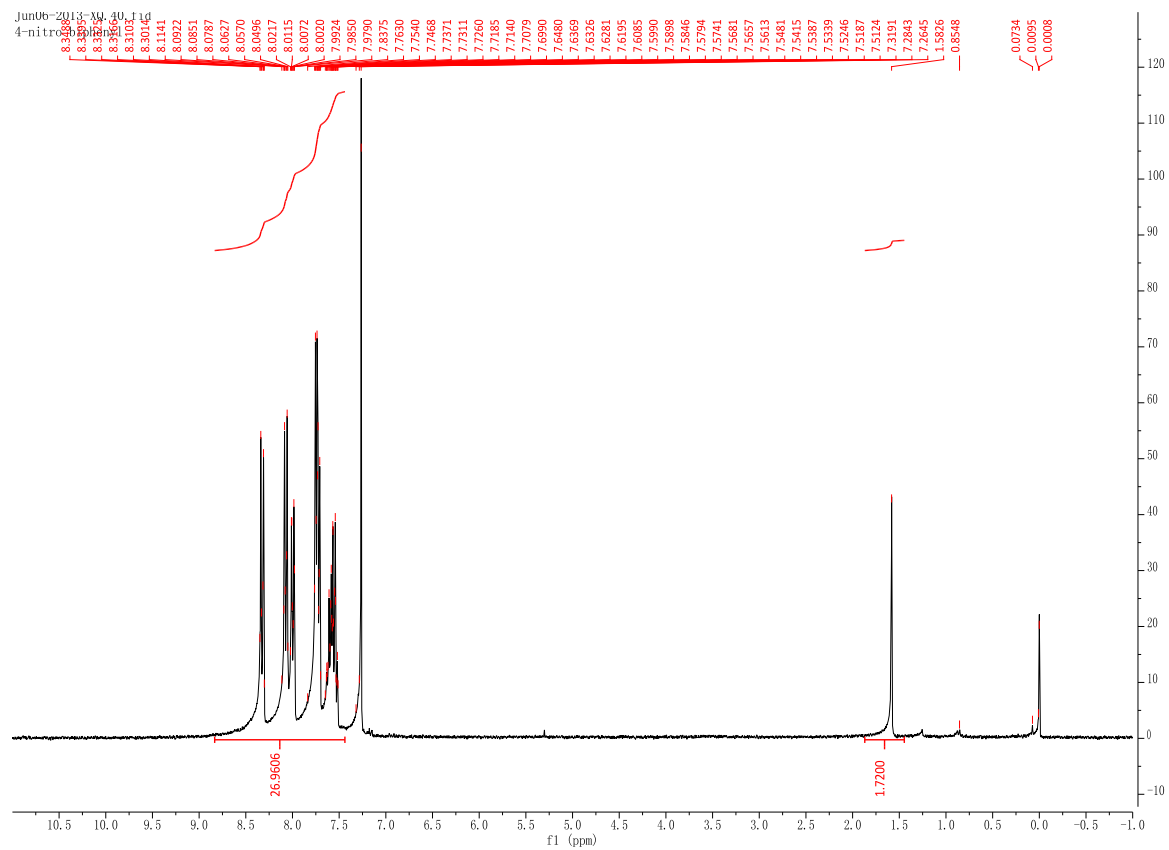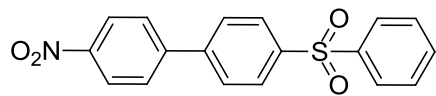
UV-absorption spectra of compound 55 recorded at a lower concentration

The UV-absorption spectra were also recorded at a lower concentration (0.712×10^{-3} mM) as this was required for quantum yield calculation, **Figure 0.1-0.6**
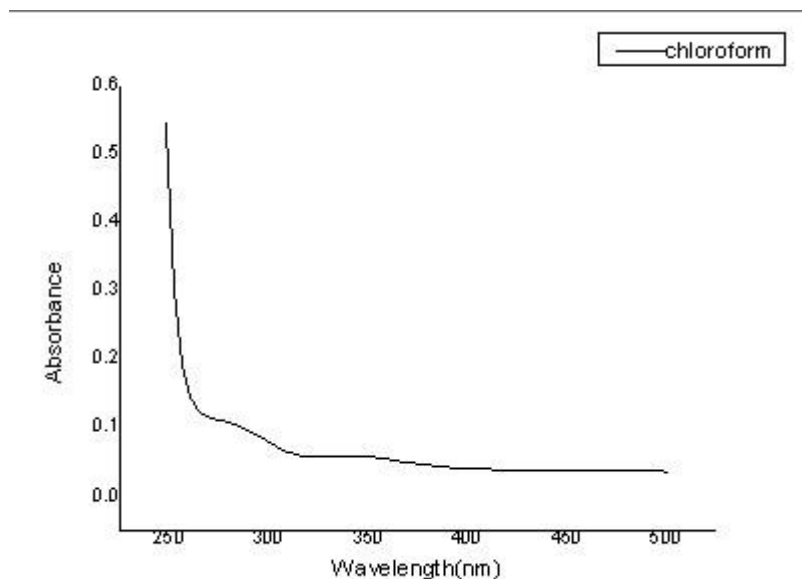
Figure 0.1 Absorption spectra of **55** (in chloroform at 0.712×10^{-3} mM)
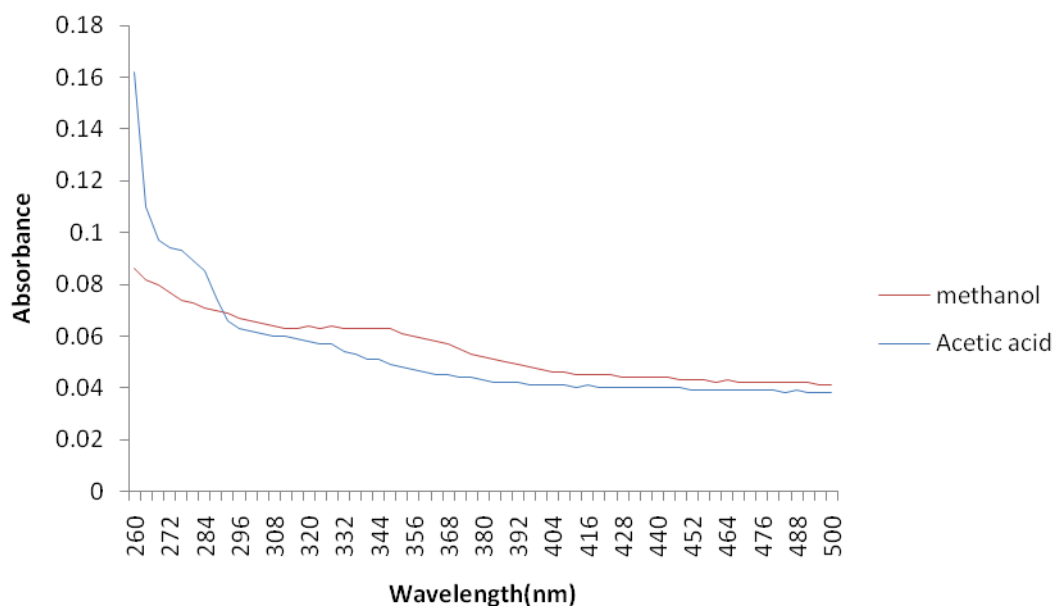
Figure 0.2 Absorption spectra of **55** (in methanol and acetic acid at 0.712×10^{-3} mM)
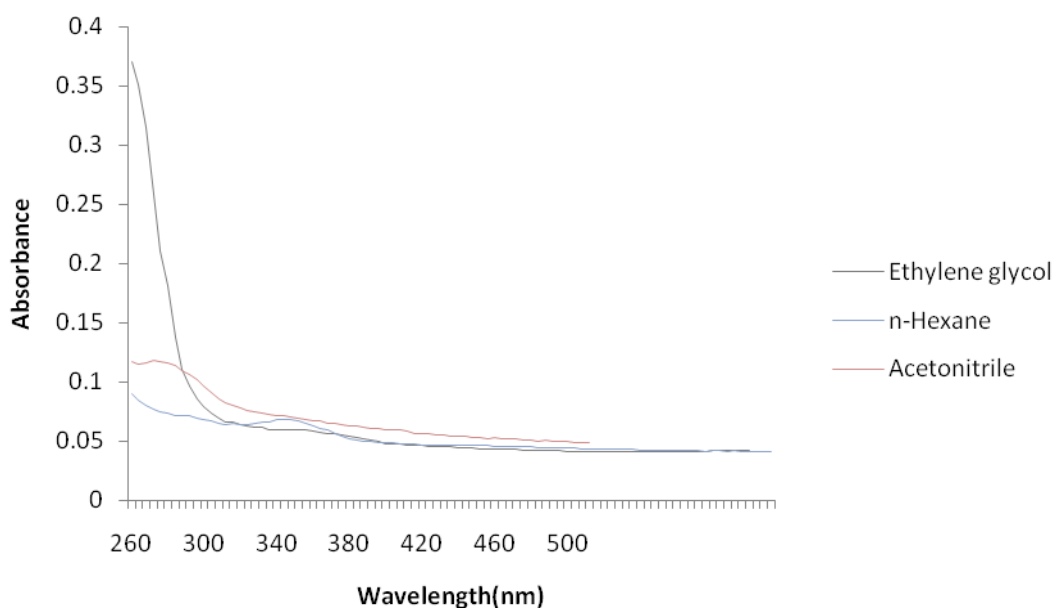
Figure 0.3 Absorption spectra of **55** (in ethylene glycol, hexane and acetonitrile at 0.712×10^{-3} mM)
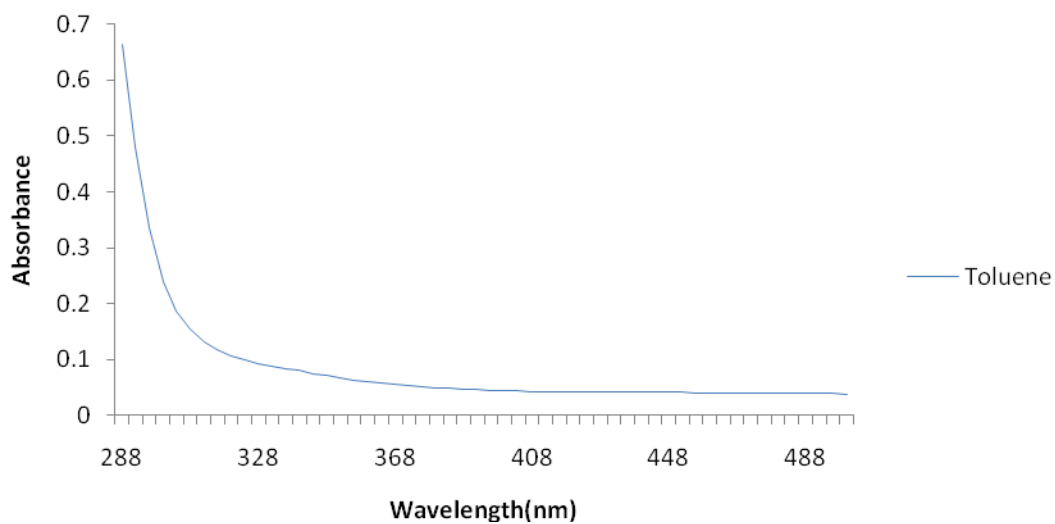
Figure 0.4 Absorption spectra of **55** (in toluene at 0.712×10^{-3} mM)
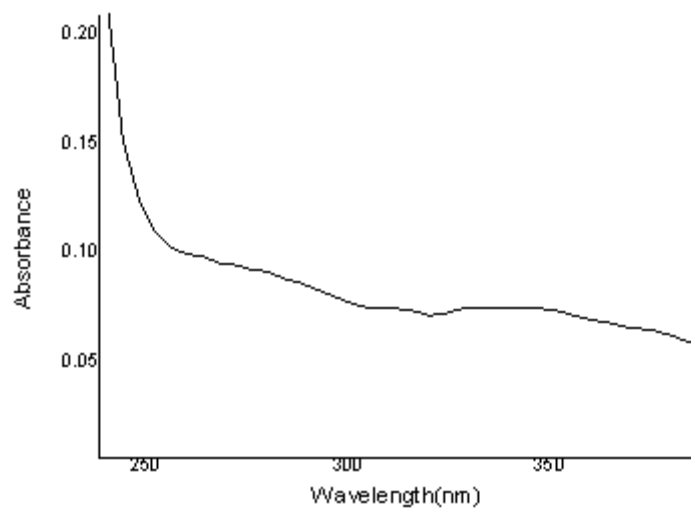
Figure 0.5 Absorption spectra of **55** (in dichloromethane at 0.712×10^{-3} mM)
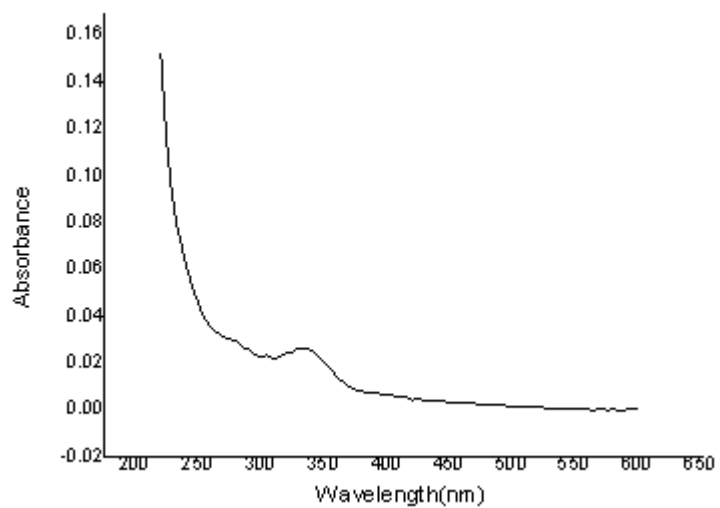
Figure 0.6 Absorption spectra of **55** (in n-hexane at 0.712×10^{-3} mM)

Molecular orbital energies

4-nitro-4'-(phenylsulfonyl)-1,1'-biphenyl **63**
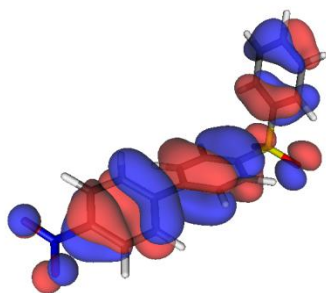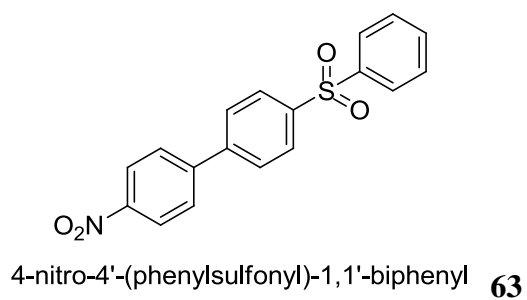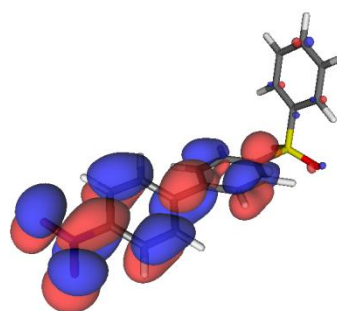
| HOMO | LUMO |
| E = -0.235 au | E = -0.127 au |
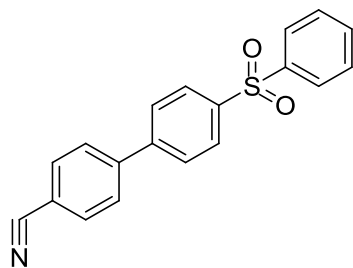
4'-(phenylsulfonyl)-[1,1'-biphenyl]-4-carbonitrile **60**
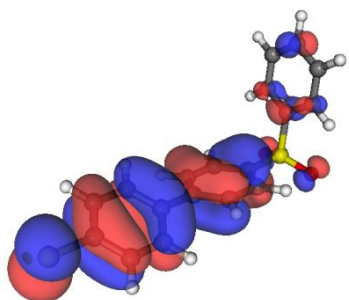
HOMO
E = -0.215 au
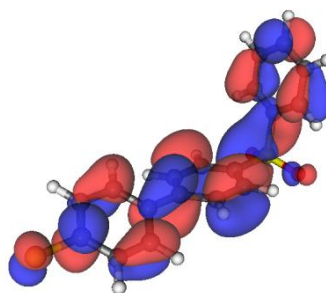
LUMO
E = -0.093 au
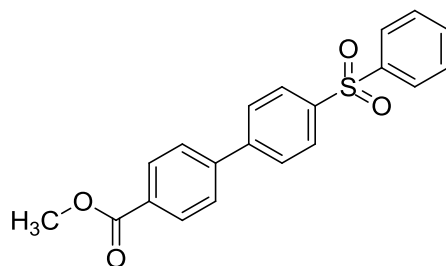
methyl 4'-(phenylsulfonyl)-[1,1'-biphenyl]-4-carboxylate **57**
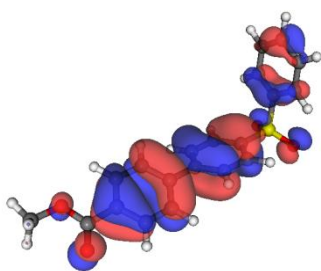
HOMO
E = -0.222 au
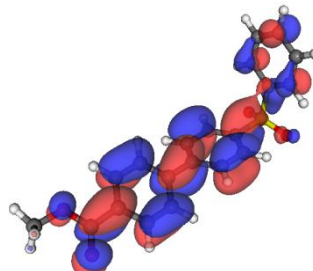
LUMO
E = -0.101 au
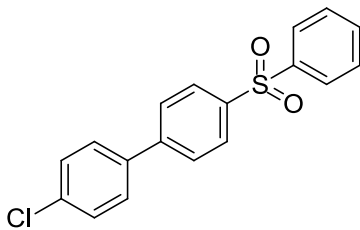
4-chloro-4'-(phenylsulfonyl)-1,1'-biphenyl **59**
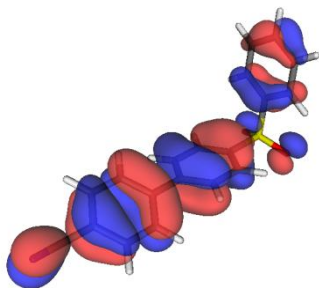
HOMO
E = -0.230 au
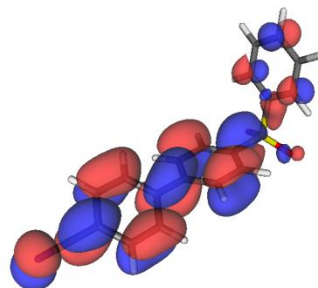
LUMO
E = -0.110 au
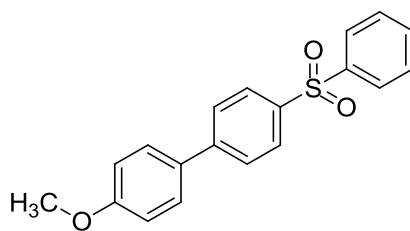
4-methoxy-4'-(phenylsulfonyl)-1,1'-biphenyl **58**
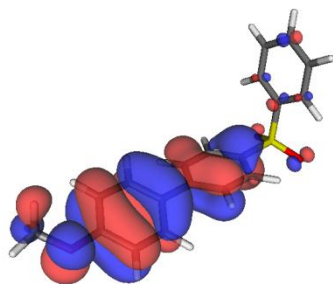
HOMO
E = -0.195 au
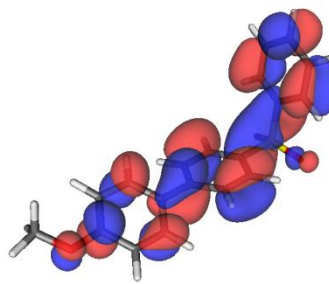
LUMO
E = -0.083 au
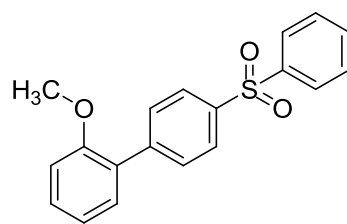
2-methoxy-4'-(phenylsulfonyl)-1,1'-biphenyl **61**
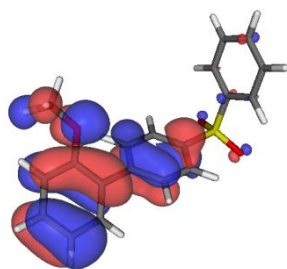
HOMO of isomer a
E = -0.199 au
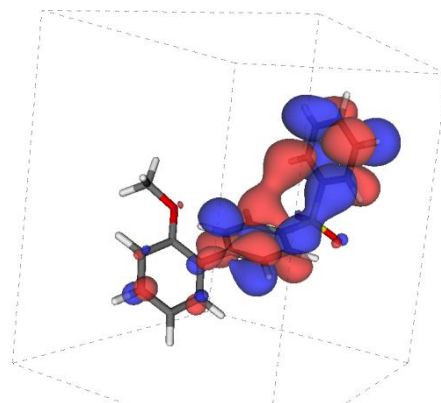
LUMO of isomer a
E = -0.055 au
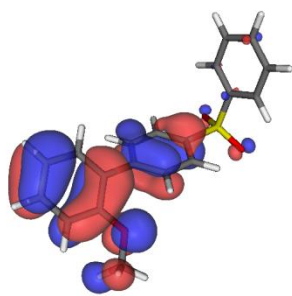
HOMO of isomer b
E = -0.198 au
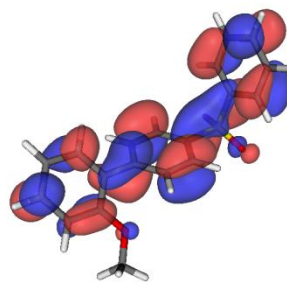
LUMO of isomer c
E = -0.082 au
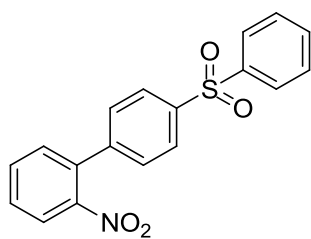
2-nitro-4'-(phenylsulfonyl)-1,1'-biphenyl **62**
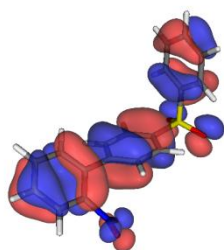
HOMO
E = -0.230 au
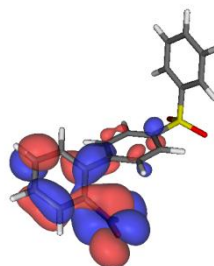
LUMO
E = -0.119 au
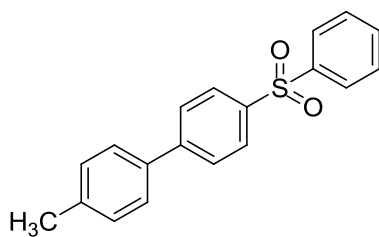
4-methyl-4'-(phenylsulfonyl)-1,1'-biphenyl **56**
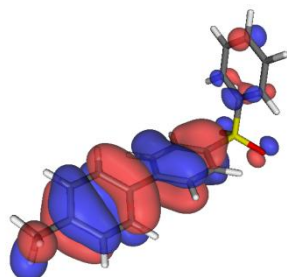
HOMO
E = -0.209 au
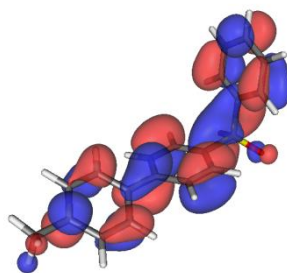
LUMO
E = -0.086 au

Table 0.11: Crystal data for 1-[(1*E*,3*E*,5*E*)-4,6-bis(phenylsulfonyl)hexa-1,3,5-trien-1-yl] -4-nitrobenzene **45**

Identification code	**45**
Empirical formula	$C_{24}H_{19}NO_6S_2$
Formula weight	481.52
Temperature	149.9(1) K
Wavelength	0.71073 Å
Crystal system	Triclinic
Space group	P 1
Unit cell dimensions	a = 5.86394(16) Å = 87.204(3)°.
	b = 8.2153(3) Å = 77.171(3)°.
	c = 11.8849(4) Å = 86.386(2)°.
Volume	556.78(3) Å^3
Z	1
Density (calculated)	1.430 Mg/m^3
Absorption coefficient	0.280 mm^{-1}
F(000)	249
Crystal size	0.40 x 0.20 x 0.20 mm^3
Theta range for data collection	2.994 to 25.348 °.
Index ranges	-7<=h<=7, -9<=k<=9, -14<=l<=7
Reflections collected	3499
Independent reflections	2552 [R(int) = 0.0122]
Completeness to theta = 25.242 °	99.9 %
Absorption correction	Semi-empirical from equivalents
Max. and min. transmission	1.00000 and 0.95971
Refinement method	Full-matrix least-squares on F^2
Data / restraints / parameters	2552 / 3 / 298
Goodness-of-fit on F^2	1.158

Final R indices [I>2sigma(I)]	R1 = 0.0336, wR2 = 0.0998			
R indices (all data)	R1 = 0.0351, wR2 = 0.1012			
Absolute structure parameter	0.03(10)			
Extinction coefficient	n/a			
Largest diff. peak and hole	0.385 and -0.217 e.Å^{-3}			

Table 0.12: Atomic coordinates (x 10^4) and equivalent   isotropic displacement parameters

(Å^2x 10^3) for **45**. U(eq) is defined as one third of the trace of the orthogonalized U^{ij} tensor.

_____

	x	y	z	U(eq)
S(1)	4500(1)	2382(1)	650(1)	21(1)
S(2)	123(2)	7415(1)	2102(1)	24(1)
O(1)	2097(5)	2404(4)	545(3)	25(1)
O(3)	-2182(6)	7481(4)	1888(3)	39(1)
O(2)	6214(5)	1314(4)	-49(3)	27(1)
O(4)	1499(6)	8812(4)	1834(3)	34(1)
O(5)	18173(6)	11565(5)	-3166(4)	49(1)
N(1)	16100(7)	11765(5)	-2676(4)	20(1)
O(6)	15123(7)	13115(4)	-2467(4)	45(1)
C(1)	14743(8)	10315(6)	-2341(4)	25(1)
C(2)	15799(8)	8789(6)	-2597(4)	28(1)
C(3)	14504(7)	7433(6)	-2247(4)	27(1)
C(4)	12167(8)	7604(6)	-1643(4)	26(1)
C(5)	11167(8)	9172(6)	-1399(5)	31(1)
C(6)	12442(8)	10528(6)	-1748(4)	28(1)
C(7)	10858(8)	6136(6)	-1304(4)	30(1)
C(8)	8641(8)	6099(6)	-678(4)	30(1)
C(9)	7580(7)	4578(6)	-312(4)	29(1)
C(10)	5451(7)	4407(6)	367(4)	24(1)

C(11)	3950(7)	5760(5)	920(4)	25(1)
C(12)	1679(8)	5724(6)	1392(4)	28(1)
C(13)	-23(8)	6810(5)	3559(4)	28(1)
C(14)	-1809(10)	5811(6)	4121(5)	42(1)
C(15)	-1908(13)	5231(8)	5209(6)	57(2)
C(16)	-250(14)	5626(10)	5751(6)	68(2)
C(17)	1536(13)	6649(10)	5252(7)	72(2)
C(18)	1664(9)	7256(7)	4099(5)	42(1)
C(19)	4593(7)	1975(5)	2123(4)	21(1)
C(20)	6679(8)	1365(5)	2383(4)	26(1)
C(21)	6726(9)	1021(6)	3525(5)	34(1)
C(22)	4740(9)	1301(6)	4390(4)	35(1)
C(23)	2677(9)	1919(7)	4125(5)	37(1)
C(24)	2584(8)	2252(6)	2977(4)	28(1)

_____

Table 0.13: Bond lengths [Å] and angles [º] for **45**

.

_____

S(1)-O(2)	1.435(3)
S(1)-O(1)	1.441(3)
S(1)-C(19)	1.779(5)
S(1)-C(10)	1.780(5)
S(2)-O(4)	1.427(3)
S(2)-O(3)	1.428(3)
S(2)-C(12)	1.758(5)
S(2)-C(13)	1.763(5)
O(5)-N(1)	1.230(5)
N(1)-O(6)	1.227(6)
N(1)-C(1)	1.463(6)
C(1)-C(2)	1.380(6)
C(1)-C(6)	1.381(6)
C(2)-C(3)	1.383(6)

C(2)-H(2)	0.9300
C(3)-C(4)	1.400(6)
C(3)-H(3)	0.9300
C(4)-C(5)	1.397(7)
C(4)-C(7)	1.463(6)
C(5)-C(6)	1.376(7)
C(5)-H(5)	0.9300
C(6)-H(6)	0.9300
C(7)-C(8)	1.348(6)
C(7)-H(7)	0.9300
C(8)-C(9)	1.437(7)
C(8)-H(8)	0.9300
C(9)-C(10)	1.339(6)
C(9)-H(9)	0.9300
C(10)-C(11)	1.460(6)
C(11)-C(12)	1.327(6)
C(11)-H(11)	0.9300
C(12)-H(12)	0.9300
C(13)-C(18)	1.369(7)
C(13)-C(14)	1.400(7)
C(14)-C(15)	1.347(8)
C(14)-H(14)	0.9300
C(15)-C(16)	1.343(11)
C(15)-H(15)	0.9300
C(16)-C(17)	1.393(11)
C(16)-H(16)	0.9300
C(17)-C(18)	1.422(9)
C(17)-H(17)	0.9300
C(18)-H(18)	0.9300
C(19)-C(20)	1.385(6)
C(19)-C(24)	1.388(6)
C(20)-C(21)	1.379(7)
C(20)-H(20)	0.9300
C(21)-C(22)	1.387(7)

C(21)-H(21)	0.9300
C(22)-C(23)	1.377(7)
C(22)-H(22)	0.9300
C(23)-C(24)	1.391(7)
C(23)-H(23)	0.9300
C(24)-H(24)	0.9300
O(2)-S(1)-O(1)	119.34(19)
O(2)-S(1)-C(19)	108.53(19)
O(1)-S(1)-C(19)	108.58(19)
O(2)-S(1)-C(10)	107.7(2)
O(1)-S(1)-C(10)	107.74(19)
C(19)-S(1)-C(10)	103.9(2)
O(4)-S(2)-O(3)	119.7(2)
O(4)-S(2)-C(12)	109.5(2)
O(3)-S(2)-C(12)	107.5(2)
O(4)-S(2)-C(13)	108.6(2)
O(3)-S(2)-C(13)	108.9(2)
C(12)-S(2)-C(13)	101.2(2)
O(6)-N(1)-O(5)	123.1(4)
O(6)-N(1)-C(1)	118.9(4)
O(5)-N(1)-C(1)	118.0(4)
C(2)-C(1)-C(6)	122.1(4)
C(2)-C(1)-N(1)	119.6(4)
C(6)-C(1)-N(1)	118.3(4)
C(1)-C(2)-C(3)	118.7(4)
C(1)-C(2)-H(2)	120.6
C(3)-C(2)-H(2)	120.6
C(2)-C(3)-C(4)	120.7(4)
C(2)-C(3)-H(3)	119.7
C(4)-C(3)-H(3)	119.7
C(5)-C(4)-C(3)	118.8(4)
C(5)-C(4)-C(7)	122.5(4)
C(3)-C(4)-C(7)	118.7(4)

C(6)-C(5)-C(4)	120.9(4)
C(6)-C(5)-H(5)	119.6
C(4)-C(5)-H(5)	119.6
C(5)-C(6)-C(1)	118.8(4)
C(5)-C(6)-H(6)	120.6
C(1)-C(6)-H(6)	120.6
C(8)-C(7)-C(4)	125.6(5)
C(8)-C(7)-H(7)	117.2
C(4)-C(7)-H(7)	117.2
C(7)-C(8)-C(9)	121.1(5)
C(7)-C(8)-H(8)	119.5
C(9)-C(8)-H(8)	119.5
C(10)-C(9)-C(8)	125.7(5)
C(10)-C(9)-H(9)	117.2
C(8)-C(9)-H(9)	117.2
C(9)-C(10)-C(11)	124.0(4)
C(9)-C(10)-S(1)	116.8(4)
C(11)-C(10)-S(1)	119.2(3)
C(12)-C(11)-C(10)	126.1(4)
C(12)-C(11)-H(11)	117.0
C(10)-C(11)-H(11)	117.0
C(11)-C(12)-S(2)	121.1(4)
C(11)-C(12)-H(12)	119.4
S(2)-C(12)-H(12)	119.4
C(18)-C(13)-C(14)	121.4(5)
C(18)-C(13)-S(2)	119.7(4)
C(14)-C(13)-S(2)	118.8(4)
C(15)-C(14)-C(13)	121.1(6)
C(15)-C(14)-H(14)	119.5
C(13)-C(14)-H(14)	119.5
C(16)-C(15)-C(14)	118.7(7)
C(16)-C(15)-H(15)	120.7
C(14)-C(15)-H(15)	120.7
C(15)-C(16)-C(17)	123.0(6)

C(15)-C(16)-H(16)	118.5
C(17)-C(16)-H(16)	118.5
C(16)-C(17)-C(18)	118.6(7)
C(16)-C(17)-H(17)	120.7
C(18)-C(17)-H(17)	120.7
C(13)-C(18)-C(17)	117.1(6)
C(13)-C(18)-H(18)	121.4
C(17)-C(18)-H(18)	121.4
C(20)-C(19)-C(24)	121.8(4)
C(20)-C(19)-S(1)	118.6(3)
C(24)-C(19)-S(1)	119.6(3)
C(21)-C(20)-C(19)	118.3(4)
C(21)-C(20)-H(20)	120.9
C(19)-C(20)-H(20)	120.9
C(20)-C(21)-C(22)	120.7(4)
C(20)-C(21)-H(21)	119.7
C(22)-C(21)-H(21)	119.7
C(23)-C(22)-C(21)	120.7(5)
C(23)-C(22)-H(22)	119.7
C(21)-C(22)-H(22)	119.7
C(22)-C(23)-C(24)	119.5(5)
C(22)-C(23)-H(23)	120.2
C(24)-C(23)-H(23)	120.2
C(19)-C(24)-C(23)	119.0(4)
C(19)-C(24)-H(24)	120.5
C(23)-C(24)-H(24)	120.5

Table 0.14: Anisotropic displacement parameters (Å^2 x 10^3) for **45**

The anisotropic displacement factor exponent takes the form: $-2\pi^2[h^2 a^{*2}U^{11} + ... + 2 h k a^* b^* U^{12}]$

	U^{11}	U^{22}	U^{33}	U^{23}	U^{13}	U^{12}
S(1)	20(1)	21(1)	22(1)	-3(1)	-6(1)	-1(1)
S(2)	23(1)	22(1)	26(1)	-3(1)	-7(1)	2(1)
O(1)	24(2)	26(2)	28(2)	-2(1)	-10(1)	-3(1)
O(3)	30(2)	41(2)	49(2)	-10(2)	-19(2)	9(2)
O(2)	28(2)	28(2)	25(2)	-5(1)	-5(1)	1(1)
O(4)	39(2)	21(2)	38(2)	1(2)	0(2)	-3(1)
O(5)	42(2)	36(2)	66(3)	7(2)	-1(2)	-11(2)
N(1)	24(2)	18(2)	16(2)	2(2)	-2(2)	-7(2)
O(6)	60(2)	27(2)	41(2)	0(2)	4(2)	-10(2)
C(1)	31(2)	27(2)	19(2)	1(2)	-9(2)	-4(2)
C(2)	25(2)	30(2)	27(3)	-1(2)	1(2)	-3(2)
C(3)	26(2)	27(2)	28(3)	0(2)	-3(2)	2(2)
C(4)	25(2)	28(2)	23(3)	0(2)	-3(2)	-5(2)
C(5)	25(2)	33(3)	32(3)	-8(2)	0(2)	0(2)
C(6)	29(2)	28(2)	26(3)	-6(2)	-3(2)	0(2)
C(7)	29(2)	31(3)	32(3)	-3(2)	-10(2)	0(2)
C(8)	32(2)	33(3)	25(3)	-1(2)	-6(2)	-2(2)
C(9)	25(2)	30(2)	31(3)	0(2)	-6(2)	-2(2)
C(10)	29(2)	27(2)	16(2)	0(2)	-8(2)	-2(2)
C(11)	23(2)	25(2)	25(3)	2(2)	-5(2)	-5(2)
C(12)	36(3)	24(2)	23(2)	-1(2)	-9(2)	1(2)
C(13)	30(2)	26(2)	25(3)	-6(2)	-2(2)	6(2)
C(14)	45(3)	38(3)	34(3)	-5(2)	8(3)	-1(2)
C(15)	72(4)	56(4)	33(4)	0(3)	6(3)	9(3)
C(16)	87(5)	71(5)	29(4)	14(3)	11(4)	34(4)
C(17)	77(5)	93(6)	54(5)	-34(4)	-37(4)	36(5)
C(18)	43(3)	52(3)	37(3)	-10(3)	-19(3)	7(3)
C(19)	22(2)	20(2)	23(2)	0(2)	-7(2)	-1(2)

C(20)	21(2)	28(2)	28(3)	1(2)	-5(2)	1(2)
C(21)	34(3)	33(3)	38(3)	2(2)	-17(2)	1(2)
C(22)	47(3)	41(3)	19(3)	1(2)	-13(2)	-7(2)
C(23)	38(3)	42(3)	27(3)	1(2)	1(2)	1(2)
C(24)	24(2)	31(2)	27(3)	2(2)	-5(2)	1(2)

Table 0.15.   Hydrogen coordinates (x 10^4) and isotropic   displacement parameters (Å^2x

10^{3}) for **45**.

	x	y	z	U(eq)
H(2)	17351	8675	-2998	37
H(3)	15191	6397	-2415	36
H(5)	9619	9300	-995	40
H(6)	11766	11569	-1587	37
H(7)	11619	5143	-1541	39
H(8)	7785	7075	-480	39
H(9)	8448	3628	-570	37
H(11)	4652	6738	944	32
H(12)	897	4787	1345	36
H(14)	-2946	5545	3736	55
H(15)	-3100	4569	5578	74
H(16)	-296	5197	6494	89
H(17)	2621	6928	5663	93
H(18)	2843	7927	3728	55
H(20)	8014	1192	1802	34
H(21)	8103	597	3718	44
H(22)	4802	1069	5156	45
H(23)	1355	2112	4710	48

H(24)	1197	2654	2784	36

_____

Table 0.21: Crystal data for 4-nitro-4'-(phenylsulfonyl)-1,1'-biphenyl **63**

Identification code	**63**
Empirical formula	$C_{18}H_{13}NO_4S$
Formula weight	339.35
Temperature	149.9(1) K
Wavelength	0.71073 Å
Crystal system	Monoclinic
Space group	P 2_1/c
Unit cell dimensions	a = 13.1110(9) Å = 90°.
	b = 7.6752(5) Å = 99.600(7)°.
	c = 15.2536(13) Å = 90°.
Volume	1513.47(19) Å^3
Z	4
Density (calculated)	1.489 Mg/m^3
Absorption coefficient	0.237 mm^{-1}
F(000)	704
Crystal size	0.30 x 0.30 x 0.25 mm^3
Theta range for data collection	2.898 to 25.346 °.
Index ranges	-15<=h<=12, -9<=k<=6, -18<=l<=14
Reflections collected	5783
Independent reflections	2766 [R(int) = 0.0426]
Completeness to theta = 25.242 °	99.9 %
Absorption correction	Semi-empirical from equivalents
Max. and min. transmission	1.00000 and 0.89631
Refinement method	Full-matrix least-squares on F^2
Data / restraints / parameters	2766 / 0 / 217
Goodness-of-fit on F^2	0.963

Final R indices [I>2sigma(I)]	R1 = 0.0538, wR2 = 0.0965		
R indices (all data)	R1 = 0.1011, wR2 = 0.1145		
Extinction coefficient	n/a		
Largest diff. peak and hole	0.230 and -0.374 e.Å^{-3}		

Table 0.22 Atomic coordinates (x 10^4) and equivalent   isotropic displacement parameters

(Å^2x 10^3) for **63**. U(eq) is defined as one third of the trace of the orthogonalized U^{ij} tensor.

	x	y	z	U(eq)
S(1)	7046(1)	6567(1)	827(1)	30(1)
O(1)	7553(2)	5780(3)	152(1)	37(1)
O(2)	6629(2)	8301(3)	698(2)	36(1)
O(3)	12214(2)	8002(3)	7186(2)	41(1)
O(4)	13202(2)	6202(3)	6627(2)	50(1)
N(1)	12403(2)	7051(3)	6580(2)	34(1)
C(1)	11637(2)	6940(3)	5765(2)	25(1)
C(2)	10686(2)	7721(4)	5747(2)	28(1)
C(3)	9963(2)	7621(4)	4979(2)	27(1)
C(4)	10182(2)	6778(3)	4224(2)	23(1)
C(5)	11161(2)	6007(3)	4278(2)	27(1)
C(6)	11880(2)	6061(3)	5046(2)	28(1)
C(7)	9407(2)	6704(3)	3396(2)	23(1)
C(8)	8571(2)	7866(4)	3244(2)	28(1)
C(9)	7862(2)	7834(4)	2472(2)	28(1)
C(10)	7951(2)	6604(4)	1824(2)	25(1)
C(11)	8763(2)	5415(4)	1958(2)	29(1)
C(12)	9479(2)	5482(4)	2731(2)	28(1)
C(13)	6057(2)	5167(4)	1045(2)	24(1)
C(14)	5242(2)	5830(4)	1410(2)	30(1)

C(15)	4493(2)	4708(4)	1602(2)	38(1)
C(16)	4554(3)	2948(4)	1428(2)	35(1)
C(17)	5368(3)	2295(4)	1072(2)	38(1)
C(18)	6130(2)	3396(4)	880(2)	36(1)

_____

Table 0.23: Bond lengths [Å] and angles [°] for **63**.

S(1)-O(2)	1.439(2)
S(1)-O(1)	1.447(2)
S(1)-C(13)	1.758(3)
S(1)-C(10)	1.766(3)
O(3)-N(1)	1.234(3)
O(4)-N(1)	1.226(3)
N(1)-C(1)	1.464(4)
C(1)-C(6)	1.370(4)
C(1)-C(2)	1.380(4)
C(2)-C(3)	1.380(4)
C(2)-H(2)	0.9300
C(3)-C(4)	1.392(4)
C(3)-H(3)	0.9300
C(4)-C(5)	1.403(4)
C(4)-C(7)	1.485(4)
C(5)-C(6)	1.377(4)
C(5)-H(5)	0.9300
C(6)-H(6)	0.9300
C(7)-C(12)	1.396(4)
C(7)-C(8)	1.402(4)
C(8)-C(9)	1.373(4)
C(8)-H(8)	0.9300
C(9)-C(10)	1.387(4)
C(9)-H(9)	0.9300
C(10)-C(11)	1.392(4)
C(11)-C(12)	1.381(4)

C(11)-H(11)	0.9300
C(12)-H(12)	0.9300
C(13)-C(14)	1.382(4)
C(13)-C(18)	1.388(4)
C(14)-C(15)	1.374(4)
C(14)-H(14)	0.9300
C(15)-C(16)	1.381(4)
C(15)-H(15)	0.9300
C(16)-C(17)	1.371(4)
C(16)-H(16)	0.9300
C(17)-C(18)	1.377(4)
C(17)-H(17)	0.9300
C(18)-H(18)	0.9300
O(2)-S(1)-O(1)	119.88(13)
O(2)-S(1)-C(13)	108.40(13)
O(1)-S(1)-C(13)	108.66(13)
O(2)-S(1)-C(10)	106.74(14)
O(1)-S(1)-C(10)	107.26(13)
C(13)-S(1)-C(10)	104.90(14)
O(4)-N(1)-O(3)	123.1(3)
O(4)-N(1)-C(1)	118.5(3)
O(3)-N(1)-C(1)	118.3(3)
C(6)-C(1)-C(2)	121.8(3)
C(6)-C(1)-N(1)	119.4(3)
C(2)-C(1)-N(1)	118.8(3)
C(1)-C(2)-C(3)	118.9(3)
C(1)-C(2)-H(2)	120.5
C(3)-C(2)-H(2)	120.5
C(2)-C(3)-C(4)	121.4(3)
C(2)-C(3)-H(3)	119.3
C(4)-C(3)-H(3)	119.3
C(3)-C(4)-C(5)	117.4(3)
C(3)-C(4)-C(7)	121.0(3)

C(5)-C(4)-C(7)	121.5(3)
C(6)-C(5)-C(4)	121.8(3)
C(6)-C(5)-H(5)	119.1
C(4)-C(5)-H(5)	119.1
C(1)-C(6)-C(5)	118.6(3)
C(1)-C(6)-H(6)	120.7
C(5)-C(6)-H(6)	120.7
C(12)-C(7)-C(8)	116.9(3)
C(12)-C(7)-C(4)	121.6(3)
C(8)-C(7)-C(4)	121.4(3)
C(9)-C(8)-C(7)	121.9(3)
C(9)-C(8)-H(8)	119.0
C(7)-C(8)-H(8)	119.0
C(8)-C(9)-C(10)	119.9(3)
C(8)-C(9)-H(9)	120.0
C(10)-C(9)-H(9)	120.0
C(9)-C(10)-C(11)	119.6(3)
C(9)-C(10)-S(1)	120.1(2)
C(11)-C(10)-S(1)	120.3(2)
C(12)-C(11)-C(10)	119.7(3)
C(12)-C(11)-H(11)	120.1
C(10)-C(11)-H(11)	120.1
C(11)-C(12)-C(7)	121.8(3)
C(11)-C(12)-H(12)	119.1
C(7)-C(12)-H(12)	119.1
C(14)-C(13)-C(18)	120.9(3)
C(14)-C(13)-S(1)	119.7(2)
C(18)-C(13)-S(1)	119.3(2)
C(15)-C(14)-C(13)	118.9(3)
C(15)-C(14)-H(14)	120.5
C(13)-C(14)-H(14)	120.5
C(14)-C(15)-C(16)	120.4(3)
C(14)-C(15)-H(15)	119.8
C(16)-C(15)-H(15)	119.8

C(17)-C(16)-C(15)	120.5(3)				
C(17)-C(16)-H(16)	119.7				
C(15)-C(16)-H(16)	119.7				
C(16)-C(17)-C(18)	120.0(3)				
C(16)-C(17)-H(17)	120.0				
C(18)-C(17)-H(17)	120.0				
C(17)-C(18)-C(13)	119.2(3)				
C(17)-C(18)-H(18)	120.4				
C(13)-C(18)-H(18)	120.4				

Table 0.24: Anisotropic displacement parameters ($Å^2$ x 10^3) for **63**. The anisotropic displacement factor exponent takes the form: $-2\pi^2[h^2 a^{*2}U^{11} + ... + 2 h k a^* b^* U^{12}]$

	U^{11}	U^{22}	U^{33}	U^{23}	U^{13}	U^{12}
S(1)	26(1)	32(1)	33(1)	1(1)	10(1)	-5(1)
O(1)	29(1)	55(2)	31(1)	-5(1)	15(1)	-7(1)
O(2)	34(1)	30(1)	45(2)	9(1)	9(1)	-3(1)
O(3)	44(2)	36(1)	42(2)	-10(1)	4(1)	1(1)
O(4)	34(1)	48(2)	65(2)	-9(1)	-4(1)	15(1)
N(1)	30(2)	27(2)	45(2)	0(1)	4(2)	-3(1)
C(1)	26(2)	14(2)	34(2)	2(1)	5(2)	-6(1)
C(2)	31(2)	21(2)	37(2)	-2(2)	16(2)	-1(1)
C(3)	26(2)	22(2)	36(2)	2(2)	14(2)	2(1)
C(4)	24(2)	14(1)	32(2)	2(1)	11(2)	-2(1)
C(5)	32(2)	18(2)	36(2)	-1(2)	17(2)	0(1)
C(6)	28(2)	19(2)	39(2)	1(2)	12(2)	0(1)
C(7)	26(2)	16(2)	31(2)	4(1)	17(2)	-3(1)
C(8)	26(2)	23(2)	37(2)	-3(2)	12(2)	-2(1)

C(9)	25(2)	22(2)	39(2)	0(2)	11(2)	2(1)
C(10)	22(2)	25(2)	31(2)	0(2)	13(1)	-7(1)
C(11)	32(2)	23(2)	36(2)	-2(2)	16(2)	-1(1)
C(12)	27(2)	21(2)	37(2)	3(2)	12(2)	4(1)
C(13)	21(2)	26(2)	26(2)	4(1)	4(1)	-3(1)
C(14)	29(2)	25(2)	37(2)	1(2)	9(2)	1(1)
C(15)	31(2)	39(2)	49(2)	5(2)	20(2)	1(2)
C(16)	32(2)	33(2)	42(2)	7(2)	8(2)	-8(2)
C(17)	40(2)	25(2)	51(3)	-7(2)	10(2)	-4(2)
C(18)	30(2)	33(2)	48(2)	-4(2)	14(2)	2(2)

———

Table 0.25: Hydrogen coordinates (x 10^4) and isotropic displacement parameters ($Å^2$x 10 ^{3})

for **63**.

———

	x	y	z	U(eq)
H(2)	10534	8306	6243	37
H(3)	9316	8127	4966	35
H(5)	11329	5444	3781	36
H(6)	12517	5513	5076	36
H(8)	8495	8683	3679	36
H(9)	7323	8637	2385	36
H(11)	8824	4580	1528	38
H(12)	10024	4690	2812	36
H(14)	5201	7016	1524	39
H(15)	3941	5136	1850	49
H(16)	4038	2201	1554	46
H(17)	5406	1107	961	50
H(18)	6686	2959	643	47

Table 0.31: Crystal data for ((1*E*,3*E*,5*E*)-6-(4-methoxyphenyl)hexa-1,3,5-triene-1,3 -diyldisulfonyl)dibenzene **50**

Identification code	**50**
Empirical formula	$C_{25}H_{22}O_5S_2$
Formula weight	466.54
Temperature	150.0(1) K
Wavelength	0.71073 Å
Crystal system	Monoclinic
Space group	P 2_1/c
Unit cell dimensions	a = 5.84331(18) Å $\quad$ = 90°.
	b = 25.5606(8) Å $\quad$ = 90.258(3)°.
	c = 14.9540(5) Å $\quad$ = 90°.
Volume	2233.49(12) Å^3
Z	4
Density (calculated)	1.387 Mg/m^3
Absorption coefficient	0.274 mm^{-1}
F(000)	976
Crystal size	0.50 x 0.25 x 0.20 mm^3
Theta range for data collection	3.157 to 25.350 °.
Index ranges	-7<=h<=7, -30<=k<=30, -18<=l<=18
Reflections collected	28233
Independent reflections	4078 [R(int) = 0.0479]
Completeness to theta = 25.242 °	99.9 %
Absorption correction	Semi-empirical from equivalents
Max. and min. transmission	1.00000 and 0.98856
Refinement method	Full-matrix least-squares on F^2
Data / restraints / parameters	4078 / 0 / 291
Goodness-of-fit on F^2	1.018

Final R indices [I>2sigma(I)]	R1 = 0.0384, wR2 = 0.0838			
R indices (all data)	R1 = 0.0463, wR2 = 0.0875			
Extinction coefficient	n/a			
Largest diff. peak and hole	0.341 and -0.328 e.Å^{-3}			

Table 0.32: Atomic coordinates (x 10^4) and equivalent isotropic displacement parameters (Å^2x 10^3) for **50**. U(eq) is defined as one third of the trace of the orthogonalized U^{ij} tensor.

	x	y	z	U(eq)
S(1)	1960(1)	6051(1)	4947(1)	24(1)
S(2)	5195(1)	6598(1)	2097(1)	23(1)
O(2)	4415(3)	6044(1)	4976(1)	30(1)
O(4)	7592(3)	6482(1)	2030(1)	31(1)
O(3)	3711(3)	6487(1)	1352(1)	31(1)
O(5)	-9912(3)	4151(1)	665(1)	38(1)
O(1)	733(3)	5756(1)	5609(1)	36(1)
C(1)	-9532(6)	4200(1)	-275(2)	47(1)
C(2)	-8338(4)	4368(1)	1232(2)	28(1)
C(3)	-8856(4)	4346(1)	2135(2)	27(1)
C(4)	-7374(4)	4555(1)	2761(2)	26(1)
C(5)	-5346(4)	4802(1)	2506(2)	23(1)
C(6)	-4853(4)	4818(1)	1593(2)	31(1)
C(7)	-6311(4)	4600(1)	964(2)	32(1)
C(8)	-3885(4)	5027(1)	3193(2)	24(1)
C(9)	-2019(4)	5328(1)	3090(2)	23(1)
C(10)	-848(4)	5533(1)	3857(2)	23(1)
C(11)	1003(4)	5851(1)	3872(2)	21(1)
C(12)	2101(4)	6076(1)	3088(2)	21(1)
C(13)	4158(4)	6295(1)	3058(2)	21(1)

C(14)	4940(4)	7268(1)	2371(2)	22(1)
C(15)	2966(4)	7534(1)	2135(2)	27(1)
C(16)	2781(5)	8058(1)	2349(2)	34(1)
C(17)	4527(5)	8308(1)	2807(2)	36(1)
C(18)	6470(5)	8036(1)	3053(2)	36(1)
C(19)	6696(4)	7515(1)	2836(2)	28(1)
C(20)	1017(4)	6708(1)	5015(2)	25(1)
C(21)	-1131(4)	6805(1)	5366(2)	35(1)
C(22)	-1874(5)	7319(1)	5425(2)	48(1)
C(23)	-512(6)	7724(1)	5130(2)	48(1)
C(24)	1597(6)	7622(1)	4781(2)	42(1)
C(25)	2393(5)	7113(1)	4719(2)	30(1)

_____

Table 0.33: Bond lengths [Å] and angles [°] for **50**.

S(1)-O(2)	1.4351(17)
S(1)-O(1)	1.4376(17)
S(1)-C(20)	1.769(2)
S(1)-C(11)	1.775(2)
S(2)-O(4)	1.4356(17)
S(2)-O(3)	1.4372(18)
S(2)-C(13)	1.745(2)
S(2)-C(14)	1.766(2)
O(5)-C(2)	1.367(3)
O(5)-C(1)	1.430(3)
C(1)-H(1A)	0.9600
C(1)-H(1B)	0.9600
C(1)-H(1C)	0.9600
C(2)-C(7)	1.385(3)
C(2)-C(3)	1.386(3)
C(3)-C(4)	1.381(3)
C(3)-H(3)	0.9300
C(4)-C(5)	1.397(3)

C(4)-H(4)	0.9300
C(5)-C(6)	1.396(3)
C(5)-C(8)	1.453(3)
C(6)-C(7)	1.383(4)
C(6)-H(6)	0.9300
C(7)-H(7)	0.9300
C(8)-C(9)	1.343(3)
C(8)-H(8)	0.9300
C(9)-C(10)	1.432(3)
C(9)-H(9)	0.9300
C(10)-C(11)	1.354(3)
C(10)-H(10)	0.9300
C(11)-C(12)	1.456(3)
C(12)-C(13)	1.327(3)
C(12)-H(12)	0.9300
C(13)-H(13)	0.9300
C(14)-C(15)	1.384(3)
C(14)-C(19)	1.389(3)
C(15)-C(16)	1.383(4)
C(15)-H(15)	0.9300
C(16)-C(17)	1.383(4)
C(16)-H(16)	0.9300
C(17)-C(18)	1.380(4)
C(17)-H(17)	0.9300
C(18)-C(19)	1.380(4)
C(18)-H(18)	0.9300
C(19)-H(19)	0.9300
C(20)-C(21)	1.385(3)
C(20)-C(25)	1.386(3)
C(21)-C(22)	1.386(4)
C(21)-H(21)	0.9300
C(22)-C(23)	1.379(5)
C(22)-H(22)	0.9300
C(23)-C(24)	1.366(4)

C(23)-H(23)	0.9300
C(24)-C(25)	1.384(4)
C(24)-H(24)	0.9300
C(25)-H(25)	0.9300
O(2)-S(1)-O(1)	118.27(11)
O(2)-S(1)-C(20)	108.81(11)
O(1)-S(1)-C(20)	107.51(12)
O(2)-S(1)-C(11)	109.55(11)
O(1)-S(1)-C(11)	108.46(11)
C(20)-S(1)-C(11)	103.18(11)
O(4)-S(2)-O(3)	119.36(11)
O(4)-S(2)-C(13)	107.96(11)
O(3)-S(2)-C(13)	109.84(11)
O(4)-S(2)-C(14)	107.44(11)
O(3)-S(2)-C(14)	108.73(11)
C(13)-S(2)-C(14)	102.11(10)
C(2)-O(5)-C(1)	117.8(2)
O(5)-C(1)-H(1A)	109.5
O(5)-C(1)-H(1B)	109.5
H(1A)-C(1)-H(1B)	109.5
O(5)-C(1)-H(1C)	109.5
H(1A)-C(1)-H(1C)	109.5
H(1B)-C(1)-H(1C)	109.5
O(5)-C(2)-C(7)	124.6(2)
O(5)-C(2)-C(3)	116.0(2)
C(7)-C(2)-C(3)	119.4(2)
C(4)-C(3)-C(2)	120.3(2)
C(4)-C(3)-H(3)	119.8
C(2)-C(3)-H(3)	119.8
C(3)-C(4)-C(5)	121.3(2)
C(3)-C(4)-H(4)	119.3
C(5)-C(4)-H(4)	119.3
C(6)-C(5)-C(4)	117.4(2)

C(6)-C(5)-C(8)	123.8(2)
C(4)-C(5)-C(8)	118.8(2)
C(7)-C(6)-C(5)	121.6(2)
C(7)-C(6)-H(6)	119.2
C(5)-C(6)-H(6)	119.2
C(6)-C(7)-C(2)	120.0(2)
C(6)-C(7)-H(7)	120.0
C(2)-C(7)-H(7)	120.0
C(9)-C(8)-C(5)	128.4(2)
C(9)-C(8)-H(8)	115.8
C(5)-C(8)-H(8)	115.8
C(8)-C(9)-C(10)	120.2(2)
C(8)-C(9)-H(9)	119.9
C(10)-C(9)-H(9)	119.9
C(11)-C(10)-C(9)	127.8(2)
C(11)-C(10)-H(10)	116.1
C(9)-C(10)-H(10)	116.1
C(10)-C(11)-C(12)	125.4(2)
C(10)-C(11)-S(1)	115.87(18)
C(12)-C(11)-S(1)	118.47(17)
C(13)-C(12)-C(11)	126.6(2)
C(13)-C(12)-H(12)	116.7
C(11)-C(12)-H(12)	116.7
C(12)-C(13)-S(2)	122.30(19)
C(12)-C(13)-H(13)	118.9
S(2)-C(13)-H(13)	118.9
C(15)-C(14)-C(19)	121.2(2)
C(15)-C(14)-S(2)	119.23(18)
C(19)-C(14)-S(2)	119.57(19)
C(16)-C(15)-C(14)	118.9(2)
C(16)-C(15)-H(15)	120.5
C(14)-C(15)-H(15)	120.5
C(15)-C(16)-C(17)	120.3(2)
C(15)-C(16)-H(16)	119.8

C(17)-C(16)-H(16)	119.8
C(18)-C(17)-C(16)	120.2(2)
C(18)-C(17)-H(17)	119.9
C(16)-C(17)-H(17)	119.9
C(19)-C(18)-C(17)	120.3(3)
C(19)-C(18)-H(18)	119.9
C(17)-C(18)-H(18)	119.9
C(18)-C(19)-C(14)	119.1(2)
C(18)-C(19)-H(19)	120.5
C(14)-C(19)-H(19)	120.5
C(21)-C(20)-C(25)	120.9(2)
C(21)-C(20)-S(1)	118.4(2)
C(25)-C(20)-S(1)	120.68(19)
C(20)-C(21)-C(22)	118.7(3)
C(20)-C(21)-H(21)	120.7
C(22)-C(21)-H(21)	120.7
C(23)-C(22)-C(21)	120.6(3)
C(23)-C(22)-H(22)	119.7
C(21)-C(22)-H(22)	119.7
C(24)-C(23)-C(22)	120.1(3)
C(24)-C(23)-H(23)	119.9
C(22)-C(23)-H(23)	119.9
C(23)-C(24)-C(25)	120.6(3)
C(23)-C(24)-H(24)	119.7
C(25)-C(24)-H(24)	119.7
C(24)-C(25)-C(20)	119.1(3)
C(24)-C(25)-H(25)	120.5
C(20)-C(25)-H(25)	120.5

Table 0.34: Anisotropic displacement parameters (Å^2x 10^3) for **50**. The anisotropic displacement factor exponent takes the form: $-2\pi^2[h^2 a^{*2}U^{11} + ... + 2 h k a^* b^* U^{12}]$

	U^{11}	U^{22}	U^{33}	U^{23}	U^{13}	U^{12}
S(1)	24(1)	28(1)	20(1)	5(1)	-1(1)	-4(1)
S(2)	25(1)	23(1)	20(1)	0(1)	3(1)	0(1)
O(2)	25(1)	39(1)	27(1)	5(1)	-4(1)	-1(1)
O(4)	28(1)	31(1)	33(1)	4(1)	11(1)	4(1)
O(3)	40(1)	32(1)	22(1)	-2(1)	-1(1)	-4(1)
O(5)	37(1)	40(1)	37(1)	-9(1)	-3(1)	-11(1)
O(1)	36(1)	44(1)	26(1)	14(1)	-1(1)	-11(1)
C(1)	60(2)	47(2)	35(2)	-9(1)	-7(1)	-15(2)
C(2)	28(1)	19(1)	36(1)	-4(1)	-2(1)	-1(1)
C(3)	23(1)	22(1)	36(1)	-2(1)	8(1)	-4(1)
C(4)	30(1)	19(1)	28(1)	-1(1)	7(1)	-1(1)
C(5)	24(1)	15(1)	29(1)	0(1)	1(1)	2(1)
C(6)	29(1)	30(1)	33(1)	4(1)	4(1)	-8(1)
C(7)	38(2)	34(1)	25(1)	2(1)	3(1)	-8(1)
C(8)	27(1)	17(1)	27(1)	2(1)	2(1)	3(1)
C(9)	26(1)	17(1)	27(1)	2(1)	1(1)	2(1)
C(10)	24(1)	20(1)	26(1)	4(1)	2(1)	2(1)
C(11)	23(1)	19(1)	22(1)	2(1)	-3(1)	1(1)
C(12)	24(1)	16(1)	22(1)	-1(1)	-1(1)	2(1)
C(13)	25(1)	18(1)	21(1)	-1(1)	2(1)	4(1)
C(14)	24(1)	22(1)	18(1)	4(1)	3(1)	-2(1)
C(15)	26(1)	31(1)	24(1)	-1(1)	-2(1)	1(1)
C(16)	39(2)	28(1)	36(2)	5(1)	-3(1)	10(1)
C(17)	49(2)	20(1)	41(2)	1(1)	2(1)	1(1)
C(18)	38(2)	27(1)	44(2)	1(1)	-5(1)	-10(1)
C(19)	24(1)	27(1)	34(1)	6(1)	-4(1)	-3(1)
C(20)	29(1)	30(1)	16(1)	-5(1)	-4(1)	-1(1)
C(21)	27(1)	49(2)	30(1)	-12(1)	-2(1)	-5(1)

C(22)	34(2)	68(2)	42(2)	-29(2)	-7(1)	14(2)
C(23)	61(2)	39(2)	44(2)	-20(1)	-16(2)	15(2)
C(24)	68(2)	29(2)	28(2)	-6(1)	-5(1)	-4(1)
C(25)	39(2)	32(1)	21(1)	-5(1)	4(1)	-4(1)

___

Table 0.35: Hydrogen coordinates (x 10^4) and isotropic displacement parameters (Å^{2}x 10^3) for **50**.

_____

	x	y	z	U(eq)

_____

H(1A)	-9453	4564	-432	62
H(1B)	-10770	4038	-596	62
H(1C)	-8119	4032	-429	62
H(3)	-10209	4188	2320	35
H(4)	-7733	4532	3365	33
H(6)	-3512	4979	1404	40
H(7)	-5931	4610	361	42
H(8)	-4296	4955	3780	31
H(9)	-1486	5402	2519	30
H(10)	-1428	5435	4410	30
H(12)	1277	6065	2555	27
H(13)	5078	6286	3567	28
H(15)	1782	7363	1837	35
H(16)	1477	8244	2184	45
H(17)	4391	8661	2950	47
H(18)	7632	8206	3366	47
H(19)	8006	7331	3000	37
H(21)	-2055	6532	5558	46
H(22)	-3305	7391	5665	63

H(23)	-1031	8067	5170	62
H(24)	2507	7897	4583	54
H(25)	3830	7045	4482	40

_____

_____

Table 0.41: Crystal data for 4'-methoxy-4'-(phenylsulfonyl)-1,1'-biphenyl **58**

Identification code	**58**
Empirical formula	$C_{19}H_{16}O_3S$
Formula weight	324.38
Temperature	296.3(1) K
Wavelength	0.71073 Å
Crystal system	Monoclinic
Space group	$P\,2_1$
Unit cell dimensions	a = 6.7378(3) Å = 90°.
	b = 7.9901(4) Å = 98.700(5)°.
	c = 15.1328(7) Å = 90°.
Volume	805.31(7) Å^3
Z	2
Density (calculated)	1.338 Mg/m^3
Absorption coefficient	0.213 mm^{-1}
F(000)	340
Crystal size	0.40 x 0.30 x 0.25 mm^3
Theta range for data collection	3.059 to 25.349 °.
Index ranges	-7<=h<=8, -7<=k<=9, -18<=l<=12
Reflections collected	3173
Independent reflections	2209 [R(int) = 0.0230]
Completeness to theta = 25.242 °	99.8 %
Absorption correction	Semi-empirical from equivalents
Max. and min. transmission	1.00000 and 0.88553
Refinement method	Full-matrix least-squares on F^2
Data / restraints / parameters	2209 / 1 / 209
Goodness-of-fit on F^2	1.056
Final R indices [I>2sigma(I)]	R1 = 0.0384, wR2 = 0.0854
R indices (all data)	R1 = 0.0482, wR2 = 0.0909

Absolute structure parameter	0.09(7)			
Extinction coefficient	n/a			
Largest diff. peak and hole	0.121 and -0.238 e.Å^{-3}			

Table 0.42 Atomic coordinates (x 10^4) and equivalent isotropic displacement parameters (Å^2x 10^3) for **58**. U(eq) is defined as one third of the trace of the orthogonalized U^{ij} tensor.

	x	y	z	U(eq)
S(1)	3306(1)	6276(1)	8194(1)	51(1)
O(3)	-7038(3)	5910(4)	2516(2)	63(1)
O(1)	5232(3)	6173(6)	7916(2)	78(1)
O(2)	2783(5)	7717(3)	8680(2)	73(1)
C(1)	-8817(6)	6888(7)	2420(3)	92(2)
C(2)	-5735(4)	6031(5)	3287(2)	45(1)
C(3)	-3971(5)	5107(5)	3334(2)	57(1)
C(4)	-2576(5)	5127(5)	4082(2)	50(1)
C(5)	-2827(4)	6058(5)	4835(2)	39(1)
C(6)	-4575(5)	6991(5)	4769(2)	58(1)
C(7)	-6016(5)	6977(5)	4017(3)	58(1)
C(8)	-1323(4)	6067(5)	5663(2)	40(1)
C(9)	582(5)	5386(6)	5687(2)	57(1)
C(10)	1968(5)	5410(5)	6455(3)	59(1)
C(11)	1486(4)	6135(6)	7221(2)	46(1)
C(12)	-381(5)	6803(5)	7218(2)	54(1)
C(13)	-1765(5)	6759(5)	6453(2)	54(1)
C(14)	3001(5)	4485(5)	8839(2)	41(1)
C(15)	3875(6)	3007(5)	8648(3)	61(1)
C(16)	3683(7)	1625(6)	9156(4)	82(1)
C(17)	2663(7)	1718(7)	9851(4)	88(2)

C(18)	1789(8)	3191(8)	10055(3)	87(2)
C(19)	1956(5)	4602(5)	9549(2)	59(1)

_____

Table 0.43: Bond lengths [Å] and angles [º] for **58**.

S(1)-O(1)	1.426(2)
S(1)-O(2)	1.438(3)
S(1)-C(14)	1.761(4)
S(1)-C(11)	1.772(3)
O(3)-C(2)	1.353(4)
O(3)-C(1)	1.420(5)
C(1)-H(1A)	0.9600
C(1)-H(1B)	0.9600
C(1)-H(1C)	0.9600
C(2)-C(7)	1.375(5)
C(2)-C(3)	1.392(5)
C(3)-C(4)	1.358(5)
C(3)-H(3)	0.9300
C(4)-C(5)	1.393(5)
C(4)-H(4)	0.9300
C(5)-C(6)	1.384(4)
C(5)-C(8)	1.487(4)
C(6)-C(7)	1.380(5)
C(6)-H(6)	0.9300
C(7)-H(7)	0.9300
C(8)-C(9)	1.390(5)
C(8)-C(13)	1.391(4)
C(9)-C(10)	1.376(5)
C(9)-H(9)	0.9300
C(10)-C(11)	1.378(5)
C(10)-H(10)	0.9300
C(11)-C(12)	1.366(4)
C(12)-C(13)	1.372(5)

C(12)-H(12)	0.9300
C(13)-H(13)	0.9300
C(14)-C(15)	1.370(5)
C(14)-C(19)	1.374(5)
C(15)-C(16)	1.362(6)
C(15)-H(15)	0.9300
C(16)-C(17)	1.344(7)
C(16)-H(16)	0.9300
C(17)-C(18)	1.372(7)
C(17)-H(17)	0.9300
C(18)-C(19)	1.377(6)
C(18)-H(18)	0.9300
C(19)-H(19)	0.9300
O(1)-S(1)-O(2)	120.1(2)
O(1)-S(1)-C(14)	107.7(2)
O(2)-S(1)-C(14)	108.03(15)
O(1)-S(1)-C(11)	107.30(13)
O(2)-S(1)-C(11)	106.5(2)
C(14)-S(1)-C(11)	106.52(18)
C(2)-O(3)-C(1)	118.5(3)
O(3)-C(1)-H(1A)	109.5
O(3)-C(1)-H(1B)	109.5
H(1A)-C(1)-H(1B)	109.5
O(3)-C(1)-H(1C)	109.5
H(1A)-C(1)-H(1C)	109.5
H(1B)-C(1)-H(1C)	109.5
O(3)-C(2)-C(7)	125.6(3)
O(3)-C(2)-C(3)	116.4(3)
C(7)-C(2)-C(3)	118.1(3)
C(4)-C(3)-C(2)	121.0(3)
C(4)-C(3)-H(3)	119.5
C(2)-C(3)-H(3)	119.5
C(3)-C(4)-C(5)	122.3(3)

C(3)-C(4)-H(4)	118.9
C(5)-C(4)-H(4)	118.9
C(6)-C(5)-C(4)	115.8(3)
C(6)-C(5)-C(8)	121.5(3)
C(4)-C(5)-C(8)	122.7(3)
C(7)-C(6)-C(5)	122.7(3)
C(7)-C(6)-H(6)	118.6
C(5)-C(6)-H(6)	118.6
C(2)-C(7)-C(6)	120.1(3)
C(2)-C(7)-H(7)	120.0
C(6)-C(7)-H(7)	120.0
C(9)-C(8)-C(13)	116.7(3)
C(9)-C(8)-C(5)	122.0(3)
C(13)-C(8)-C(5)	121.3(3)
C(10)-C(9)-C(8)	121.5(3)
C(10)-C(9)-H(9)	119.2
C(8)-C(9)-H(9)	119.2
C(9)-C(10)-C(11)	120.0(3)
C(9)-C(10)-H(10)	120.0
C(11)-C(10)-H(10)	120.0
C(12)-C(11)-C(10)	119.7(3)
C(12)-C(11)-S(1)	120.0(3)
C(10)-C(11)-S(1)	120.3(3)
C(11)-C(12)-C(13)	120.1(3)
C(11)-C(12)-H(12)	120.0
C(13)-C(12)-H(12)	120.0
C(12)-C(13)-C(8)	121.9(3)
C(12)-C(13)-H(13)	119.0
C(8)-C(13)-H(13)	119.0
C(15)-C(14)-C(19)	120.7(4)
C(15)-C(14)-S(1)	119.6(3)
C(19)-C(14)-S(1)	119.6(3)
C(16)-C(15)-C(14)	120.0(4)
C(16)-C(15)-H(15)	120.0

C(14)-C(15)-H(15)	120.0
C(17)-C(16)-C(15)	120.1(5)
C(17)-C(16)-H(16)	120.0
C(15)-C(16)-H(16)	120.0
C(16)-C(17)-C(18)	120.7(5)
C(16)-C(17)-H(17)	119.6
C(18)-C(17)-H(17)	119.6
C(17)-C(18)-C(19)	120.2(4)
C(17)-C(18)-H(18)	119.9
C(19)-C(18)-H(18)	119.9
C(14)-C(19)-C(18)	118.3(4)
C(14)-C(19)-H(19)	120.8
C(18)-C(19)-H(19)	120.8

Table 0.44: Anisotropic displacement parameters ($\text{Å}^2 \text{x } 10^3$) for **58**. The anisotropic displacement factor exponent takes the form: $-2\pi^2[h^2 a^{*2}U^{11} + ... + 2 h k a^* b^* U^{12}]$

	U^{11}	U^{22}	U^{33}	U^{23}	U^{13}	U^{12}
S(1)	54(1)	53(1)	46(1)	4(1)	5(1)	-14(1)
O(3)	56(1)	72(2)	57(1)	1(2)	-5(1)	4(2)
O(1)	50(1)	121(3)	63(1)	17(2)	8(1)	-29(2)
O(2)	108(2)	39(2)	66(2)	-7(2)	-7(2)	-8(2)
C(1)	60(2)	123(5)	85(3)	1(3)	-9(2)	21(3)
C(2)	45(2)	42(2)	48(2)	7(2)	8(1)	-3(2)
C(3)	68(2)	54(3)	49(2)	-11(2)	10(2)	16(2)
C(4)	50(2)	49(2)	51(2)	-2(2)	7(2)	16(2)
C(5)	44(2)	33(2)	42(2)	4(2)	14(1)	2(2)

C(6)	55(2)	69(3)	51(2)	-8(2)	13(2)	17(2)
C(7)	43(2)	71(3)	62(2)	-3(2)	9(2)	18(2)
C(8)	41(1)	36(2)	45(2)	1(2)	12(1)	0(2)
C(9)	51(2)	75(3)	47(2)	-11(2)	13(2)	11(2)
C(10)	45(2)	80(3)	54(2)	-4(2)	8(2)	15(2)
C(11)	50(2)	46(2)	42(2)	5(2)	10(1)	-8(2)
C(12)	59(2)	63(3)	43(2)	-4(2)	17(2)	8(2)
C(13)	49(2)	68(3)	46(2)	-3(2)	16(2)	10(2)
C(14)	38(2)	42(2)	41(2)	-2(2)	1(2)	-3(2)
C(15)	59(2)	55(3)	67(3)	-10(2)	4(2)	1(2)
C(16)	76(3)	49(3)	110(4)	-3(3)	-23(3)	6(2)
C(17)	79(3)	74(4)	97(4)	43(3)	-30(3)	-23(3)
C(18)	91(3)	108(5)	66(3)	24(3)	25(2)	-20(3)
C(19)	63(2)	63(3)	56(2)	6(2)	22(2)	3(2)

___

Table 0.45 Hydrogen coordinates (x 10^4) and isotropic displacement parameters (Å^2x 10 ^{3}) for **58**.

_____

	x	y	z	U(eq)
H(1A)	-9559	6631	2896	119
H(1B)	-9624	6640	1856	119
H(1C)	-8470	8054	2442	119
H(3)	-3745	4466	2846	74
H(4)	-1412	4496	4092	65
H(6)	-4786	7654	5251	75
H(7)	-7179	7610	4004	76
H(9)	929	4903	5173	74
H(10)	3230	4937	6457	77

H(12)	-714	7288	7734	70
H(13)	-3035	7206	6464	70
H(15)	4599	2946	8173	79
H(16)	4259	617	9021	107
H(17)	2548	773	10199	114
H(18)	1081	3237	10537	113
H(19)	1376	5608	9684	77

_____